Investigation of the role of nutrients for protection against acute kidney injury

Hui-Hsuan Liu, BSc, MSc

University of Nottingham
School of Biosciences

Thesis submitted to the University of Nottingham for the degree of Doctor of Philosophy

May 2017

Abstract

Ischaemia reperfusion injury and nephrotoxicity are the common insults of acute kidney injury. Drug induced nephrotoxicity can also lead to an ischaemic phenomenon. The key mediator to both insults is oxidative injury caused by reactive oxygen species, and prolonged injury can result in irreversible kidney fibrosis and chronic kidney disease. This thesis developed a simulated ischaemia reperfusion injury in an *in-vitro* model to investigate whether amino acid supplementation may facilitate human proximal tubule cell recovery and protect from H_2O_2 damage following starvation and whether this was mediated by pH. The findings showed that resupply of amino acids at pH 7.5 under H_2O_2 injury after starvation exacerbated cell death. The mammalian target of rapamycin was also activated in response to amino acids in a concentration dependent manner even if under H_2O_2 damage, but the link between mammalian target of rapamycin activation and endoplasmic reticulum stress leading to cell death was not yet identified in this thesis. The constant expression of chaperone protein Grp78 may suggest the persistent cellular stress caused by starvation. While amino acids at pH 6.4 failed to activate the mammalian target of rapamycin and potentially reduced protein synthesis, it still exacerbated cell death under H_2O_2 damage. It also inhibited Grp78 expression, but the link between Grp78 inhibition and cell death was unclear. Moreover, this thesis established an aristolochic acid induced nephrotoxicity in mice and investigated whether another putative nutrient, sodium nitrite, could be renoprotective. However, the therapeutic effects of sodium nitrite remain to be confirmed, as aristolochic acid did not induce any injury in this animal model. Overall, this thesis implicated that the return of circulating amino acids may be detrimental for ischaemia reperfusion injury and that antioxidant therapy may be the priority for acute kidney injury.

Acknowledgments

I would like to thank the University of Nottingham for sponsoring my three year PhD programme and thank my supervisors Dr. Simon Welham and Prof. Andy Salter for their invaluable and patient guidance and help during my study. I also would like to thank Associate Prof. David Gardner from School of Veterinary Medicine and Science for sharing his knowledge in this field of research and helping with the experimental protocol, providing some reagents and instruments for my animal study. I also appreciate and enjoyed discussing the statistical analysis with Jim Craigon from Animal Sciences.

Furthermore, I would like to thank my family for their full support and encouragement for my study during these three years. Also, I greatly thank to my partner Andrew Burlinson for all his help, encouraging me and always being there for me. Andrew's family is always kind to me and treats me as part of their family during my study in the UK, always offering their help and being supportive.

Additionally I would like to thank all my friends including Yihe, Jessica, Maddy, Bashair, Lujain, Kimberly and PhD students from office 50 and 51 for being there for me, the technicians including Kirsty, Zoe, Sarah and others (Ceri and Alan) from the Veterinary School for their help with experiment and for teaching me a variety of experimental techniques and instruments. I am glad to have met them, and I have developed many experimental skills, learned a lot from them and really enjoyed their company during my study.

Contents

Abstract ii
Acknowledgments iii
Contents iv
Table of figures vii
Table of tables ix
Abbreviations x
Chapter 1: Introduction 2
1.1 World prevalence of AKI 2
1.2 Kidney structure and function 3
1.2.1 Glomerular filtration 7
1.2.2 Tubular function 9
1.3 AKI 12
1.3.1 Definition 12
1.3.2 Classification and causes of AKI 14
1.4 Mechanism and pathophysiology of I/R injury 17
1.5 Nephrotoxicity 23
1.5.1 ArisA-induced nephrotoxicity 26
1.6 Experimental models of AKI 29
1.7 Prevention and current treatment for AKI 36
1.8 The mTOR signalling pathways 45
1.9 ER stress and UPR 53
1.10 Cellular repair process and long-term consequences 58
1.11 Pathophysiology of renal interstitial fibrosis 66
1.12 Other strategies for renoprotection 70
1.13 Acidic infusion 76
1.14 Dietary nitrite, I/R injury and a link to RIPC 81
1.14.1 Metabolism and circulation of nitrate and nitrite 84
1.14.2 NO bioavailability and I/R injury 91
1.14.3 Possible mechanisms of protection by nitrite derived NO 92
1.15 Summary 94
Chapter 2: Material and methods 97
2.1 Cell culture 97
2.1.1 HK-2 cells 97
2.1.2 C2C12 cells 98

2.1.3 Simulated I/R and D/R protocol 98
2.1.4 MTT assay 103
2.1.5 Immunocytochemistry 105
2.1.6 Calcein AM assay 106
2.1.7 ROS measurement 106
2.1.8 Mitochondrial and lysosomal morphology 108
2.1.9 Western blot analysis 108
2.2 Kidney tissue sections 112
2.2.1 Animals and experimental design 112
2.2.2 Kidney processing and paraffin-embedding 114
2.2.3 Sectioning 115
2.2.4 Renal histology 116
2.2.5 Masson's trichrome staining 117
2.2.6 Immunohistochemistry 118
2.2.7 Quantification of BrdU and pH3 labeled tubular cells 119
2.2.8 Total RNA extraction from snap frozen kidneys 120
2.2.9 Total RNA quality and cDNA synthesis 121
2.2.10 Quantitative real time PCR 123
2.3 Imaging 127
2.3.1 Cell culture images 127
2.3.2 Cell culture immunofluorescence images 127
2.3.3 Electrophoresis and western blot images 128
2.3.4 Kidney tissue histological images 128
2.3.5 Kidney tissue immunofluorescence images 128
2.4 Statistics 129
Chapter 3: The detrimental effects of amino acids on HK-2 cells following simulated I/R injury 131
3.1 Introduction 131
3.2 Results 134
3.2.1 Induction of simulated I/R injury in HK-2 cells 134
3.2.2 Detrimental effects of AAS at acidic pH on HK-2 cells following simulated I/R injury 136
3.2.3 Detrimental effects of low pH on HK-2 cells following simulated I/R injury 140
3.2.4 Detrimental effects of AAS at physiological pH on HK-2 cells following simulated I/R injury 142
3.2.5 Effects of AAS at low pH on HK-2 cells following D/R injury 148
3.2.6 Effects of AAS and pH on HK-2 cell viability following D/R injury 152

3.2.7 F-actin cytoskeleton alterations in HK-2 cells in response to AAS following simulated I/R injury 162
3.2.8 F-actin cytoskeleton alterations in HK-2 cells in response to pH following D/R injury 173
3.2.9 Intracellular ROS in HK-2 cells treated with AAS after simulated I/R injury 177
3.3 Conclusion 181
Chapter 4: Cellular responses to amino acids during oxidative stress following nutrient deprivation 185
4.1 Introduction 185
4.2 Results 189
4.2.1 Effects of AAS at physiological pH following D/R injury on mTOR signalling 189
4.2.2 Effects of AAS at acidic pH following D/R injury on mTOR signalling 193
4.2.3 Effects of pH without pre-starvation on mTOR signalling 195
4.2.4 Intracellular localisation of mTOR to mitochondria in response to AAS following D/R injury 197
4.2.5 Intracellular localisation of mTOR to lysosomes in response to AAS following D/R injury 206
4.2.6 Effects of AAS at physiological and acidic pH on ER stress sensor protein following D/R injury 216
4.3 Conclusion 220
Chapter 5: The effects of sodium nitrite on ArisA-induced AKI 225
5.1 Introduction 225
5.2 Results 229
5.2.1 Histopathology of the kidneys 229
5.2.2 Tubulointerstitial fibrosis assessment by Masson's trichrome stain 232
5.2.3 Cell proliferation, survival and recovery 236
5.2.4 Effects of sodium nitrite on renal gene expression in ArisA-induced AKI 241
5.3 Conclusion 245
Chapter 6: Discussion 250
6.1 The detrimental effects of amino acids on HK-2 cells following simulated I/R injury 250
6.2 Cellular responses to amino acids during oxidative stress following nutrient deprivation 259
6.3 The effects of sodium nitrite on ArisA-induced AKI 265
Chapter 7: Conclusion 272
Future work 277
Chapter 8: References 280

Table of figures

Figure 1. 1 The structure of kidney and a nephron. 6
Figure 1. 2 Diagram of a glomerular structure. 8
Figure 1. 3 A schematic diagram of nephron segments involved in urine concentrating mechanisms. 12
Figure 1. 4 Diagram shows the mitochondrial ROS generation in I/R injury. 21
Figure 1. 5 Diagram of mTOR signaling pathways in response to nutrients and growth factors. 52
Figure 1. 6 The proposed mechanism of amino acid sensing pathways in activation of mTORC1. 53
Figure 1. 7 Diagram of UPR signalling pathways. 58
Figure 1. 8 A schematic diagram of repair process in proximal tubular cells. 66
Figure 1. 9 Outcomes of wound healing process in tubular cells after injury. 70
Figure 1. 10 A schematic diagram of active NOS enzyme homodimer and NOS catalysis for NO synthesis. 90
Figure 1. 11 Endogenous and exogenous pathways for NO formation in mammals. 91
Figure 2. 1 The diagram depicts experimental protocols for I/R and D/R injury. 102
Figure 2. 2 The diagram shows the experimental design and protocol. 114
Figure 2. 3 The figure shows the ideal amplication curves and metlting curves from qRT-PCR of eNOS gene. 125
Figure 3. 1 Effects of simulated I/R injury on HK-2 cells. 135
Figure 3. 2 Effects of AAS on HK-2 cells following simulated I/R injury. 137
Figure 3. 3 Effects of AAS following starvation on mitochondrial morphologies in HK-2 cells. 139
Figure 3. 4 Effects of a varying pH on HK-2 cells following simulated I/R injury. 141
Figure 3. 5 Effects of AAS at pH 7.5 on HK-2 cells following simulated I/R injury. 143
Figure 3. 6 Effects of KOH on HK-2 cells following simulated I/R injury. 145
Figure 3. 7 Effects of AAS at pH 7.5 following starvation on mitochondrial morphologies in HK-2 cells. 147
Figure 3. 8 Effects of AAS at physiological and low pH on HK-2 cells following starvation. 151
Figure 3. 9 HK-2 cell viability after treatment with AAS following starvation in normoxia or hypoxia. 154
Figure 3. 10 HK-2 cell viability after treatment with AAS in the presence of H_2O_2 following starvation in normoxia or hypoxia. 155
Figure 3. 11 HK-2 cell viability after treatment with AAS at pH 7.5 following starvation in normoxia or hypoxia. 156
Figure 3. 12 HK-2 cell viability after treatment with AAS at pH 7.5 in the presence of H_2O_2 following starvation in normoxia or hypoxia. 157
Figure 3. 13 Effects of pH on HK-2 cell viability following starvation in normoxia. 158
Figure 3. 14 Effects of pH on HK-2 cell viability following starvation in hypoxia. 159
Figure 3. 15 Effects of pH on HK-2 cell viability in the presence of H_2O_2 following starvation in normoxia. 160
Figure 3. 16 Effects of pH on HK-2 cell viability in the presence of H_2O_2 following starvation in hypoxia. 161

Figure 3. 17 Time course images of phalloidin-labelled HK-2 cells treated with AAS following starvation. 165
Figure 3. 18 Time course images of phalloidin-labelled HK-2 cells treated with AAS following starvation. 167
Figure 3. 19 Effects of AAS on F-actin in HK-2 cells at 2 hours following starvation. 168
Figure 3. 20 Time course images of phalloidin-labelled HK-2 cells treated with AAS in the presence of H_2O_2 following starvation. 170
Figure 3. 21 Time course images of phalloidin-labelled HK-2 cells treated with AAS in the presence of H_2O_2 following starvation. 172
Figure 3. 22 Time course images of phalloidin-labelled HK-2 cells treated with HBSS at varying pH following starvation. 175
Figure 3. 23 Effects of pH on F-actin in HK-2 cells at 6 hours following starvation. 176
Figure 3. 24 ROS detection in AAS solutions at pH 7.5 with and without H_2O_2. 179
Figure 3. 25 ROS detection in HK-2 cells after treatment with AAS at pH 7.5 with and without H_2O_2 following starvation. 180
Figure 4. 1 Effects of AAS at pH 7.5 after starvation on mTOR signalling. 192
Figure 4. 2 Effects of AAS at pH 6.4 after starvation on mTOR signalling. 194
Figure 4. 3 Effects of pH 7.5 and 6.4 in the presence or absence of H_2O_2 without pre-starvation on mTOR signalling. 196
Figure 4. 4 Intracellular localisation of mTOR in HK-2 cells incubated in complete DMEM and rapamycin. 199
Figure 4. 5 Intracellular localisation of mTOR in response to AAS at pH 7.5 following starvation was independent of mitochondria. 200
Figure 4. 6 Intracellular localisation of mTOR in response to AAS at pH 7.5 with H_2O_2 following starvation was independent of mitochondria. 201
Figure 4. 7 Intracellular localisation of mTOR and mitochondria in response to nutrients at pH 7.5 following starvation was independent of mitochondria. 202
Figure 4. 8 Intracellular localisation of mTOR and mitochondria in response to AAS at pH 6.4 following starvation. 203
Figure 4. 9 Intracellular localisation of mTOR and mitochondria in response to AAS at pH 6.4 with H_2O_2 following starvation. 204
Figure 4. 10 Intracellular localisation of mTOR and mitochondria in response to nutrients at pH 6.4 following starvation. 205
Figure 4. 11 Intracellular localisation of mTOR and lysosomes in response to AAS at pH 7.5 following starvation. 208
Figure 4. 12 Intracellular localisation of mTOR and lysosomes in response to AAS at pH 7.5 with H_2O_2 following starvation. 209
Figure 4. 13 Intracellular localisation of mTOR and lysosomes in response to nutrients at pH 7.5 following starvation. 210
Figure 4. 14 Intracellular localisation of mTOR and lysosomes in response to AAS at pH 6.4 following starvation. 211
Figure 4. 15 Intracellular localisation of mTOR and lysosomes in response to AAS at pH 6.4 with H_2O_2 following starvation. 212
Figure 4. 16 Intracellular localisation of mTOR and lysosomes in response to nutrients at pH 6.4 following starvation. 213
Figure 4. 17 Effects of amino acids at pH 7.5 and 6.4 with and without H_2O_2 following starvation on total mTOR protein levels. 214

Figure 4. 18 Effects of nutrients at pH 7.5 and 6.4 following starvation on total mTOR. 215
Figure 4. 19 Effects of amino acids at pH 7.5 with and without H_2O_2 following starvation on Grp78.....218
Figure 4. 20 Effects of amino acids at pH 6.4 with and without H_2O_2 following starvation on Grp78.....219
Figure 5. 1 Representative images of H&E stain in 48-hour kidneys. 230
Figure 5. 2 Representative images of H&E stain in 35-day kidneys. 231
Figure 5. 3 Representative images of Masson's trichrome stained kidneys. 233
Figure 5. 4 Representative images of Masson's trichrome stain in 35-day kidneys.234
Figure 5. 5 Analyses of Masson's trichrome positive stain in 35-day kidneys. 235
Figure 5. 6 Representative images of positive control for pH3 labelling in sections from mouse embryos.....238
Figure 5. 7 Representative images of BrdU and pH3 labelling in 48-hour kidneys. 239
Figure 5. 8 Quantification of BrdU and pH3 positive cell number in cortex. 240
Figure 5. 9 Effects of treatments on renal gene expression in 48-hour kidneys. 243
Figure 5. 10 Effects of treatments on renal gene expression in 48-hour kidneys. 244

Table of tables

Table 1. 1 Common *in-vitro* models of AKI.....35
Table 1. 2 Common *in-vivo* models of AKI. 36
Table 2. 1 Comparison of amino acid contents between 50x MEM essential amino acid solution and the complete 1x DMEM. 103
Table 2. 2 All primers were designed using Primer Express software and NCBI-Primer BLAST. 126
Table 5. 1 Effects of sodium nitrite on gene expression in 48-hour kidneys.....245

Abbreviations

A

AAS	Amino acid supplementation
AAN	Aristolochic acid nephropathy
AKI	Acute kidney injury
AKIN	Acute Kidney Network
Alpha-SMA	Alpha-smooth muscle actin
AMP	Adenosine monophosphate
ANOVA	Analysis of variance
ANT	Adenine nucleotide translocase
ArisA	Aristolochic acid
ATF4	Activating transcription factor 4
ATF6	Activating transcription factor 6
ATM-Chk2	Ataxia telangiectasia mutated serine/threonine kinase-checkpoint kinase 2
ATN	Acute tubular necrosis
ATP	Adenosine 5'-triphosphate

B

Bcl-2	B-cell lymphoma 2
BH4	(6R-)5,6,7,8-tetrahydrobiopterin
β-ME	β-Mercaptoethanol
BrdU	5-Bromo-2'-deoxyuridine
BrdU+ cells	BrdU positive cells
BrdU+pH3+ cells	BrdU and pH3 copositive cells
BSA	Bovine serum albumin

C

C2C12 cells	Mouse embryonic myoblast cells
cDNA	Complementary DNA
CHOP	C/EBP homologous protein
CKD	Chronic kidney disease
CM	Complete DMEM
Col1A1	Collagen-I alpha 1 gene
Col4A1	Collagen-IV alpha 1 gene
Ct	Threshold cycle
CTGF	Connective tissue growth factor
Ctgf	Connective tissue growth factor gene
CYP	Cytochrome P450
Cyba	Nox2 cytochrome b-245 alpha chain gene
Cybb	Nox2 cytochrome b-245 beta chain

D

DAPI	4',6-Diamidino-2-phenylindole
DDIT3	DNA damage inducible transcript 3
DDT	DL-Dithiothreitol
dH_2O	Distilled water
DMEM	Dulbecco's modified Eagle's medium
DMSO	Dimethyl sulfoxide
D/R	Nutrient depletion/replenishment

E

4EBP1	Eukaryotic translation initiation factor 4E -binding protein 1
ECM	Extracellular matrix
eIF2a	Eukaryotic translation initiation factor 2 alpha
eIF4E	Eukaryotic translation initiation factor 4E
EMT	Epithelial-mesenchymal-transition
eNOS	Endothelial nitric oxide synthase
ER	Endoplasmic reticulum
ESRD	End-stage renal disease

F

F-actin	Filamentous actin
FBS	Foetal bovine serum
Fe^{2+}	Ferric ions
FITC-conjugated swine anti-rabbit immunoglobulins	Fluorescein isothiocyanate isomer 1-conjugated swine anti-rabbit immunoglobulins

G

GFR	Glomerular filtration rate
GRP	Glucose-regulated protein
GSH	Reduced glutathione
GSSG	Oxidised glutathione
GTPase	Guanosine-5'-triphosphatase

H

HBSS	Hank's balanced salts solution
HCl	Hydrochloric acid solution
H&E	Haematoxylin and eosin
HEPES	4-(2-Hydroxyethyl)piperazine-1-ethanesulfonic acid
HK-2 cells	Human renal proximal tubular epithelial cells

H_2O_2	Hydrogen peroxide

I

ICU	Intensive care units
IGF-1	Insulin-like growth factor-1
IL	Interleukin
iNOS	Inducible nitric oxide synthase
I/R injury	Ischaemia reperfusion injury
IRE1	Inositol-requiring transmembrane kinase/endoribonuclease
IRS	Insulin receptor substrate
ITS	Insulin-transferrin-selenium

J

JNK	cJUN N-terminal kinase

K

KDIGO	Kidney Disease Improving Global Outcomes
KOH	Potassium hydroxide
KIM-1	Kidney injury molecule-1
Kim1 or Havcr1	Kidney injury molecule-1 gene

L

LLC-PK1 cells	Porcine proximal tubular epithelial cells
LSD	Least significant difference

M

mLST8	SEC13 protein 8
MMP	Metalloproteinases
MPTP	Mitochondrial permeability transition pore
mSin1	Mammalian stress-activated protein kinase-interacting protein
MTT	3-(4,5-Dimethylthiazol-2-yl)-2,5-diphenyltetrazolium bromide
mTOR	Mammalian target of rapamycin
mTORC1	mTOR complex 1
mTORC2	mTOR complex 2

N

Na^+/K^+ ATPase	Sodium potassium adenosine triphosphatase
$NaNO_2$	Sodium nitrite
NO	Nitric oxide
NO_2^-	Nitrite ion
NO_3^-	Nitrate anion
NOS	Nitric oxide synthase
Nos2	Inducible nitric oxide synthase gene
Nos3	Endothelial nitric oxide synthase gene
NOX-2	NADPH oxidase-2
Nox2	NADPH oxidase-2 gene
NOX-4	NADPH oxidases-4
Nox4	NADPH oxidases-4 gene
NSAIDs	Non-steroidal anti-inflammatory drugs

O

P

PBS	Phosphate buffered saline
PBST	PBS with Tween 20
PERK	Protein kinase RNA-like ER kinase
PFA	Paraformaldehyde
pH3	Anti-Histone H3 (phospho S10)
pH3+ cells	pH3 positive cells
pHi	Intracellular pH
PI3K	Phosphoinositide3-kinase
PKB	Protein kinase B
pS6	Phospho ribosomal protein S6
pS6K	Phospho ribosomal kinase S6

Q

qRT-PCR	Quantitative real time polymerase chain reaction

R

Raf-MAPK-ERK	Raf-mitogen activated kinases-extracellular signal regulated kinases
Rheb	Ras homolog enriched in brain
RIPC	Remote ischaemic preconditioning
ROS	Reactive oxygen species
RPTECs	Renal proximal tubular epithelial cells
RRT	Renal replacement therapy
RT reaction	Revert transcriptase reaction

S

SCr	Serum creatinine
SDS	Sodium dodecyl sulfate
SEM	Standard error of the means
SF media	Serum free media
S6	Ribosomal protein S6
S6K	Ribosomal kinase S6

T

TAE buffer	Tris-acetate-EDTA buffer
Tbp	TATA box binding protein gene
TBST	Tris buffer saline with Tween 20
TGF-b1	Transforming growth factor-β1
Tgfb1	Transforming growth factor-β1 gene
TIM	Inhibitors of metalloproteinases
TSC1/TSC2	Tuberous sclerosis complex/tuberin

U

UPR pathways	Unfolded protein folding response pathways

V

V-ATPase	Vacuolar-H^+-adenosine triphosphatase
Vim	Vimentin gene

W

X

XBP1	X-box binding protein 1
XOR	Xanthine oxidoreductase

Y

Z

Chapter 1: Introduction

Chapter 1: Introduction

1.1 World prevalence of AKI

A general demographic characteristic shared by high-income countries (e.g. Australia, Switzerland, Germany, UK and Japan) is an ageing population (The World Bank, 2015a; The World Bank, 2015b). Although high-income countries tend to have high quality health care, an ever-increasing proportion of elderly people remains a challenge. The prevalence of acute kidney injury (AKI) is expected to be lower in the high-income countries due to adequate medical care system; however, it is still increasing owing to the increased ageing population. For instance, Susantitaphong et al. (2013) reported that Australia and New Zealand have a higher incidence rate (25.6%) of AKI than Asia (15.6%).

In the UK, between 13% and 18% of all patients admitted to hospital are found to suffer from AKI (NICE, 2013). It is estimated that over 40,000 inpatient deaths are linked to AKI in England (Kerr et al., 2014). In general UK population, the incidence of AKI was estimated to be 172 per million population per year and to be up to 486-630 per million population per year, depending on the time of estimation (Lewington and Kanagasundaram, 2011). A history of single or more episodes of AKI has been found to increase the risk of developing chronic kidney disease (CKD) and end-stage renal disease (ESRD) and resulting in other organ failure with the increase in the severity (Coca, Singanamala and Parikh, 2012). The prevalence of CKD (stage 3-5) in the UK is estimated to be between 2.3 million and 3 million people in England aged over 16 (Public Health England, 2014). It increases significantly with age, for example, around 32% of people with CKD (stage 3-5) have been found to be aged

over 75 and 13.4% aged between 65-74 (Public Health England, 2014). With normal ageing, kidney and other organ systems exhibit progressive deterioration of structural and functional changes. In particular, the decreased renal blood flow and glomerular filtration rate are profoundly associated with ageing-related kidney dysfunction due to the impaired vasodilatory responsiveness and increased sensitivity to vasoconstrictive stimuli (Weinstein and Anderson, 2010). The impaired haemodynamics occurs with other structual changes such as reduced kidney mass, increased sclerotic glomeruli and development of tubulointerstital fibrosis (Weinstein and Anderson, 2010). The age-related kidney dysfunction was also found to be further accelerated by several risk factors such as hypertension, atherosclerotic disease, male gender, smoking and a history of AKI (Weinstein and Anderson, 2010). Hence, ageing kidneys are more susceptible to any acute insults such as AKI as well as CKD.

AKI not only causes a burden on the long-term quality of life (particularly those requiring dialysis or hospitalisation) but also has an economic impact (Kerr et al., 2014). For instance, in England it was estimated to cost the NHS £434-620 millions each year on AKI including the acute admissions, critical care and renal replacement therapy (RRT) from 2009 to 2010 (NICE, 2013). It has been suggested that 30% of cases are preventable. Were this to be achieved, it could potentially save the NHS up to £130-186 millions per year (Taylor et al., 2011). Hence, early detection and prevention are the key to managing AKI.

1.2 Kidney structure and function

Kidneys are two bean-shaped organs located in the lower back of abdominal cavity and weigh approximate 150 g each (Briggs et al., 2014). Kidneys receive 25% of the

cardiac output and filter around 1.25 L blood/minute. The major function is to maintain the body fluid compositions in terms of volume, osmolality, concentration and acidity and to remove metabolic waste products such as urea and xenobiotic/toxic substances (Eaton and Pooler, 2013; Briggs et al., 2014). This is achieved through reabsorption and excretion to balance between water, electrolyte and ion contents and through urinary excretion of waste products and foreign substances. In addition, kidneys are responsible for several enzyme and hormone production and activity. For instance, renin is known to catalyse formation of angiotensin (a vasoconstrictor) and increase aldosterone secretion in kidneys to promote sodium chloride reabsorption and increase blood pressure (Danilczyk and Penninger, 2006). This system is essential for regulating blood pressure and cardiac output and contractility (Danilczyk and Penninger, 2006). Furthermore, kidneys also play a role as a pH sensor due to the abundant pH sensitive proteins (e.g. Na^+/H^+ exchangers) located on proximal and distal tubular cells (Brown and Wagner, 2012). Renal regulation of blood pH is mediated by reabsorption of bicarbonate and excretion of H^+ and ammonium in dependence of acid-base state (Kim, 2009; Briggs et al., 2014).

The functional unit in the kidney is called nephron. Each nephron is composed of a glomerulus, the Bowman's capsule, the proximal tubule, the loop of Henle, the distal tubule and the collecting duct (Koeppen and Stanton, 2013) (Figure 1.1). The glomerulus is a ball-shaped network of capillaries, across the walls of which the filtrate passes into the encapsulating Bowman's capsule. The Bowman's capsule connects to renal tubulue at the proximal tubule, the loop of Henle, the distal tubule and the collecting duct (Koeppen and Stanton, 2013). The glomerular filtrate is further processed when entering the tubules, and the urine is formed.

The kidney parenchyma comprises two distinct regions, including the outer cortex and the inner medulla (Briggs et al., 2014). The cortical regions of the kidney consist of all the glomeruli, most of the proximal tubules and some distal tubules. The medullary regions comprise the loop of Henle and the collecting ducts. In the human kidney, there are approximate one million nephrons (Briggs et al., 2014). Nephrons are bundled in parallel into cone-shaped regions called pyramids (7-9 in the human kidney). At the tips of each pyramid are the regions called papillae from which urine passes into calyx, renal pelvis and to the ureter and is then transferred to the bladder (Briggs et al., 2014) (Figure 1.2).

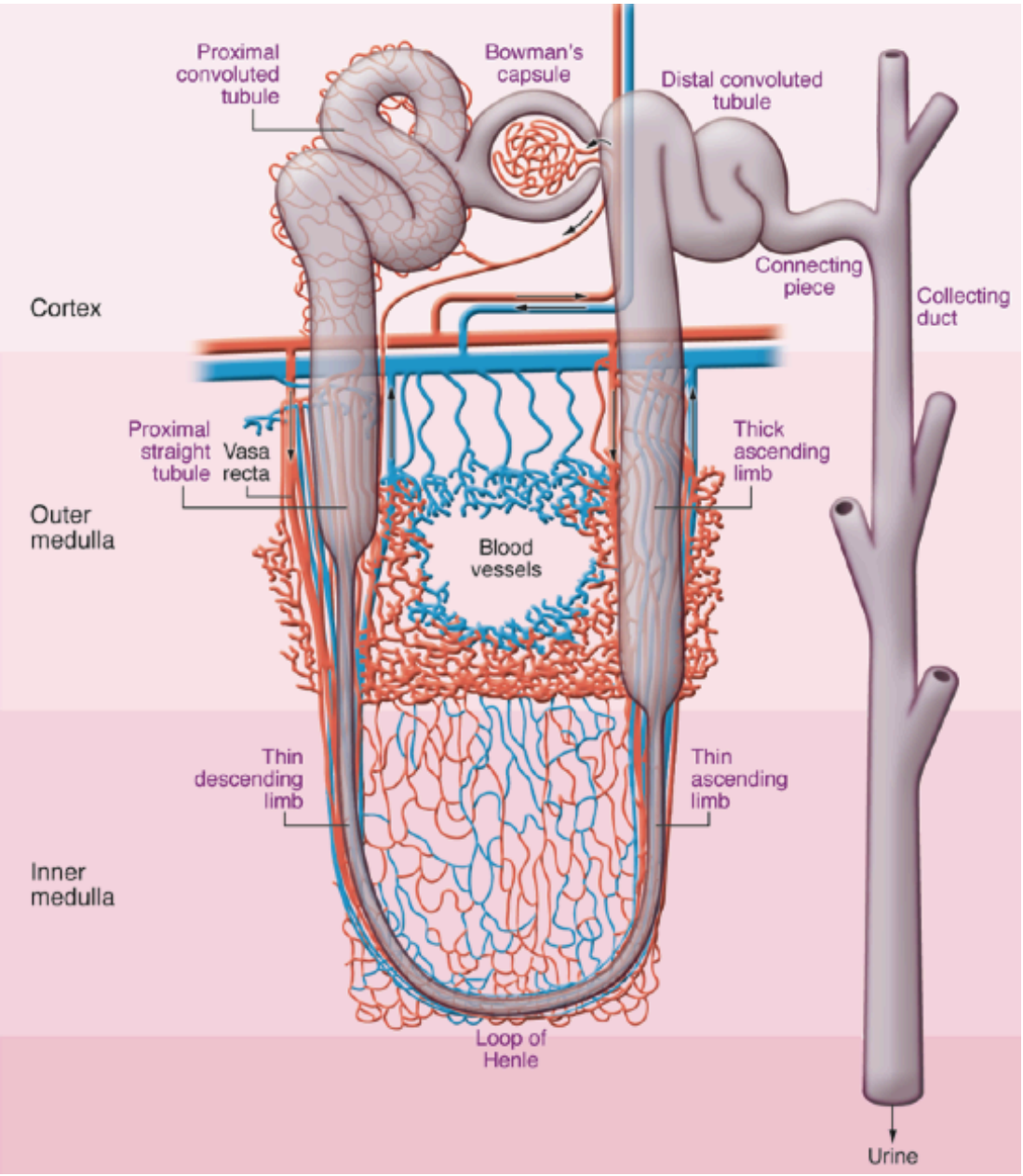


Figure 1. 1 The structure of kidney and a nephron.

A nephron is composed of a glomerulus, the Bowman's capsule, the proximal tubule, the loop of Henle, the distal tubule and the collecting duct. This diagram was republished from 'Bonventre, J. V. and Yang, L. (2011) Cellular pathophysiology of ischemic acute kidney injury. The Journal of Clinical Investigation, 121, 4210-4221.' by permission of American Society of Clinical Investigation, conveyed through Copyright Clearance Center, Inc.

1.2.1 Glomerular filtration

The glomerulus is a ball-shaped structure formed by a series of capillaries, which are held together by the mesangial cells (Briggs et al., 2014) (Figure 1.2). The surface of the capillaries is covered with specialised and highly differentiated cells called podocytes, which form a foot process to become a membranous layer that overlies the capillaries (Haraldsson and Sorensson, 2004; Greka and Mundel, 2012) (Figure 1.3). The glomerular filtration barrier comprises three layers, and these include endothelium, glomerular basement membrane and epithelial podocytes (Figure 1.3). The podocyte foot processes form filtration slit diaphragms, which are the gaps between podocytes. These filtration slits allow small substances with molecular size less than 60-70 kDa (e.g. insulin, small proteins, glucose, amino acids, urea, sodium and potassium) to pass through into the Bowman's capsule, whilst passage of substances with molecular size greater than 70 kDa (e.g. albumin) is prevented (D'Amico and Bazzi, 2003). This filtered fluid then enters the tubular lumen as the primary urine (or plasma ultrafiltrate).

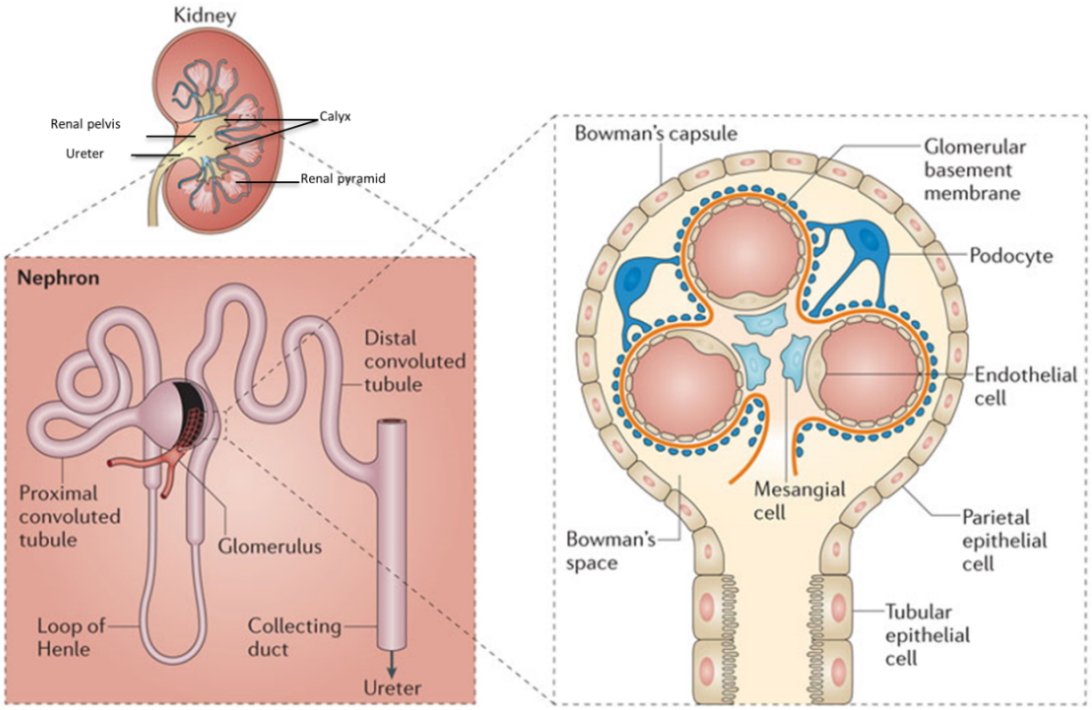


Figure 1. 2 Diagram of a glomerular structure.

This figure shows the Bowman's capsule, glomerular basement membrane endothelial cells, mesangial cells, proximal tubular epithelial cells, perital epithelial cells and epithelial podocytes. This diagram was adapted and republished from 'Kurts, C., Panzer, U. Anders, H. J. and Rees, A. J. (2013) The immune system and kidney disease: Basic concepts and clinical implications. Nature Reviews Immunology, 13, 738-753.' by permission of Macmillan Publishers Ltd, granted by Nature Publishing Group.

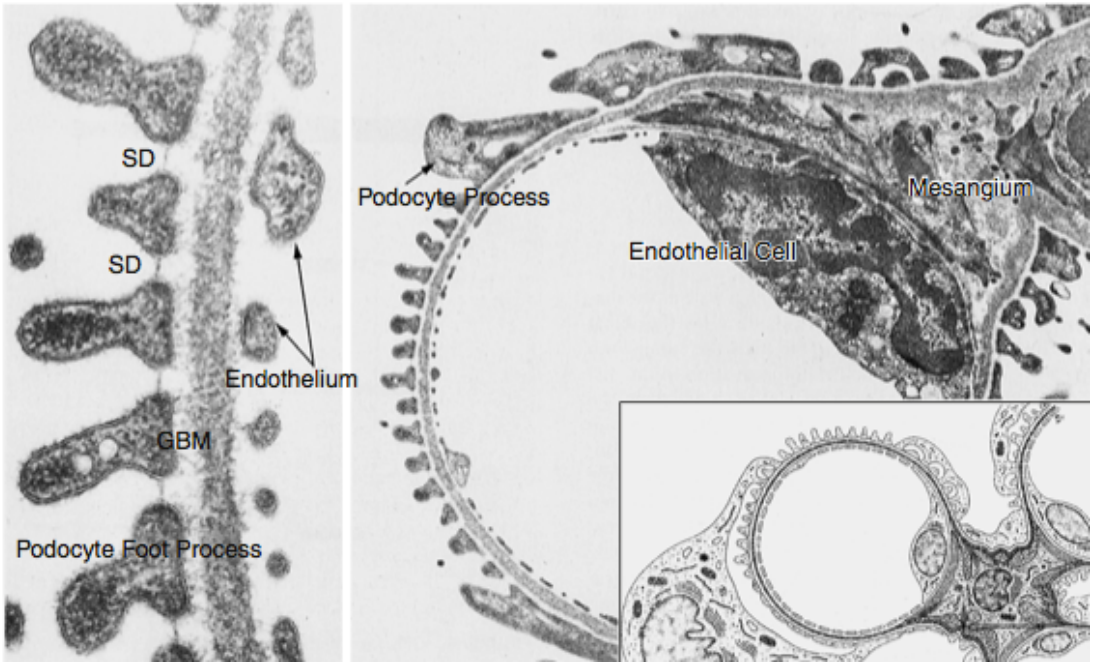


Figure 1. 3 Image of a glomerular loop and the filtration barrier.

This image shows the structure of a glomerular filtration barrier composed of endothelial cells, glomerular basement membrane (GBM) and the slit diaphragms (SD) between podocyte foot processes. This image was republished from 'Briggs, J. P., Kriz, W. and Schnermann, J. B. (2014) Chapter 1 - Overview of kidney function and structure. In: Gilbert, S. and Weiner, D. E. (Eds.) National kidney foundation primer on kidney diseases, 6th edition, 6. Philadelphia: Saunders Elsevier and Lancet.' by permission of Elsevier.

1.2.2 Tubular function

After glomerular filtration, the primary urine passes into the proximal tubules which undergo the reabsorption and secretion process to further adjust the volume, composition, concentration, osmolality and pH of the filtrate by exchanging the substances across the tubular lumen, tubular cells and blood (Briggs et al., 2014). The majority of solutes are reabsorbed by the proximal tubules. These include all nutrients (e.g. glucose, amino acids and lactate) and 90% of the filtered HCO_3^-. Approximately 67% water and 60% filtered ions including Na^+, Cl^-, K^+, Ca^{2+} and

phosphate are also reabsorbed (Briggs et al., 2014). Reabsorption relies on transport proteins (sodium dependent co-transporters) and diffusion. An example is the Na^+/H^+ antiporter on the apical membrane, it transports Na^+ into intracellular space and excretes H^+. Other substances including glucose, amino acids, lactate, Cl^-, Ca^{2+} and phosphate are also transported with Na^+ into cells through synporters (Koeppen and Stanton, 2013; Blaine, Chonchol and Levi, 2015). Sodium potassium adenosine triphosphatase (Na^+/K^+ ATPase) on the basolateral membrane actively transports Na^+ out of the cell in exchange for K^+. This creates an elevated concentration of extracellular Na^+ which permits the sodium linked co-transport of solutes (nutrients and ions) from the luminal filtrate to the tubular cell, and solutes are transported into the blood through their individual transporters on the basolateral membrane (Koeppen and Stanton, 2013). The diffusion of Cl^- into the blood through K^+/Cl^- symporters and through Cl^- channels also leads to K^+ reabsorption (Koeppen and Stanton, 2013). Moreover, some substances such as Ca^{2+} and NaCl can be reabsorbed through passive diffusion across tight junctions (a paracellular route), facilitating their reabsorption (Koeppen and Stanton, 2013; Blaine, Chonchol and Levi, 2015).

After the reabsorption of all these solutes, it spontaneously creates an osmotic gradient that drives water reabsorption (Koeppen and Stanton, 2013). Approximately 67% water is reabsorbed due to this osmosis, and many aquaporin water channels on the apical and basolateral membranes and the water permeable tight junctions in the proximal tubular cells also facilitate water reabsorption (Koeppen and Stanton, 2013). As most solutes are reabsorbed here, proximal tubular cells are characterised by brush borders which increase the surface area to facilitate the reabsorption (Briggs et al., 2014). Additionally proximal tubular cells have large mitochondria which can constantly supply energy for Na^+/K^+ ATPase to support their function (Briggs et al.,

2014). In addition to reabsorption, the proximal tubules excrete excess K^+, H^+, uric acid and ammonium ions, drugs and toxins (Briggs et al., 2014). This corrects the concentration of solutes and acid-base balance of plasma fluids and removes harmful substances (Briggs et al., 2014).

Proximal tubules also reabsorbs 50% urea by solvent drag created by water reabsorption, with 50% urea secreted into the tubular lumen (Koeppen and Stanton, 2013). The luminal urea contributing to the osmolar urea gradient between tubular lumen and medulla is essential for concentrating urine (Weiner, Mitch and Sands, 2015). When the fluid passes through the loop of Henle water is continuously reabsorbed in the descending limb, and such a water loss increases luminal urea concentration, causing the fluid to be concentrated (Weiner, Mitch and Sands, 2015) (Figure 1.4). The thin ascending limb is impermeable to water and relatively more permeable to NaCl, and the reabsorption of NaCl causes the filtered fluid to be diluted as water still remains in the tubule (Imai and Kokko, 1974). When the fluid proceeds to the thick ascending limb and the distal tubule, it becomes much more diluted due to reabsorption of Na^+, Cl^- and urea but not water, and meanwhile the tubule excretes K^+ and H^+ (Sands and Layton, 2009). When the fluid reaches the collecting duct, water is reabsorbed through diffusion (Koeppen and Stanton, 2013) (Figure 1.4). At this point, urea comprises the principle osmotically active solute. At the end of the collecting duct cells are permeable to urea, high concentration of urea in the filtrate creates a gradient force to drive urea reabsorption back to interstitium in the medullary region, maximising water reabsorption and subsequently concentrating the urine (Sands and Layton, 2009; Koeppen and Stanton, 2013).

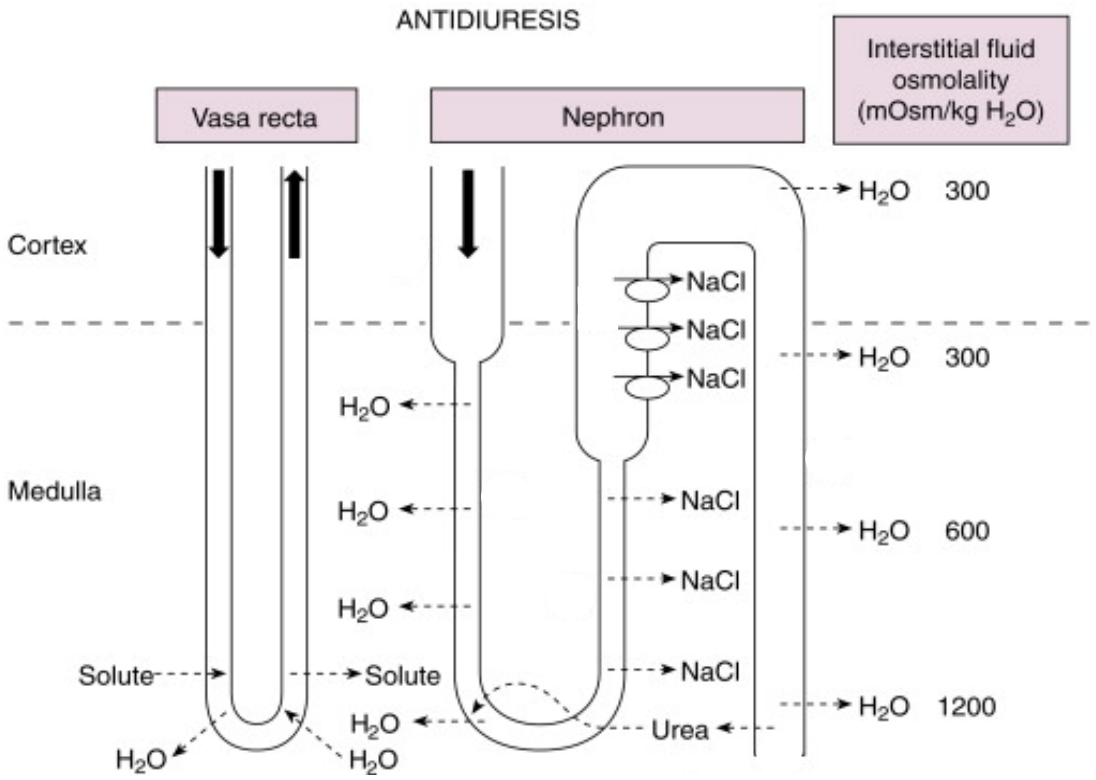


Figure 1. 4 A schematic diagram of nephron segments involved in urine concentrating mechanisms.

This diagram shows the mechanisms for excretion of concentrated urine. When the filtrate passes through the collecting duct water is continuously reabsorbed, with the presence of urea the fluid becomes more concentrated. At the end of the collecting duct, high urea concentration in the filtrate creates a gradient force to drive urea reabsorption to the medullary interstitium. This further drives water reabsorption and concentrates the urine. This diagram was republished from 'Koeppen, B. M. and Stanton, B. A. (2013) Regulation of body fluid osmolality: Regulation of water balance. In: Renal physiology, fifth edition, 85. Philadelphia: Saunders Elsevier and Lancet.' by permission of Elsevier.

1.3 AKI

1.3.1 Definition

AKI is defined as an abrupt and continuous decrease in kidney function leading to the accumulation of waste products including creatinine, plasma urea and uric acid

(Guarnieri, Situlin and Toigo, 2005). It can widely range from less severe kidney dysfunction to severe kidney impairment which requires RRT. Currently the severity of AKI is determined by RIFLE (risk, injury, failure, loss of renal function, end-stage renal disease) criteria established by the Acute Dialysis Quality Initiative group (Lameire, Van Biesen and Vanholder, 2005). This widely used system classifies the severity into three levels including 'risk', 'injury' and 'failure' based on the increased amount of serum creatinine (SCr) and the change in urine output at specific time duration, and it defines the clinical consequences including 'loss of renal function' and 'end-stage renal disease' depending on the duration of kidney dysfunction (Singbartl and Kellum, 2012) (Figure 1.5). Following RIFLE, Acute Kidney Network (AKIN) subsequently established broader and more sensitive criteria for diagnosis of AKI. AKIN includes the 0.3 mg/dl increase in SCr in the stage 1 and categorises patients with RRT as 'failure' regardless of SCr levels or urine output (Mehta et al., 2007; Case et al., 2013) (Figure 1.5). The increase in the sensitivity of criteria was due to the observation of a positive correlation between a subtle change of SCr and an increased mortality in a study by Chertow and coworkers in 2005 (Case et al., 2013). Although RIFLE criteria appears to be more commonly used in most clinical data, both guidelines have standardised the level of AKI and facilitated the diagnosis of AKI (Case et al., 2013).

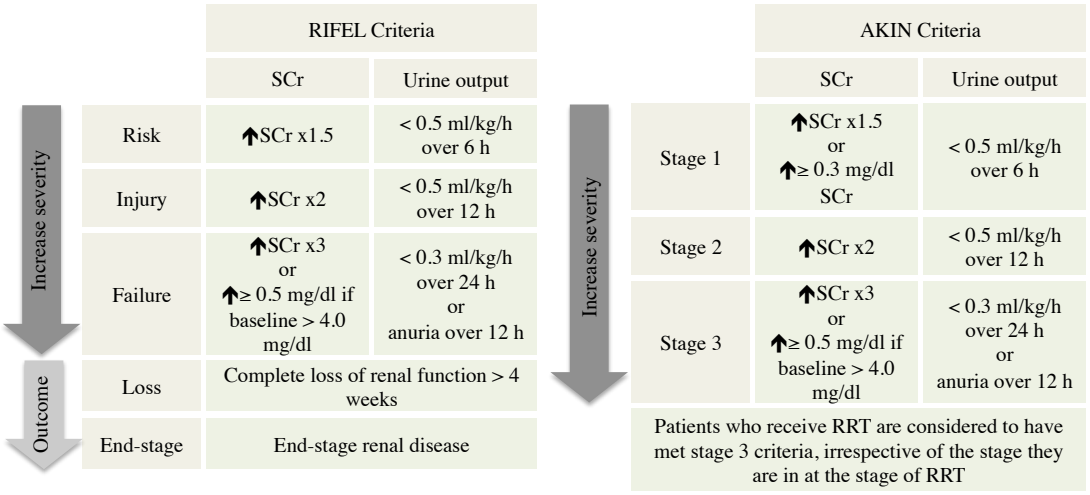


Figure 1. 5 Categories of AKI by RIFLE and AKIN criteria.

Compared with RIFLE, AKIN includes a slight increase in SCr (0.3 mg/dl) in the stage one and classifies the patients with RRT as 'failure'. This table was adapted and republished from 'Singbartl, K. and Kellum, J. A. (2012) AKI in the ICU: Definition, epidemiology, risk stratification, and outcomes. Kidney International, 81, 819-825.' by permission of Elsevier.

1.3.2 Classification and causes of AKI

Clinically AKI can be divided into pre-renal, post-renal and intrinsic AKI (Holley, 2005). Pre-renal AKI results from the reduced renal perfusion, for instance, the decreased blood volume caused by haemorrhage, congestive heart failure or arterial occlusion (Lameire, Van Biesen and Vanholder, 2005). It leads to the increase in SCr and plasma urea levels and the reduction in glomerular filtration rate (GFR), but it is also reversible (Lameire, Van Biesen and Vanholder, 2005). Post-renal AKI generally results from the obstruction of urinary system and kidneys (e.g. obstruction of the collecting ducts or kidney stones) caused by pre-renal or intrinsic AKI, and it can be completely recovered by promptly relieving the obstruction (Lameire, Van Biesen and Vanholder, 2005). The intrinsic AKI mainly refers to structural damage of nephrons including glomeruli, tubules, vessels and interstitium, and tubular injury

or acute tubular necrosis (ATN) is the most common case (Devarajan, 2006; Rennke and Denker, 2014).

ATN mostly refers to AKI or vice versa as it contributes to over 90% cases of AKI, and it mainly occurs in hospitalised and critically ill patients (Bonventre and Yang, 2011). While it is termed as ATN, necrotic cell death is more commonly observed in experimental models of AKI as animal models of AKI are developed with intense insults such as high doses of nephrotoxins or a prolonged ischaemia to achieve reproducible experimental acute renal failure (Rosen and Stillman, 2008). In human biopsies a single tubular epithelial cell necrosis may be observed in some cases, but ATN is not frequently seen (Rosen and Stillman, 2008). Most cases display some degree of a loss of brush borders in proximal tubule cells and tubule swelling due to the defect of water reabsorption, while the tubular dilation and interstitial oedema/inflammation with some regenerative areas are more commonly observed in patients at the early stage of AKI (Solez, Morel-Maroger and Sraer, 1979). Tubular necrosis is more restricted to medullary areas or occurs more commonly in the sustained period of AKI (e.g. over 28 days) (Solez, Morel-Maroger and Sraer, 1979; Davarajan, 2006).

In the severe cases such as a prolonged injury or AKI with underlying comorbidities, the tubular cell damage and death by apoptosis or necrosis are commonly observed (Bonventre and Yang, 2011). Whether injured cells undergo apoptosis or necrosis depends on the severity of insults (Daghar, 2004). The major events in establishing necrosis are the prolonged ischaemic or toxic insults where severe adenosine 5'-triphosphate (ATP) depletion occurs and the induction of inflammation cascades, whereas apoptosis requires ATP and triggers minimal inflammatory responses

(Kaushal, Basnakiana and Shah, 2004). In the AKI setting, both forms of cell death can occur (Basile, Anderson and Sutton, 2012). The overlap between apoptotic and necrotic cell death has been suggested to involve the pathophysiological process of AKI and is termed as necropotosis (Basile, Anderson and Sutton, 2012). If the ATP level is still maintained after injury, apoptosis accurs, despite that necrosis may occur in the susceptible outer medullary regions. During apoptosis, if the injury causes ATP depletion, necrosis ensues (Basile, Anderson and Sutton, 2012). With severe injury both non-viable and viable tubular cells are desquamated into the tubular lumens, which is evidenced by the appearance of tubular cells in the urine (Bonventre and Zuk, 2004). These detached cells and cell debris with the proteins (e.g. fibronectin) in the tubular lumen form casts which lead to tubule obstruction and reduce GFR (Bohle et al., 1990; Bonventre and Zuk, 2004). The increase in the tubular pressure caused by obstruction can further lead to filtrate backleak into interstitium and cause interstitial inflammation (Lameire, Van Biesen and Vanholder, 2005).

Although ATN can be resolved by RRT, the mortality rate still remains over 50% in most cases due to underlying diseases and comorbidities (Esson and Schrier, 2002; Metcalfe et al., 2002). Several factors including previous episode of kidney disease, hypotension, vascular disease, organ failure (e.g. heart or liver), diabetes, ageing, post-surgery (particularly cardiac surgery) and medications (e.g. vessopressors, antibiotics or non-steroidal anti-inflammatory drugs) have been identified to increase risk of developing ATN and contribute to long-term mortality (Nash, Hafeez and Hou, 2002; Lameire, Van Biesen and Vanholder, 2005; Case et al., 2013; Farooqi and Dickhout, 2016). Three major causes of ATN are sepsis, nephrotoxic injury and

ischaemia/reperfusion (I/R) injury, with the latter two being the most common insults (Bonventre and Yang, 2011).

1.4 Mechanism and pathophysiology of I/R injury

I/R injury is the most common cause of AKI. Ischaemia is a temporary disruption of renal blood through kidneys, leading to a decrease in oxygen and nutrient supply and a build up of waste products (Schrier et al., 2004). It frequently occurs after surgery (e.g. open heart surgery and organ transplantation) and in patients with vascular-associated diseases (e.g. heart failure) due to anaesthesia or a loss of fluid leading to intravascular volume depletion which causes the decreased renal blood flow and GFR (Humes, 1995; Sharfuddin and Molitoris, 2011). The persistent reduction of renal blood flow causes severe damage particularly in the corticomedullary region. Under normal physiological condition, the corticomedullary junction only receives ~10% of total renal blood flow, which is sufficient for its high consumption of oxygen for tubules undergoing solute exchange (Janssen et al., 1995). After ischaemia, this region was found to have a severe reduction of blood flow, and hence this further reduced oxygen supply, exacerbating hypoxic damage (Janssen et al., 1995). Even if the blood flow was restored after ischaemia, this region still displayed a profound reduction of blood flow and persistent cell injury (Karlberg et al., 1983). In contrast, at the same stage the blood flow in the outer cortex recovered back to normal, with tubular cells undergoing repairing process (Karlberg et al., 1983). Furthermore, the most sensitive region of the nephron to ischaemic injury is the S3 segment of the proximal tubule and the medullary thick ascending limb of loop of Henle due to their physiological location in relatively low oxygen regions (Brezis and Rosen, 1995). In particular, the S3 segment of the proximal tubule is most

susceptible to ischaemia (Wilson and Schrier, 1986). Cells in this areas are highly metabolically active and have a high demand for ATP; however, they have low capacity of undergoing glycolysis to produce energy under anaerobic conditions (Sabbahy and Vaidya, 2010). Hence, the S3 segment of the proximal tubule located in the cortical or medullary areas is vulnerable to ischaemia (Bonventre and Zuk, 2004). Additionally, this region is susceptible to direct nephrotoxicity as most toxins are reabsorbed and concentrated here (Sabbahy and Vaidya, 2010).

ATP depletion caused by ischaemia can result in morphological alterations including a loss of brush borders and cell polarity, alteration in cytoskeletal structure and adherent and tight junctions in the renal tubular cells (Schrier et al., 2004; Rennke and Denker, 2014). This leads to a loss of cellular functions including reabsorption of water and sodium and causes viable and dead cells shedding and accumulating in the tubular lumen to form casts which obstruct the tubular lumen and subsequently lead to a decrease in GFR (Schrier et al., 2004; Rennke and Denker, 2014). These structural and functional changes are reversible, and kidney function can be preserved if the sublethal injury is mitigated (Devarajan, 2006; Sharfuddin and Molitoris, 2008). However, severe and prolonged ischaemic insults leading to a severe ATP depletion can limit recovery capacity and cause subsequent lethal damage to tubular epithelial cells (Bush, Keller and Nigam, 2000; Lameire and Vanholder, 2004).

Reperfusion, that is, the return of renal blood flow, is normally considered to help kidney recover from ischaemic insults by restoring energy, oxygen and nutrient supply and removing metabolic wastes (Chatterjee, 2007). Yet, it leads to adverse

effects due to a burst generation of reactive oxygen species (ROS) and reactive nitrogen species (Chamoun et al., 2000; Yazihan and Kavas, 2010).

The increase in oxidative stress by ROS generation has been implicated to play a key role in I/R injury, and this was evidenced by the observation of a decrease in antioxidant enzyme activity during reperfusion. Dobashi et al. (2000) reported that the level and activity of several antioxidant enzymes including catalase, glutathione peroxidase and superoxide dismutases significantly decreased in kidneys subjected to 60 or 90 minutes of ischaemia following 2 or 24 hours reperfusion. The authors pointed out that without reperfusion these enzyme activities were not affected. Also, a longer duration of reperfusion after ischaemia led to a further reduction of the enzyme activity and increased the enzyme mRNA turnover rate. Cruthirds et al. (2003) also showed that manganese superoxide dismutase was rapidly inactivated in the rodents subjected to 16 hours of reperfusion following 30 minutes ischaemia.

It was proposed that ROS generation during reperfusion was caused by the accumulation of hypoxanthine and hypoxanthine oxidoreductase (XOR) activity in the kidney (Weight and Nicholson, 1996). During reperfusion, the accumulation of hypoxanthine, a metabolite from ATP breakdown during ischaemia, is converted to xanthine by xanthine oxidoreductase (XOR) and spontaneously generates hydrogen peroxide (H_2O_2) and superoxide (Weight and Nicholson, 1996). This was demonstrated by Rhoden et al. (2000) that pretreatment of allopurinol (xanthine oxidase inhibitor) significantly decreased oxidant activity and ameliorated renal damage in rat model of I/R injury. However, some conflicting results were also reported. Zager et al. (1994) showed that pretreatment with antioxidant agents including XO inhibitor (oxypurinol) and ROS scavenger (sodium benzoate) before

ischaemia did not protect against renal cell death and improve renal function in rats subjected to I/R injury. Doctor and Mandel (1991) also reported that XO was not involved in anoxia or hypoxia/reoxygenation in proximal tubular cells as XO inhibitor did not protect from cell death. Recently, Wijermars et al. (2017) suggested that XO participating in human renal I/R injury was unlikely. The authors found that XO activity in human kidney was low and that there was no release of the oxidative stress markers such as renal malondialdehyde, isoprostane and allantoin during reperfusion in patients with transplantation induced I/R injury, despite a great accumulation of hypoxanthine during ischaemia.

While ROS generation by XO is controversial, there are other sources of ROS. The mitochondrial electron respiratory chain is a potential source of ROS and has been suggested to contribute to I/R injury in many organs. Recently, the mechanism was revealed by Chouchani et al. (2014). This group found that during ischaemia the metabolite, citric acid cycle intermediate succinate, accumulated in a variety of tissues including kidney. Accumulation of succinate was due to that fumarate overflow, caused by purine nucleotide breakdown, drove complex II to run in a reverse mode to reduce fumarate into succinate (Figure 1.6). Upon reperfusion, with oxygen restoration the mitochondria complex II rapidly oxidised succinate (Figure 1.6). However, there was an insufficient ATP generation upon reperfusion. This limited electron flow through ATP synthase, causing a reverse electron flow which led to a burst ROS generation at complex I and initiated I/R injury (Figure 1.6). The authors also showed that controlling succinate accumulation during ischaemia and its oxidation upon reperfusion limited mitochondria ROS production.

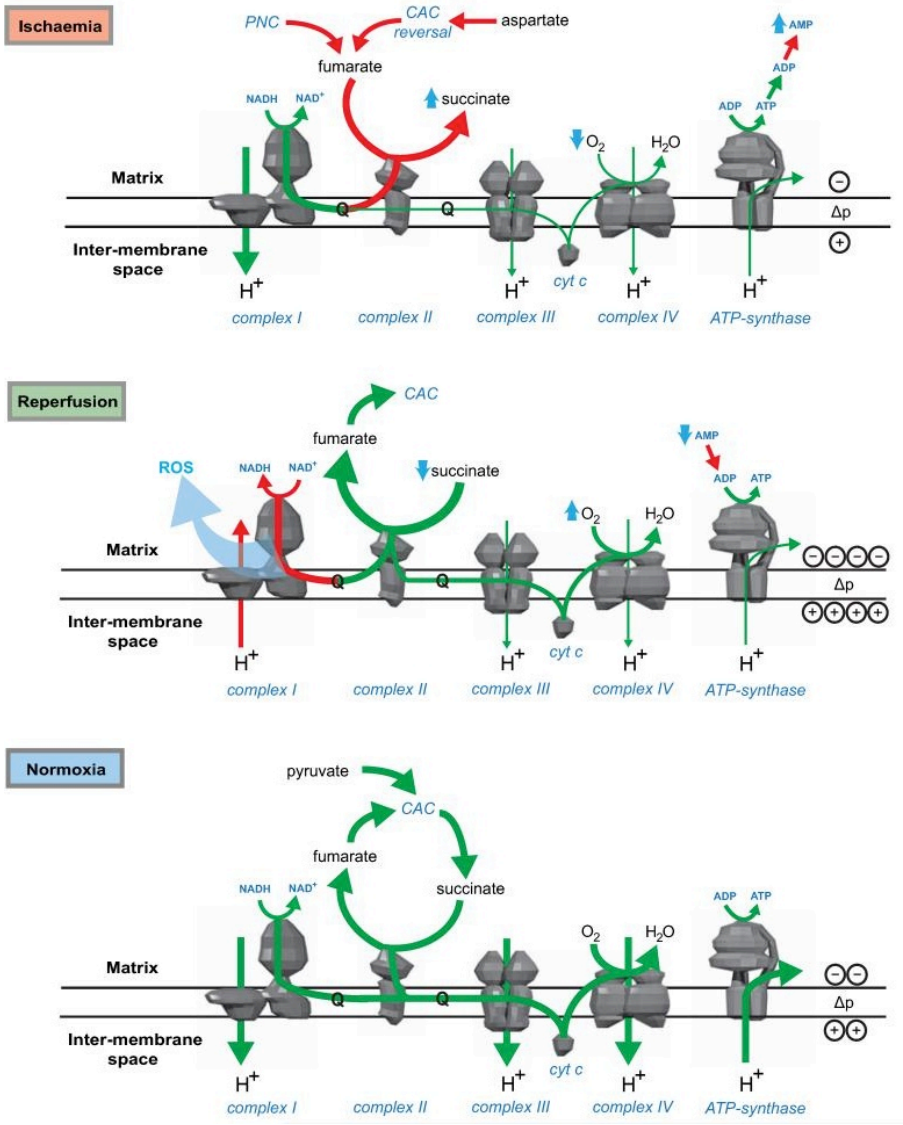


Figure 1. 6 Diagram shows the mitochondrial ROS generation in I/R injury.

During ischaemia, fumarate overflow due to purine nucleotide breakdown drives complex II to run in a reverse mode to reduce fumarate into succinate, leading to accumulation of succinate. Upon reperfusion oxygen restores, mitochondria complex II rapidly oxidises succinate. However, insufficient ATP generation upon reperfusion limits electron flow through ATP synthase. This results in a reverse electron flow which leads to a burst ROS generation at complex I and initiates I/R injury. Republished from 'Chouchani, E. T., Pell, V. R., Gaude, E., Aksentijević, D., Sundier, S. Y., Robb, E. L., Logan, A., Nadtochiy, S. M., Ord, E. N. J., Smith, A. C., Eyassu, F., Shirley, R., Hu, C. H., Dare, A. J., James, A. M., Rogatti, S., Hartley, R. C., Eaton, S., Costa, A. S. H., Brookes, P. S., Davidson, S. M., Duchen, M. R., Saeb-Parsy, K., Shattock, M. J., Robinson, A. J., Work, L. M., Frezza, C., Krieg, T. and Murphy, M. P. (2014) Ischaemic accumulation of succinate controls reperfusion injury through mitochondrial ROS. Nature, 515(7527), 431-435.' by permission of Macmillan Publishers Ltd, granted by Nature Publishing Group.

With the presence of ferric irons (Fe^{2+}), the Fenton reaction is driven to convert ROS including H_2O_2 and superoxides into reactive hydroxyl radicals which induce a series of oxidative stress in tissues (Sharfuddin and Molitoris, 2008). The increase in oxidative stress contributes to the cellular damage and death after I/R injury through several mechanisms including lipid membrane peroxidation, protein oxidation and DNA damage (Sharfuddin and Molitoris, 2008). Noiri et al. (2001) found that oxidative stress caused by I/R injury in rats led to the increased epithelial cell permeability by lipid peroxidation and DNA damage, a loss of cell-matrix adhesion and integrity and kidney dysfunction. Pretreatment of antioxidant agents was found to reverse the outcomes. Erdogan et al. (2006) also showed a great increase in lipid peroxidation and protein oxidation, evidenced by the observation of the increased thiobarbituric acid-reactive substances levels and protein carbonyl contents in rat kidneys subjected to I/R injury. The authors found that antioxidant agents ameliorated lipid peroxidation and protein oxidation and reduced renal damage such as tubular dilation and epithelial cell necrosis. Kadkhodaee et al. (1998) also showed that oxidative stress caused by oxygen derived free radicals resulted in DNA fragmentation which caused tubular damage (e.g. tubular cast formation and epithelial cell blebbing and death) in the isolated rat kidneys subjected to I/R injury. Pretreatment with antioxidant agents prevented DNA and structural damage and cell death.

In addition to the direct tubular cell death, ROS can also directly or indirectly influence haemodynamics and induce inflammation (Basile, Anderson and Sutton, 2012). For instance, ROS recruits leukocytes adhesion to the endothelial cells. Leukocytes were proposed to generate vasoconstriction mediators such as ROS and impair capillary flow to exacerbate hypoxia, further compromising kidney function

(Basile, Anderson and Sutton, 2012). Alongside, ROS-activated inflammatory cytokines such as tumour necrosis factor-alpha and interleukin-1 were found to disrupt actin cytoskeleton, cell-matrix adhesions and junction proteins in renal proximal tubular epithelial cells (RPTECs) (Bonventre and Zuk, 2004). This eventually results in epithelial cells exfoliating into the tubular lumens (Bonventre and Zuk, 2004).

1.5 Nephrotoxicity

Nephrotoxicity induced by pharmacological agents, particularly numerous commonly used clinical drugs, is the second common cause of AKI (Sharfuddin and Molitoris, 2008). High risk populations include the elderly over 60 years old and patients on medication and with underlying diseases including previous kidney disease, underlying renal insufficiency, heart failure or diabetes or those continuously exposed to many nephrotoxins (Liu and Chertow, 2008). The mechanisms of kidney impairment induced by several clinical drugs have been recognised, including alterations in glomerular haemodynamics, tubular cell toxicity and acute/chronic interstitial fibrosis (Naughton, 2008).

The glomerular filtration rate is regulated by the afferent and efferent arterioles. The vasodilation of afferent arteriole by circulating vasodilators (e.g. prostaglandins and nitric oxide) predominantly contributes to the volume of blood flow through the kidney (Naughton, 2008). Meanwhile, the efferent arteriole plays a key role in modulating intraglomerular pressure through vasoconstriction regulated by angiotensin-II, as its constriction creates pressure upstream and hence increases GFR (Ren, Garvin and Carretero, 2001). Therefore, drugs including anti-prostaglandin agents such as non-steroidal anti-inflammatory drugs (NSAIDs) and cardiovascular

agents such as anti-angiotensin-II (e.g. angiotensin converting enzyme inhibitors) and the vasoconstriction agents (e.g. cyclosporine) can profoundly affect the glomerular pressure and decrease GFR (Palmer, 2002). Tubular cell toxicity can be induced readily by numerous clinical and prescribed medications as renal tubules function to reabsorb and concentrate the filtrate from glomeruli, and the high level of circulating toxins causes renal tubules to be more vulnerable to nephrotoxicity (Leblanc et al., 2005; Schetz et al., 2005; Liu and Chertow, 2008). Common agents including antimicrobials (e.g. aminoglycosides such as gentamycin), anti-cancer drugs (e.g. cisplatin) and radiocontrast dye contribute a vast majority of nephrotoxicity in hospitalised patients, and the direct tubular cell injury involves many diverse mechanisms (Markowitz and Perazella, 2005; Chirino and Pedraza-Chaverri, 2009).

For instance, after biotransformation through enzyme systems such as cytochrome P450 in the microsomes, many drugs such as cisplatin form reactive oxygen metabolites (Liu and Baliga, 2003). The metabolites can degrade cytochrome P450 hemeprotein and promote the release of iron ion which leads to a potent ROS generation through the Fenton reaction (Liu and Baliga, 2003). The increase in oxidative stress that overwhelms local antioxidant capacity leads to tubular injury through protein oxidation, lipid peroxidation and DNA strand break, eventually causing cell death (Liu and Baliga, 2003; Perazella, 2009). Accumulation of these drugs and their metabolites within cells can cause phospholipid damage, organelle dysfunction and the formation of ROS with an increase in oxidative stress (Perazella, 2009). Promotion of phospholipid damage results in membrane rupture in the cellular membranes and organelles. The disruption of cellular membranes causes the increase in the cellular permeability, leading to cell swelling and lysis (Perazella, 2009). The

membrane rupture in organelles, such as lysosomes, leads to protease release into cytosols and induces cell lysis or triggers apoptosis/necrosis (Schnellmann and Williams, 1998; Chwieralski, Welte and Bühling, 2006). Mitochondrial injury is another common event in drug induced nephrotoxicity, evidenced by the observation of several structural abnormalities such as enlarged mitochondria, clumped cristae and a reduced number of mitochondria in the proximal tubule cells (Herlitz et al., 2010). Mitochondrial damage further leads to overproduction of ROS which is a key contributor to tubular cell injury and death. ROS can result in permeability transition pore opening that stimulates cytochrome c release to induce apoptotic cascades; DNA damage leading to cell cycle arrest; lipid peroxidation causing cellular membrane disruption; stress on other organelles such as endoplasmic reticulum; and oxidative inhibition of Na^+/K^+ ATPase leading to cell swelling, loss of membrane integrity and necrosis (Kruidering et al., 1997; Hickey et al., 2001; Liu and Baliga, 2005; Price, 2006; Morales et al., 2010; Quiros et al., 2011).

Furthermore, an acute or chronic interstitial fibrosis is commonly caused by drugs that induce inflammation in glomerular cells, renal tubular cells and interstitial regions where uncontrolled scarring/repairing process and immune reaction occur (Naughton, 2008). The drugs identified to induce acute kidney fibrosis include antibiotic, diuretics, NSAIDs, cyclosporine and herbal remedies containing aristolochic acid. Long term and high dose exposure can lead to chronic fibrosis, progressing to irreversible chronic kidney disease (CKD) and end-stage renal disease (ESRD) (Markowitz and Perazella, 2005; Debelle, Vanherweghem and Nortier, 2008). Additionally, the therapy with a combination of these drugs can induce synergistic nephrotoxic effect, and the increase in exposure time and dosage can result in kidney impairment (Coffman, 2005; Schetz et al., 2005). However, tubular

cell toxicity can be alleviated by discontinuing, reducing the dose or limiting the duration, whereas it can progress to irreversible CKD if the exposure is continued (Coffman, 2005).

1.5.1 ArisA-induced nephrotoxicity

Aristolochic acid (ArisA) refers to the extracts from several traditional Chinese herbs from *Aristolochiaceae* family of plants (IARC, 2002). These Chinese traditional herbal remedies were used as anti-inflammatory agents, anti-septic agents and diuretics for the treatment of oedema or weight-loss (IARC, 2002; Debelle, Vanherweghem and Nortier, 2008). However, in the early 1990s it has been reported to cause AKI, tubular atrophy and progressive renal tubulointerstitial fibrosis in those who ingested ArisA containing pills for the weight-loss purposes and had no history of kidney disease (Debelle, Vanherweghem and Nortier, 2008).

The nephrotoxicity and genotoxicity of ArisA appear after metabolism throughout the body. Its activation is involved in the nitrogroup reduction by the cytosolic and microsomal enzymes (e.g. hepatic cytochrome P450 (CYP) 1A2 and renal microsomal NADPH:CYP reductase) which predominantly exist in livers and kidneys (Stiborová et al., 2008), and ArisA is converted into N-acylnitrenium ion which forms DNA adducts with purine bases (Grollman et al., 2007). Several reports have evidenced the development of malignant tumor in liver, kidney, ureter and urinary bladder in animals injected with ArisA (Rossiello et al., 1993; Cosyns et al., 2001; Mei et al., 2006). In kidneys, ArisA mainly damages cortex, with RPTECs being the major target of aristolochic acid nephropathy (AAN) (Chang et al., 2001; Sato et al., 2004; Shibutani et al., 2007). Evidence has shown that ArisA induces DNA damage/adduct formation and leads to G2/M cell cycle arrest via ataxia

telangiectasia mutated serine/threonine kinase (ATM)-checkpoint kinase 2 (Chk2)-p53-p32 pathway. This has been demonstrated in human renal proximal tubule epithelial (HK-2) cells, porcine proximal tubular epithelial cells (LLC-PK1 cells) and IRPTC rat proximal cells (Li, Y. et al., 2006; Yang et al., 2010; Romanov et al., 2015). Li, Y. et al. (2006) showed that treatment with ArisA (80, 320 and 1280 ng/ml) for 24 hours induced DNA damage and G2/M cell cycle arrest in pre-starved LLC-PK1 cells in a dose dependent manner, despite no effects on cell viability. Yang et al. (2010) demonstrated that treatment with ArisA (5 μg/ml) for 48 hours greatly induced G2/M cell cycle arrest in HK-2 cells, LLC-PK1 cells and IRPTC rat proximal cell line. The authors also demonstrated that male BALB/c mice treated with one-time peritoneal injection of ArisA (5 mg/kg) induced a high number of cells arrested at G2/M phase from day 5 through day 42. They found that this cell cycle arrest was mainly observed in tubular cells. Romanov et al. (2015) also reported that treatment with lower minimal dose of ArisA (4 μM) for 48 hours caused cell cycle arrest in HK-2 cells. These cells arrested in G2/M phase were found to express the senescence associated secretory phenotype and contribute to the production and secretion of fibrotic factors and cytokines, eventually leading to development of fibrosis (Yang et al., 2010; Canaud and Bonventre, 2015). This was shown by Yang et al. (2010) that treatment with ArisA (5 μg/ml) for 48 hours led to upregulation of profibrogenic genes in HK-2, LLC-PK1 and IRPTC rat proximal cell line. The authors observed that after treated with ArisA HK-2 cells continuously cultured in fresh media were still arrested in the G2/M phase. Strikingly, they further found that the conditioned media in which ArisA treated HK-2 cells was cultured contained high levels of transforming growth factor-β1 and connective tissue growth factor and

could enhance pre-starved NIH 3T3 fibroblast cell proliferation and collagen production.

Recently it was identified that this cell cycle arrest was associated with an increase in oxidative stress in cell organelles, particularly in the endoplasmic reticulum (ER) and mitochondria in both *in-vitro* and *in-vivo* studies (Pozdzik et al., 2008; Yu et al., 2011; Zhu et al., 2012; Romanov et al., 2015). Pozdzik and colleagues (2008) reported that male Wistar rats receiving subcutaneous injection of ArisA (10 mg/kg) daily showed tubular cell regeneration greatly initiated at the acute phase during day 1-5. However, the proliferation and differentiation ability significantly declined, resulting in tubular atrophy, inflammation, fibrosis and apoptosis at the chronic phase on day 35. The authors suggested that such damage by ArisA was associated with the increased oxidative stress and mitochondrial injury, evidenced by the observation of the reduction in activities of antioxidant enzymes including antioxidant catalases, mitochondrial antioxidative enzyme and Cu/Zn superoxide dismutases and the cytochrome c release at the chronic phase. Romanov et al. (2015) reported that intracellular ROS production increased in HK-2 cells treated with ArisA (4 or 40 μM) for 4 hours in a dose and time dependent manner. Yu et al. (2011) determined that the increased ROS production induced by ArisA (25-200 μM) was associated with the depletion of glutathione contents which was detected 30 minutes after treatment in HK-2 cells. In contrast, pretreatment with glutathione or N-acetyl cysteine was found to suppress ROS generation and attenuate DNA damage and apoptosis. Zhu et al. (2012) also showed an increase in ER stress protein expression and cell apoptosis in HK-2 cells treated with ArisA (100 μM) for 24 hours. Conversely, pretreatment of antioxidants glutathione or N-acetyl cysteine could

suppress ER stress and ER stress related apoptosis, suggesting that ROS mediated ArisA-induced ER stress.

In addition to oxidative stress, De Broe (1999) found that ArisA caused endothelial wall thickening in the afferent arterioles, suggesting an ischaemic phenomenon in AAN. This may explain why proximal tubular cells, known to be highly metabolically active and high demanding in ATP, are more susceptible to ArisA tubulotoxicity (Brezis and Rosen, 1995). Collectively, AAN and I/R shared some identical features including proximal tubular cells as a main target, G2/M cell cycle arrest and oxidative stress.

1.6 Experimental models of AKI

In-vitro models including renal cell cultures, isolated renal tubules and isolated perfused kidneys are widely used for investigating pathophysiological mechanisms of ischemic AKI due to the independence of complexity of human body system. The most widely used approach to mimic renal I/R injury in the *in-vitro* model is the induction of ATP depletion by maintaining in the nutrient depleted media in hypoxic condition followed by resupply of complete media in normoxic condition (Sáenz-Morales et al., 2009; Jiang et al., 2010; Razvickas et al., 2013; Kurian et al., 2014) (Table 1.1). Another approach is the chemical induced ischaemia/ATP depletion by mitochondria respiration inhibitors (e.g. rotenone, antimycin and sodium azide) in hypoxia followed by replacement of complete media in normoxia (Brooks et al., 2009; Kurian et al., 2014) (Table 1.1). An alternative method to induce I/R injury is the provision of exogenous hydrogen peroxide to mimic oxidative stress after I/R (Yoshida et al., 2008) (Table 1.1). Among these methods, hypoxia/reoxygenation is widely used as it mimics clinical I/R injury where blood supply, that is, oxygen and

nutrient supply, is disrupted and restored. This can be achieved simply by incubating cells in nutrient depleted media in hypoxia followed by maintaining cells in complete media in normoxia. However, to entirely mimic the *in-vivo* condition a specialised automated chamber with a gas and fluid controller to control oxygen concentration and media would be ideal to achieve the hypoxia/reoxygenation condition. Moreover, drug induced AKI by clinically used drugs such as cyclosporine, gentamycin and cisplatin and nephrotoxic compounds such as ArisA, is also commonly carried out in cell models (Table 1.1). The cell models generally display a consistent dose and duration dependent responses. However, triggering sublethal injury by these drugs in cells, particularly the transformed cells, normally requires higher dose and longer treatment time, which does not reflect the clinical condition.

All approaches have been carried out in a variety of cell lines, and some biological changes caused by sublethal injury are consistent with the *in-vivo* models. For instance, ischaemia/ATP depletion in *in-vitro* and *in-vivo* models and postischaemic patients led to disruption of actin cytoskeleton and loss of cell polarity, cellular junctions and monolayer integrity (Kellerman et al., 1990; Molitoris, 1993; Kroshian, Sheridan and Lieberthal, 1994; Alejandro et al., 1995). Cell model systems also showed that ROS production upon reperfusion/reoxygenation contributed to tubular cell injury, consistent with *in-vivo* models of I/R injury (Paller et al., 1991; Greene and Paller, 1994; Yonehana and Gemba, 1995).

Immortalised cell lines such as HK-2, LLC-PK1 and rat proximal epithelial cells are mostly used by the literature as transformed cells can be continuously cultured for over a year (Ryan et al., 1994). HK-2 cells, in particular, are widely adopted. While it is a transformed cell line, it still maintains several differentiated (e.g. alkaline

phosphatase and gamma glutamyltranspeptidase in the brush border) and functional (e.g. sodium dependent sugar transport and adenylate cyclase responsiveness to parathyroid) features of human proximal tubular cells (Ryan et al., 1994). However, some features are altered after transformation and may be a limitation for the study. For instance, HK-2 cells can undergo glycolysis which is not seen in human proximal tubular cells. Therefore, they can continue growing in serum starved media (Ryan et al., 1994).

In contrast, primary cell culture and isolated tubules have been suggested to be more relevant to *in-vivo* models as they retain renal physiology and fully differentiated features and functions (Lieberthal and Nigam, 2000). Additionally, primary culture is more sensitive to ATP depletion as observed in the *in-vivo* models; for instance, severe anoxia/hypoxia could induce necrosis within 30 minutes (Weinberg, 1985; Nurko et al., 1996). However, primary culture is tedious to harvest, with limited cell number from any isolate, higher risk of contamination during experimental procedure and a short lifespan (Racusen et al., 1996). Overall, the *in-vitro* model has its value for studying pathophysiological mechanisms of AKI owing to its independence of complex physiological interactions, but this also becomes a limitation due to being less clinically relevant. Hence, because of this imperfection the *in-vivo* models are normally adopted.

In-vivo models of AKI have been established for decades. Different approaches are taken to induce AKI in different animal models as many factors such as species, strains, age and gender can affect the severity of AKI. Induction of AKI in small animals such as mice and rats requires shorter ischaemic time (e.g. within 25 minutes) which can generate an overt necrosis (Wu et al., 2007). In contrast, AKI in

pigs requires up to 3 hours to induce a modest necrosis (Sabbagh et al., 2011). Additionally, smaller animals such as mice are preferred because a relatively smaller amount of experimental drugs are used to induce nephrotoxicity, compared with relatively larger animals such as rats (Basile, Anderson and Sutton, 2012). Inbred strain of animals may produce a consistent and reproducible response to insults due to the homogenous genetic background, despite its high susceptibility to insults (Festing, 2010). By contrast, outbred strain often generates variable results due to the heterogeneous phenotypes and is more resistant to experimental insults, but the diverse genetic backgrounds are closely relevant to human (Festing, 2010). Older animals are more susceptible to AKI insults compared with younger ones, even a age difference of over one week can lead to different results (Kusaka et al., 2012). Moreover, sex hormones have been known to determine the susceptibility to AKI. Males are generally more sensitive to AKI than females as testosterone was found to inhibit nitric oxide synthase activity and reduce nitric oxide production which is a vasodilator, hence enhancing susceptibility to I/R injury (Park et al., 2004). Because of the consistent and sensitive response to AKI insults, male animals are generally preferred as an experimental model of AKI.

To date, the widely used AKI model is the warm I/R injury, classified as the unilateral and bilateral I/R injury (Table 1.2). In particular, the bilateral I/R is more commonly used as it is closely relevant to human pathological condition where both kidneys are affected by the alteration of blood flow (Wei and Dong, 2012). However, to achieve the consistent results in I/R injury induction, it depends on several factors such as selection of animal models. More importantly, a successful induction of I/R injury requires a good surgery protocol and a well-trained skilful surgeon to perform

the operation, minimise surgical trauma and carry out postsurgery care (Wei and Dong, 2012).

In addition to I/R injury, other models of AKI are induced by several clinically used drugs and nephrotoxic compounds such as cyclosporine, gentamycin, cisplatin, folic acid and ArisA (Table 1.2). Drug induced nephrotoxicity can also generate ischaemic insults by interfering renal haemodynamics (Singh et al., 2012). It can also cause tubular injury through several mechanisms including ATP depletion, ROS generation and mitochondrial damage, similar to I/R injury (Singh et al., 2012). The consecutive administration of these clinically used drugs such as cyclosporine, gentamycin and cisplatin to induce renal dysfunction closely mimics the clinical setup where patients are also continuously on the medication (Suzuki et al., 1995; Li et al., 2004; Bing et al., 2006; Wei and Dong, 2012) (Table 1.2). Folic acid induced injury is a classic nephrotoxic AKI and a widely accepted model for studying pathogenesis of AKI (Gupta et al., 2012; Wen et al., 2012). Unlike other clinically used drugs, the induction of AKI requires one-time injection of high dose of folic acid, and renal dysfunction can be observed within 1-14 days (Yang, Zuo and Fogo, 2010; Gupta et al., 2012; Wen et al., 2012) (Table 1.2). Furthermore, aristolochic acid induced injury, termed as aristolochic acid nephropathy, is a commonly used compound for investigating AKI and tubulointerstitial fibrosis (Lim, Yang and Fogo, 2014). It has been shown that a single low dose could result in modest AKI at the early stage (within 1-5 days) and lead to interstitial fibrosis after 2-5 weeks (Pozdzik et al., 2008; Yang et al., 2010; Novitskaya et al., 2014; Declèves et al., 2016) (Table 1.2). While drug induced AKI may have less technical issues than I/R injury, the consecutive injection and high consumption of these drugs (except ArisA) are the disadvantages. Additionally, high dose of drugs is normally administered to animals

in order to rapidly produce renal dysfunction and damage. However, high dose of drugs and the overt damage such as necrosis at the early stage of AKI may not be clinically relevant as these drugs only cause structural alteration of apical membranes during uptake by proximal tubules (Mingeot-Leclercq and Tulkens, 1999).

Table 1. 1 Common *in-vitro* models of AKI.

In-vitro model	Dose/duration for induction of AKI	Factors for successful AKI
I/R injury	▪ Cells incubated in nutrient depleted media in anoxia (0% O_2) or hypoxia (1% O_2) for 30 minutes-48 hours followed by incubation in complete media in normoxia (21% O_2) for various duration depending on the experimental design and models (Sáenz-Morales et al., 2009; Jiang et al., 2010; Razvickas et al., 2013; Kurian and Pemaih, 2014). ▪ Chemical induced ATP depletion by mitochondria inhibitors such as rotenone, antimycin and sodium azide for 1-3 hours followed by replacemnt with complete media (Brooks et al., 2009; Kurian and Pemaih, 2014). ▪ Exogenous H_2O_2 at different concentration and duration (Yoshida et al., 2008).	▪ Models: transformed cell lines, primary cell lines and isolated tubules. ▪ Require a specialised chamber with a compact gas oxygen controller to maintain oxygen concentration for hypoxia and reoxygenation condition. ▪ Dose and duration dependence.
Nephrotoxicity	▪ Cyclosporine A: >10 μM for 24 hours induces cell death or low dose for 14 days induce cell cycle arrest (Bakker et al., 2002; Jennings et al., 2007; Puigmulé et al., 2009). ▪ Gentamycin: 10 mM for 3-15 days to induce cell death (Regec, Trifillis and Trump, 1986; El Mohammed et al., 2000; Choi et al., 2000). ▪ Cisplatin: 20 μM for 4 days or >25 μM for 24 hours (Cummings et al., 2002; Price et al., 2004; Kawai and Gemba, 2007). ▪ ArisA: lower minimal dose ~4 μM for 24-48 hours to induce cell cycle arrest without affecting cell viability (Yang et al., 2010). High dose 40-200 μM for 24-48 hours to induce cell death (Yu et al., 2011; Romanov et al., 2015).	▪ Models: transformed cell lines, primary cell lines and isolated tubules. ▪ Dose and duration dependence.

Table 1. 2 Common *in-vivo* models of AKI.

In-vivo model	Dose/duration for induction of AKI	Factors for successful AKI
I/R injury	▪ Unilateral or bilateral I/R. ▪ Clamping renal artery, vein or pedicle for 20-60 minutes depending on experimental design followed by reperfusion for 24 hours (Bagetti-Filho et al., 2012; Funk et al., 2012; Li et al., 2012). Male animals are preferred.	▪ Animal species, strains, age and sex. ▪ Technical issues such as operation time, surgeon skills and postsurgery care to maintain consistent AKI model.
Nephrotoxicity	▪ Cyclosporine: Administration of 7.5 or 15 mg/kg for 14 days (Bing et al., 2006). Female mice are preferred. ▪ Gentamycin: Administration of 10-80 mg/kg for 7 days or longer (Suzuki et al., 1995). Male rats are preferred. ▪ Cisplatin: A single dose ~30 mg/kg (Li et al., 2004; Wei et al., 2007). Male mice are preferred. ▪ Folic acid: A single dose 250 mg/kg to induce AKI at early stage (1-14 days) (Yang, Zuo and Fogo, 2010; Wen et al., 2012). Male mice are preferred. ▪ ArisA: A single dose ~5 mg/kg to induce AKI at early stage (3-10 days) (Yang et al., 2010; Novitskaya et al., 2014). Male mice are preferred.	▪ Animal species, strains, age and sex. ▪ Dose and time dependence.

1.7 Prevention and current treatment for AKI

Even if AKI is known to contribute to a high risk of progression to irreversible CKD and ESRD and significant morbidity and mortality, to date there is still no specific treatment for AKI. Currently RRT is the common and readily available clinical strategy, and it has been performed for patients with severe AKI or multiple organ failure in the past decades. While some cases showed full recovery, most patients

developed CKD and ESRD and had high mortality rate (Cerdá et al., 2015). A variety of complications such as hypotension, sepsis, anaemia and metabolic acidosis/alkalosis caused by over removal of fluid and solutes or volume overload, malnutrition and infection can delay kidney recovery, worsen pre-exisiting renal diseases and lead to other organ failure (e.g. cardio renal syndrome) (Hall and Fox, 2006; Cerdá et al., 2015). This strategy may be effective for the short-term, but the long-term complications and outcomes remain unresolved. Other approaches including management of hypotension by adjustment of circulating blood volume with vasodilators and discontinuation of nephrotoxic drugs are also recommended in Kidney Disease Improving Global Outcomes (KDIGO) guidelines (2012). In addition, nutritional support is often required as AKI normally occurs with critical illness which is a hypermetabolic/hypercatabolic state and an important contributor to the high morbidity and mortality in the hospitalised patients (Fiaccadori, Parenti and Maggiore, 2008; Bellomo, Kellum and Ronco, 2012).

Patients with AKI are normally at higher risk of protein-energy malnutrition as a result of skeletal muscle breakdown, impaired amino acid transport into muscle, suppressed protein synthesis, body energy and protein depletion and increased urea production (Btaiche et al., 2008). In particular, protein catabolism is further promoted by metabolic acidosis which is typically observed in patients with AKI (Btaiche et al., 2008). Together with protein degradation, serum amino acid profile is also altered due to the impaired kidney metabolic function. For example, the serum level of some amino acids such as phenylalanine, methionine and cysteine are increased, whilst others such as valine and leucine have an increased turnover rate in these patients (Btaiche et al., 2008). In addition, some non-essential amino acids such

as glutamine, arginine and tyrosine become indispensible or conditionally essential under metabolic stress (Druml et al., 1994; Btaiche et al., 2008).

As protein-energy malnutrition is inevitable in the critically ill patients in general and patients with AKI, exogenous supplementation of amino acids and nutritional support clinically aim to correct the protein catabolic state and net body loss for treatment of AKI (Druml, 2001). Accordingly, it was suggested by KDIGO guidelines (2012) that administration of 0.8-1.0 g/kg/d, 1.0-1.5 g/kg/d and up to 1.7 g/kg/d protein for non-catabolic patients with AKI, patients with AKI on RRT and patients with continuous RRT and hypercatabolism, respectively. In addition, the provision of 1.7 g amino acids/kg/d maximum was also recommended for patients with peritoneal dialysis or continuous RRT as these patients have additional amino acid losses varying individually. The clinically used standard parenteral and enteral amino acid formulation is a balanced mix of both non-essential and essential amino acids, since non-essential amino acids become indispensible in patients with AKI (Btaiche et al., 2008). The energy requirement is suggested range from 25 to 35 kcal/kg/d, which is set up to be equivalent to 100-130% resting energy expenditure (KDIGO guidelines, 2012). A higher energy intake is not recommended as it does not have positive effects on nitrogen and fluid balance; instead, it contributes to a higher incidence of hyperglycaemia (KDIGO guidelines, 2012). However, such nutrient requirement for patients with AKI is the same as that recommended for critically ill patients with functional kidneys (Fiaccadori, Parenti and Maggiore, 2008; Bellomo, Kellum and Ronco, 2012). The optimal nutrition composition and formulation, particularly amino acid and protein intake, specific for patients with AKI have not yet been clearly defined due to varying protein catabolic rate ranging from 1.4 to 1.8 g/kg/d in this clinical condition (Fiaccadori, Regolisti and Cabassi,

2010). Also, a wide variety of clinical situations including etiology, severity, previous nutritional status and underlying diseases also make it difficult to develop a specialised formulation (Guarnieri, Situlin and Toigo, 2005). This clinical standard amino acid composition may not correct the nitrogen balance and amino acid profile for all the patients with AKI, and hence it is suggested that at least 1.6-1.7 g amino acids/kg/d is required to ensure a less negative to positive nitrogen balance (Fiaccadori, Regolisti and Cabassi, 2010). Additionally, a higher amino acid intake (over 2.0 g/kg/d) has been further stated to ensure a positive nitrogen balance (Fiaccadori, Regolisti and Cabassi, 2010). The advantage of such a high amino acid intake was evaluated by several clinical studies, and it was shown that increasing amino acid intake was directly correlated to the increased plasma amino acid concentration and the positive nitrogen balance. A prospective cohort study by Bellemo et al. (1991) observed that parenterally receiving 1.25-1.87 g amino acids /kg/d with 1850 kcal/d of nonprotein calories achieved a positive nitrogen balance in nine critically ill patients with AKI requiring haemodialysis. Another prospective and non-randomised study by Macias et al. (1996) also observed that enterally or parenterally receiving 1.0 g amino acids/kg/d or more maintained a positive nitrogen balance in AKI patients requiring continuous venovenous haemofiltration. The authors suggested that a higher amino acid intake (over 1.5 or 2.0 g/kg/d) with 25-35 kcal/kg/d of nonprotein calories further improved the positive nitrogen balance. Scheinkestel et al. (2003) further identified that in most cases maintaining a positive nitrogen balance was more likely to be correlated to amino acid intake greater than 2.0 g/kg/d for 2 days in fifty critically ill patients with AKI and requiring haemodialysis. This was also suggested by Bellomo et al. (1997) and Bellemo et al. (2002) that approximately 2.0 g/kg/d of amino acid intake may be optimal to

improve nitrogen balance and that 2.5 g/kg/d of amino acids can provide a neutral to positive amino acid balance for critically ill patients with AKI and requiring haemodialysis or haemofiltration. These studies recommended that over 2.0 g/kg/d amino acid intake could be the optimal concentration to improve nitrogen balance and correct serum amino acids. However, these studies either did not evaluate or observe the significant relationship between amino acid intake and survival rate or patient outcomes despite an improved nitrogen balance.

Moreover, available evidence to suggest the advantages of increasing amino acid intake for critically ill patients with AKI and not requiring RRT or haemodialysis is limited and inconclusive, and most trials were small and based on a single-centre. For instance, Abel et al. (1973) reported that intravenous provision of 8-essential amino acids (12.6 g/24 hours) in hypertonic dextrose solution for at least 24 hours facilitated urea reutilisation and protein synthesis in AKI patients without requiring RRT (>60 years old; with underlying diseases). However, the trial was too small, with two deaths out of six patients. Another clinical trial by Mocan et al. (1995) also showed that receiving 13.4 g of intravenous essential amino acids with a 500 ml/g hypertonic glucose solution daily significantly reduced the daily increase in blood urea nitrogen, increased serum protein and albumin level, reduced complication and mortality rate and improved survival after 15 days of therapy in 30 patients with AKI. Singer (2007) reported that fourteen critically ill patients with AKI receiving 75g or 150 g amino acids with 2000 kcal/d of nonprotein calorie intake parenterally showed a significant improvement of nitrogen balance in the group with greater amino acid intake, despite no differences in creatinine clearance between two groups.

The recommendation of a greater amino acid or protein intake (at least >1.0 g/kg/d) for treatment of AKI is continuously suggested by clinical studies and guidelines, as the negative nitrogen balance is key contributor to the increased mortality and metabolic complications. However, the evidence and current clinical data are lacking to support such a recommendation as there was no association observed between maintaining positive nitrogen and serum amino acid balance through increasing amino acid or protein intake and survival/outcomes in patients with AKI. Rather, some negative results of a higher amino acid intake were reported. Bellemo et al. (2014) conducted a secondary analysis on five of the Randomized Evaluation of Normal versus Augmented Level (RENAL) studies, which are the largest randomised, prospective and multicentre studies of AKI treatment to date. The authors also reported that a higher daily protein intake (>1.0 g protein/kg/d) was not associated with the improved clinical outcomes in AKI patients without requiring continuous RRT during ICU stay. Additional assessment on the mortality rate in patients surviving through the first 96 hours showed that patients with a greater daily protein intake had a higher mortality rate (40% death in 415 patients) than those with a low daily protein intake (23.9% death in 515 patients). Another multicentre randomised clinical trial by Doig et al. (2015) recruiting 475 patients showed that daily intravenous infusion of 100 g/L L-amino acids which reached the maximum total daily protein intake (2.0 g/kg/d) for patients with AKI until discharge from ICU also did not reverse the outcomes and duration of renal dysfunction. In fact, it was indicated that AKI patients with hypercatabolism cannot be resolved simply by increasing amino acid intake, as there is a concern of greater amino acid intake exceeding muscle protein synthetic capacity that contributes to higher urea production (Btaiche et al., 2008; Cano et al., 2009).

Despite inconclusive evidence for supporting benefits of high amino acid intake for improvement of clinical outcomes of AKI, maintaining positive nutritional status is still the primary target for these patients in the clinical settings as pre-existing and in-hospital malnutrition is known as a key factor to increasing mortality rate in patients with AKI. In addition to preserving the protein-energy status, the acute increase in protein or amino acid infusion/intake (1-1.2 g/kg) was found to significantly increase GFR within 2 hours in both healthy individuals and patients with renal diseases (Sharma, Mucino and Ronco, 2014). The increase in GFR was due to the globally increased renal blood flow in response to the acute high amino acid infusion, and it has been found to improve the outcomes in animal models of I/R injury. Tolins and Raij (1991) reported that rats pre-fasted or fed with low protein chow for 20 hours followed by a diet containing 10% amino acids for a week or amino acid infusion through renal artery significantly increased renal vasodilation and GFR. The authors found that the increased renal vasodilation and GFR was positively correlated to the elevated endothelium-derived relaxing factor and nitric oxide synthesis in response to the presence of amino acids (particularly L-arginine) and amino acid metabolism. Roberts et al. (1997) also demonstrated that enteral administration of amino acids (peptide based formula) for 6 hours before glycerol-induced ischaemia improved the kidney function by increasing vasodilation and GFR and hence increased survival rate in rats. Evidence from a recent clinical trial by Doig et al. (2015) also showed that intravenously receiving a short-term high dose of amino acid supplementation or higher protein intake daily (2.0 g/kg/d) preserved GFR and diuresis despite no improved primary outcomes.

Moreover, the clinical effect of increasing an individual amino acid on AKI is unknown. The effects and the underlying mechanisms of single amino acids were

mainly investigated in the experimental models of AKI. Amino acids such as glycine, alanine, glutamine and arginine were shown to have renoprotective effects on I/R injury. Alanine and glycine were found to restore mitochondrial functions and inhibit mitochondria-mediated cell death in the renal proximal tubular cell models of hypoxia and hypoxia/reoxygenation (Garza-Quintero et al., 1990; Weinberg et al., 1997; Petrat et al., 2012). In particular, the protection of glycine against I/R injury in many organs including kidney has been evaluated in several *in-vitro* and *in-vivo* studies and clinical trials, and these studies were listed in a review study by Petrat et al. (2012). However, the authors concluded that glycine to serve as a renoprotective agent was unlikely in treating kidney I/R injury due to its protection either diminishing in a short period (e.g. protection only appeared during 15 minutes of ischaemia) or no protection in the *in-vivo* studies.

Furthermore, glutamine is one of the precursors of glutathione, known as an antioxidant detoxifier and responsible for maintaining redox state homeostasis in cells (Amores-Sánchez and Medina, 1999). Glutamine itself was also found to attenuate apoptosis and preserve renal function after I/R injury through induction of stress response protein expression such as heat shock proteins (Zhang et al., 2009; Hwang et al., 2013) or heme oxygenase-1 (Shi et al., 2009). Furthermore, it was reported by Esposito et al. (2011) that intraperitoneal administration of glutamine prior to reperfusion attenuated expressions of inflammatory mediators and oxidative stress markers and profoundly improved renal function in the rat model of I/R injury. Such therapeutic effects of glutamine were also evidenced and suggested to protect from surgically or medically relevant oxidative injury and improve survival rate particularly in critically ill patients, as it attenuated inflammation and oxidative stress and enhanced stress response protein expression (Amores-Sánchez and Medina,

1999; Wischmeyer, 2007). Moreover, arginine is known as a precursor of nitric oxide. Its protection against renal I/R injury was found to be due to the anti-inflammation, improvement of microvascular and renal blood flow and inhibition of ROS formation. Schneider et al. (2003) demonstrated that intraperitoneal arginine supplementation following arterial clamping in rats with continuous supplementation of arginine in drinking water for 2 weeks fully restored kidney function. Another study by Jerkic et al. (1999) also demonstrated that arginine supplemented in drinking water for 4 weeks before ischaemic injury (induced by left renal arterial clamping for 45 minutes) in rats improved renal blood flow by 96% and water and sodium reabsorption and protected from necrosis. Basile et al. (2003) also observed that arginine supplemented in drinking water for 5-20 weeks enhanced the renal function recovery from I/R injury in rats and also attenuated the development of CKD in rats subjected to unilateral ischaemia nephrectomy. However, some negative results were also reported. Schwartz et al. (2002) showed that increased arginine uptake and nitric oxide production worsened I/R injury in rats induced by right nephrectomy and left renal artery clamping for 60 minutes following reperfusion owing to the peroxynitrite formation during reperfusion period.

Overall, the current clinical and experimental data are limited and inconclusive to support the requirement and benefits of amino acid intake and the physiological effects of increasing individual amino acids for AKI. More laboratory investigations as well as larger, randomised and multicentre clinical trials are required to define the optimal amino acid requirement for patients with AKI, the safety of a high amino acid intake and its effects on the clinical outcomes and survival.

1.8 The mTOR signalling pathways

Prompt nutritional support and high amino acid or protein requirement are frequently recommended in the clinical settings for patients with AKI and particularly those requiring continuous RRT and haemodialysis. Such recommendation is solely based on the point of view in maintaining positive nitrogen balance and attenuating protein catabolism, which is associated with the increased comorbidity and mortality rate (Fiaccadori, Parenti and Maggiore, 2008). However, to date clinical evidence to support the direct relationship between amino acid intake and improved outcomes or survival of AKI is lacking. Rather, it was found that increasing amino acid/protein in early parenteral nutrition for AKI patients substantially contributed to extra amino acid catabolism, urea production, prolonged RRT duration and a higher mortality rate (Gunst et al., 2013; Bellemo et al., 2014). These findings revealed doubts on the advantages of early full nutritional supports in the current clinical practices.

Emerging evidence began to suggest that permissive under feeding (Arabi et al., 2011), low volume trophic feeding (Rice et al., 2011; National Heart, Lung, and Blood Institute Acute Respiratory Distress Syndrome (ARDS) Clinical Trials Network et al., 2012) and late initiation of parenteral feeding (Casaer et al., 2011) could be superior to current approaches. These approaches were found to enhance the recovery from various diseases such as acute lung injury or acute respiratory injury and other complications such as gastrointestinal intolerance and infection. Among these studies, Casaer et al. (2011) reported that early target macronutrient feeding and increasing amino acid or protein intake delayed the recovery and worsened the outcomes in critically ill patients (early full feeding: 204.2 ± 46.7 g glucose/day and 47.2 ± 15.1 g amino acids/day; late feeding after one week: 91.8 ± 44.3 g

glucose/day and 14.2 ± 14.6 g amino acids/day). The lowest dose of macronutrients was also found to be associated with fastest recovery and earlier alive discharge from intensive care units. This group also showed that late initiation of parenteral feeding (8 days after ICU admission) reduced 3 days in the duration of continuous RRT. The explanation for the delayed recovery or worse outcomes by target full feeding (increasing macronutrient delivery) was proposed by Vanhorebeek et al. (2011). This group suggested that the underlying mechanism was the inhibition of autophagy, known as a cellular stress response system for clearance of damaged organelles and damaged protein aggregation and degradation of bulk cytoplasmic materials to maintain cellular integrity. The authors observed autophagy deficiency in organs and tissues from the prolonged critically ill patients fed with full parenteral and enteral nutrition. The insufficient clearance of cellular damage by autophagy process explained why the prolonged critically ill patients never recovered from multiple organ failure and had adverse outcomes. Although clinical studies directly evaluating the beneficial effects of late and low dose of macronutrient delivery on outcomes of AKI are limited, there is a necessity to revise current nutritional approach, i.e. the early target feeding. The molecular mechanisms of the deleterious effects by autophagy inhibition in the patients fed with full parenteral and enteral nutrition remain unclear, but it is certain that autophagy is negatively regulated by the nutrient sensing pathway, the mammalian target of rapamycin (mTOR). Recent studies have begun to uncover that the activation of mTOR may lead to ER stress and contribute to renal I/R injury.

The mammalian target of rapamycin (mTOR) is a highly conserved protein kinase responsible for regulating cell growth and metabolism (Benjamin et al., 2011). There are two structurally and functionally distinct multiprotein complexes named as

mTOR complex 1 (mTORC1) and mTOR complex 2 (mTORC2) (Benjamin et al., 2011). The mTORC1 is composed of regulatory-associated protein of mTOR (Raptor), SEC13 protein 8 (mLST8), proline-rich AKT substrate of 40 kDa (also known as AKT1S1 or PRAS40) and can be inhibited by rapamycin (Loewith et al., 2002). It regulates cell growth through protein synthesis, ribosome biosynthesis, lipogenesis, glycolysis and autophagy (Betz and Hall, 2013). The mTORC2 contains rapamycin-insensitive companion of mTOR (Rictor), mLST8, proline-rich protein 5 and mitogen-activated protein kinase-associated protein 1.

The mTORC2 mainly regulates actin cytoskeleton and is only activated by phosphoinositide3-kinase (PI3K) stimulated by growth factors including insulin and insulin-like growth factor-1 (IGF-1) (Benjamin et al., 2011). Unlike mTORC2, the activity of mTORC1 is mediated by a variety of intracellular and extracellular factors including oxygen/nutrient condition, energy levels, growth factors and stresses (Loewith et al., 2002). The mTORC1 activity is negatively regulated by a heterodimer of tuberous sclerosis complex (TSC1)/tuberin (TSC2) which inhibits Ras homolog enriched in brain (Rheb) responsible for mTORC1 activation (Efeyan, Zoncu and Sabatini, 2012) (Figure 1.7). Generally, in the nutrient/growth factor/energy sufficient condition the TSC2 is inhibited through Akt/protein kinase B (PKB) pathway, and mTORC1 is then activated by Rheb (Efeyan, Zoncu and Sabatini, 2012). The activated mTORC1 stimulates downstream substrates ribosomal kinase S6 (S6K) which phosphorylates ribosomal protein S6 (S6) to promote cell growth (cell mass/size) and inhibits eukaryotic translation initiation factor 4E (eIF4E)-binding protein 1 (4EBP1) to release eIF4E which promotes translation for protein synthesis (Reiling and Sabatini, 2006) (Figure 1.7).

Several nutrients and factors have been recognised to regulate mTORC1 activity, and this includes glucose, amino acids (leucine in particular) and growth factors such as insulin and IGF-1 (Sengupta, Peterson and Sabatini, 2010). Glucose sensing pathway is related to energy status in cells (Sengupta, Peterson and Sabatini, 2010). Deprivation of glucose or energy level elevates adenosine monophosphate (AMP)/ATP ratio, and AMP binds AMP kinase which then phosphorylates/activates TSC2 to maintain mTORC1 inactive (Inoki, Zhu and Guan, 2003; Sanders et al., 2007). On the other hand, the growth factor activated mTORC1 pathway is through insulin receptor substrate (IRS)-PI3K-Akt, as described in mTORC2 signalling pathway (Figure 1.7). In the amino acid sensing pathways, the removal of individual amino acids in cell culture media can inhibit mTORC1 activity (Hara et al., 1998). In particular the removal of leucine or arginine has been identified to profoundly inhibit mTORC1 activity, and the inhibition level was identical to total amino acid deprivation (Hara et al., 1998).

The amino acid signalling pathways to mTORC1 are still not fully understood, but studies have revealed that the activation of mTORC1 by amino acids may be independent of TSC1/TSC2 (Smith et al., 2005). Emerging data has shown that the activation of mTORC1 by amino acids was independent of TSC1/TSC2 (Smith et al., 2005). Instead, it was identified that the amino acid sensing pathway requires vacuolar-H^+-adenosine triphosphatase (V-ATPase) of lysosomes (Figure 1.8). It was confirmed that this sensing pathway was associated with the amino acid pool in the lysosomes rather than the cytoplasm (Zoncu et al., 2011). The mechanism proposed currently was that amino acids are rapidly transported into lysosomes and activate Ragulator complex via V-ATPase on lysosomes, and Ragulator activates the RagA and RagB proteins to their guanosine-5'-triphosphatase (GTPase)-bound

conformation which recruits mTOR and promotes its translocation to the lysosomal membrane where Rheb switches on mTOR kinase activity (Sancak et al., 2008; Sancak et al., 2010; Zoncu et al., 2011) (Figure 1.8). In contrast, mTORC1 activity is inhibited under stresses including low oxygen/nutrient conditions (Kim et al., 2002; Liu et al., 2006), low energy levels (Hardie, Hawley and Scott, 2006), oxidative stress (Li et al., 2010) and low pH (Marino et al., 2012; Crean et al., 2013) in order to attenuate cell growth and initiate autophagy processes (Jung et al., 2010).

The active mTOR in renal epithelial cells is normally found at the embryonic stage and during postnatal development (Murakami et al., 2004). However, in normal adult kidneys mTOR activity has been found to be low or absent, particularly in renal epithelial cells (Lieberthal and Levine, 2009). This has been evidenced by the observation of downregulated phosphorylation of S6K and mTOR in the normal rat, mouse and human kidney tissues (Lieberthal et al., 2001; Shillingford et al., 2006; Baba et al., 2008). Conversely, a marked activation of mTOR is more commonly observed in various pathological conditions such as I/R injury, polycystic kidney disease, diabetic nephropathy, glomerulosclerosis and tubulointerstitial fibrosis (Lieberthal et al., 2001; Shillingford et al., 2006; Torres et al., 2010). This is due to its essential role in regenerative and recovery process by promoting cell proliferation and fibrosis in response to injuries (Torres et al., 2010). These findings suggested that mTOR activity is more essential for the response to injury but not for regulation of normal kidney function.

During ischaemia the mTOR activity is highly suppressed, whilst upon reperfusion mTOR is markedly activated for renal regeneration and recovery by enhancing cell proliferation (cell number) and growth (cell size) due likely to the sudden return of

growth factors, amino acids and ATP (Lieberthal et al., 2006). Currently there is no data to support a further suppression of mTOR in the ischaemic kidney, as virtually all studies measured mTOR expression levels after reperfusion. However, it is certain that ischaemia is unlikely to activate mTOR due to no nutrients and oxygen supply whereas mTOR is reasonably activated during reperfusion. The mTOR activation during reperfusion is crucial for the complete repopulation and renal functional restoration after injury, and its inhibition was found to delay recovery process (Lieberthal and Levine, 2009). However, recent data showed that in fact inhibition of mTOR and activation of autophagy was more protective against renal I/R injury. A more potent renoprotection of mTOR inhibition was observed in the diabetic nephropathy and kidney interstitial fibrosis due to the immunosuppressive and anti-inflammatory effects (Declèves et al., 2011; Chen et al., 2012; Zhang et al., 2014). Others reported that the induction of autophagy was the key to the protection, but the mechanism was unknown. For instance, Wang et al. (2013) observed that induction of autophagy by mTOR inhibitors protected against pig renal tubular cell apoptosis after I/R injury. In addition to pharmacologic inhibition of mTOR and activation of autophagy, the dietary intervention and preconditioning are alternative means. For instance, Chen et al. (2014) reported that quercetin, an antioxidant, also displayed a renoprotection through downregulation of mTOR and activation of autophagy in both *in-vitro* and *in-vivo* models of I/R injury. Mitchell et al. (2010) showed that the survival rate and lifespan were improved by a 30% dietary restriction for 2-4 weeks or one day fasting prior to I/R injury in mice. Verweij et al. (2011) demonstrated that 3 days of fasting with water or glucose solution also provided beneficial effects on I/R injury in mice. Peng et al. (2012) reported that dietary restriction by the removal of a single essential amino acid (tryptophan or leucine) or total protein deprivation

protected against renal and liver I/R injury caused by surgery and extended longevity in mice. Robertson et al. (2015) demonstrated that mice fed with protein and calorie restricted diet for a week before I/R injury showed a lower level of serum urea and lesser tubular destruction and obstruction, compared with mice fed with complete diet. Protein restricted diet exhibited a similar level of protection as non-essential amino acids only diet, but mice fed with essential amino acid only diet had a great increase in serum urea. The authors suggested that the compromised protection by the essential amino acids was due to the presence of leucine, as a specific mTOR activator. The authors further identified that activation of mTOR by the addition of leptin (an mTOR activator) to protein and calorie restricted diet negated the protection due to the observation of increased serum urea. Taken together, these studies suggested that mTORC1 inhibition may serve as a potential therapeutic strategy for kidney I/R injury.

Furthermore, the direct correlation between mTORC1 activation and I/R injury was found to be associated with endoplasmic reticulum (ER) stress. For instance, Ozcan et al. (2008) have identified that *Tsc1*$^{-/-}$ and *Tsc2*$^{-/-}$ cells and *Tsc2*$^{+/-}$ mice showed a dysregulation of mTOR which led to an uncontrolled protein synthesis and increased ER stress and triggered UPR mediated apoptosis. Recently Kato et al. (2012) reported that mTORC1 was rapidly activated in the ER-stressed rat tubular epithelial cells (NRK-52E) and rat mesangial cells (SM43). Dong et al. (2015) also demonstrated similar results in the rat kidney proximal tubular cell line. Both studies demonstrated that inhibition of mTOR signalling by rapamycin mitigated the apoptotic cell death mediated by the unfolded protein response pathways. These studies suggested that mTORC1 activation contributes to ER stress which has been found to regulate a variety of renal diseases, including diabetic nephropathy,

nephrotoxicity and I/R injury (Peyrou and Cribb, 2007; Prachasilchai et al., 2008; Cunard and Sharma, 2011; Cybulsky, 2013; Inagi, Ishimoto and Nangaku, 2014).

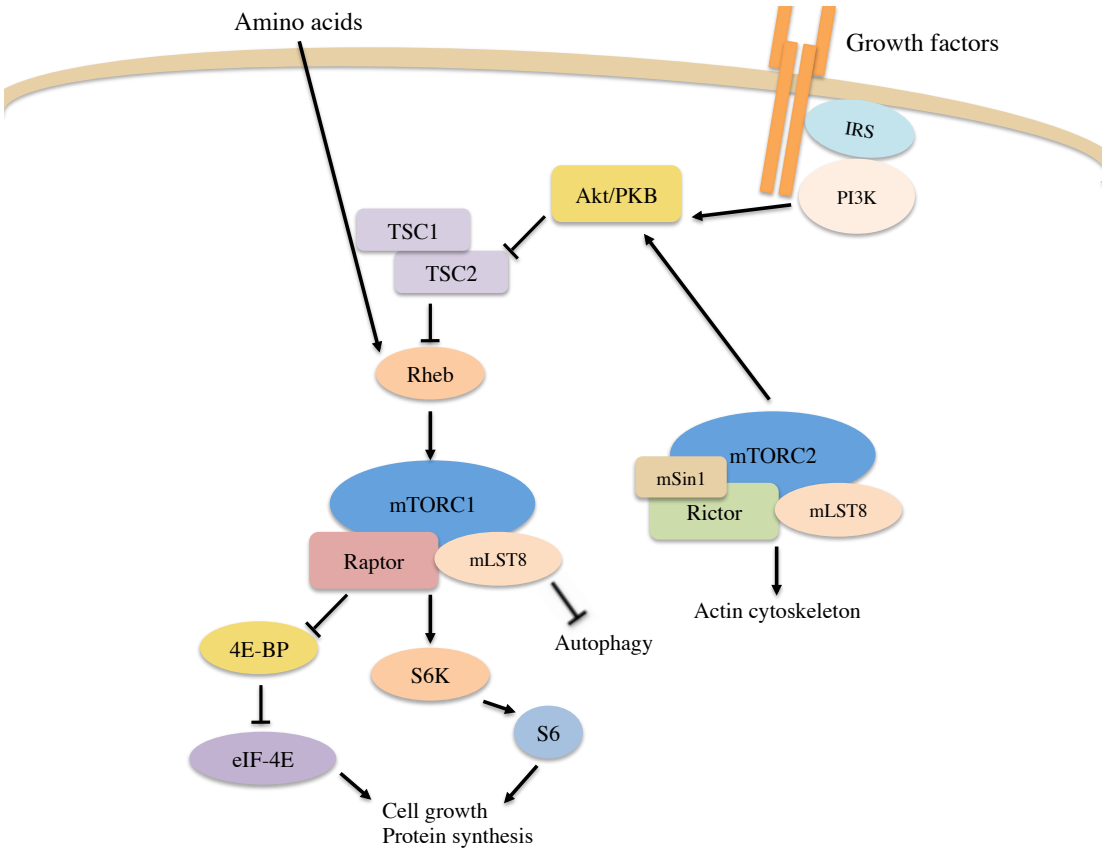


Figure 1. 7 Diagram of mTOR signaling pathways in response to nutrients and growth factors.

The cell growth and protein synthesis are regulated through mTORC1 and mTORC2 pathways in responses to availability of nutrients and growth factors and energy levels. Akt/PKB, Akt/protein kinase B; 4E-BP, eukaryotic translation initiation factor 4E-binding protein; eIF-4E, eukaryotic translation initiation factor 4E; IRS, insulin receptor substrate; mLST8, SEC13 protein 8; mTORC1, mTOR complex 1; mTORC2, mTOR complex 2; mSin1, mammalian stress-activated protein kinase-interacting protein; PI3K, phosphoinositide3-kinase; Rheb, Ras homolog enriched in brain; S6, ribosomal protein S6; S6K, ribosomal kinase S6; TSC1/TSC2, heterodimer of tuberous sclerosis complex/tuberin. This diagram was adapted and republished from 'Reiling, J. H. and Sabatini, D. M. (2006) Stress and mTORture signalling. Oncogene, 25(48), 6373-6383.' by permission of Macmillan Publishers Ltd, granted by Nature Publishing Group.

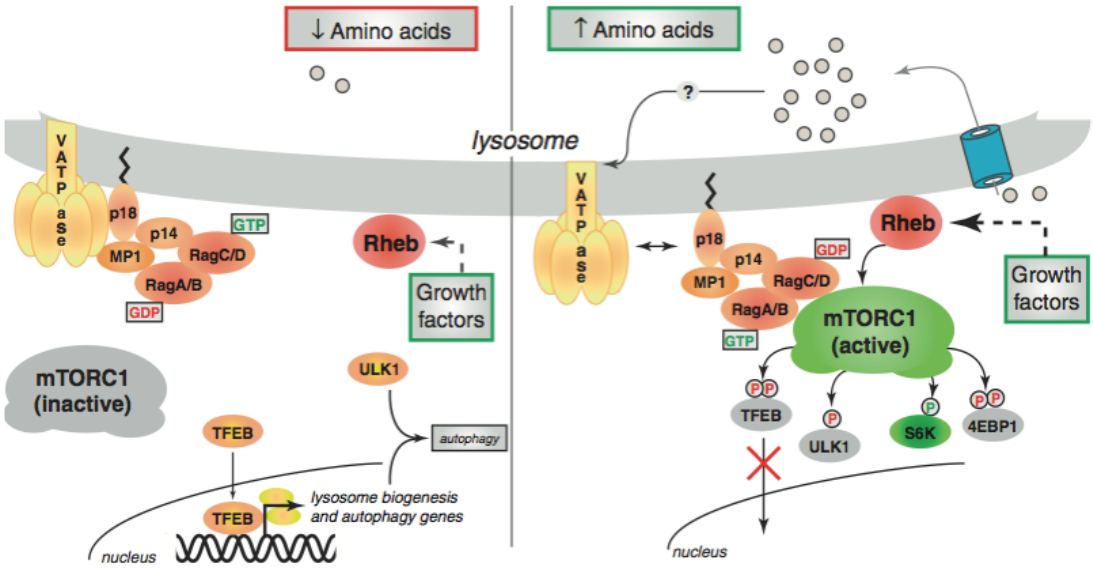


Figure 1. 8 The proposed mechanism of amino acid sensing pathways in activation of mTORC1.

Amino acids in lysosomes signal V-ATPase to activate Ragulator complex which activates RagA/B into GTPase-bound conformation. This subsequently recruits mTORC1 to lysosomal surface where Rheb switches on mTOR kinase activity. This diagram was republished from 'Efeyan, A., Zoncu, R. and Sabatini, D. M. (2012) Amino acids and mTORC1: From lysosomes to disease. Trends in Molecular Medicine, 18(9), 524-533.' by permission of Elsevier.

1.9 ER stress and UPR

The major function of endoplasmic reticulum is to ensure that the newly synthesised proteins are properly assembled and folded for optimal biological functions by regulating protein biosynthesis, folding, trafficking and modification (Rao and Bredesen, 2004; Inagi, 2009). Post-translational modification including proper folding is essential to ensure optimal protein function, and this requires interaction with chaperone proteins which assist protein folding and recognise differences between normal and abnormal (misfolded) proteins (Rao and Bredesen, 2004). Misfolded proteins can be generated not only under normal physiological condition due to the expression of mutant proteins, excess unassembled protein subunits and

inefficient protein biogenesis (Voisine, Pedersen and Morimoto, 2010) but also under pathological conditions such as oxidative stress, metabolic stress, cancer and ageing (Haigis and Yankner, 2010). In I/R injury, it was proposed that the production of ROS could interfere with the protein disulfide bonding and lead to protein misfolding and accumulation in the ER (Inagi, 2009). In addition, the activation of mTOR caused by a rebound of nutrients, growth factors and ATP during reperfusion promotes protein synthesis and may lead to an increase in misfolded protein load in the ER (Lieberthal et al., 2006; Inagi, 2009). This subsequently overwhelms the ER ability of processing these proteins, resulting in cell death (Douglas and Dillin, 2010). The direct correlation between mTOR activation leading to ER stress and I/R injury remains unknown as it was only recently proposed and demonstrated in the cell work (Ozcan et al., 2008; Kato et al., 2012; Dong et al., 2015). Neverthelss, this mechanism may be in agreement with the study by Vanhorebeek et al. (2011) suggesting that prolonged critically patients fed with target nutrition never recover from organ failure due to the autophagy deficiency. The activation of mTOR by nutrients inhibits autophagy and results in accumulation of damaged protein and organelles, and meanwhile increasing protein synthesis further leads to ER stress. This may also explain why increasing amino acid intake did not reverse the outcomes in AKI patients.

The mechanism of how ROS interferes with protein disulfide bonding is not fully understood. The current available explanation was that ROS disrupts homeostatic redox state in the ER lumen and leads to mispairing of cysteine residues that cause inappropriate disulfide bonds or protein unfolding (Chakravarthi, Jessop and Bulleid, 2006; Malhotra and Kaufman, 2007). In eukaryotic cells, a correct protein folding process requires the thiol-disulfide pair formation between cysteine residues and

isomerisation for polypeptide arrangements to maintain protein structural and functional stability (Cao and Kaufman, 2014). This process is regulated mainly by protein disulfide isomerase, glutathione and ER oxidoreductase through exchanging disulfide bonds and protein oxidation (Cao and Kaufman, 2014). As the disulfide bond formation involves oxidation reaction, it reveals that the ER is a rather oxidising environment. It was also evidenced that the ratio of reduced glutathione (GSH)/oxidised glutathione (GSSG) ranging from 1:1 to 3:1 in the ER, compared with GSH/GSSG ratio ranging from 30:1 to 100:1 in the cytoplasm (Hwang, Sinskey and Lodish, 1992). Given that such an oxidising environment preferably promotes oxidative protein folding, maintaining a redox state is essential to ensure a correct protein folding process (Hwang, Sinskey and Lodish, 1992; Malhotra and Kaufman, 2007). When under a greater oxidising condition (e.g. diminishing glutathione level or exogenous H_2O_2), the ER becomes more prone to oxidation, increasing protein disulfide bond formation (Van der Vlies et al., 2003; Chakravarthi, Jessop and Bulleid, 2006; Malhotra and Kaufman, 2007). However, it is also accompanied by an increase in disulfide bond mispairing and unfolded protein accumulation (Chakravarthi and Bulleid, 2004; Molteni et al., 2004). The decreased folding capacity is a result of inactivation/hyperoxidation of ER resident proteins such as disulfide isomerase (Van der Vlies et al., 2003; Chakravarthi and Bulleid, 2004).

Unfolded/misfolded proteins can aggregate and accumulate and subsequently impose a burden on the ER (Buchberger, Bukau and Sommer, 2010; Ferris, Kodali and Kaufman, 2014). Normally, chaperones can assist misfolded proteins to refold properly or promote their degradation and clearance via the ubiquitin-proteasome system (McClellan et al., 2005). Chaperone proteins such as glucose-regulated protein (Grp or Bip) can recognise the exposed hydrophobic regions/residues from

aggregation of misfolded proteins (Buchberger, Bukau and Sommer, 2010; Ferris, Kodali and Kaufman, 2014). Grp/Bip contains an N-terminal nucleotide-binding domain and a C-terminal substrate-binding domain (Bukau, Weissman and Horwich, 2006). It binds to the hydrophobic regions of unfolded/misfolded proteins or nascent polypeptides and hold the substrates inside the C-terminal substrate-binding domain (Ferris, Kodali and Kaufman, 2014). This prevents from substrate aggregation and allows the substrates to refold, the subunits to assemble and other enzymes such as protein disulfide bond isomerases to amend the mispaired protein disulfide bonds or promotes protein degradation (Ferris, Kodali and Kaufman, 2014), hence alleviating misfolded protein load in the ER. However, the increasing accumulation of oxidatively damaged proteins causes an imbalance between the newly synthesised proteins and the ability of ER to process these proteins (Douglas and Dillin, 2010). This results in ER stress and eventually leads to toxicity and cell death (Douglas and Dillin, 2010). In eukaryotes, a set of cellular responses to ER stress is termed unfolded protein response (UPR) which is regulated by three proximal ER stress sensor proteins including protein kinase RNA-like ER kinase (PERK), activating transcription factor 6 (ATF6) and inositol-requiring transmembrane kinase/endoribonuclease (IRE1) (Tsai and Weissman, 2010) (Figure 1.9). These ER transmembrane proteins are normally bound by chaperone protein Grp/Bip to maintain in an inactive form (Bertolotti et al., 2000). In the presence of misfolded proteins, Grp/Bip dissociates from these sensors and binds to misfolded proteins, and meanwhile these sensors becoming active, signal downstream URP pathways (Rao and Bredesen, 2004) (Figure 1.9).

The downstream parallel pathways that help relieve ER stress are as follows (Figure 1.7). Active PERK inactivates eukaryotic translation initiation factor 2 alpha (eIF2a)

by phosphorylation to shut down global mRNA translation (Harding et al., 2000). Hence, PERK pathway reduces the protein flow to the ER and alleviates the ER stress. Meanwhile, the phosphorylated eIF2a also signals to activating transcription factor 4 (ATF4) to induce several stress response genes encoding chaperones and anti-oxidant enzymes including glutathione S-transferase and heme-oxygenase-1, protecting cells from ER and oxidative stress (Zhang, 2006). The activation of ATF6 after chaperone protein dissociation requires its site-1 and site-2 proteolysis in the Golgi apparatus (Tsai and Weissman, 2010). After cleavage, the fragmented ATF6 translocates to nucleus and then transcriptionally upregulates ER chaperones (e.g. Grp78) to enhance protein folding capacity (Yamamoto et al., 2007; Tsai and Weissman, 2010). On the other hand, active IRE1 after chaperone protein dissociation cleaves X-box binding protein 1 (XBP1), and the spliced XBP1 can induce the transcript encoding chaperones and ER associated degradation components to reduce protein load in the ER (Tsai and Weissman, 2010). Additionally active IRE1 can directly cleave mRNA encoding secretory proteins to reduce the protein load in the ER, hence facilitating the restoration of ER homeostasis (Lee et al., 2002; Hollien et al., 2009).

UPR can serve as an adaptive response, but it can also lead to cell death if the activation is prolonged or fails to resolve ER stress (Tsai and Weissman, 2010). When failing to relive ER stress, the UPR-induced apoptosis is initiated by PERK and IRE1. PERK increases the expression of C/EBP homologous protein (CHOP), a transcription factor which up-regulates pro-apoptotic genes and also activates cJUN N-terminal kinase (JNK) to initiate the apoptotic cascade (e.g. initiation of B-cell lymphoma 2 (Bcl-2) apoptotic signalling to release cytochrome c) (Darling and Cook, 2014). Meanwhile, IRE1 also activates JNK to promote apoptosis and also can

directly cleave caspases to initiate downstream apoptotic cascades, leading to UPR mediate cell death (Sykes, Mactier and Christopherson, 2016). Therefore, the downstream signalling pathways determine the fate of a cell.

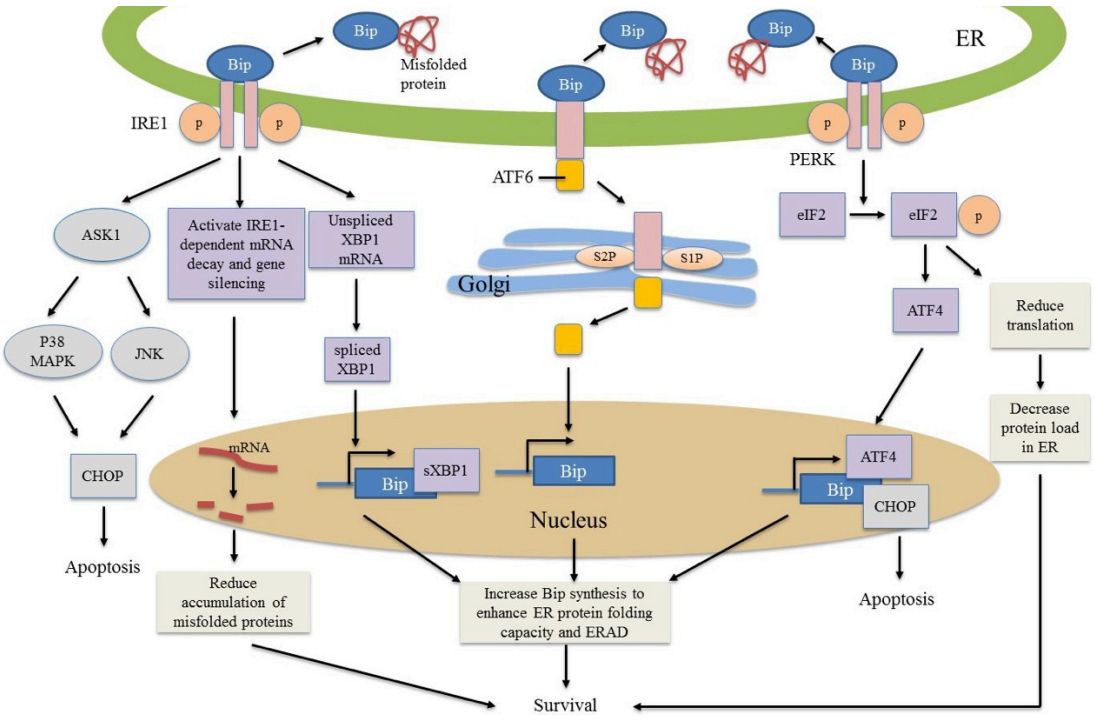


Figure 1. 9 Diagram of UPR signalling pathways.

The increased misfolded proteins lead to Bip dissociation from the ER stress sensors including PERK, ATF6 and IRE1, inducing adaptive or maladaptive UPR pathways which determine the fate of cells. This diagram was adapted and republished from 'Wang, M. and Kaufman, R. J. (2014) The impact of the endoplasmic reticulum protein-folding environment on cancer development. Nature Reviews Cancer, 14(9), 581-597.' by permission of Macmillan Publishers Ltd, granted by Nature Publishing Group.

1.10 Cellular repair process and long-term consequences

The recovery responses to injury have been shown in biopsies from patients with ischaemic or nephritic injury and animal models of acute or severe insults caused by I/R injury and nephrotoxins (Solez, Morel-Maroger and Sraer, 1979; Solez et al.,

1993; Megyesi et al., 1995; Spurgeon, Donohoe and Basile, 2005). The regeneration process mainly occurs in the proximal tubules and is normally observed 24 hours after injury, evidenced by a rapid cellular proliferation (Megyesi et al., 1995; Spurgeon, Donohoe and Basile, 2005). After sublethal injury, the surviving tubular cells can undergo a repair process by dedifferentiation, proliferation and differentiation to restore cellular functions (Bonventrre and Yang, 2011) (Figure 1.10). These injured cells appear as a flattened and elongated morphology with a loss of polarity, brush borders and tight junctions and misallocation of integral proteins on membranes (Bonventrre and Yang, 2011). To repopulate the denuded area of the basement membrane, these cells dedifferentiate, migrate, markedly proliferate to restore the lost cells and redifferentiate to recover nephron functions (Bonverntre and Weinberg, 2003; Nony and Schnellmann, 2003; Hallman, Zhuangand and Schnellmann, 2008).

After injury, surviving epithelial cells first undergo dedifferentiation, and this can be detected by the expression of Vimentin which is normally expressed by mesenchymal cells but not by mature proximal tubules (Witzgall et al., 1994). Such dedifferentiated phenotype allows tubular cells to undergo a rapid proliferation and migrate to repopulate the denuded areas on the basement membrane (Bard, 2002). During proliferation process, several genes encoding growth factors including insulin-like growth factor-1, hepatocyte growth factor and fibroblast growth factor (Matejka and Jennische, 1992; Igawa et al., 1993; Ichimura et al., 1996) and others encoding transcription factors such as paired box gene 2 (Kramann, Kobayashi and Humphreys, 2013) are found to be upregulated to promote the regeneration process. Some genes, such as epidermal growth factor, are downregulated after injury whereas it is highly activated during recovery (Schaudies and Johnson, 1993).

Regulation of these genes is similar to and is essential for nephrogenesis; however, the role of endogenous growth factors during the recovery process is not well defined.

In addition to tubular cell proliferation, the re-establishment of basement membrane and expression of adhesion molecules are also essential for tubular cell proliferation, migration and differentiation. Injured renal tubular epithelial cells can express basement membrane extracellular matrix components such as fibronectin and collagen IV during regeneration process to enhance integrin binding (Basile, Martin and Hammerman, 1998; Zuk and Bonventre, 2001). Also, the flattened and dedifferentiated proximal tubular cells are found to persistently express cell adhesion molecules such as neural cell adhesion molecule (Bonventre, 2003). The expression of both matrix components and adhesion molecules enables to maintain cell-matrix integrity and promote cell adhesion, migration and proliferation (Bonventre, 2003). Following repopulation of the denuded areas, tubular cells differentiate possibly by re-expression of genes related to embryonic and fetal development such as paired box gene 2 and *WNT-4* (Imgrund et al., 1999; Terada et al., 2003). This allows reinitiating chromatin modification by histone acetylation after dedifferentiation, and hence cells can re-enter the cell cycle and restore normal morphology and function (Surendran and Kopan, 2011).

In addition to the high regeneration capacity, tubular cells have been suggested to play an important role in immune system which further supports the repairing process. Tubular cells constitutively express toll-like receptors, which mediate signalling pathways controlling expression of proinflammatory cytokines and chemokines (Maeshima et al., 2015). After injury, tubular cells express several

proinflammatory cytokines and chemokines to recruit leukocytes such as neutrophils, M1 macrophages and various lymphocyte subsets to the injured areas (Maeshima et al., 2015). The activated leukocytes secrete proinflammatory cytokines (e.g. interleukin (IL)-6, IL-13, IL-1β, tumour necrosis factor and transforming growth factor β) and chemokines (e.g. monocyte chemoattractant protein-1 and IL-8) to recruit more leukocytes and amplify the wound healing process (Lech and Anders, 2013). These immune cells also secrete growth factors such as platelet derived growth factor, vascular endothelial growth factor and epidermal growth factor to promote epithelial cell proliferation, adhesion and migration (Humes, 1993; Lech and Anders, 2013). These cytokines, chemokines and growth factors also activate local fibroblast transformation to myofibroblasts and enhance myofibroblast proliferation (Wynn, 2007). Myofibroblasts are responsible for producing extracellular matrix components and basement membrane remodeling and maturation by wound contraction (Wynn, 2007). Meanwhile, leukocytes particularly macrophages produce matrix metalloproteinase (MMP) and tissue inhibitor of matrix metalloproteinase (TIMP) for balancing deposition and degradation of extracellular matrix to eliminate scar tissues (Lech and Anders, 2013). This process restores the normal basement membrane and hence enables epithelial cell proliferation, adhesion and migration during regeneration (Wynn, 2007).

This process involving immune cell activation and infiltration is an inflammatory phase during recovery and is essential for removal of dead cells and tissue debris and supporting epithelial cell proliferation (Lech and Anders, 2013). However, persistent inflammation suppresses the regenerative process, and the tubular regeneration process does not occur until inflammation is resolved (Lech and Anders, 2013). Hence, controlling inflammation is critical for an efficient recovery and preserving

tissue morphology and function, and several immune cells play an important role in resolution of inflammation during the repairing process (Lech and Anders, 2013). Immune cells such as M2 macrophages, regulatory T cells and dendritic cells are known to possess anti-inflammatory properties and promote tissue regeneration (Lech and Anders, 2013; Maeshima et al., 2015). The proinflammatory M1 macrophages can change their phenotype towards anti-inflammatory M2 macrophages during phagocytosis of apoptotic cells (Lech and Anders, 2013). M2 macrophages then release several anti-inflammatory mediators such as IL-4, IL-13, IL-10 and a large amount of transforming growth factor-β1 (TGF-b1) to promote tubular regeneration (Filardy et al., 2010; Lee et al., 2011; Zhang et al., 2012). It was also recently found that M2 macrophages could trigger signalling pathways related to kidney development. For instance, M2 macrophages were found to secrete Wnt7b to promote tubular regeneration through Wnt-β-catenin signalling pathways (Lin et al., 2010) or release Notch ligands to enhance cell proliferation (Bielesz et al., 2010). Such alternatively activated macrophages have been suggested to play a crucial role in supporting the transition from tubule injury to recovery (Lech and Anders, 2013).

Among all lymphocyte subsets, only regulatory T cells possess anti-inflammatory properties (Maeshima et al., 2015). The regulatory T cells have been shown to promote tubular recovery by reducing proinflammatory cytokines generated by other lymphocyte T cells and the accumulation of leukocytes (Gandolfo et al., 2009). Dendritic cells play an important role in both early phase of AKI and recovery (Kulkarni et al., 2014). It was identified that during the healing phase dendritic cell derived IL-22 suppressed inflammation and accelerated tubular regenerative process in the surviving tubular cells through signal transducer and activator of transcription 3 (STAT3) and extracellular signal-regulated kinases 1/2 (ERK1/2) (Kulkarni et al.,

2014). Collectively, termination of inflammation during repairing process through switching proinflammatory immune cells to anti-inflammatory phenotypes supports an efficient tubular regenerative process.

Moreover, activation of mTOR signalling after I/R injury has been known to mediate tubular regeneration process (Lieberthal and Levine, 2009). It was found that inhibition of mTORC1 delayed kidney function recovery in patients and experiemental models (Lieberthal et al., 2006; Lieberthal and Levine, 2009; Grahammer et al., 2014). Because of this finding, rapamycin, a clinically used immunosuppressant and an mTOR inhibitor, is routinely administered after the transplanted kidney is functional or is temporarily discontinued in patients with transplantation and AKI in the clinical setting (Smith et al., 2003; Loverre et al., 2004).

The mTORC1 stimulates mitochondrial activity and ATP production to supply energy for renal recovery and is responsible for regulating cell growth and proliferation through promoting protein synthesis (Lieberthal and Levine, 2012; Grahammer et al., 2014). The mTORC2 may also promote renal recovery potentially by mediating cell survival, cell polarity, cytoskeletal organisation and re-establishment of tight junctions and cell adhesions (Lieberthal and Levine, 2012). After cell division, the size of two daughter cells is half of a normal cell (Lieberthal and Levine, 2009). The daughter cell mass must be doubled before entering another cell cycle to continue proliferation (Fingar et al., 2002; Fingar et al., 2004). Hence, mTORC1 is required for increasing cell size/mass as it is responsible for promoting protein synthesis, and this enables cells to progress through the G0/1 cell cycle and promotes a sustained cell proliferation (Fingar et al., 2002; Fingar et al., 2004).

Additionally, mTOR signalling also negatively regulates autophagy. Autophagy has been found to be induced by oxidative stress and ER stress during I/R injury and nephrotoxicity, and it participates in renal injury and contributes to cell death (Suzuki et al., 2008; Wu et al., 2009; Bolisetty et al., 2010). However, emerging studies discovered that induction of autophagy through inhibition of mTOR exerted potent protection against I/R injury and nephrotoxicity (Pallet et al., 2008; Jiang et al., 2010; Wang et al., 2013; Zhang et al., 2015). The mechanism is likely to be that autophagy degrades bulk cytoplasmic materials such as the damaged organelles and proteins to maintain cellular integrity (Vanhorebeek et al., 2011). Also, degradation of these cellular contents can supply nutrients for cells to rebuild energy and essential cellular structures (Lieberthal, 2008). Hence, these findings partially argue against the role of mTOR in the recovery process. Nevertheless, mTOR signalling still plays a significant role in the tubular regenerative process as it regulates cell growth and proliferation and arranges cytoskeletal structures to restore kidney morphology and function.

The evidence of mTOR regulating cell proliferation and cell mass expansion can be observed in not only tubular cells but also other types of cells such as glomerular cells, fibroblasts and inflammatory cells, and it also increases matrix protein synthesis (Lieberthal, 2008). Although these appear to further support its role during recovery, these features are mostly observed in pathological conditions such as diabetic nephropathy and interstitial inflammation/fibrosis (Lloberas et al., 2006; Chen et al., 2012). This reveals that mTOR also plays a substantial role in the progression of CKD. The activation of mTOR at the early stage of injury would be beneficial as it activates immune cells such as macrophages to clean up dead cells and tissue debris, but the persistent mTOR activation was found to promote

inflammation and fibrosis (Chen et al., 2012). This suggested that the balance of mTOR activation determined the outcomes of renal injury and repair (Chen et al., 2012).

An efficient repairing process involves a complex system. To achieve full recovery, it requires an adaptive immunity and the balanced activation of various signalling pathways. Althoguh tubular cells have a high generative capacity, patients with history of AKI were still found to have higher risk of developing CKD and ESRD (Ishani et al., 2009; Lo et al., 2009; Wald et al., 2009). Patients with history of severe AKI (requiring hospital admission without RRT) were found to be at higher risk of long-term mortality (Lafrance and Miller, 2010; Pereira, Zanetta and Abdulkader, 2012). This is because that the repairing process after AKI is frequently maladaptive particularly in the prolonged and severe cases. The maladaptive repairing process can cause a sustained inflammation in the interstitial areas, proliferation of fibroblasts, macrophage invasion and the increased extracellular matrix deposition, eventually developing into postischaemic fibrosis and progressing to CKD and ESRD (Brown et al., 2010; Chawla et al., 2011; Chawla and Kimmel, 2012).

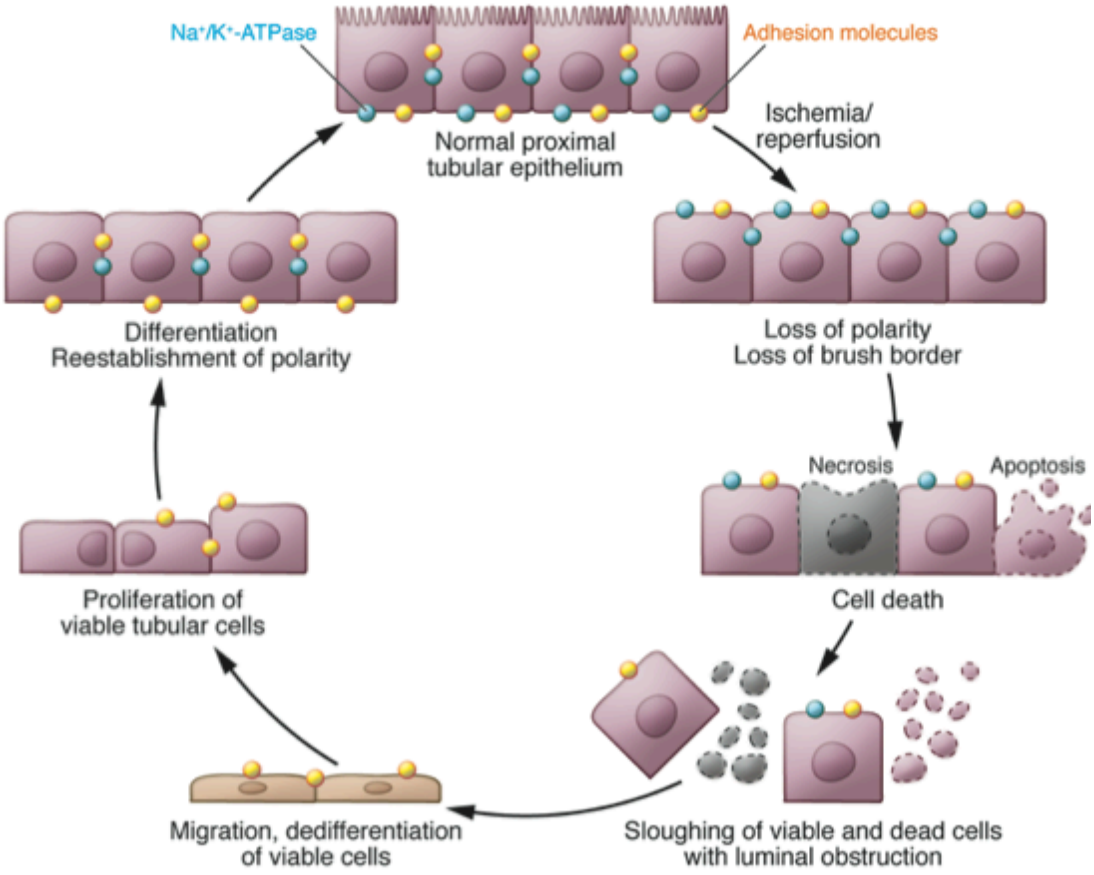


Figure 1. 10 A schematic diagram of repair process in proximal tubular cells.

After injury, proximal tubular cells can dedifferentiate, migrate and proliferate to restore the lost cells and then redifferentiate to recover nephron functions. This diagram was republished from 'Bonventre, J. V. and Yang, L. (2011) Cellular pathophysiology of ischemic acute kidney injury. The Journal of Clinical Investigation, 121, 4210-4221.' by permission of American Society of Clinical Investigation, conveyed through Copyright Clearance Center, Inc.

1.11 Pathophysiology of renal interstitial fibrosis

Interstitial fibrosis is a common event before progression to CKD. It is characterised as a maladaptive repairing/scarring process; that is, an uncontrolled wound healing response (Wynn, 2007). After injury, the tissue can undergo a normal repair process by regenerating the same cells to replace the damaged ones and fully recover from the damage. However, the wound healing process can be pathogenic when out of

control and result in organ failure and death because the connective tissue replaces the normal parenchymal tissue and form the permanent scarring tissue which loses its phenotypic functions (Wynn, 2007).

Briefly, interstitial fibrosis involves the deregulation of a variety of cells including epithelial cells, endothelial cells, fibroblasts, myofibroblasts, inflammatory cells including lymphocytes, monocytes, leukocytes and macrophages and the inflammatory mediators synthesised and secreted by these cells (Vahed, Samadi and Ardalan, 2014) (Figure 1.11). Upon injury, the epithelial and endothelial cells produce inflammatory mediators such as cytokines and chemokines which stimulate the inflammatory cells to recruit to the injured basement membranes and proliferate (Farris and Colvin, 2012). The activated leukocytes such as neutrophils and macrophages are first recruited to remove the dead cells, tissue debris and invading organisms and produce cytokines and chemokines to enhance the repairing process (Wynn, 2007; Farris and Colvin, 2012).

Macrophages, in particular, participate in not only various stages of tissue injury and the repairing process but also the profibrotic process (Bielesz et al., 2010; Braga, Agudelo and Camara, 2015; Kim et al., 2015). Persistent activation and infiltration of proinflammatory macrophages have been found to turn the acute inflammation to chronic inflammation, leading to impaired wound healing (Lech and Anders, 2013). Macrophages are classified into two subtypes including M1 and M2 macrophages. M1 macrophages have endocytotic and phagocytotic ability and secrete IL-1, IL-2, IL-23, tumour necrosis factor and ROS (Lech and Anders, 2013). Proinflammatory M1 macrophages amplify inflammation and play an important role in many renal diseases including I/R injury (Lech et al., 2009; Lee et al., 2011). M1 macrophages

are predominantly activated after injury, and their production of inflammatory cytokines can exacerbate injury (Braga, Agudelo and Camara, 2015). Persistent proinflammatory stimuli is known to preserve M1 macrophage activity, and a sustained secretion of these proinflammatory cytokines by M1 macrophages results in cell cycle arrest and apoptosis, leading to anti-regenerative effects and tubular injury (Lee et al., 2011; Maeshima et al., 2015). After injury or termination of this acute inflammation caused by M1 macrophages, M2 macrophages are activated and recruited by T helper 2 cells to create an anti-inflammatory environment to promote the repairing process (Braga, Agudelo and Camara, 2015). Additionally, proinflammatory M1 macrophages can switch their phenotypes to anti-inflammatory M2 macrophages during phagocytosis of apoptotic cells or by tubular epithelial cell derived factors (Filardy et al., 2010; Lee et al., 2011). M2 macrophages promote resolution of inflammation and tubular regeneration (Filardy et al., 2010; Lee et al., 2011; Zhang et al., 2012), but they also play a key role in the development of renal fibrosis after I/R injury (Kim et al., 2015). Persistent activation of M2 macrophages can lead to insufficient repairing process as M2 macrophages secrete a large amount of TGF-b1 which is an anti-inflammatory cytokines with fibrotic functions (Lech and Anders, 2013). Other growth factors such as platelet derived growth factor, vascular endothelial growth factor and fibronectin are also secreted by M2 macrophages to activate local fibroblasts, promote myofibroblast proliferation and increase extracellular matrix deposition (Lech and Anders, 2013). Hence, excessive activation of M2 macrophages can exacerbate the fibrotic process (Lech and Anders, 2013).

Several cytokines and growth factors, such as interleukins, platelet derived growth factor and transforming growth factor-β1 (TGF-b1), have been recognised to involve the fibrotic process (Borthwick, Wynn and Fisher, 2013). In particular, TGF-b1 is

known as the core mediator in regulating renal fibrosis (Borthwick, Wynn and Fisher, 2013). It activates resident fibroblasts to transform into myofibroblasts and also activates myofibroblast proliferation (Li, M. O. et al., 2006; Wynn, 2007; Boor and Floege, 2011). These myofibroblasts are charactersied by their expression of alpha-smooth muscle actin (alpha-SMA) which has become a hallmark of the fibrotic process (Wynn, 2007). More importantly, TGF-b1 also induces the epithelial cells to undergo the epithelial-mesenchymal-transition (EMT); that is, epithelial cells transform into myofibroblasts and no longer maintain their phenotypes (Boonla et al., 2011). This can be detected by several biomarkers including the decreased epithelial markers (e.g. E-cadherin and cytokeratin) and increased mesenchymal markers (e.g. Vimentin and alpha-SMA) (Boor and Floege, 2011; Tang et al., 2011; Zella et al., 2013). During this uncontrolled repairing process/lesion formation, TGF-b1 and myofibroblasts cause an excessive accumulation of extracellular matrix (ECM) components such as hyaluronic acid, fibronectin, laminin and collagens, activate metalloproteinases (MMP) expression and production and suppress tissue inhibitors of metalloproteinases (TIM) expression and production (Wynn, 2007; Liu, 2011; Genovese et al., 2014). Another key mediator of fibrogenic response, connective tissue growth factor (CTGF), has also been suggested to contribute to the ECM accumulation. CTGF can activate the RPTECs and fibroblasts to synthesise and secrete several ECM components including fibronectin and type I and IV collagen (Okada et al., 2005; Qi et al., 2005). Additionally, it can also act as a downstream mediator of TGF-b1 in modulating renal fibrogenesis (Okada et al., 2005). Subsequently, the failure in terminating tissue repair process results in the permanent fibrotic lesions, leading to a loss of renal functions and progression to CKD and ESRD.

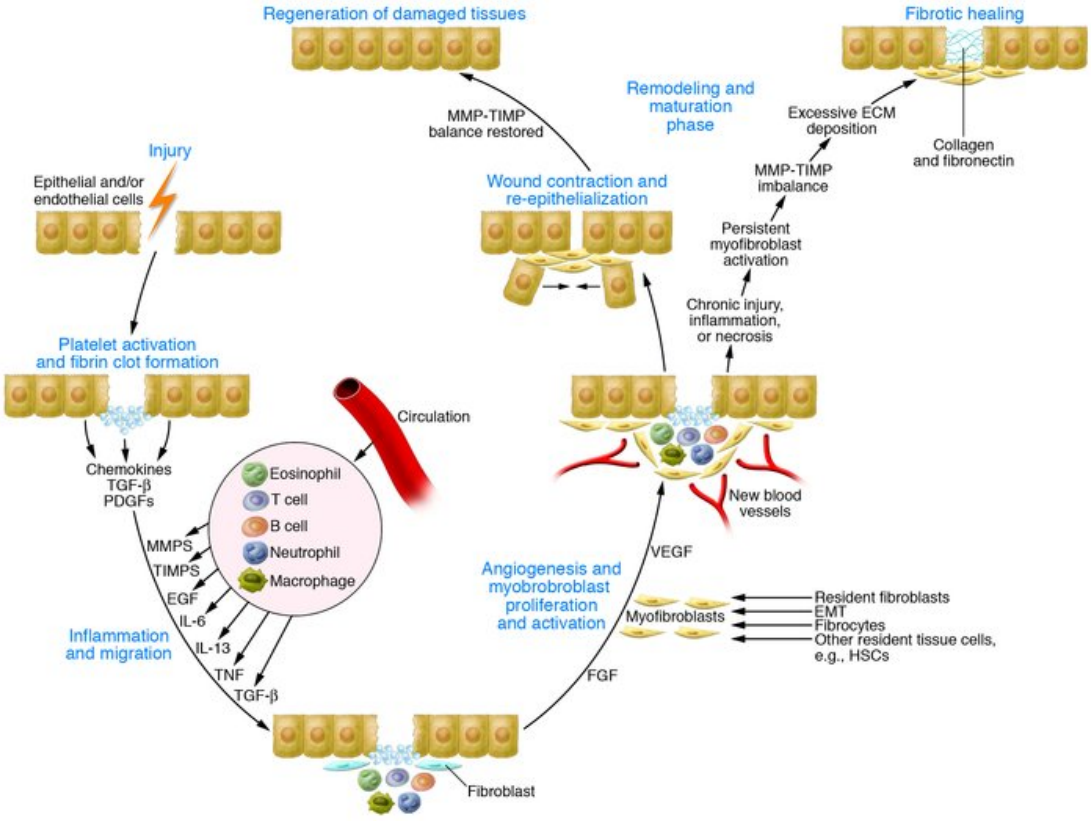


Figure 1. 11 Outcomes of wound healing process in tubular cells after injury.

An adaptive repairing process can lead to tissue regeneration and full recovery; however, an uncontrolled repairing process can cause permanent scar tissue and lead to fibrosis. This diagram was republished from 'Wynn, T. A. (2007) Common and unique mechanisms regulate fibrosis in various fibroproliferative diseases. The Journal of Clinical Investigation, 117, 524-529.' by permission of American Society of Clinical Investigation, conveyed through Copyright Clearance Center, Inc.

1.12 Other strategies for renoprotection

To date there is no specific treatment for AKI except RRT and renal transplantation, but these approaches still do not improve high morbidity and mortality. The ongoing pre-clinical research continues to explore renoprotective strategies and therapeutic targets for AKI. Several key factors involving pathogenesis of AKI including oxidative stress, ER stress, inflammation and degeneration are the main focus for seeking novel treatments. Oxidative stress, as a result of mitochondria dysfunction,

has been known to play a key role in AKI. It has been widely accepted that ischaemia leading to ATP depletion results in mitochondria injury (e.g. swelling and fragmentation) which further enhances ROS production, and upon reperfusion mitochondrial permeability transition pore (MPTP) opening leads to cell death (Brooks et al., 2009). Hence, restoration of functional mitochondria has been suggested to be key to ameliorating I/R injury. This was found to be achieved by treatment of mitochondria targeted superoxide scavenger, Mito-TEMPO, which restored mitochondria function, superoxide dismutase activity and in turn attenuated renal I/R injury in mice (Patil et al., 2014). It was also demonstrated by Jesinkey et al. (2014) that stimulation of mitochondrial biogenesis through beta2-adrenergic receptor by formoterol (drug to treat asthma) after I/R injury diminished necrosis and improved renal function in mice.

The increase in ER stress was also found to be associated with AKI, and there are some potential strategies to target ER stress. ER stress is known to be caused by the accumulation of misfolded proteins, and in mammalian cells the damaged proteins can be resolved by chaperone proteins through refolding and degradation process. It was found that inducing chaperone protein (heat shock proteins) expression by heat stress for 4-8 minutes prior to ischaemia reduced blood urea nitrogen and creatinine level, cast formation and necrotic cell death in rat model of I/R injury (Kelly, Baird and Greene, 2001). Additionally, a direct provision of chaperone protein 4-phenylbutyrate (clinically used drug for urea cycle disorder) in drinking water significantly protected from tunicamycin induced AKI through inhibiting ER stress in mice (Carlisle et al., 2014). Targeting ER stress has been suggested to be a promising strategy for not only I/R injury but also a variety of chronic kidney diseases (Dickhout, Carlisle and Austin, 2014). In addition to targeting these stresses,

accumulated studies have suggested that increasing the kidney resistance to stress by preconditioning or postconditioning strategies (by dietary restriction, acidic infusion, remote ischaemia or pre-treatment with stress inducers) has a profound protection against development of I/R injury induced by surgery (Prachasilchai et al., 2008; Crean et al., 2013; Gallinetti et al., 2013; Saat et al., 2016).

Furthermore, targeting immunity is another potential solution for AKI since inflammation participates in the early stage of injury and contributes to renal degeneration when becoming maladaptive at the chronic phase. After triggering inflammation for clearance of dead cells, the adaptive immune cells such as regulatory T cells are activated to suppress inflammation through modulating other immune cells to promote the recovery process (Maeshima et al., 2015). Studies have found that administration of regulatory T cells or IL-2 to expand regulatory T cells in animal models of I/R injury significantly improved renal function and recovery (Gandolfo et al., 2009; Kim et al., 2013).

In addition to the strategies for attenuating early stage of renal injury, other approaches to prevention from progression to fibrosis and CKD were also investigated. For instance, it is known that hypertension caused by renin-angiotensin system and overactive sympathetic nerve system contribute to progressive loss of renal function (Boor et al., 2007). In particular, studies showed that blockade of the sympathetic nerve system by injection of selective alpha- and beta-blocker at the antihypotension dose through the renal artery protected against the development of renal fibrosis (Amann et al., 2000; Amann et al., 2001; Pawluczyk, Patel and Harris, 2006). Surprisingly, such a protection did not involve reducing blood pressure, and therefore this may exclude the concern of hypotension which is also a contributor to

renal failure. However, it is unknown whether selective alpha- and beta-blocker may affect intraglomerular pressure despite the administration of antihypotension dose. Other strategies by targeting inflammation to ameliorate progression to fibrosis include immunosuppresants (e.g. rapamycin) or cytokine and chemokine receptor antagonists have also been studied (Boor et al., 2007; Chen et al., 2012). However, suppressing immunity can cause side effects such as infection and may limit clinical trials (Boor et al., 2007). Another approach by targeting growth factors including connective tissue growth factor, hepatocyte growth factor and vascular endothelial growth factor has also been found to attenuate development of fibrosis. Among these, inhibition of connective tissue growth factor, a potent fibrotic mediator, has been shown to significantly reduce fibrogenesis in many experimental models such as diabetic nephropathy (Yokoi et al., 2004; Van Nieuwenhoven et al., 2005). Hepatocyte growth factor possesses antifibrotic properties; however, overexpression has been found to exacerbate renal fibrosis and may raise the concern of carcinogenic effects (Wang et al., 2000; Jiang et al., 2005). Vascular growth factor promotes angiogenesis and fibrogenesis, but it remains uncertain whether administration or inhibition may ameliorate fibrosis due to the conflicting experimental results (Kang et al., 2001; Hakroush et al., 2009).

In addition to targeting these key contributors of AKI and fibrosis, other researchers focus on regeneration medicine such as stem cell therapy, which may be beneficial for AKI, fibrosis and CKD. The research of stem/progenitor cell therapy was initiated because some evidence showed that the progenitor cells such as bone marrow derived cells and hematopoetic stem cells may contribute to the regeneration process due to the ability to travel to the injured site and transdifferentiate into functional tubular cells (Lin et al., 2003; Patschan, Patschan and Müller, 2011; Tögel

and Westenfelder, 2012). However, it has been widely confirmed that the major cells for regeneration were surviving tubular cells after sublethal injury (Humphreys et al., 2008). Despite the fact that progenitor cells do not participate in the repairing process, studies have developed stem cell therapy using different cell populations and showed some positive effects on renal recovery in animals. Progenitor populations such as mesenchymal stromal cells, hematopoetic stem cells, endothelial progenitor cells and renal derived progenitor cells have been shown to be beneficial for preserving renal and vascular function and accelerating recovery in animal models of AKI (Patschan et al., 2006; Lazzeri et al., 2007; Li et al., 2010; Wang et al., 2013). However, some negative results were also presented. For instance, administration of hematopoetic stem cells in mice was found to exacerbate renal inflammation (Tögel, Isaac and Westenfelder, 2004). Among these cell population, mesenchymal stem cells are perhaps the most promising population for treatment of AKI. Many studies have consistently reported the beneficial effect on AKI; for instance, mesenchymal progenitor cells protected from AKI when administered upon injury or accelerated recovery when administered after injury (Morigi et al., 2010; Wang et al., 2013).

Although these novel targets and treatments have been identified to be promising for renal diseases in experimental models, there are a number of issues for these treatments to be tested clinically. Since the pathogenesis of renal diseases involves a variety of factor interactions, simply targeting one factor; for example, suppressing inflammation or increasing/inhibiting some mediators, cannot resolve the condition. Rather, it can lead to side effects such as infection, exacerbate disease conditions or raise other concerns such as carcinogenic effects. Cell therapy including administration and expansion of adaptive regulatory T cells and administration of

progenitor cells may hold a great promise for AKI and CKD. However, it still faces numerous challenges such as selection of progenitor cell population, difficulty of cell isolation procedure, limited amount of isolated cells for treatment, undefined route and timing of administration and unaddressed long-term safety (Silver et al., 2015).

Moreover, most preconditioning or postconditioning strategies still face the challenge of controlling an optimal level of stress and therapeutic window. These strategies still need to be validated before becoming clinical applications. Compared with these potential treatments, dietary intervention is non-invasive and readily achievable. Since the nutritional support is indispensible in the clinical practices, manipulation of the dietary requirement becomes essential to achieve an individual's condition. In particular for amino acids, the clinically used formulation is a standardised combination of essential and non-essential amino acids for patients with and without renal diseases. The current knowledge and aims of nutritional support are to maintain protein-energy status and support immunity. However, some amino acids possess other therapeutic properties such as antioxidant, anti-inflammation, vasodilation and promotion of stress response protein expression (Amores-Sánchez and Medina, 1999; Schneider et al., 2003; Basile et al., 2003; Wischmeyer, 2007). Therefore, redesigning the formulation specific for patients with AKI, for instance, increasing concentration of certain amino acids, may be beneficial for recovery. In addition, recent studies have pointed out that clinically used early target macronutrient (increasing amino acid/protein intake) feeding may have to be reconsidered as it did not benefit organ recovery but worsened the clinical outcomes (Vanhorebeek et al., 2011; Casaer et al., 2013). These findings further implicated the necessity of revising nutrition formulation. Moreover, other strategies such as acidic infusion and dietary intervention were also found to be renoprotective, readily

achievable and less invasive and can generate the same effects as those pre-clinical strategies such as tissue conditioning. For example, it was found that acidic infusion and dietary nitrite or nitrate may provide a similar level of protection to ischaemic postconditioning and remote ischaemic preconditioning (RIPC), respectively (Shiva et al., 2007b; Rassaf et al., 2014).

1.13 Acidic infusion

Ischaemic postconditioning, a brief induction of several cycles of ischaemia and reperfusion in the early phase of reperfusion after prolonged ischaemic episode, has been shown to be cytoprotective against I/R injury for many organs in various species (Moradi and Wang, 2013). Its renoprotective effect has been confirmed in animal models of I/R injury (Wever et al., 2012). The mechanisms of cytoprotection by ischaemic postconditioning were not fully understood, but several mediators such as slow return of intracellular pH during reperfusion, increased nitric oxide and other vasodilator production and reduced inflammation have been proposed to be key to its cytoprotective properties (Moradi and Wang, 2013). The mechanism mediated by slow pH return has been an area of special interest for decades.

During tissue ischaemic injury acidosis occurs (pH < or = 7.0), and the tissue pH is abruptly restored back to normal upon reperfusion. Such prompt return of intracellular pH or so-called pH paradox has been known as one of the key mediators to triggering cell death upon reperfusion. Ischaemia may result in a rapid loss of cell integrity and polarity mainly due to the increase in intracellular calcium caused by the ATP depletion and the decrease in intracellular pH (pHi) (Devarajan, 2005; Kalogeris et al., 2012). These structural and functional changes are reversible, and kidney function can be fully recovered if the injury is mitigated (Devarajan, 2006;

Sharfuddin and Molitoris, 2008). After ischaemia, the renal blood flow restoration is crucial for recovery (Chatterjee, 2007). Yet, reperfusion has been found to be rather catastrophic and can lead to a rapid cell death due to a burst ROS generation upon reoxygenation (Sharfuddin and Molitoris, 2008). In addition to the elevated oxygen free radical formation, an abrupt return of extracellular pH to physiological levels is also a key contributor to triggering lethal cell injury during reperfusion as it triggered MPTP opening which released apoptotic factors and initiated apoptotic cascades (Gores et al., 1988; Shanley et al., 1988; Currin et al., 1991; Zager, Schimpf and Gmur, 1993; Weinberg et al., 1994). The potential mechanisms proposed are as follows.

Ischaemia is normally accompanied by acidosis due to the anaerobic metabolism (Kalogeris et al., 2012). The accumulation of hydrogen ions in tissue stimulates the Na^+/H^+ antiporters to excrete excess protons to exchange for sodium ions (Kalogeris et al., 2012). Sodium ions accumulate as Na^+/K^+ ATPase is inhibited due to ATP depletion, resulting in the reduced calcium ion efflux through decreased Na^+/Ca^{2+} exchanger activity or the increase in calcium influx through activating Na^+/Ca^{2+} exchanger (Karmazyn, Sostaric and Gan, 2001; Linz and Busch, 2003). This causes calcium overload in the cytoplasm and mitochondria. At this point, MPTP still remains closed as a result of protons antagonising the calcium triggering sites due to the low pHi (Haworth and Hunter, 1979; Bernardi et al., 1992). Upon reperfusion, the pHi and the mitochondrial membrane potential and respiration were restored to normal in order to drive ATP synthesis, but this also enables the accumulation of calcium and the rapid ROS generation (Crompton, 1999; Carlson, Rao and Yan, 2013). This leads to MPTP opening for the release of calcium and cytochrome c into cytoplasm, triggering apoptotic cascade or necrosis if ATP is depleted (Martinou and

Green, 2001; Zimmermann and Green, 2001).

Recently another mechanism was proposed. Zhang and Lemasters (2013) investigated the mitochondria mediated cell death after I/R injury in the primary culture of the rat hepatocytes. It was proposed that during ischemia ATP depletion inhibited V-ATPase and this caused lysosomal alkalisation which released Fe^{2+} from lysosome to cytoplasm. Reperfusion resulted in Fe^{2+} translocation into mitochondria through mitochondrial calcium uniporters and participated in the free radical generation through the Fenton reaction. The authors also clarified that MPTP-dependent cell death does not occur during ischaemia as it requires the return of oxygen and normal pHi for restoring mitochondrial respiration where ROS is generated. Collectively, these studies indicated that the deleterious effect of reperfusion requires Ca^{2+} and Fe^{2+} overload in mitochondria (via disturbed ionic homeostasis), the prompt return of pHi to physiological levels and subsequent ROS production.

Such cell death caused by the abrupt recovery of pH upon reperfusion could be resolved by ischaemic postconditioning which was reported to maintain acidosis during first few minutes (3-5 minutes) of reperfusion and attenuate mitochondrial mediated cell death (Cohen et al., 2007). Since 1988, many experimental cell work using direct acidic infusion (pH < 7.0) upon reperfusion to mimic ischaemic postconditioning and to induce delayed intracellular pH normalisation to attenuate the abrupt increase in cell death. The efficacy has been demonstrated in heart, liver and kidney cells using a wide range of acidic pH ranging from pH 6.1 to pH 7.0 or slow pH return by adjusting pH of perfusates from pH 6.1 to pH 7.3 (Gores et al.,

1988; Shanley et al., 1988; Currin et al., 1991; Zager, Schimpf and Gmur, 1993; Weinberg et al., 1994).

However, currently studies applying direct acidotic perfusion on animal models of I/R injury are limited. Only a few studies investigated its efficacy in heart I/R injury, but none was yet carried out in renal I/R injury. For instance, Qiao et al. (2013) demonstrated that acidotic perfusion with Krebs bicarbonate buffer at pH 6.9 in rat hearts upon first 3 minutes of reperfusion after 30 minutes of no-flow global ischaemia reduced infarct size and inhibited ROS production by increasing nitric oxide generation through PI3k-Akt-endothelial nitric oxide synthase (eNOS) pathways. Another study by Rodríguez-Sinovas et al. (2009) reported that intracoronary perfusion with Krebs bicarbonate solution at pH 6.4 upon the first 3 minutes of reperfusion in pigs subjected to 60 minutes of coronary occlusion significantly reduced the infarct size. The effect of acidic infusion was found to be equivalent to ischaemic postconditioning, although there was a higher risk of ventricular fibrillation. Both ischaemic postconditioning and application of direct acidotic perfusion remains restricted to experimental studies and are not applied in clinical settings. These strategies still require the knowledge of how to induce an optimal intervention (e.g. the number of cycles, duration and timing of intervention and optimal pH) and meanwhile prevent from adverse effects (e.g. sustained ischaemia and acidosis).

In addition to these mechanisms, recent studies further discovered that cytoprotection by acidic pH may be due to inhibiton of other pathways including mTOR and UPR pathways. The marked activation of mTORC1 upon reperfusion due to the sudden return of nutrients, growth factors and ATP is considered to enhance renal

regeneration and functional recovery (Lieberthal et al., 2006). However, emerging evidence showed that mTORC1 activation mediated a variety of renal diseases including I/R injury and directly contributed to ER stress mediated apoptotic cell death (Prachasilchai et al., 2008; Kato et al., 2012; Dong et al., 2015). The inhibition of mTORC1 activity by mTOR inhibitors was observed to be more protective as a result of induction of autophagy, immunosuppression and anti-inflammation (Declèves et al., 2011; Chen et al., 2012; Wang et al., 2013; Zhang et al., 2014). Furthermore, attenuation of mTOR signalling pathways through dietary restriction, particularly amino acid and protein restriction, also demonstrated a certain level of protection against renal I/R injury in animal models (Mitchell et al., 2010; Verweij et al., 2011; Peng et al., 2012; Robertson et al., 2015). Studies suggested that such protection afforded by nutrient restriction or deprivation (fasting) was due to the increase in cell resistance to oxidative stress after renal I/R injury.

Nutrient (glucose and amino acids) or oxygen deprivation can result in cell death and tissue injuries due to the accumulated oxidative stress in the metabolic organelles such as mitochondria and the ER if prolonged (Crean et al., 2012). However, cells may survive by regulating metabolism for stress adaptation. Under oxidative stress and DNA damage, the important cellular functions including protein synthesis, cell growth and proliferation are downregulated through the inhibition of mTORC1 (Reiling and Sabatini, 2006). Moreover, in mammalian cells the UPR pathways in the ER may also be activated to participate in the protection from stress. Activation of UPR inhibits protein synthesis through downregulation of gene transcription or translation in order to reduce the misfolded protein overload in the ER (Walter and Ron, 2011). It could be the case that ER stress activates UPR which forms a feedback loop to inhibit mTOR, but the interaction between UPR and mTOR still remains

unclear and complicated (Appenzeller-Herzog and Hall, 2012; Kapuy, Vinodb and Bánhegyia, 2014). Collectively, reducing global protein synthesis and protein load in the ER is key to cell survival through stressed condition.

Recently, it was reported that acidic pH could also attenuate cell growth and protein synthesis by inhibiting mTOR signalling pathways as observed in nutrient deprivation. Balgi et al. (2011) showed that reperfusion at acidic pH following starvation interfered with the protein synthesis in MCF-7 human breast cancer cells through the inhibition of growth signalling pathways and Raf/mitogen activated kinases (MEK)/extracellular signal regulated kinases (ERK) of mTOR pathways to negatively affect the energy-consuming anabolic process to respond to metabolic stresses. Marino et al. (2012) suggested that acidic extracellular pH reduced the uptake of amino acids and subsequently inhibited mTOR in melanoma cells. Crean et al. (2013) proposed that acidic pH (pH 6.4) protected against cell death induced by oxygen and glucose deprivation in HK-2 cells through reducing protein synthesis/translation. The authors further observed that acidic pH attenuated UPR activated pro-apoptosis by inhibiting DNA damage inducible transcript 3 (DDIT3) gene mediated by ATF6-CHOP signalling pathway. However, it still remains unknown whether acidic pH is protective against oxidative stresses in renal I/R injury due to the limited literature. The effectiveness was mostly shown in treating heart and liver I/R injury (Kim et al., 2006; Zhang and Lemasters, 2013), and others were mainly associated with cancer research (Balgi et al., 2011; Marino et al., 2012).

1.14 Dietary nitrite, I/R injury and a link to RIPC

The dietary nitrite is another non-inavsive strategy to mimic tissue conditioning, in particular the remote ischemic preconditioning. The principle of RIPC is to induce

brief periods of I/R in the distant organs or tissues to render the target organs more tolerant to the insult of the subsequent ischaemia, and its profound protection in I/R injury has also been well established in many organs including heart (Hausenloy et al., 2007; Heusch et al., 2013; Thielmann et al., 2013), liver (Abu-Amara et al., 2011), small intestine (Sileria et al., 2004) and kidney (Torras et al., 2002). This potentially implicates its promising clinical applications such as an intervention before transplantation surgeries. Rassaf and colleagues (2014) successfully demonstrated the robust protection of RIPC in myocardial I/R injury. The authors proposed that RIPC generated a shear-stress stimulating endothelial nitric oxide synthase (eNOS) in the femoral artery to release nitric oxide (NO) which then was oxidised to nitrite circulating to heart. Circulating nitrite was converted into NO by myoglobin, and NO interfered mitochondrial respiration through S-nitrosation of the mitochondria complex, reducing ROS production and infarct size.

Overall, the increase in circulating and tissue nitrite levels appeared to be the key to the cytoprotection in I/R injury, and this can also be rapidly and readily achieved by oral administration of either inorganic (McKnight et al., 1997; Lundberg and Govoni, 2004) or dietary (Webb et al., 2008) nitrite/nitrate. Shiva and colleagues (2007b) suggested that exogenous administration of nitrate/nitrite could also generate the RIPC-like effect as both shared an identical mechanism involved in NO signalling pathway and provided similar levels of protection. The authors demonstrated that the protection of intraperitoneal injection of nitrite either before or during the subsequent ischemic episode in hepatic I/R injury in mice was as robust as RIPC programme. Accumulated experimental animal data also revealed the therapeutic benefits of exogenous nitrate/nitrite in preventing and treating I/R injury mostly in heart (Zhan et al., 2009), liver (Patel et al., 2005) or brain (Jung et al., 2006), but few studies

were carried out in kidneys and remained controversial. Only one study by Basireddy et al. (2006) showed intraperitoneal administration of nitrate/nitrite solution (0.12, 1.2 and 12 nmol/g body weight) either 15 minutes before or midway through 45 minutes of ischaemia did not protect against renal I/R injury in male Sprague-Dawley rats subjected to left renal pedicle clamping. Intravenous administration of nitrate/nitrite 45 minutes before clamping also did not show any effects. However, a later study by Tripatara et al. (2007) reported that topical administration of nitrite (0.12 nmol/g body weight) onto kidneys 1 minute before reperfusion following 60 minutes bilateral ischaemia attenuated renal injury in male Wistar rats. In contrast, the intravenous injection of nitrite did not show any effects on kidney dysfunction and injury. The authors suggested that the topical route could reach the highest nitrite level in the tissue whereas systematic administration could cause nitrite to be metabolised by deoxyhaemoglobin to NO in the circulation. In 2008, Kanematsu and colleagues also reported that nitrite supplemented in drinking water (0.1, 1 and 10 mg/L) for 8 weeks ameliorated renal injury induced by chronic administration of Nω-Nitro-L-arginine methyl ester hydrochloride (a NO inhibitor) in male Sprague-Dawley rats in a dose dependent manner. The authors found that the medium dose (1 mg/kg) which was lower than the maximum vegetarian dose (0.24 mg/kg in human equals to 2.4 mg/kg in rats) greatly improved kidney function and attenuated renal damage. According to the current understanding of all molecular pathways being proposed, the bioactive form of exogenous nitrate/nitrite; that is, nitric oxide, is the key to the cytoprotection. Hence, we intended to investigate whether the oral administration of sodium nitrite could protect against renal I/R injury.

1.14.1 Metabolism and circulation of nitrate and nitrite

Generally the mammalian cells can endogenously produce NO through catalysing L-arginine (a non-essential amino acid) by nitric oxide synthase (NOS) to regulate physiological functions including vasodilation (Maher et al., 2008), inhibition of platelet aggregation (Radomski, Palmer and Moncada, 1990), neutrophil aggregation (Kubes, Suzuki and Granger, 1991), improvement of cell growth (Contestabile and Ciani, 2004) and inhibition of mitochondrial respiration (Brown, 1999). In the kidney, eNOS serves basal renal vascular control and function through balancing with the effect of renin-angiotensin system and other vasoconstrictor such as acetylcholine by catalysing arginine to produce NO (Forbes et al., 2007). Lacking eNOS by genetic deletion has been evidenced to cause high blood pressure, decreased heart rate and increased plasma renin activity (Huang et al., 1995; Wang et al., 2004). Further, it was demonstrated that genetic deletion of *Nos3* resulted in hypertension and in turn elevated renal arterial pressure and reduced renal blood flow in mice (Wang et al., 2004). Forbes et al. (2007) also showed that *Nos3* knockout mice displayed an abnormal renal structure such as glomerular hypoplasia and tubular cell death despite a normal appearance of renal anatomy. Even if the appearance seems normal, *Nos3* knockout animals appeared to be more susceptible to a variety of renal diseases including AKI, diabetic nephropathy and CKD and have accelerated progression of renal injury (Nakagawa et al., 2007; Nakayama et al., 2009; Nakayama et al., 2010). In addition to genetic inhibition of eNOS, sex hormone difference has been found to be an important determinant of eNOS activity and renal diseases. Studies have identified that eNOS is an essential component that leads to females to be less susceptible to renal I/R injury compared with males. The

female sex hormone, estrogen, has been identified to act via its receptor to activate eNOS through phosphatidylinositol-3 kinase/Akt to induce NO production, contributing to renoprotection (Satake et al., 2008). In contrast, the presence of testosterone in males or administration of testosterone in female animals was found to inhibit NOS activity, leading to the increased susceptibility to ischaemic injury (Park et al., 2004).

In addition to NOS expression and activity, NO bioavailability is also mediated by (6R-)5,6,7,8-tetrahydrobiopterin (BH4), an essential co-factor required for all three NOS isoforms during NO synthesis. NOS enzymes are active as homodimers (Tejero and Stuehr, 2013). Each monomer contains the N-terminal oxygnase domain which binds heme and arginine and the C-terminal which binds flavin adenine dinucleotide, flavin mononucleotide and nicotinamide (Tejero and Stuehr, 2013) (Figure 1.12). BH4 acts to stabilise this dimer structure with its high affinity with NOS enzymes and substrates and may also enhance NOS dimer formation (Klatt et al., 1995; Tejero and Stuehr, 2013). Another important role of BH4 is serving as an electron donor to the ferrous-dioxygen complex for the catalytic reaction (Bendall et al., 2014). After receiving an electron from flavin adenine dinucleotide, BH4 transfers the electron to the heme iron in the oxygenase domain to form an active heme-bound molecule oxygen, which rapidly hydrosylates arginine for NO synthesis (Monens and Kass, 2006; Tejero and Stuehr, 2013) (Figure 1.12). During electron transfer, BH4 is oxidised to trihydrobiopterin (BH3.H+) radical intermediate which is subsequently reduced back to BH4 in the next catalytic cycle by flavins (Bendall et al., 2014).

BH4 bioavailability is strongly correlated to the NO synthesis (Mayer and Werner 1995), and it is profoundly mediated by the balance of biosynthesis/recycling and

degradation (Bendall et al., 2014). It has been shown that oxidative stress in many pathological conditions resulted in the depletion of intracellular BH4 pool due to BH4 oxidation to BH3 or 7,8-tetrahydrobiopterin (BH2), an inactive form of BH4 without co-factor activity (Cunnington et al., 2012; Bendall et al., 2014). BH4 depletion causes NOS enzyme to be uncoupled and converted to monomer, and in the absence of BH4 the electron is transferred directly to ferrous oxygen to form superoxide rather than NO (Takimoto et al., 2005).

As BH4 plays a key role in producing vasoactive molecule to regulate cardiovascular development and homeostasis and organ perfusion, BH4 deficiency has been found to link to a variety of cardiovascular and pulmonary disorders (e.g. cardiovascular dysfunction, hypertension and atherosclerosis pulmonary hypertension) and renal I/R injury (Kakoki et al., 2000; Cunnington et al., 2012; Bendall et al., 2014). It has been shown that treatment with BH4 supplementation can reverse these disease consequences associated with BH4 depletion in experimental models and patients. In experimental models, Kase et al. (2005) showed that BH4 supplementation (20 mg/kg/d in drinking water) for a week improved vascular response to acetylcholine and endothelial relaxation and reduced blood pressure in rat model of hypertension induced by angiotensin-II. Yamamizu et al. (2007) reported that oral administration of BH4 (10 mg/kg/d in food) for 2 weeks significantly improved endothelium dependent relaxation in the aortic segment, decreased blood pressure and superoxide formation and improved kidney function in rats with CKD. Combining BH4 treatment with arginine supplemented in drinking water exerted a synergistic effect on these outcomes. Several clinical studies have also demonstrated that oral or infusion of BH4 supplementation has markedly improved endothelium dependent vasodilation and vessel relaxation in the healthy individuals, elderly and patients

with vascular related diseases and other underlying diseases such as kidney failure. It was found that ingestion of BH4 (10 mg/kg/body weight) increased circulating BH4 and subsequently reduced blood pressure and improved large elastic artery stiffness in the elderly patients with coronary artery disorder (Pierce et al., 2012). Infusion of 500 mg/min BH4 in healthy individuals and patients with hypertension improved the forearm vascular response to acetylcholine and restored endothelium dependent vasodilation (Higashi et al., 2002). Other studies reported that intracoronary infusion of BH4 at low concentration (250 μg/min to 1 mg/min) significantly improved endothelium dependent vasorelaxation in patients with atherosclerosis, coronary artery disease and chronic heart failure (Setoguchi et al., 2001; Fukuda et al., 2002; Woethley et al., 2007)

In addition to the therapeutic effect on cardiovascular diseases, it has been discovered that BH4 supplementation also protected against renal I/R injury. Kakoki et al. (2000) showed that oral administration of BH4 (5 or 20 mg/kg) before 45 minutes of renal artery clamping significantly restored BH4 level in kidney and plasma, NOS activity in kidney and NO production through eNOS in a dose dependent manner in rats. The pretreatment of BH4 improved vasodilation during ischaemia and preserved renal function, as evidenced by the observation of a significant reduction in serum creatinine, urea nitrogen and renal structural damage. The authors also observed that treatment with BH4 1 hour after reperfusion was beneficial on endothelial function. This finding suggested that BH4 treatment may have less restricted therapeutic window, without raising the risk of peroxynitrite formation that worsens tissue damage observed in supplementation of NO substrates after reperfusion (Schwartz et al., 2002). Sucher et al. (2010) also demonstrated that BH4 supplementation (20 mg/kg) intramuscularly 15 minutes before artery clamping

or 15 minutes before organ recovery and revascularisation following transplantation restored tissue BH4 level in rats. The authors reported that treatment of BH4 before ischaemia reduced renal damage and peroxynitrite formation and restored kidney function. Also, BH4 was found to preserve renal capillary and kidney function after transplantation through scavenging peroxynitrite. These data may suggest that BH4 supplementation may be promising for renal I/R injury by improving intracellular BH4 level, NOS catalysis and NO synthesis and scavenging superoxide. Clinical studies are required to support the efficacy of BH4 on renal I/R injury, as most investigations focused on the cardiovascular related diseases.

The bioactive NO is normally oxidised rapidly into nitrite and nitrate to circulate in the blood and tissues, and nitrate/nitrite can also be reduced back to NO by mammalian enzymes (e.g. xanthine oxidase) and recycled (Lundberg et al., 2011) (Figure 1.13). It is important to note that this L-arginine-NOS-NO pathway is an oxidation reaction and therefore requires oxygen as a substrate; hence, under ischaemia/hypoxia NOS will become dysfunctional, reducing NO bioavailability (Garg and Bryan, 2009). In addition to the endogenous pathway, nitrate/nitrite/NO can also be formed exogenously. In fact, the daily diet predominantly contributes to the body nitrite pool (Lidder and Webb, 2012). Over 80% of dietary nitrate comes from vegetables (particularly green leafy vegetables such as spinach and beetroot) with the rest from tap drinking water, and the dietary nitrite is mainly from cured meats which are processed with nitrates/nitrites added as an anti-bacterial agent (Lidder and Webb, 2012). Hence, the main source of nitrite is mainly from dietary nitrate. The ingestion of nitrite/nitrate can facilitate the exogenous NO production without oxygen's participation (Figure 1.13); thus, NO production can still occur during ischaemia or hypoxemia (Webb et al., 2008).

The exogenous nitrate/nitrite circulation and metabolism is as follows. After ingestion, dietary nitrate is first reduced to nitrite by the nitrate reductases produced by commensal anaerobic bacteria in the oral cavity (Lundberg and Weitzberg, 2005). Once swallowed, nitrite is further reduced enzymatically (e.g. XOR, respiratory chain enzymes in mitochondria, haemoglobin or NOS) or non-enzymatically (e.g. gastric acidity, vitamin C or polyphenols) into bioactive NO and other nitric oxides in tissues and the blood (Lundberg et al., 2011). These one-electron reduction pathways to form NO from nitrite are ubiquitous in the tissues and the circulation and are accelerated especially in low oxygen (Lundberg et al., 1994) and acidosis condition (Zweier et al., 1995) which commonly occurs in ischaemic tissues (Sola et al., 2003) (Figure 1.13). This serves as an alternative pathway to compensate the endogenous eNOS-derived NO production when NOS and oxygen supply are impaired during ischaemia/hypoxia (Suschek et al., 2006).

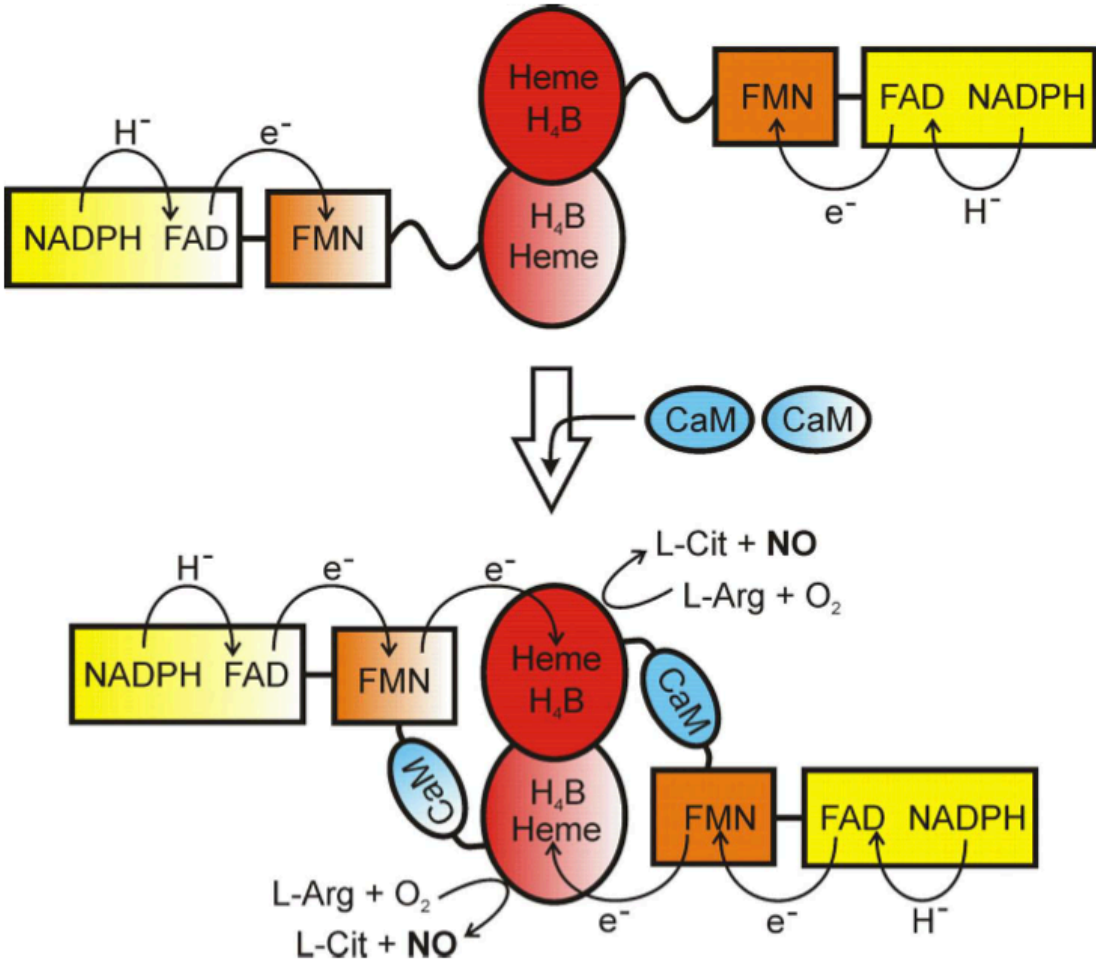


Figure 1. 12 A schematic diagram of active NOS enzyme homodimer and NOS catalysis for NO synthesis.

This diagram depicts an NOS enzyme homodimer and the catalytic reaction for NO synthesis. Each monomer is composed of the N-terminal oxygnase domain that binds heme and arginine and the C-terminal that binds flavin adenine dinucleotide (FAD), flavin mononucleotide and nicotinamide (FMN). BH4 acts to stabilise the dimer structure with its high affinity with NOS enzymes and substrates. After receiving an electron from FMN, BH4 transfers the electron to the heme iron in the oxygenase domain to form an active heme-bound molecule oxygen, which rapidly hydrosylates arginine for NO synthesis. Republished from 'Tejero, J. and Stuehr, D. (2013) Tetrahydrobiopterin in nitric oxide synthase. IUBMB Life, 65(4), 358-365.' by permission of John Wiley and Sons, conveyed through Copyright Clearance Center, Inc.

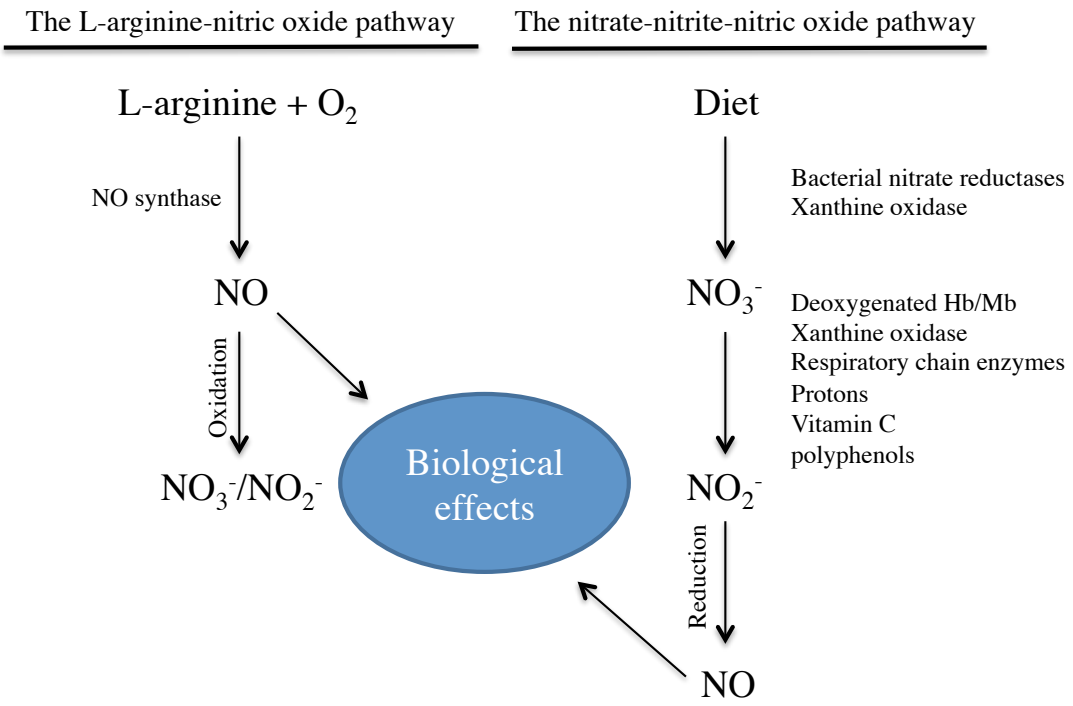


Figure 1. 13 Endogenous and exogenous pathways for NO formation in mammals.

NO can be formed through the endogenous pathway, L-arginine-NOS-NO pathway, which requires oxygen. It can also be formed through the exogenous pathway, nitrate-nitrite-NO pathway, which is a ubiquitous reduction reaction and can occur under ischaemia. NO_3^-, nitrate anion; NO_2^-, nitrite ion. This diagram was adapted and republished from 'Lundberg, J. O., Carlstro ¨m, M., Larsen, F. J. and Weitzberg, E. (2011) Roles of dietary inorganic nitrate in cardiovascular health and disease. Cardiovascular Research, 89, 525-532.' by permission of Oxford University Press.

1.14.2 NO bioavailability and I/R injury

NO is involved in a variety of physiological regulations. In normal kidney, NO is known to mediate the vascular function and renal blood pressure regulation (Majid et al., 2001). A growing body of evidence indicated that the insufficient NO bioavailability was associated with I/R injury and several human vascular dysfunctions (Huang, 2009). However, the nutritional approach to the prevention and the treatment of these diseases may be readily achieved by daily diet or

supplementation. For instance, Bryan et al. (2007) reported that nitrite insufficiency by restricting dietary nitrite (low nitrogen oxide chow) for a week in rats resulted in the deleterious myocardial injury, whereas sodium nitrite or nitrate supplemented in drinking water for a week restored the levels of bioactive nitrogen oxides and reversed the outcome. In 2008, Bryan and colleagues again demonstrated that nitrite supplemented in drinking water could replenish the levels of nitrite and other nitrite oxides in the eNOS knockout mice and protect against heart I/R injury. More recently, Declèves et al. (2016) showed that 5% L-arginine (also a source of NO) supplemented in drinking water for a week protected against ArisA-induced AKI (4 days injection of 2.5 mg/kg ArisA) in mice. The authors showed that arginine improved NO bioavailability, kidney function (decreased plasma creatinine, polyuria and proteinuria) and structure (less tubular injury, apoptosis and necrosis) and reduced oxidative stress (increased antioxidant enzyme level and decreased ROS production). Collectively, these studies suggested that the body pool of nitrite is the critical source to achieve the sufficient NO production for a variety of physiological regulations.

1.14.3 Possible mechanisms of protection by nitrite derived NO

Several mechanisms of nitrite cytoprotection involved in inhibition of mitochondrial respiratory chain have been proposed, although it is not yet fully elucidated. It was proposed that NO may compete with mitochondrial membrane complex IV for electrons and slow down mitochondrial respiration and therefore reduce superoxide formation and also prevent from superoxide reacting with NO to form a more potent reactive nitrogen species such as peroxynitrite (Gryglewski et al., 1986). Recently, emerging evidence suggested that nitrite attenuated ROS generation by blocking

electron flow through electron transport chain through NO-mediated thiol-nitrosation inhibition at complex I and subsequently inhibited MPTP opening and cytochrome c release (Burwell, Nadtochiy and Brookes, 2009; Dezfulian and Shiva, 2009; Raat et al., 2009). In addition, it was found that nitrite could be converted to NO by complex III or IV (also named cytochrome c oxidase) and thereby became competitive with oxygen for the binding site on complexes and therefore inhibited respiration and reduced ROS formation (Shiva et al., 2007a; Hendgen-Cotta et al., 2008; Larsen et al., 2011). Furthermore, some studies showed that nitrite greatly suppressed expression and activity of adenine nucleotide translocase (ANT) which is responsible for MPTP formation during hypoxia and hence had a profound effect on maintaining mitochondrial function (Larsen et al., 2011).

Moreover, other mechanisms being proposed were involved in the enzyme xanthine oxidoreductases. XOR, an enzyme responsible for purine catabolism, converts hypoxanthine (an ATP breakdown product after ischaemia) into xanthine and simultaneously produces H_2O_2 and superoxide (Weight and Nicholson, 1996). Thus, it is generally considered as a key contributor to I/R injury. Interestingly, XOR has been found to play a role in converting nitrite to NO especially in a hypoxic condition (Millar et al., 1998; Harrison, 2002). This was evidenced by many animal studies that inhibition of NO formation by allopurinol, a specific XOR inhibitor, negated the protective effect of nitrite against I/R injury (Li et al., 2003; Lu et al., 2005; Dejam et al., 2007; Tripatara et al., 2007). Webb et al. (2004) also reported that the nitrite supplementation could compete with purine metabolites as a substrate for XOR in I/R injury and suggested that this subsequently shifted a part of XOR activity from generating harmful superoxide to producing protective NO. That is,

nitrite might be able to render XOR less harmful and more protective during I/R injury.

While the formation of S-nitrosothiols of mitochondrial complexes was proposed to be the potential mechanism of protection by nitrite, this was still arguable as it was also shown that these thiol-proteins could lead to more potent oxidation and a rapid increase in superoxide formation (Dahm, Moore and Murphy, 2006). Additionally the role of XOR in AKI in human was argued to be unlikely (Basile, Anderson and Sutton, 2012). Hence, the mechanism of cytoprotection by nitrite was more likely to be the formation of S-nitrosothiols and S-nitrosamines through the reaction of nitrite with haemeproteins in tissues or deoxyhaemoglobin in red blood cells (Duranski et al., 2005). The increase in such a bioactive form of nitrite stored in the tissue and circulation allows NO to readily release and hence protects against I/R injury.

1.15 Summary

The prevalence of AKI is still increasing worldwide, and early detection and prevention are the strategy for managing AKI. To date, there is no specific treatment for AKI except haemodialysis and RRT. However, these treatments can impose a heavy burden on an individual's quality of life in the long term, and the cost can be considerable. Nutritional support for these patients is frequently required, but the nutrient requirement is not yet to be established and is the same as that for critically ill patients. The key concept of renal I/R injury and nephrotoxicity is the increased oxidative stress caused by ROS, which contributes to most human diseases and ageing. Current ongoing research discovered that increasing cell resistance (by means of preconditioning or postconditioning with diet, acidosis, remote ischaemia or stress inducers) prior to exposure to the oxidative stress is critical for cell

adaptation and survival. Several strategies including nutrient restriction and acidosis are identical to clinical trials of ischaemia conditioning and have been proposed to protect against I/R injury. Moreover, increasing the antioxidant capacity is also known to defend oxidative stress associated diseases. Hence, this thesis investigated the effects of putative nutrients including amino acids and sodium nitrite against AKI. The aims of this thesis were to investigate whether amino acid supplementation could rescue human renal proximal tubular cells from a simulated I/R injury and promote recovery and to determine whether acidic pH may be renoprotective in an *in-vitro* model. It was hypothesised that resupply of amino acids at physiological pH exacerbated cell death under oxidative stress following starvation whereas acidic pH may reverse the consequences. This thesis also aimed to examine whether dietary sodium nitrite could protect proximal tubular cells from nephrotoxic drug induced AKI in an *in-vivo* model. It was hypothesised that pretreatment with sodium nitrite could serve as a renoprotection against aristolochic acid induced AKI and prevent from development of tubulointerstitial fibrosis.

Chapter 2: Material and methods

Chapter 2: Material and methods

2.1 Cell culture

All cell culture work was performed using sterile techniques inside an Escoglobal Class II biological safety cabinet (Model AC2-4S1, Esco Micro Pte Ltd., Hoyland, Barnsley, UK).

2.1.1 HK-2 cells

Immortalised adult human proximal tubular epithelial (HK-2) cells were a kind gift from Dr. Karen Price (Institute of Child Health, University College London, London). This cell line was generated by exposing primary proximal tubule cells from the normal adult human renal cortex to the recombinant retrovirus containing human papilloma virus 16 E6/E7 genes (Ryan et al., 1994). While it is a transformed cell line, it still retains differentiated and functional features of human proximal tubular cells and allows to study various pathology of human kidney cells in response to injury and recovery process (Ryan et al., 1994). Cells stored in liquid nitrogen were thawed at 37°C (90% thawed) and were transferred to a T75 cell culture flask containing 13 ml warm media and grown in a 37°C humidified incubator with 5% CO_2. The high-glucose Dulbecco's modified Eagle's medium (DMEM, containing 4500 mg/L glucose and sodium pyruvate without L-glutamine, D6546, Sigma-Aldrich, Poole, Dorset, UK) supplemented with 10% foetal bovine serum (FBS, 10500-064, Gibco, Life Technologies Ltd., Paisley, UK), 100 μg/ml penicillin-streptomycin (11548876, Gibco, Life Technologies Ltd., Paisley, UK) and 1% L-glutamine (25030-024, Gibco, Life Technologies Ltd., Paisley, UK) were used for

culturing HK-2 cells. All supplements were sterile filtered through 0.2 μm syringe filters (Minisart® NML syringe filters 16534----------K, Sartorius Mechatronics UK Ltd., Surrey, UK) into DMEM. Culture media was replaced every 2 days, and cells were normally split after reaching 70-80% confluence and subcultured. To subculture cells, cells were washed in sterile phosphate buffer saline (PBS, phosphate buffer saline tablets, P4417, Sigma-Aldrich, Poole, Dorset, UK). A 2 ml trypsin-EDTA solution (0.25% trypsin-EDTA, Gibco, Life Technologies Ltd., Paisley, UK) was added for 20 seconds, 8 ml complete media was added to terminate the trypsin activity. Cells were spun down at 157 xg for 5 minutes in an Eppendorf 5702R centrifuge (Eppendorf UK Ltd., Stevenage, UK), and the supernatant was discarded. The cell pellet was resuspended in fresh media, and the cell suspension (1 in 10) was added to a new T75 flask containing 13 ml fresh media.

2.1.2 C2C12 cells

The cell culture procedures for mouse myoblast (C2C12) cells were the same as HK-2 cells. C2C12 cell line is a subclone, originally generated through serial passage of myofibroblasts from dystrophic C3H mouse muscle (Yaffe and Saxel, 1977). The C2C12 cells were cultured in the high-glucose DMEM (D5796, containing 4500 mg/L glucose and L-glutamine without sodium pyruvate, Sigma-Aldrich, Poole, Dorset, UK) supplemented with 10% FBS and 100 μg/ml penicillin-streptomycin was used. After reaching 70-80% confluence, cells were split into 1 in 15 and were subcultured.

2.1.3 Simulated I/R and D/R protocol

Cells at 100% confluence were grown 24 hours prior to all experiments. The I/R

injury protocol was conducted according to the MSc dissertation by Liu (2013). It was also similar to the widely used protocol in the published literature where cells were maintained in the nutrient depleted media in hypoxia (1% O_2) followed by incubation in the complete media in normoxia (21% O_2). However, preliminary results by Liu (2013) showed that this protocol did not affect HK-2 cells as the immortalised cell line tends to have high resistance to experimental injury. Hence, exogenous H_2O_2 was included in the reperfusion media to mimic oxidant injury during reperfusion. The exogenous H_2O_2 concentration between 0.01-1 mM has been indicated to directly mimic endogenous release of H_2O_2 in the diseased tissues (Schröder and Eaton, 2008). In the previous study by Liu (2013) 1 mM H_2O_2 was adopted, but it led to lethal cell death in the control group after starvation. To induce a modest/sublethal injury, this thesis adopted 0.5 mM H_2O_2. It is also important to acknowledge that in the later experiments starvation in hypoxia was excluded due to no influence of hypoxia and restricted access to the hypoxic incubator during the study. Nevertheless, the main interest of this thesis is investigate the cellular response to oxidant injury and nutrients following starvation, and this could still be achieved by the nutrient deprivation/replenishment (D/R) protocol.

To carry out a simulated I/R injury protocol, cells were maintained in the sterile Hank's balanced salt solution (HBSS, 14025-050, Gibco, Life Technologies Ltd., Paisley, UK) in a 37°C humidified hypoxic incubator (containing 1% O_2 and 5% CO_2) for 24 hours followed by 24 hours of treatment with amino acid supplementation (AAS, 50x MEM amino acids, 11130-036, Gibco, Life Technologies Ltd., Paisley, UK) with or without 0.5 mM H_2O_2 (hydrogen peroxide solution, H-1009, Sigma-Aldrich, Poole, Dorset, UK) in a 37°C humidified normoxic incubator (containing 21% O_2 and 5% CO_2). For the nutrient depletion/replenishment

(D/R) protocol, confluent cells were maintained in sterile HBSS in a 37°C humidified normoxic incubator (containing 21% O_2 and 5% CO_2) for 24 hours followed by resupply of nutrients in a 37°C humidified normoxic incubator (containing 21% O_2 and 5% CO_2) for the indicated periods. Figure 2.1 depicted the experimental protocols.

The MEM amino acid solution utilised for reperfusion media is commercially formulated to contain 50x the essential amino acids found in the complete DMEM (Thermo Fisher Scientific, 2016), but it is exclusive of glycine, L-glutamine and L-serine (Table 2.1). These three amino acids were excluded in the study, as the transformed and cancer cell lines can use these amino acids as substrates through metabolic reprogramming to synthesise energy and antioxidants such as glutathione to rapidly proliferate and survive through hypoxic and glucose deprived conditions (Metallo et al., 2011; Jain et al., 2012; Maddocks et al., 2012; Tanava et al., 2013). The 1x AAS is almost equivalent to the amount of essential amino acids found in the standard DMEM. The provision of AAS during reperfusion for 24 hours was to mimic clinical condition where patients with restored renal blood were administered with parenteral or enteral nutrition after I/R injury.

Any treatments were prepared in sterile hoods. AAS treatments were prepared by adding 0, 0.5 and 1 ml sterile amino acid supplements to each tube with and without 0.5 mM H_2O_2, and sterile HBSS was added to make up to 50 ml. In some experiments, cells were treated with 10% FBS, 25 mM glucose (G7528, Sigma-Aldrich, Poole, Dorset, UK), 1% insulin-transferrin-selenium (ITS, ITS-G 100x, 41400045, Gibco, Life Technologies Ltd., Paisley, UK) and 52 μg/ml L-leucine (L5652, Sigma-Aldrich, Poole, Dorset, UK) in HBSS for 15 and 60 minutes after 24

hours of starvation. The concentration for these nutrients to serve as a positive control for mTOR signalling was chosen according to the published literature and was known to stimulate mTOR signalling after starvation in renal tubular cells such as HK-2 cells and human embryonic kidney cells (Ramírez-Rangel et al., 2011; Velagapudi et al., 2011). Cells treated with 100 nM rapamycin (R8781, Sigma-Aldrich, Poole, Dorset, UK) or 0, 2.5, 5 and 10 μg/ml tunicamycin (T7765, Sigma-Aldrich, Poole, Dorset, UK) for 24 hours (unless specified) at the 37°C served as positive controls.

In some experiments, a biological buffer, 10 mM 4-(2-hydroxyethyl)piperazine-1-ethanesulfonic acid (HEPES, H3375, Sigma-Aldrich, Poole, Dorset, UK) was added to buffer AAS. Following preparation, a concentrated (31.5-33.0%) hydrochloric acid solution (HCl, 11483703, Fisher Scientific Ltd., Loughborough, Leicestershire, UK) and 2 M potassium hydroxide (KOH, P/5640/60, Fisher Scientific Ltd., Loughborough, Leicestershire, UK) solution were used for final adjustment of treatment pH with a Microprocessor pH meter (P210, Hanna Instruments Ltd., Leighton Buzzard, Bedfordshire, UK). All treatments were sterile filtered through 0.2 μm syringe filters into sterile tubes before adding to cells. The buffering systems and pH values were stated in the results.

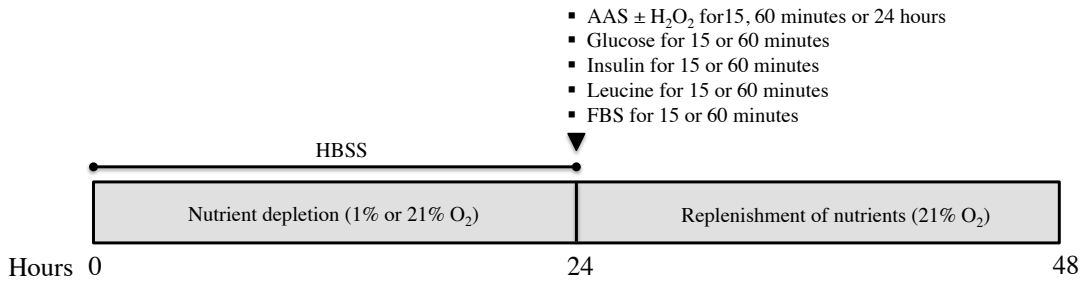


Figure 2. 1 The diagram depicts experimental protocols for I/R and D/R injury.

Confluent cells were maintained in HBSS for 24 hours in a hypoxic or normoxic incubator for nutrient depletion followed by resupply of nutrients for the indicated periods in a normoxic incubator.

Table 2. 1 Comparison of amino acid contents between 50x MEM essential amino acid solution and the complete 1x DMEM.

	50x MEM amino acid solution	**Complete 1x DMEM**
Amino acids	Concentration (mg/L)	Concentration (mg/L)
L-Arginine hydrochloride	6320.0	84.0
L-Cystine	1200.0	62.6
L-Glutamine	-	584.0
Glycine	-	30.0
L-Histidine hydrochloride-H_2O	2100.0	42.0
L-Isoleucine	2620.0	105.0
L-Leucine	2620.0	105.0
L-Lysine hydrochloride	3625.0	146.0
L-Methionine	755.0	30.0
L-Phenylalanine	1650.0	6.06
L-Serine	-	42.0
L-Threonine	2380.0	95.0
L-Tryptophan	510.0	16.0
L-Tyrosine	1800.0	103.8
L-Valine	2340.0	94.0

This table shows the content of amino acids in MEM essential amino acid solution and in the complete DMEM. MEM essential amino acid solution contains 50x the essential amino acids found in the complete DMEM except glycine, L-glutamine and L-serine.

2.1.4 MTT assay

MTT assay is a widely used, inexpensive and simple colourimetric assay to indirectly determine viable cell numbers. However, the amount of signal detected depends on

the cell metabolic activity as MTT measures the activity of mitochondria enzyme, NADPH dependent cellular oxidoreductase (Riss et al., 2013). The change of culture condition such as nutrient deprivation or cell line with lower metabolic activity can influence the MTT results (Riss et al., 2013). Hence, such an imperfection in determining cell viability has been argued. Other commonly used techniques for directly measuring viability are trypan blue, propidium iodine, LDH release assay and calcein AM. While these methods have the advantage of exclusion of viable cells from dead cells, some are costly and require cell counting which generates variable results, high content imaging or flow cytometry for an accurate quantitative analysis. Compared with other methods, MTT may provide a simpler and effective measurement for our study since we only investigated single cell line. Also, HK-2 cells are highly metabolically active to allow detection of signals.

Cells at 100% confluence were plated in 96-well cell culture plates, and a simulated I/R or D/R protocol (2.1.3) was carried out. The Vybrant MTT [3-(4,5-dimethylthiazol-2-yl)-2,5-diphenyl-2H-tetrazolium bromide] cell proliferation assay kit (V13154, Gibco, Life Technologies Ltd., Paisley, UK) was used according to the manufacturer's protocol. The treatment media was replaced with 100 μl HBSS in each well, and 10 μl of 12 mM MTT was added to each well (except negative controls). After incubation at 37°C for 4 hours, 85 μl was removed from each well. A 50 μl dimethyl sulfoxide (DMSO, 154938, Sigma-Aldrich, Poole, Dorset, UK) was added to each well and mixed thoroughly followed by incubation at a 37°C for 10 minutes. The plate was then read on a Model 680 XR microplate reader (Bio-Rad Ltd., Watford, Hertfordshire, UK) at an absorbance of 550 nm. A negative control of HBSS with DMSO alone was also performed. Each treatment had triplicates per plate and was repeated on three plates for an n = 3. Data were presented as a

percentage of mitochondrial function (%) with respect to the control (HBSS treated cells after starvation in each condition. The formula for calculation was as follows.

Mitochondrial function (%) = [(absorbance of treated cells - absorbance of negative control)/(absorbance of control cells - absorbance of negative control)] × 100.

2.1.5 Immunocytochemistry

Confluent cells cultured on 16-mm circular glass coverslips (631-0152, VWR International Ltd., Lutterworth, Leicestershire, UK) were fixed with 4% paraformaldehyde (PFA, P/0840/53, Fisher Scientific Ltd., Loughborough, Leicestershire, UK) in PBS for 15 minutes at room temperature and washed in PBS three times. Cells were permeabilised with 0.1% Triton X-100 (93420, Sigma-Aldrich, Poole, Dorset, UK) in PBS for 15 minutes followed by three times wash in PBS. For assessing the filamentous actin (F-actin) cytoskeleton, Alexa Fluor 555-phalloidin (A34055, Invitrogen, Life Technologies Ltd., Paisley, UK, 1:100) diluted in PBS was applied and left at room temperature in the dark for 2 hours. For the detection of total mTOR, cells on coverslips were blocked with 5% bovine serum albumin (BSA, 11423164, Sigma-Aldrich, Poole, Dorset, UK) in PBS for 1 hour at room temperature followed by incubation with (7C10) rabbit mAb mTOR (#2983, Cell Signaling Technology, New England Biolabs (UK) Ltd., Herts, UK, 1:100) in 5% BSA at 4°C in the dark overnight. Cells were washed in PBS three times, and fluorescein isothiocyanate isomer 1 (FITC)-conjugated swine anti-rabbit immunoglobulins (F0205, Dako UK Ltd., Stockport, Cheshire, UK, 1:100) in 5% BSA was applied as a secondary antibody to mTOR for 1 hour at room temperature in the dark. After incubation with antibodies, cells were washed three times in PBS. Coverslips were mounted on microscope glass slides (Adhesion slides, Polysine®,

VWR International Ltd., Lutterworth, Leicestershire, UK) with Vectashield Hardset mounting medium containing 4',6-diamidino-2-phenylindole (DAPI, H-1500, Vector Laboratories Ltd., Peterborough, UK) and stored at 4°C in the dark overnight and at room temperature in the dark thereafter. It is important to note that a positive control (performing the staining on the sample which significantly expresses the protein of interest) and a negative control (carrying out the same protocol without addition of primary antibody) should be included in each experiment to ensure the efficiency of the primary antibody and to confirm that the secondary antibody does not nonspecifically bind to cellular compartments. However, these were not performed in this thesis.

2.1.6 Calcein AM assay

According to the manual from Life Technologies, the live cells can take up and covert non-fluorescent calcein AM (C3099, Gibco, Life Technologies Ltd., Paisley, UK) into green fluorescent calcein by intracellular esterases. Therefore, this dye can be used for determining cell viability by exclusion of dead cells from live cells. This assay was performed to confirm MTT assay. Cells at 100% confluence were grown in black-walled 96-well plates with clear bottoms 24 hours before the experiment, and simulated I/R or D/R protocol (2.1.3) was performed. Cells were washed in HBSS and then incubated with 2 μM calcein AM in HBSS at a 37°C humidified incubator for 30 minutes.

2.1.7 ROS measurement

There are several reagents for detecting intracellular ROS production, such as dihydroethidium, MitoSOX Red and CM-H_2DCFDA. Dihydroethidium is commonly

used for detecting cytosolic superoxide anions, peroxynitrite and hydroxyl radicals. MitoSOX Red is derived from dihydroethidium, and it directly measures superoxides in mitochondria matrix (Wojtala et al., 2014). However, there is a concern of cytotoxicity and mitotoxicity for the utility of both probes (Wojtala et al., 2014). It was also found that these ROS indicators often generate unspecific oxidation products which further require high performance liquid chromatography based analysis to separate the unspecific products for interpreting results (Nazarewicz, Bikineyeva and Dikalov, 2013). The dye CM-H_2DCFDA mainly probes intracellular hydrogen peroxide and a broad range of ROS such as hydroxyl radicals, carbonate radicals and thiol radicals, and it has been suggested to detect general intracellular oxidative stress (Wojtala et al., 2014). Compared with other indicators, this probe provides a simpler and effective ROS measurement. Also, after being improved by the manufacturer, this dye can retain inside the live cells after oxidation reaction with ROS longer than other ROS indicators and hence benefits the long-term study.

Therefore, the cellular oxidative stress was estimated by detecting intracellular ROS generation using fluorescent dye CM-H_2DCFDA (C6827, Invitrogen, Life technologies Ltd., Paisley, UK). According to the manufacture's manual, this fluorescent dye can be taken up by cells and usually deacetylated by intracellular esterases. Subsequent oxidation of H_2DCF leads to fluorescent dichlorofluorescein which retains within the cells and can be visualised and detected. Cells at 100% confluence were grown in black-walled 96-well plates with clear bottoms 24 hours prior to the experiment. After 24 hours of starvation with HBSS in normoxia and hypoxia, cells were treated with bicarbonate buffered AAS containing 5 μM CM-H_2DCFDA with or without 0.5 mM H_2O_2 and incubated at 37°C for 120 minutes. The CM-DCF fluorescence was determined using a FLUORstar OPTIMA microplate

reader at an excitation wavelength of 485 nm and an emission wavelength of 520 nm at 0, 10, 30, 60, 90 and 120 minutes. Each treatment had triplicates per plate and was repeated on three plates for an n = 3. The background readings were removed by subtracting negative control (cells without dye). For measuring the ROS formation in AAS solutions with or without 0.5 mM H_2O_2, 5 μM dye was added to bicarbonate buffered AAS at pH 7.5 and incubated for 120 minutes at 37°C. The CM-DCF fluorescence was also measured at 0, 10, 30, 60, 90 and 120 minutes. Each treatment had twelve wells in a plate and was repeated on three plates for an n = 3.

2.1.8 Mitochondrial and lysosomal morphology

MitoTracker® Red CMXRos (9082S, Cell signaling Technology, New England Biolabs (UK) Ltd., Herts, UK) and LysoTracker® Red DND-99 (L7528, Thermo Fisher Scientific, Paisley, UK) were used to probe mitochondria and lysosomes in live cells, respectively. Cells at 100% confluence were grown on 16-mm coverslips. In some experiments, cells were incubated with 100 nM Mitotracker diluted in warm HBSS at 37°C for 15 minutes following a simulated D/R protocol (2.1.3). For detecting co-localisation of mTOR and Mitotracker or Lysotracker, 100 nM Mitotracker was added to cells 15 minutes before the end of treatments, whereas 1 μM Lysotracker was incubated with treatments at 37°C for 1 hour. Cells were washed three times in cold PBS, and the immunocytochemistry procedure (2.1.6) was performed.

2.1.9 Western blot analysis

Cells at 100% confluence were grown in 6-well cell culture plates prior to experiments, and a simulated D/R protocol (2.1.3) was carried out. Each treatment

had triplicates and was repeated on three plates for an n = 3. To extract proteins, cells were washed twice in iced-cold PBS and lysed with 200 μl/well of 1x sodium dodecyl sulfate (SDS) buffer containing 2% (w/v) SDS, 5% DL-Dithiothreitol (DDT, D9779, Sigma-Aldrich, Poole, Dorset, UK), 10% glycerol (G5516, Sigma-Aldrich, Poole, Dorset, UK), 0.0625 M Tris-HCl (pH 6.8), 5 mg bromophenol blue (53H3640, Sigma-Aldrich, Poole, Dorset, UK), 1% protease inhibitor cocktail (cOmplete, 11697498001, Sigma-Aldrich, Poole, Dorset, UK) and 1% phosphatase inhibitor cocktail (PhosSTOP, 04906837001, Sigma-Aldrich, Poole, Dorset, UK). Cells were scraped into microcentrifuge tubes and left on ice. Whole Cell lysates were heated up at 95°C for 5 minutes, spun down at 15,588 xg for 3 minutes in a Microfuge® 22R microcentrifuge (Beckman Coulter UK Ltd., High Wycombe, UK) and left on ice.

Total protein concentrations in all samples were determined using 2D-Quant kit (80-0483-56, GE Healthcare Life Sciences, Little Chalfont, Buckinghamshire, UK) according to the manufacturer's protocol as follows. Standard solutions were prepared using 2 mg/ml bovine serum albumin stock solution provided from the kit to generate 0, 10, 20, 30, 40 and 50 μg/ml of protein standards. A 10 μl cell lysates of each sample was transferred to a new microcentrifuge tube. A 500 μl precipitant and 500 μl co-precipitant were added to each tube, briefly mixed with a vortex and then spun down at 9,224 xg for 10 minutes at 4°C in a Microfuge 22R® microcentrifuge to precipitate protein. Supernatants were removed carefully with a micropipette. All samples were spun down again at 9,224 xg for 5 minutes at 4°C, and supernatants were discarded completely. The precipitated protein pellets were dissolved in 100 μl copper solution and 400 μl dH_2O and mixed with a vortex. A 500 μl working colour reagent (colour reagent A:B = 100:1) was added to all tubes and mixed well with a vortex. Each sample was transferred to a disposable polystyrene

cuvette (67742, Sarstedt Ltd., Nümbrecht, Germany). The absorbance was measured at 480 nm with an Ultrospec™ 2100 pro UV/visible spectrophotometers (Amersham, GE Healthcare Life Sciences, Little Chalfont, Buckinghamshire, UK). A linear standard curve was generated by the absorbance of protein standards against concentration to determine total protein concentrations of all samples. All samples were then normalised with 1x SDS loading buffer.

Equal amount of proteins from each sample (15 μg per lane) and 8 μl protein ladder (1610373, Bio-Rad Ltd., Watford, Hertfordshire, UK) were loaded on a 4-15% Criterion™ TGX™ Precast Midi protein gel (5671085, Bio-Rad Ltd., Watford, Hertfordshire, UK). Proteins were separated by running the gel in Tris/Glycine/SDS buffer (EC-870, National Diagnostics Ltd., Nottingham, UK) in a Ctiterion™ cell (Bio-Rad Ltd., Watford, Hertfordshire, UK) at 200 V for 35 minutes. A transfer sandwich was assembled with a gel holder cassette, 3 fibre pads, 4 filter papers, a nitrocellulose membrane (Amersham Protran Supported 0.45 NC, 10600018, Amersham, GE Healthcare Life Sciences, Little Chalfont, Buckinghamshire, UK) and a protein gel, without generating any bubbles. The protein gel was placed on the cathode, and the nitrocellulose membrane was placed on the anode. The transfer sandwich was then placed into a Transfer-Blot® cell (Bio-Rad Ltd., Watford, Hertfordshire, UK) with a cooling system and ran in the transfer buffer made up of 30% glycine (G/P460/53, Fisher Scientific Ltd., Loughborough, Leicestershire, UK), 3% Tris-base (BP152-1, Fisher Scientific Ltd., Loughborough, Leicestershire, UK) and 10% isopropanol (P/7500/17, Fisher Scientific Ltd., Loughborough, Leicestershire, UK) at 0.5 A for 2 hours. It was run at 1.0 A for 2 hours for transferring total mTOR protein due to the high molecular weight. The membrane was stained with Ponceau S solution to confirm that proteins were successfully

transferred from gel to nitrocellulose membrane. The membrane was cut based on the desirable molecular weights and rinsed in 1x Tris buffer saline (containing 7.2 g NaCl and 0.016 M Tris-base in 1 L dH_2O at pH 7.5) with 0.1% Tween 20 (TBST) followed by blocking in 5% Marvel instant dried skimmed milk (Premier Brands UK Ltd.)/TBST at room temperature for 1 hour. Membranes were then incubated with appropriate primary antibodies in 5% instant dried skimmed milk/TBST at 4°C overnight on a rocker and were washed in TBST for 30 minutes with several changes of TBST. Membranes were incubated with appropriate secondary antibodies in 5% skimmed milk/TBST for 2 hours at room temperature on a rocker. It is noted that antibodies were prepared in 5% BSA/TBST for detecting phosphorylated proteins. Membranes were washed in TBST for 30 minutes with several changes of TBST. ECL western blotting detection reagent (RPN2209, Amersham, GE Healthcare Life Sciences, Little Chalfont, Buckinghamshire, UK) was applied on membranes for 1 minute, and excess liquids were tapped off. Membranes were placed on a Hypercassette (Amersham, GE Healthcare Life Sciences, Little Chalfont, Buckinghamshire, UK) and then developed on Amersham Hyperfilm ECL (28906837, Amersham, GE Healthcare Life Sciences, Little Chalfont, Buckinghamshire, UK). Films were then immersed in a Kodak GBX developer solution (1900984, Carestream Health Ltd., Hemel Hempstead, Hertfordshire, UK), rinsed with tap water, immersed in an Ilford Hypam rapid film fixer solution (1758285, Ilford Photo, Harman Technology Ltd., Mobberley, Cheshire, UK), rinsed again with tap water and air dried.

Primary antibodies (1:1000) were as follows: anti-β-actin (A1978, Sigma-Aldrich, Poole, Dorset, UK), Vimentin XP (D21H3) rabbit mAb Alexa Fluor 488 conjugate (9854, Cell Signaling Technology, New England Biolabs (UK) Ltd., Herts, UK),

phospho-S6 ribosomal protein (Ser235/236) (D57.2.2E) XP® rabbit mAb (#4858, Cell Signaling Technology, New England Biolabs (UK) Ltd., Herts, UK) and S6 ribosomal protein (54D2) mouse mAb (#2317, Cell Signaling Technology, New England Biolabs (UK) Ltd., Herts, UK), phospho-p70 S6 kinase (Thr389) antibody (#9205, Cell Signaling Technology, New England Biolabs (UK) Ltd., Herts, UK), p70 S6 kinase (49D7) rabbit mAb (#2708, Cell Signaling Technology, New England Biolabs (UK) Ltd., Herts, UK) and (7C10) rabbit mAb mTOR. Secondary antibodies (1:5000) were as follows: Amersham ECL sheep HRP-conjugated anti-mouse IgG secondary antibody (NA931, Amersham, GE Healthcare Life Sciences, Little Chalfont, Buckinghamshire, UK) and Amersham ECL donkey HRP-conjugated anti-rabbit IgG secondary antibodies (NA934, Amersham, GE Healthcare Life Sciences, Little Chalfont, Buckinghamshire, UK).

2.2 Kidney tissue sections

2.2.1 Animals and experimental design

All animal procedures were conducted by Dr. Simon Welham and animal technicians. All procedures were performed in accordance with the UK Animals (Scientific Procedures) Act, 1986 and were approved by the local ethical review committee of the University of Nottingham. This was a blind study where the treatment information was kept from the participants until any experimental data were obtained, and the animal codes representing treatments were then decoded for statistical analysis.

While male mice are frequently preferred in renal research due to high susceptibility to I/R injury, this thesis selected female mice as an experimental model with an

intention of inducing a modest injury (without an overt damage) which can be recovered by dietary intervention. The utility of ICR outbred strain is to mimic human population which is genetically variable. One hundred sixty-four female ICR outbred mice at the age of 6-8 weeks from 40 litters were separated into two groups receiving either drinking water (n = 79) or drinking water supplemented with 1 mM $NaNO_2$ (n = 85) (CHE5938, Scientific Laboratory Supplies Ltd., Nottingham, UK) for 24 hours. The concentration of $NaNO_2$ was chosen according to the literature. The commonly used therapeutic dose of dietary inorganic nitrate/nitrite ranges from 0.1 to 1.0 mmol/kg/d for various cardiovascular related diseases and renal I/R injury (Lundberg et al., 2011). In the study by Kanematsu et al. (2008), a very low dose of nitrite in drinking water (1 mg/L) protected against renal injury induced by chronic NOS blockade. Most studies investigated the effect of chronic administration (over 3 days to weeks) of dietary nitrite/nitrate (Lundberg et al., 2011). However, it is important to note that dietary nitrite is readily absorbed and distributed in most tissues and that nitrite bioavailability reaches 95-98% within 1 hour after ingestion (Bryan et al., 2005; Hunault et al., 2009). Therefore, the dose and duration of sodium nitrite used in this thesis may theoretically achieve sufficient nitrite bioavailability prior to subsequent injury. In fact, some mice (n = 42) were sacrificed after nitrite administration for plasma nitrite measurement, but it was not performed due to the equipment and time restriction. Each group was then intraperitoneally injected with 100 μl volume of saline/PBS (n = 58) or 5 mg/kg ArisA (n = 64) (A5512, Sigma-Aldrich, Poole, Dorset, UK) for 24 hours and sacrificed, with some mice (n = 63) once injected with 100 mg/kg 5-bromo-2'-deoxyuridine (BrdU, B5002, Sigma-Aldrich, Poole, Dorset, UK) to label S-phase cells 24 hours prior to sacrifice. The remaining animals (n = 59) were sacrificed 5 weeks thereafter (Figure 2.2). The dose

of ArisA was selected according to the study by Yang et al. (2010), and it should theoretically induce AKI at the early stage and tubulointerstitial fibrosis at the chronic phase. While the dose and duration of these drugs and supplementation were selected according to the literature, a pilot study which was not performed in this thesis should be carried out before the experimental trial.

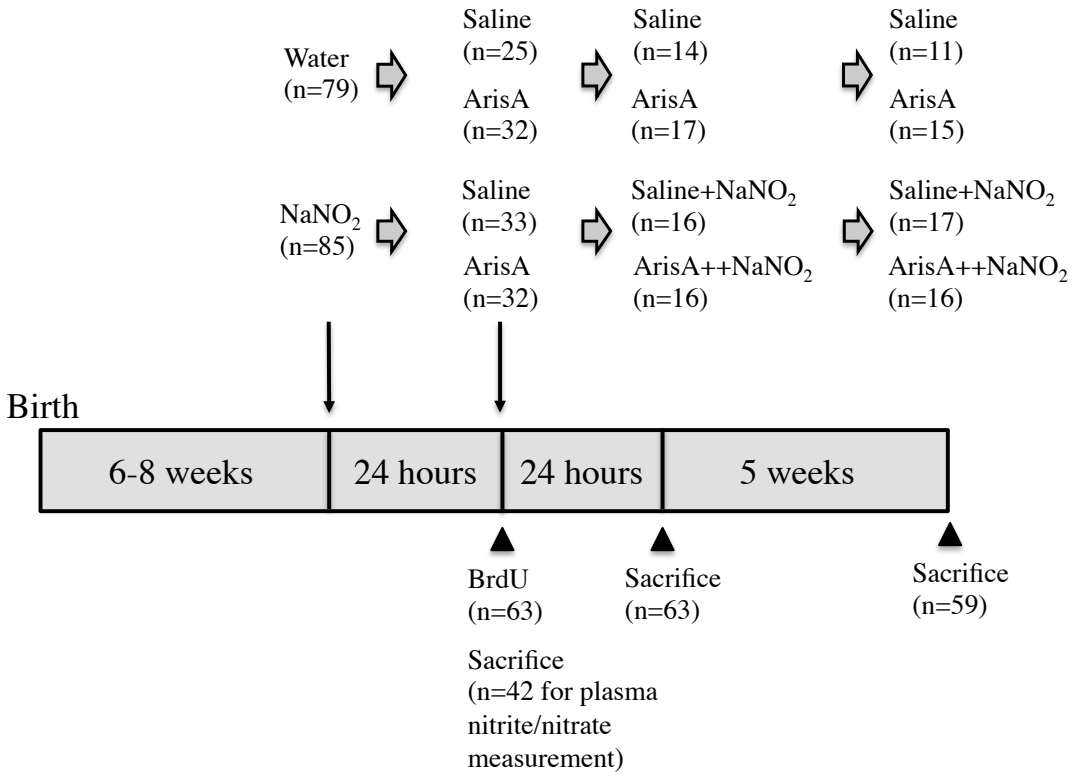


Figure 2. 2 The diagram shows the experimental design and protocol.

Mice at the age of 6-8 weeks were given drinking water or drinking water supplemented with 1 mM $NaNO_2$ for 24 hours followed by injection of saline or 5 mg/kg ArisA. After 24 hours, mice were sacrificed, with some injected with 100 mg/kg BrdU 24 hours prior to sacrifice. The remaining animals were sacrificed 5 weeks thereafter.

2.2.2 Kidney processing and paraffin-embedding

The female mouse kidney sections was prepared by technicians in the department. For preparing paraffin-embedded whole mouse embryo blocks, 4% PFA-fixed mouse

embryos provided by Dr. Simon Welham were processed manually as follows. The mouse embryos were to serve as a positive control of anti-Histone H3 labelling.

Tissues fixed with 4% PFA in PBS were washed three times for 20 minutes each in PBS until fixative was completely removed. Tissues were dehydrated in 70% ethanol (10437341, Fisher Scientific Ltd., Loughborough, Leicestershire, UK) for at least 4 hours or overnight followed by dehydration in 80%, 95% and 100% ethanol for 15 minutes each at room temperature. Tissues were then maintained in Histoclear, a hydrophobic clearing agent, for 30 minutes to replace ethanol and left in clean Histoclear overnight at room temperature. Paraffin wax was molten in a 60°C incubator, and tissues were maintained in the liquefied paraffin wax for 30 minutes twice in a 60°C incubator to replace Histoclear. Tissues were transferred to a mold and were covered with fresh paraffin wax, and the mold was left on the hot platform of a Leica EG1660 embedding centre (Leica Biosystems Ltd., Milton Keynes, UK) to maintain paraffin wax liquefied. Tissues were oriented as desired before hardening (placed in the middle and oriented the desired cut surface down in a mold). A cassette was placed on top of the wax surface, and fresh molten wax was filled in until covering the space on top of the cassette**.** The whole set was then placed on the -4°C platform of a Leica EG1660 embedding centre, and a tissue block can be detached from a mold once solidified and stored at 4°C thereafter.

2.2.3 Sectioning

Before sectioning, all tissue blocks were placed on ice to cool down to improve sectioning results. A steel blade (3050835, MB35 premier disposable microtome blade, Thermo Fisher Scientific, Paisley, UK) mounted on a Leica RM2235 manual microtome (Leica Biosystems Ltd., Milton Keynes, UK) was used to trim 5-10 μm

wax off until the tissue was exposed. Tissue blocks were then cut into 5 μm sections which were transferred with a brush and a forceps onto a few drops of 30% ethanol on a glass plate to flatten the section appropriately. Tissue sections were left on 40°C clean water in a Leica HI1210 water bath (Leica Biosystems Ltd., Milton Keynes, UK) surface until flattened. A microscope glass slide was vertically placed into water and vertically removed from water until a section was mounted on it. Excess water from beneath sections was drained by vertically placing slides, and slides were dried flat on a 40°C Leica HI1220 flattening table (Leica Biosystems Ltd., Milton Keynes, UK) for 10 to 20 minutes. All slides can be stored at room temperature indefinitely.

2.2.4 Renal histology

Sections were deparaffinised with two changes of Histoclear (HS-202, Histo-Clear II, National Diagnostics Ltd., Nottingham, UK) for 15 minutes each. Slides were immersed in 100%, 90%, 70% and 50% ethanol and tap water twice for 1 minute each, respectively. Slides were immersed in Harris haematoxylin (230-D, Raymond A Lamb Ltd., Eastbourne, UK) for 15 minutes and were rinsed in a running tap water for 15 minutes. Sections were differentiated in 1% acid ethanol (1% HCl in 70% ethanol) for 30 seconds followed by rinsing in dH_2O. Slides were immersed in eosin Y 0.5% alcoholic solution (102439, Merck Millipore Ltd., Watford, Hertfordshire, UK) for 30 minutes and then rinsed in dH_2O for 1 minute. Sections were dehydrated in 95% and 100% ethanol twice for 20 seconds each and immersed in Histoclear twice for 5 minutes each. Excess liquids on slides were tapped off, and a few drops of DPX mountant (10050080, Fisher Scientific Ltd., Loughborough, Leicestershire, UK) were applied on the tissue sections. Coverslips (MENZBB024050AZ, Menzel Glaser, VWR International Ltd., Lutterworth, Leicestershire, UK) in an appropriate

size were added to slides, and slides were allowed to flat dry in the fume cupboard overnight.

2.2.5 Masson's trichrome staining

Sections were deparaffinised with two changes of Histoclear for 15 minutes each and were rehydrated in 100%, 95%, 70% ethanol and tap water twice for 1 minute each respectively. For nuclei staining, sections were stained with Harris haematoxylin for 15 minutes and rinsed in a running tap water for 15 minutes and left in dH_2O. For cytoplasm and tubular basement membrane staining, each section was stained with 300 μl Biebrich scarlet acid-fuchsin solution (HT151, Sigma-Aldrich, Poole, Dorset, UK) for 2 minutes. Excess liquids on slides were tapped off, and each slide was differentiated with 300 μl of 5% phosphomolybdic acid (HT153, Sigma-Aldrich, Poole, Dorset, UK) for 15 minutes. For collagen staining, 300 μl of 2% fast green (F/0025/46, Fisher Scientific Ltd., Loughborough, Leicestershire, UK) in 1% glacial acetic acid (A/0400/PB17, Fisher Scientific Ltd., Loughborough, Leicestershire, UK) was applied on each section for 15 minutes. Sections were rinsed in dH_2O, differentiated in 1% glacial acetic acid for 1 minute and rinsed in dH_2O for 5 minutes. Sections were dehydrated in 95% and 100% ethanol twice for 1 minute each and Histoclear twice for 5 minutes each. Excess liquids on each slide were tapped off, and a few drops of DPX mounting medium were applied on each tissue section. A coverslip in an appropriate size was added to each slide and allowed to flat dry in the fume cupboard overnight.

2.2.6 Immunohistochemistry

Sections were deparaffinised with two changes of Histoclear for 15 minutes each and were rehydrated in 100%, 90%, 70% ethanol and dH_2O for 5 minute each respectively. Antigen retrieval was carried out using preheated citrate buffer (pH 6.0) containing 10 mM tri-sodium citrate dehydrate (10112880, Fisher Scientific Ltd., Loughborough, Leicestershire, UK) and 0.5% Tween 20 (27434-8, Sigma-Aldrich, Poole, Dorset, UK) as an antigen retrieval buffer. Slides were immersed in the preheated antigen retrieval buffer, steamed with a preheated food steamer (800 watts, available through the retail markets) for 20 minutes and were allowed to cool for 20 minutes. Slides were rinsed in PBS with 0.5% Tween 20 (PBST) for 5 minutes, and a Dako pen (S2002, Dako UK Ltd., Stockport, Cheshire, UK) was used to draw a hydrophobic circle around slide-mounted tissues. Tissue sections were blocked with secondary antibody host serum containing 10% normal pig serum (NPIS-10, Alpha Diagnostic International Ltd., Nottingham, UK) and 10% normal goat serum (S-1000, Vector Laboratories Ltd., Peterborough, UK) in 0.3% Triton X-100 in PBS for 1 hour at room temperature in a humidified chamber. Tissue sections were rinsed in PBST for 5 minutes. An appropriate primary antibody diluted in PBST was applied on sections and incubated overnight at 4°C in a humidified dark chamber. Slides were rinsed in PBST twice for 5 minutes each. An appropriate secondary antibody diluted in PBS containing 2% secondary antibody host serum was applied on each section for 1 hour at room temperature in a humidified dark chamber. Slides were then rinsed with PBST twice for 5 minutes each and rinsed in PBS again. Nuclear counterstaining was performed by adding 5 μg/ml Hoescht 33258 (B1155, Sigma-Aldrich, Poole, Dorset, UK) in PBS for 15 minutes. Tissue sections were mounted in Vectashield Hardset containing DAPI with coverslips and were stored at 4°C in the

dark. It is important to note that a positive control (performing the staining on the sample that significantly express the protein of interest) and a negative control (carrying out the same protocol without addition of primary antibody) should be included in each experiment to ensure the efficiency and specificity of the primary antibody and to confirm that secondary antibody does not nonspecifically bind to cellular compartments. However, only a positive control for anti-Histone H3 staining was performed in the mouse embryonic sections in this thesis.

Primary antibodies were as follows: anti-BrdU [clone BU 1/75 (ICR1)] (ab6326, Abcam, Cambridge, UK, 1:300) and anti-Histone H3 (phospho S10) (pH3, ab5176, Abcam, Cambridge, UK, 1:500). Secondary antibodies (1:500) were as follows: Alexa Fluor 488 anti-rat IgG (H+L) (A11006, Invitrogen, Life Technologies Ltd., Paisley, UK) and FITC-conjugated swine anti-rabbit immunoglobulins.

2.2.7 Quantification of BrdU and pH3 labeled tubular cells

For immunofluorescence images, three randomly chosen areas of each kidney section under x20 magnification were quantitated for thymidine analog uptake and pH3 in the cortical and medullary regions to assess the proliferative activity and cell cycle. Three fields at x20 magnification were sufficient for each kidney section, since there were not many proliferative cells observed in all cases. The size of counting areas was determined by Nikon's NIS Elements D4. 13. 04 software (Nikon Instruments UK Ltd., Surrey, UK). The number of BrdU positive (BrdU+), pH3 positive (pH3+) and BrdU and pH3 copositive (BrdU+pH3+) cells in the specific areas of cortex and medulla (three fields per kidney section) were counted and averaged for an n = 3. This thesis intended to present data as positive cell number per total cell number, but the nuclei staining with DAPI was unstable in some sections. Hence, data were

presented as cell number per mm^2 for the densities of BrdU+, pH3+ and BrdU+pH3+ cells per kidney section.

2.2.8 Total RNA extraction from snap frozen kidneys

Total RNA was isolated from snap frozen ground kidneys with an RNeasy Mini Kit (74104, QIAGEN Ltd., Manchester, UK) following the standard protocol in a MACH-AIRE fume cupboard. Prior to RNA extraction, 10 μl β-mercaptoethanol (β-ME) was added to 1 ml buffer RTL; 4 volumes of ethanol were added to buffer RPE before use; and DNase 1 stock solution was prepared by dissolving lyophilised DNase 1 in 550 μl RNase-free water and mixing gently by inversion and aliquot if necessary.

Snap frozen ground kidneys were quickly weighed up to 20 mg into new microcentrifuge tubes. A 350 μl buffer RTL containing β-ME was added to each tube and immediately homogenised with squishers and 1 ml syringes (300013, BD Plastipak, Oxford, UK) with 0.9 mm hypodermic needles (BD Microlance™ 3 needles, 3301300, BD Plastipak, Oxford, UK) until uniformly homogeneous. Tissue lysates were spun down at 15,588 xg for 3 minutes in a Microfuge 22R® microcentrifuge, and supernatants were transferred to 1.5 ml microcentrifuge tubes. One volume 70% ethanol was added to each lysates and mixed immediately with a pipette. A 700 μl sample was transferred to an RNeasy spin column placed in a 2 ml collection tube and spun down at 13,282 xg for 15 seconds, and the flow through was discarded. A 350 μl buffer RW1 was added to a spin column and spun down at 13,282 xg for 15 seconds, and the flow through was discarded. A 10 μl DNase 1 (79254, QIAGEN Ltd., Manchester, UK) stock solution in 70 μl buffer RDD was mixed gently by inverting briefly and added directly to each spin column membrane

followed by 15 minutes of incubation at room temperature. A 350 μl buffer RW1 was then added and spun down at 13,282 xg for 15 seconds, and the flow through was discarded.

A 500 μl buffer RPE was added to each spin column. A spin column was spun down at 13,282 xg for 15 seconds to wash spin column membrane, and the flow through was discarded. A 500 μl buffer RPE was added again to spin column membrane and spun down at 13,282 xg for 2 minutes to wash spin column membrane. The spin column was placed into a new 2 ml collection tube and spun down at 13,282 xg for 2 minutes and was placed in a new 1.5 ml eppendorf. A 30 μl RNase-free water was directly added to the spin column membrane and left for 1 minute, and it was spun down at 13,282 xg for 1 minute to elute the RNA.

2.2.9 Total RNA quality and cDNA synthesis

The RNA concentration and purity were determined using a NanoDrop 2000 spectrophotometers (Thermo Fisher Scientific, Paisley, UK). The absorbance ratio at A260 nm/A280 nm estimates the RNA purity, and ratio around 2.0 was considered pure for RNA samples. The ratios below 2.0 indicate contaminants which increase the absorbance near 280 nm.

The integrity of RNA was assessed by separating total RNA with electrophoresis through the 1% gel followed by visualisation of 18S and 28S ribosomal RNAs. A 1% gel was made up by dissolving agarose (BP1356, Fisher Scientific Ltd., Loughborough, Leicestershire, UK) in 1x Tris-acetate-EDTA buffer (TAE, 50x TAE buffer, H19109, Flowgen Bioscience Ltd., Nottingham, UK) by boiling in a microwave for 2 minutes until the liquid becomes clear. Agarose solution was chilled

by running the flask under a cold tap and continuing swirling until it can be handled. Agarose was poured in a RunOne™ gel casting system (Embi Tec Ltd., Crewe, Cheshire, UK) slowly without generating any bubbles and left to set at room temperature. Combs were removed from gels, and gels were placed in RunOne™ electrophoresis cells (Embi Tec Ltd., Crewe, Cheshire, UK) filled with 1x TAE buffer. RNA samples were kept on ice following dilution in RNase-free distilled water (10977035, Gibco, Life Technologies Ltd., Paisley, UK) into 100 ng/μ1. A 5 μ1 RNA was mixed with 2 μl of 6x loading buffer (G190A, Promega UK Ltd., Southampton, UK) and loaded to each well, and the gel was run at 100V for 15-20 minutes. Gels were placed in ethidium bromide for at least 15 minutes and were visualised with a Gel Doc 2000 system (Bio-Rad Ltd., Watford, Hertfordshire, UK). Samples that showed two sharp 18S and 28S bands were considered intact. The samples were stored at -80 °C until use.

A 5 μ1 of 100 ng/μ1 RNA sample was taken for the first strand complementary DNA (cDNA) synthesis using RevertAid RT kit (K1691, Thermo Fisher Scientific, Paisley, UK). The revert transcriptase (RT) reaction was initiated by incubation of 0.5 μg template RNA with 1 μl random hexamer primer and 6 μl nuclease-free water at 65°C for 5 minutes in a GeneAmp PCR system 9700 (Thermo Fisher Scientific, Paisley, UK) followed by chilling on ice immediately. A 4 μl of 5x reaction buffer, 1 μl RiboLock RNase inhibitor, 2 μl of 10 mM dNTP mix and 1 μl RevertAid RT were added to each sample and incubated at 25°C for 5 minutes followed by 42 °C for 60 minutes in a GeneAmp PCR System 9700. A no template control (nuclease-free water containing all RT reaction components except RNA template) was also included in RT reaction to assess reagent contamination. The total volume at the end of the reaction was 20 μ1. The cDNA samples were chilled on ice followed by 1 in 5

dilution in RNase-free distilled water and then can be used directly or stored at -80 °C for long term.

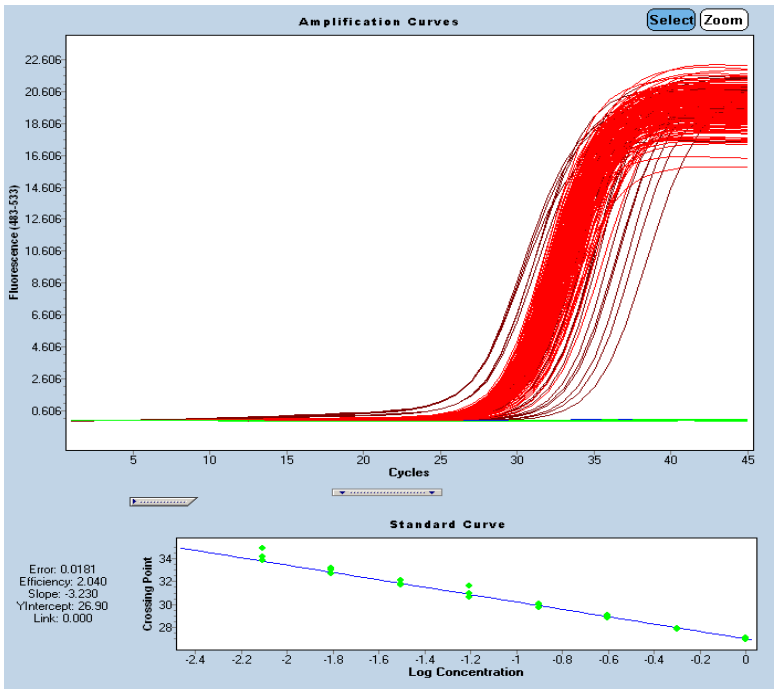
2.2.10 Quantitative real time PCR

Quantitative real time polymerase chain reaction (qRT-PCR) was performed using a Roche LightCycler 480 (Roche Diagnostics Ltd., West Sussex, UK) on both cDNA and RNA samples. Primers for TATA box binding protein (*Tbp*) designed to be located on exon-exon boundaries were used to verify cDNA products and to assess the genomic DNA contamination in RNA samples. The reaction mixture volume was 15 μ1, and it contained 7.5 μ1 LightCycler 480 SYBR Green I Master (04887352001, Roche Diagnostics Ltd., West Sussex, UK), 5 μ1 cDNA or RNA sample, 300 nM forward and reverse primers and 1.6 μ1 RNase-free distilled water. A negative control (RNase-free distilled water) was also included in each qRT-PCR reaction to assess reagent contaminations. The threshold cycle (Ct) values of all cDNA samples were averaged, and a neat cDNA pool was generated by pooling samples that showed Ct values within the range of mean Ct ± standard deviation (SD).

All primers were designed on exon-exon boundaries using Primer Express software 3.0.1 (Thermo Fisher Scientific, Paisley, UK) and NCBI-Primer BLAST and purchased from Sigma-Aldridge (Poole, Dorset, UK) (Table 2.1). Primers for genes encoding endothelial nitric oxide synthase (eNOS; *Nos3*), inducible nitric oxide synthase (iNOS; *Nos2*), NADPH oxidase-2 (NOX-2; *Nox2*) cytochrome b-245 alpha chain (*Cyba*) and beta chain (*Cybb*), NADPH oxidases-4 (NOX-4; *Nox4*), kidney injury molecule-1 (KIM-1; *Kim1* or *Havcr1*) and profibrotic factors including transforming growth factor-β1 (*Tgfb1*) and connective tissue growth factor (*Ctgf*),

collagen-I alpha 1 (*Col1A1*), collagen-IV alpha 1 (*Col4A1*), Vimentin (*Vim*) and *Tbp* as an internal control were tested with an 8-point standard curve generated by half dilution of a neat cDNA pool in triplicate. The efficiency and slope values indicate primers' working efficiency, and melting curves indicate whether primers produce a single specific product. Primers that showed values around 1.9-2.1 for the efficiency and around -3.35 for the slope with a single melting curve were used for the study (Figure 2.3). Each sample was repeated in triplicate, and the relative gene expression levels were normalised with the internal control; that is, the value of fluorescence signal of the gene from each animal was divided by that from *Tbp*.

A



B

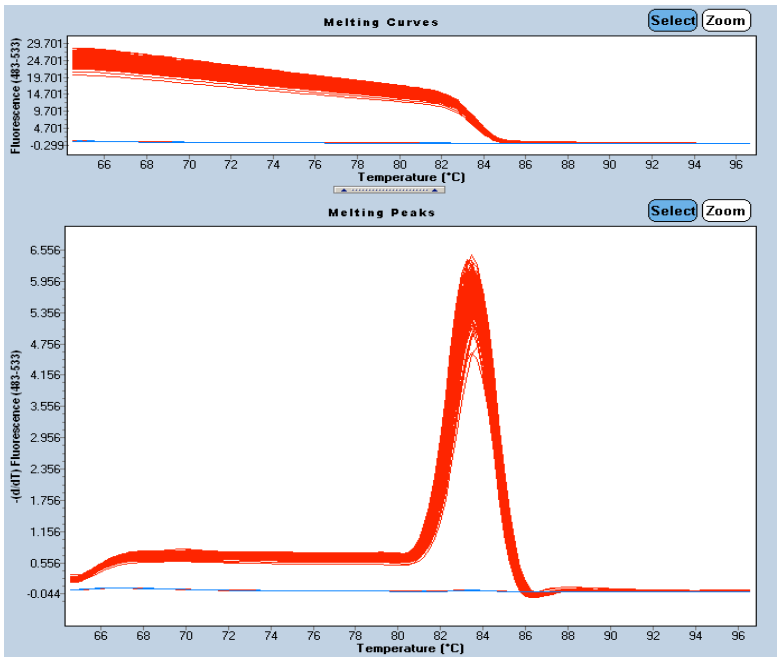


Figure 2. 3 The figure shows the ideal amplication curves and melting curves from qRT-PCR of eNOS gene.

(A) The amplication curves show that the accumulation of products occur during 25-30 cycles. The efficiency (2.040) and slope value (-3.230) are within the range of 1.9-2.1 and close to -3.35, respectively, indicaing that amplication efficiency of the primer is close to 100%. (B) The melting curves reveal a sigle peak, indicating that a single specific product was produced.

Table 2. 2 All primers were designed using Primer Express software and NCBI-Primer BLAST.

Gene	Primer sequence (5'-3')	Size
Tbp	Forward: TGTACCGCAGCTTCAAAATATTGT	147 bp
	Reverse: TGTCCGTGGCTCTCTTATTCTCA	
Nos2	Forward: CATCAGGTCGGCCATCACT	86 bp
	Reverse: CGTACCGGATGAGCTGTGAA	
Nos3	Forward: GAAGTAGCCAATGCAGTGAAGATC	93 bp
	Reverse: AGTCTCAGAGCCATACAGAATGGTT	
Cyba	Forward: CGTCTGGCCTGATTCTCATCA	79 bp
	Reverse: GAGTAGGCGCCGAAATACCA	
Cybb	Forward: GAGGTCTTATTTTGAAGTGTTCTGGTATAC	89 bp
	Reverse: CAATTCGTTCAGCTCCATGGA	
Nox4	Forward: AAGTAGTAGGAGACTGGACAGAACGAT	81 bp
	Reverse: TGAAGGGCAGAATCTCAGAGTCTT	
Havcr1	Forward: CTGGAGTAATCACACTGAAGCAATC	76 bp
	Reverse: GATGCCAACATAGAAGCCCTTAGT	
Tgfb1	Forward: CGAAGCGGACTACTATGCTAAAGA	75 bp
	Reverse: GTTTTCTCATAGATGGCGTTGTTG	
Ctgf	Forward: GGCCTCTTCTGCGATTTCG	65 bp
	Reverse: CCATCTTTGGCAGTGCACACT	
Col1A1	Forward: AAGGGAGCCACATCGATGAT	97 bp
	Reverse: ACGGCTGCACGAGTCACA	
Col4A1	Forward: TGCCAGCCGTACCCAAGT	128 bp
	Reverse: CAGGCATAGTCAGACAACAGATGA	
Vim	Forward: CCCTGAACCTGAGAGAAACTAACC	115 bp
	Reverse: GTCTCATTGATCACCTGTCCATCT	

Tbp, TATA box binding protein; *Nos2*, inducible nitric oxide synthase; *Nos3*, endothelial nitric oxide synthase; *Cyba*; cytochrome b-245 alpha chain; *Cybb*, cytochrome b-245 beta chain; *Nox4*, NADPH oxidases 4; *Havcr1*, kidney injury molecule-1; *Tgfb1*, transforming growth factor-β1; *Ctgf*, connective tissue growth factor; *Col1A1*, collagen-I alpha 1; *Col4A1*, collagen-IV alpha 1; *Vim*, Vimentin.

2.3 Imaging

2.3.1 Cell culture images

Light images were acquired on using a Leica DMIL inverted microscope, Leica DFC420c camera and Leica Application Suite v.3.2 software (Leica Microsystems Ltd., Milton Keynes, UK). The microscope settings were the same for all slides. The magnification was stated in each figure.

2.3.2 Cell culture immunofluorescence images

For imaging the fluorescence in live cells, a fluorescent Leica DMIL inverted microscope equipped with fluorescence filters and Leica DFC420c camera and Leica Application Suite v.3.2 software (Leica Microsystems Ltd., Milton Keynes, UK) were used. For fixed cell imaging, immunofluorescence microscopy was carried out using a Leica CTR 5000 digital microscope (Leica Microsystems Ltd., Milton Keynes, UK), and images were acquired using a Leica DFC420 microscope camera and Leica Application Suite v.3.8 software. The microscope settings should ideally be maintained the same for all slides; however, the exposure time and gain were occasionally altered where necessary. Overlay images were automatically created by Leica Application Suite v.3.8 software for green, red and blue fluorescence. All cell culture immunofluorescence images had triplicates (one randomly chosen field per slide and three slides per treatment for an n = 3); however, more fields for each slide are required for quantative analysis which was not performed in this thesis. The magnification was stated in each figure.

2.3.3 Electrophoresis and western blot images

RNA stained with ethidium bromide was visualised and imaged with a Gel Doc 2000 imaging system (Bio-Rad Ltd., Watford, Hertfordshire, UK). Western blot films were imaged with Gel Doc XR+ imaging system (Bio-Rad Ltd., Watford, Hertfordshire, UK), and the intensity and area of protein bands were quantified with Quantity One software (Bio-Rad Ltd., Watford, Hertfordshire, UK).

2.3.4 Kidney tissue histological images

Kidney sections stained with Haematoxylin and eosin (H&E) and Masson's trichrome were observed using a Leica CTR 5000 microscope equipped with different objectives. Brightfield images were acquired using a Leica DFC420 microscope camera and Leica Application Suite v.3.8 software. The microscope settings were the same for all slides by setting it for automatic white balance. Ten randomly chosen fields each for cortical and medullary region per slide and ten animals per treatment group were captured. The magnification was stated in each figure. The positive areas in Masson's trichrome stained kidneys were quantified using an ImageJ software. The setup of colour threshold for quantifying the stained areas was based on the colour of basement membrane of blood vessels as there were no obvious fibrosis in the interstial areas to be used as a standard threshold. The same setup was applied for all images.

2.3.5 Kidney tissue immunofluorescence images

Immunofluorescence microscopy was carried out using a Leica CTR 5000 digital microscope equipped with different objectives. Immunofluorescence images were

acquired using a Leica DFC420 microscope camera and Leica Application Suite v.3.8 software. The microscope settings should ideally be maintained the same for all slides; however, the exposure time and gain were occasionally altered where necessary. Overlay images were automatically created by Leica Application Suite v.3.8 software for green, red and blue fluorescence. Three randomly chosen fields for each slide were captured. The magnification was stated in each figure.

2.4 Statistics

All experiments were performed in triplicate unless specified. The results are presented as means ± standard error of the means (SEM). Statistical analyses were carried out with Genstat version 16. For all cell culture data, the data distribution normality and residual scatter plots were checked first. Most data demonstrated a normal distribution and random residual scatter pattern. General analysis of variance (ANOVA) was performed for comparison of the differences in means at multiple levels of treatment interactions. Polynomial contrasts were also applied to partition the factor into separate single degree of freedom to test for linear and quadratic relationship. A value of $p < 0.05$ was considered statistically significant. For the animal trial, an Unbalanced ANOVA was performed using Genstat version 16 to compare the differences in means at multiple levels of treatment effects and interactions. For the analyses of positive areas in Masson's trichrome stained kidneys, a General ANOVA was performed as ten animals per treatment group were assessed. Data distribution normality and residual scatter plots were also checked, and data were log10 or square root transformed where appropriate. Data transformation mostly improved the data distribution without changing the statistical results. A value of $p < 0.05$ was considered statistically significant.

Chapter 3: The detrimental effects of amino acids on HK-2 cells following simulated I/R injury

Chapter 3: The detrimental effects of amino acids on HK-2 cells following simulated I/R injury

3.1 Introduction

AKI is known as the most common contributor to morbidity and mortality among hospitalised patients and patients in intensive care units (ICU) (Bonverntre and Yang, 2011), and the patients with history of AKI have been indicated to be at higher risks of developing CKD and ESRD (Ishani et al., 2009; Lo et al., 2009; Wald et al., 2009). There are three major causes of AKI including I/R injury, nephrotoxicity and sepsis, and I/R injury is the most common insult (Bonverntre and Yang, 2011). Most cases occur after surgery (e.g. open heart surgery and organ transplantation) and in the patients requiring ICU, but a prompt treatment can reverse such outcomes (Bonverntre and Yang, 2011). Clinically nutritional support is frequently required for patients with AKI as these patients are normally at a risk of protein-energy depletion. However, the nutrient requirement and formulation for AKI patients remain to be defined as the catabolic rate, particularly protein catabolism, varies individually due to a variety of clinical situations including severity, previous nutritional status and underlying diseases (Guarnieri, Situlin and Toigo, 2005). The nutrient requirement for patients with AKI is the same as that for critically ill patients with functional kidneys, and such standard formulation may not meet the individual's condition (Fiaccadori, Parenti and Maggiore, 2008).

A greater amino acid or protein intake (at least >1.0 or 2.0 g/kg/d) for AKI patients is continuously recommended by clinical studies and guidelines to ensure a positive nitrogen balance, as negative nitrogen balance and protein hypercatabolism are

highly associated with the increased comorbidity and mortality rate (Fiaccadori, Parenti and Maggiore, 2008; Fiaccadori, Regolisti and Cabassi, 2010). In addition to preserving the protein-energy status, the acute increase in protein or amino acid infusion/intake (1-1.2 g/kg) was found to significantly increase GFR within 2 hours in both healthy individuals and patients with renal disease (Sharma, Mucino and Ronco, 2014). The increase in GFR was due to the globally increased renal blood flow in response to the acute high amino acid infusion, and it has been found to improve the survival rate in animal models of I/R injury (Tolins and Raij, 1991; Roberts et al., 1997). However, to date clinical evidence to support the direct relationship between amino acid intake and improved outcomes or survival in AKI patients is lacking. Rather, increasing amino acids for AKI patients did not improve nitrogen balance but substantially contributed to extra amino acid catabolism, urea production and prolonged RRT duration (Gunst et al., 2013). Also, a higher mortality rate was reported in severe AKI patients receiving higher amino acid or protein intake despite the improved nitrogen balance (Bellemo et al., 2014).

In addition to clinical trials, some experimental work investigated the effects and the underlying mechanisms of single amino acids on AKI. Amino acids including glycine, alanine, glutamine and arginine were found to have potential renoprotective effects on I/R injury in several *in-vitro* and *in-vivo* studies (Garza-Quintero et al., 1990; Weinberg et al., 1997; Amores-Sánchez and Medina, 1999; Esposito et al., 2011; Petrat et al., 2012), and some negative results showed that arginine could worsen I/R injury (Schwartz et al., 2002). Little is known regarding the effect of increasing individual amino acid on AKI patients. Nevertheless, the clinically used standard amino acid formulation is a balanced mix of both non-essential and essential amino acids for patients with AKI (Btaiche et al., 2008). The investigation

of the effects of essential amino acids on AKI is limited. The current available data showed a positive effect on survival rate in AKI patients receiving intravenous formulation of essential amino acids with hypertonic solution, despite the small-scale of studies (Abel et al. 1973; Mocan et al., 1995). Hence, this chapter intended to investigate the effects of a combination of essential amino acid supplementation on HK-2 cell recovery from simulated ischaemia reperfusion (I/R) and nutrient depletion/replenishment (D/R) injury.

Aims and Hypothesis

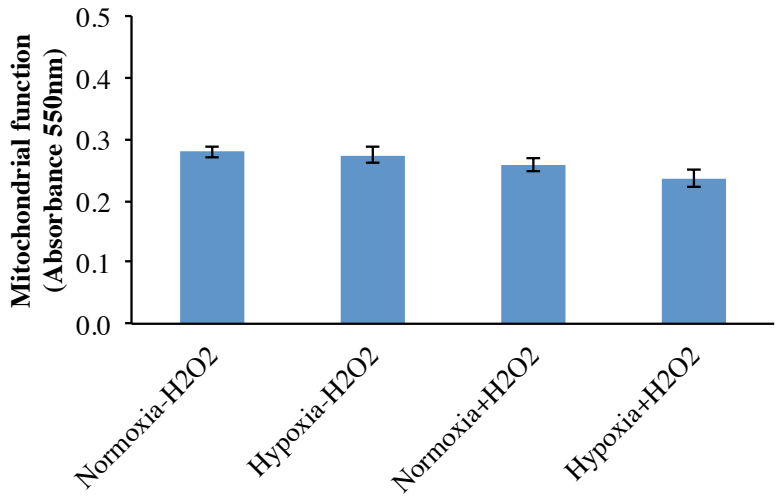
This chapter intended to investigate whether the provision of AAS may protect HK-2 cells from simulated I/R injury and promote recovery. To achieve this aim, this chapter established simulated I/R injury in HK-2 cells by 24 hours of starvation in HBSS in normoxia or hypoxia followed by resupply of AAS in the presence or absence of H_2O_2 for 24 hours. It was hypothesised that increasing AAS may protect HK-2 cells from H_2O_2 induced oxidative stress following nutrient deprivation. As it was found that increasing amino acid concentration in HBSS led to a decline in pH, the observation of deleterious effects of AAS in the presence of H_2O_2 might be attributed to pH. Hence, this thesis further examined the effects of a range of pH on HK-2 cells.

3.2 Results

3.2.1 Induction of simulated I/R injury in HK-2 cells

As the aim of this chapter was to investigate whether resupply of AAS during reperfusion might be protective against I/R injury, we first examined whether nutrient deprivation in normoxia and hypoxia followed by exposure to H_2O_2 damage in normoxia could induce a sublethal injury in HK-2 cells. The MTT assay was used to indirectly measure the viable cell number by detecting the mitochondrial enzyme activity. The mitochondrial function was only disrupted by exogenous H_2O_2 ($p = 0.021$; Figure 3.1). There were no effects of oxygen levels during nutrient deprivation and the interaction between H_2O_2 and oxygen levels during starvation on the mitochondrial function (Figure 3.1). Hence, in this thesis nutrient deprivation followed by H_2O_2 induced damage in the normoxic condition was mainly used to mimic oxidant injury in I/R injury.

A



B

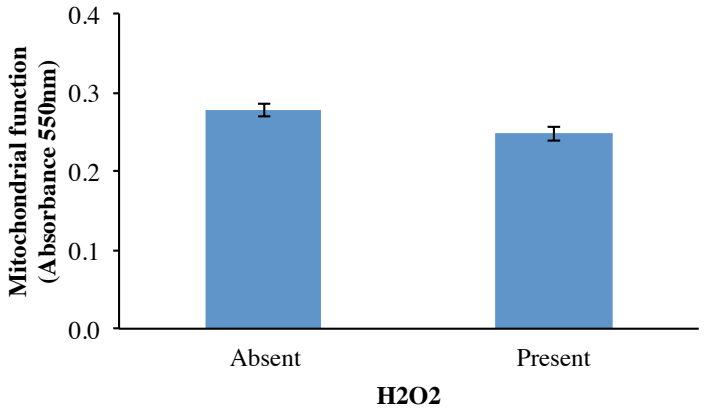


Figure 3. 1 Effects of simulated I/R injury on HK-2 cells.

(A) Mitochondrial function was measured by MTT assay after exposure to the presence or absence of H_2O_2 in normoxia following nutrient deprivation in normoxia or hypoxia. Each treatment had triplicates per plate and was repeated on three plates for an n = 3. (B) The bar graph summarised the statistical analyses. Only H_2O_2 had significant effects on mitochondrial function ($p = 0.021$). Data were presented as means ± SEM.

3.2.2 Detrimental effects of AAS at acidic pH on HK-2 cells following simulated I/R injury

It has been shown that low pH may be protective against I/R injury. In this study, the addition of amino acids to HBSS drove pH down to pH 6.4 and 3.8 in 0.5x and 1x AAS respectively. Hence, this chapter investigated whether the provision of AAS at these two pH levels was able to show a similar result. Overall, there were strong effects of AAS and H_2O_2 on the mitochondrial function (Figure 3.2 A). The mitochondrial dysfunction was observed with an increasing concentration of AAS, with a strong negative linear relationship between AAS concentration and mitochondrial function ($p < 0.001$; Figure 3.2 B). The mitochondrial function was lower in the presence of H_2O_2 compared with that in the absence of H_2O_2 ($p < 0.001$; Figure 3.2 C). There was also a strong interaction between AAS and H_2O_2 ($p < 0.01$; Figure 3.2 D). The negative linear relationship between mitochondrial function and AAS concentration was further exacerbated by the presence of H_2O_2 ($p = 0.027$; Figure 3.2 D). This suggested that increasing concentration of AAS in the presence of H_2O_2 exacerbated mitochondrial dysfunction; however, such damage could also be attributed to the pH levels of AAS. Again, the oxygen levels during nutrient deprivation did not have any effect on HK-2 cells and did not have any interactions with AAS and H_2O_2.

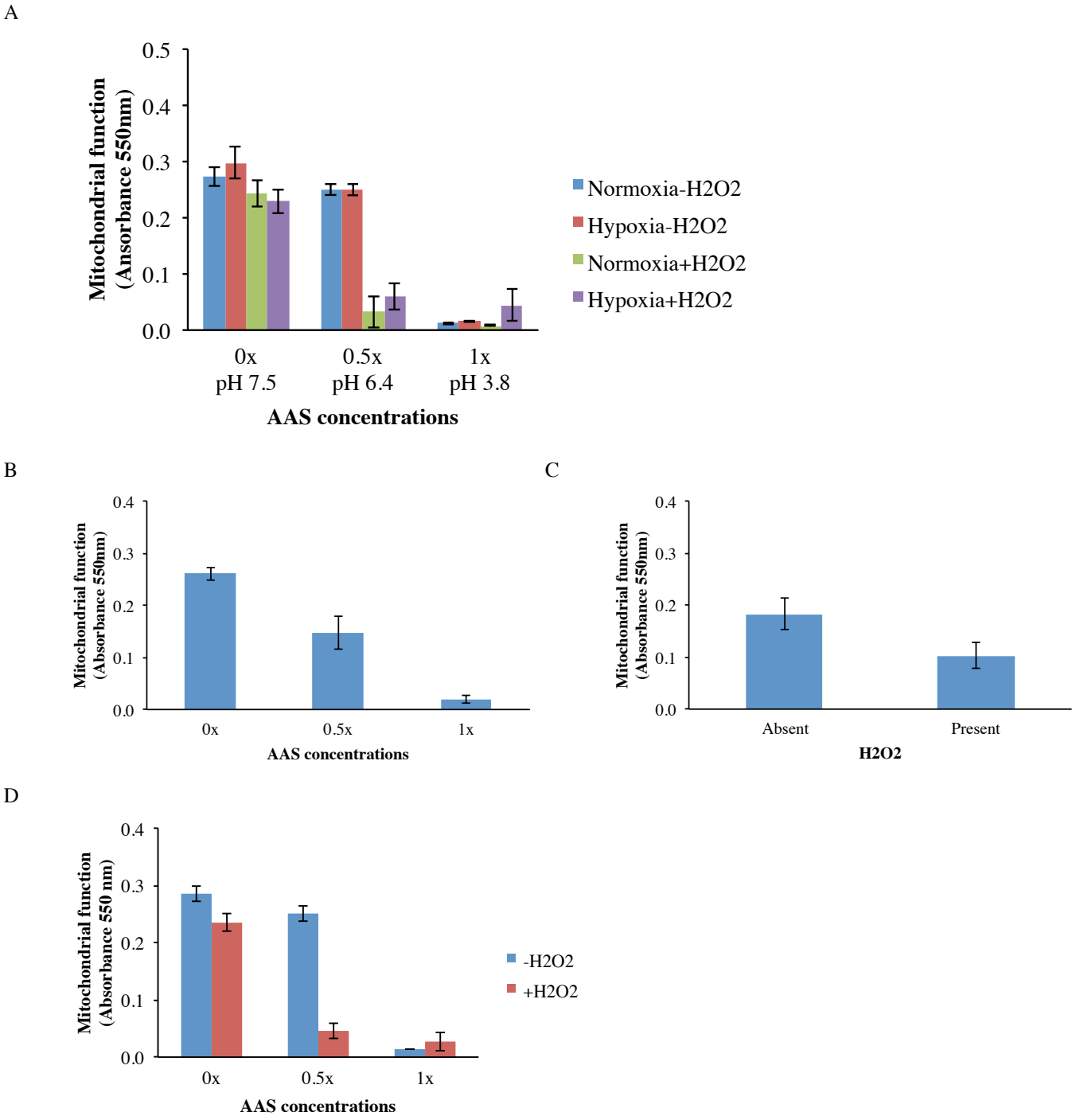


Figure 3. 2 Effects of AAS on HK-2 cells following simulated I/R injury.

(A) Mitochondrial function was measured by MTT assay after treatment with AAS with and without H_2O_2 in normoxia following nutrient deprivation in normoxia or hypoxia. Each treatment had triplicates per plate and was repeated on three plates for an n = 3. (B-D) The bar graphs summarised the statistical analyses. There were strong effects of (B) AAS ($p < 0.001$, Lin. $p < 0.001$), (C) H_2O_2 ($p < 0.001$) and (D) the interaction of AAS and H_2O_2 ($p < 0.01$, Lin. $p = 0.027$) on mitochondrial function. Data were presented as means ± SEM.

Further, we investigated whether the mitochondrial membrane potential and morphologies may be altered in response to amino acids with or without H_2O_2 following starvation. HK-2 cells were labelled with Mitotracker Red after 24 hours of treatment with AAS with or without H_2O_2 following starvation in normoxia. To determine membrane potential in live cells, the fluorescence was measured using a plate reader. However, no signals were detected. Hence, some representative images were shown here. As one field per slide and three slides per treatment group were obtained, these representative images might be biased and less generalisable.

In the absence of H_2O_2 following starvation, the mitochondrial tubular network was observed after treatment with 0x (pH 7.5) and 0.5x (pH 6.4) AAS (Figure 3.3 A and B). In contrast, the morphology was disrupted after treatment with 1x AAS (pH 3.8; Figure 3.3 C). In the presence of H_2O_2 following starvation, treatment with 0x AAS (pH 7.5) showed mitochondrial fragmentation as punctate morphologies (Figure 3.3 D). The loss of cells in 0.5x AAS at this time point made it difficult to make comparisons with other treatments and to interpret the data (Figure 3.3 E). Again, cells treated with 1x AAS (pH 3.8) showed a disruption of mitochondrial morphologies (Figure 3.3 F).

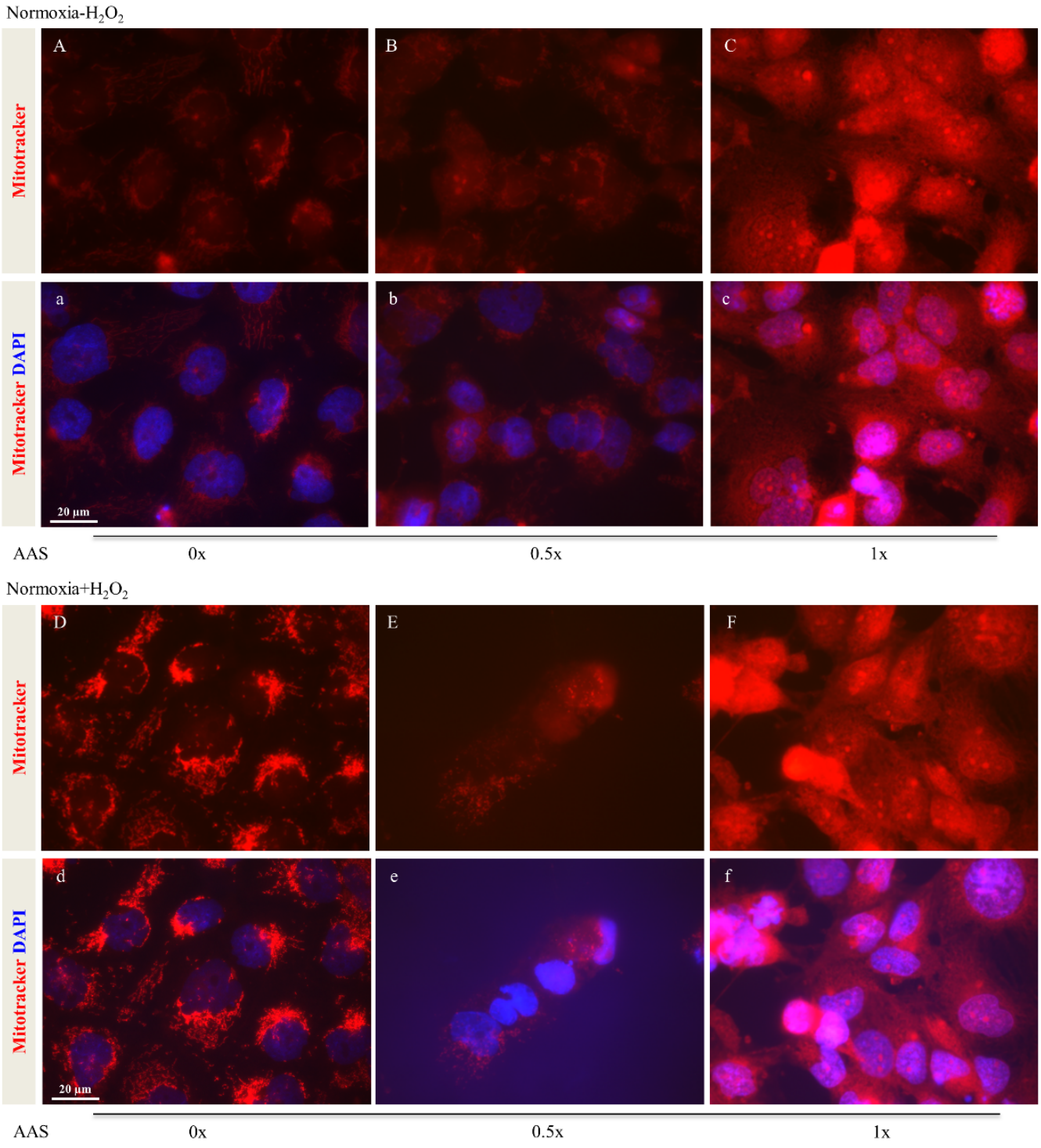


Figure 3. 3 Effects of AAS following starvation on mitochondrial morphologies in HK-2 cells.

(A-F) Representative images of Mitotracker-labelled HK-2 cells after treatment with 0x (pH 7.5), 0.5x (pH 6.4) and 1x AAS (pH 3.8) in the absence or presence of H_2O_2 following starvation. (a-f) Overlay images showed that Mitotracker (red) and DAPI (blue) were the same area. Magnification, x100; Scale bars = 20 μm. One field per slide and three slides per treatment group were performed for an n = 3.

3.2.3 Detrimental effects of low pH on HK-2 cells following simulated I/R injury

Although the increasing concentration of AAS in the presence of H_2O_2 exacerbated mitochondrial dysfunction, it was unknown whether this was driven by AAS or pH levels. Hence, we investigated the effects of varying pH levels across pH 7.8 to 3.8 on mitochondrial function in the absence of AAS. From pH 5.8 to 3.8 in the absence or presence of H_2O_2 and pH 6.4 in the presence of H_2O_2 following starvation, there was no mitochondrial function at all (Figure 3.4 A). These were excluded in statistical analyses due to the zero values.

Overall, there were significant differences between the mean mitochondrial function at pH 7.8-6.8 and that at pH 6.4. The mean mitochondrial function at pH 6.4 was significantly lower than that at pH 7.8-6.8 ($p = 0.001$; Figure 3.4 B). There was an interaction between pH and H_2O_2 ($p < 0.001$; Figure 3.4 C). The mean mitochondrial function at pH 7.8-6.8 in the presence of H_2O_2 was significantly lower compared with that in the absence of H_2O_2, but it was still higher than that at pH 6.4 in the absence H_2O_2 (Figure 3.4 C). This may suggest that pH 6.4 was more detrimental than H_2O_2 damage. There was also an interaction between pH and oxygen levels ($p = 0.035$; Figure 3.4 D), and the mitochondrial function after starvation in hypoxia was lower than normoxia and was further exacerbated by treatment with pH 6.4 compared with pH 7.8-6.8 (Figure 3.4 D).

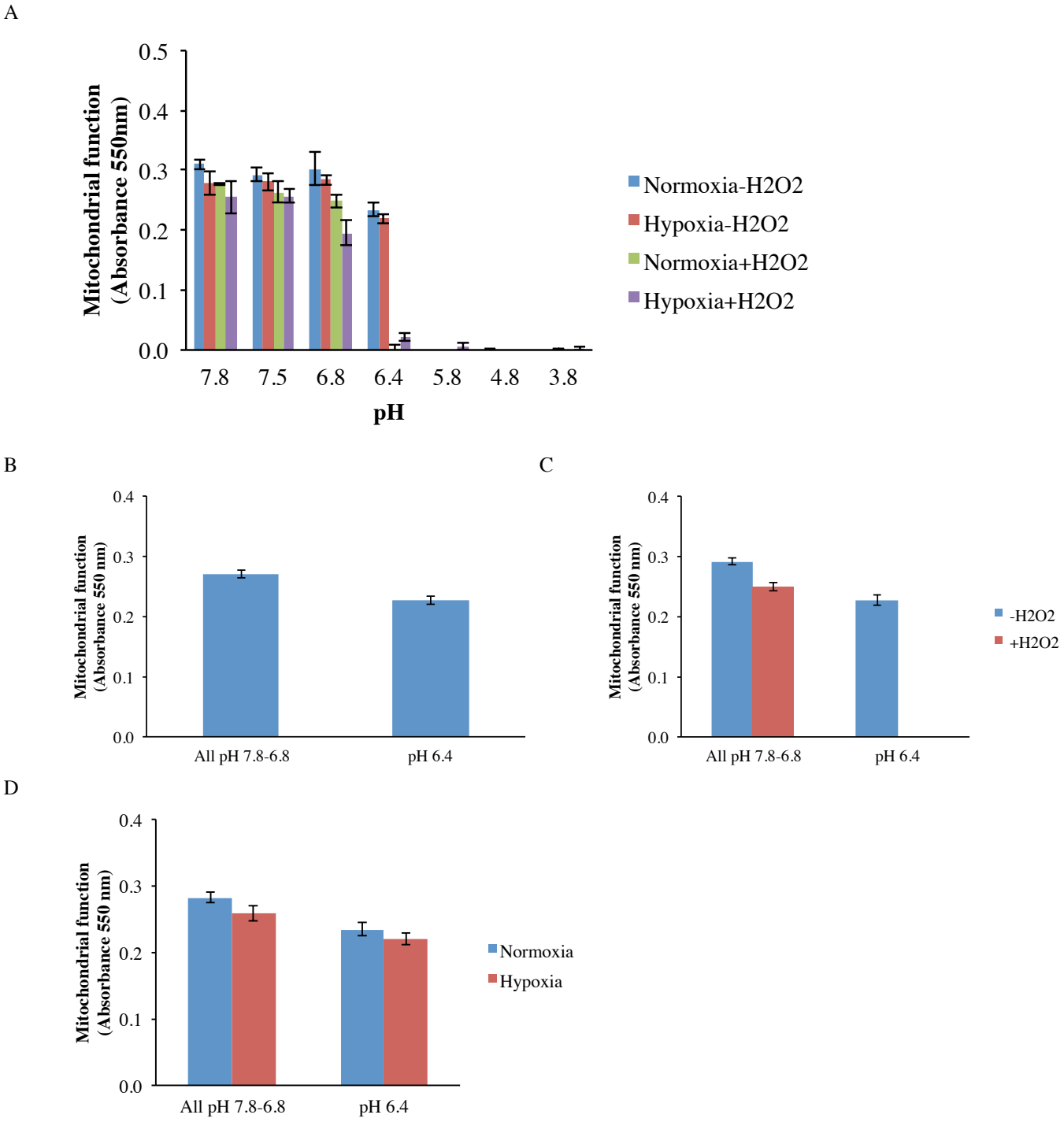


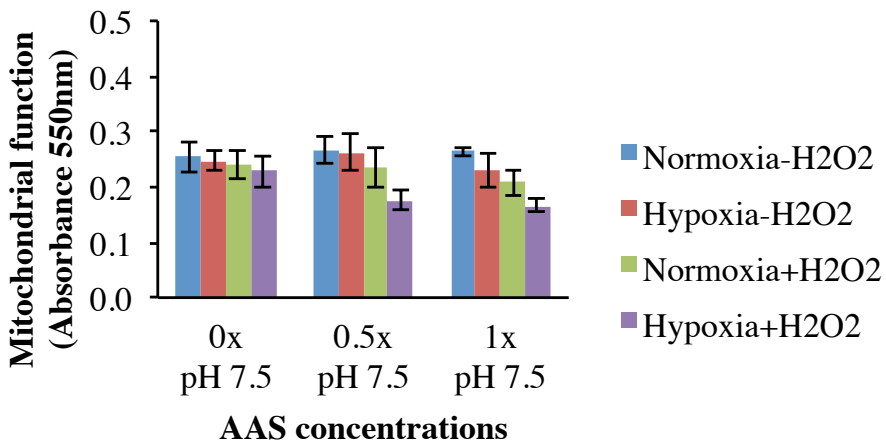
Figure 3. 4 Effects of a varying pH on HK-2 cells following simulated I/R injury.

Mitochondrial function was measured by MTT assay after exposure to HBSS at pH 7.8-3.8 with and without H_2O_2 in normoxia following nutrient deprivation in normoxia or hypoxia. Each treatment had triplicates per plate and was repeated on three plates for an n = 3. (B-D) The bar graphs summarised the statistical analyses. There were strong effects of (B) pH 6.4 ($p = 0.001$), (C) the interaction between pH 6.4 and H_2O_2 ($p < 0.001$) and (D) the interaction between pH and oxygen levels on mitochondrial function ($p = 0.035$). Data were presented as means ± SEM.

3.2.4 Detrimental effects of AAS at physiological pH on HK-2 cells following simulated I/R injury

As it was observed that the decline in pH in AAS showed no protective influence on H_2O_2 mediated damage, we investigated the effects of AAS at physiological pH (pH 7.5) adjusted by KOH on the mitochondrial function. Overall, only H_2O_2 had a negative effect on mitochondrial function (Figure 3.5 A). The mitochondrial function was significantly lower in the presence of H_2O_2 compared with that in the absence of H_2O_2 ($p < 0.002$; Figure 3.5 B). Other factorials including AAS and oxygen levels did not have any effects, and no treatment interactions were observed. Although there was no strong relationship between AAS and mitochondrial function, a decline in mitochondrial function by approximately 10% in cells treated with 1x AAS (0.21 ± 0.03 in normoxia; 0.17 ± 0.01 in hypoxia) compared with 0x AAS (0.24 ± 0.02 in normoxia; 0.23 ± 0.03 in hypoxia) in the presence of H_2O_2 was still observed (Figure 3.5 A).

A



B

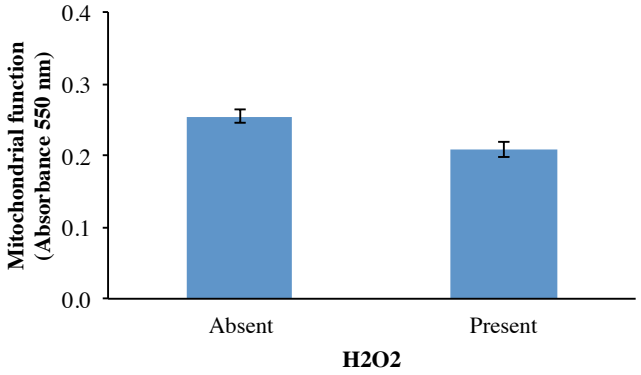
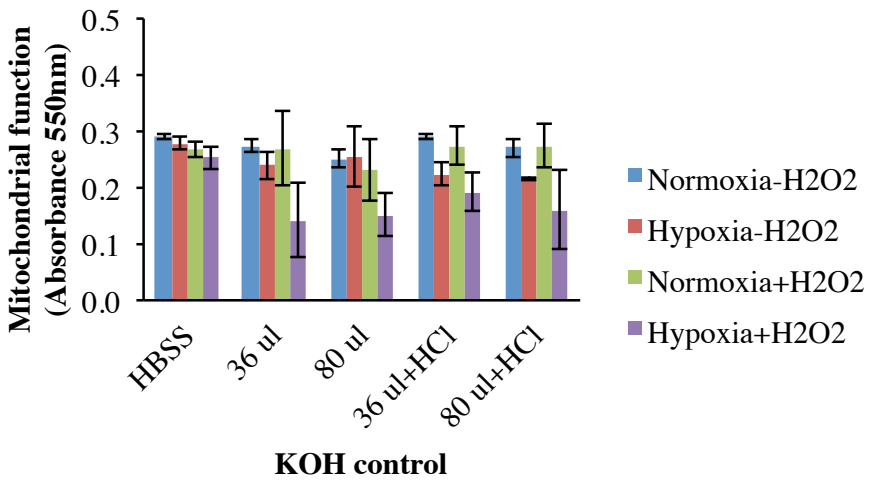


Figure 3. 5 Effects of AAS at pH 7.5 on HK-2 cells following simulated I/R injury.

(A) Mitochondrial function was measured by MTT assay after treatment with AAS at pH 7.5 with and without H_2O_2 in normoxia following nutrient deprivation in normoxia or hypoxia. Each treatment had triplicates per plate and was repeated on three plates for an n = 3. (B) The bar graph summarised the statistical analyses. There was a strong effect of H_2O_2 on mitochondrial function (p = 0.002). Data were presented as means ± SEM.

In order to ensure that KOH used for pH adjustment did not influence the cellular responses to AAS, we examined the mitochondrial function after treatment with i) the equivalent amount of KOH for adjusting AAS and ii) the equivalent amount of KOH adjusted pH back to pH 7.5 with HCl. Overall, only oxygen had an effect on mitochondrial function (Figure 3.6 A), and the mitochondrial function was lower in cells starved in hypoxia compared with normoxia ($p = 0.031$; Figure 3.6 B). More importantly, the amount of KOH did not have any effects on the mitochondrial function (Figure 3.6 A), confirming that KOH added to AAS for buffering did not interfere with mitochondrial functional responses to amino acids.

A



B

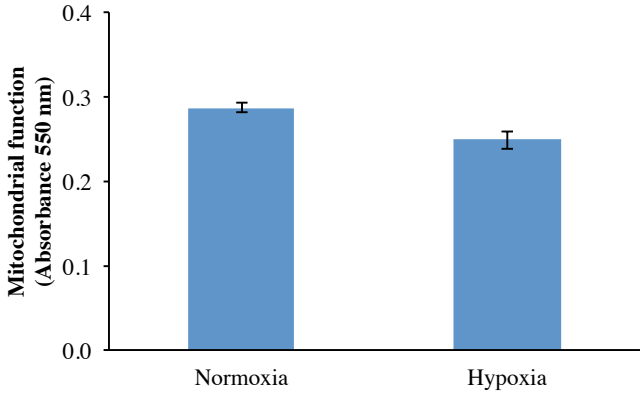


Figure 3. 6 Effects of KOH on HK-2 cells following simulated I/R injury.

(A) Mitochondrial function was measured by MTT assay after treatment with HBSS+KOH or with HBSS+KOH adjusted back to pH 7.5 by HCl with and without H_2O_2 in normoxia following nutrient deprivation in normoxia or hypoxia. Each treatment had triplicates per plate and was repeated on three plates for an n = 3. (B) The bar graph summarised the statistical analyses. Only oxygen levels had effects on mitochondrial function (p = 0.031). Data were presented as means ± SEM.

Further, we investigated the mitochondrial morphological alterations in response to amino acids at pH 7.5 with or without H_2O_2 following starvation in normoxia. In the absence of H_2O_2 following starvation, the mitochondrial tubular network was observed after 24 hours of treatment with 0x, 0.5x and 1 x AAS at pH 7.5 (Figure 3.7 A-C). In the presence of H_2O_2 following starvation, cells treated with 0x, 0.5x and 1x AAS at pH 7.5 all displayed mitochondrial fragmentation as punctate morphologies (Figure 3.7 D-F). As one representative area per slide and three slides per treatment group were obtained, these representative images might be less generalisable. To identify the differences in mitochondrial length for determining mitochondrial tubulation and fragmentation, higher power images from a confocal microscope and more fields per slide per treatment are required. Here it was difficult to clearly identify the differences in mitochondrial length between treatments. Nevertheless, the mitochondrial degradation suggested that treatment of H_2O_2 following starvation induced a certain level of oxidative stress.

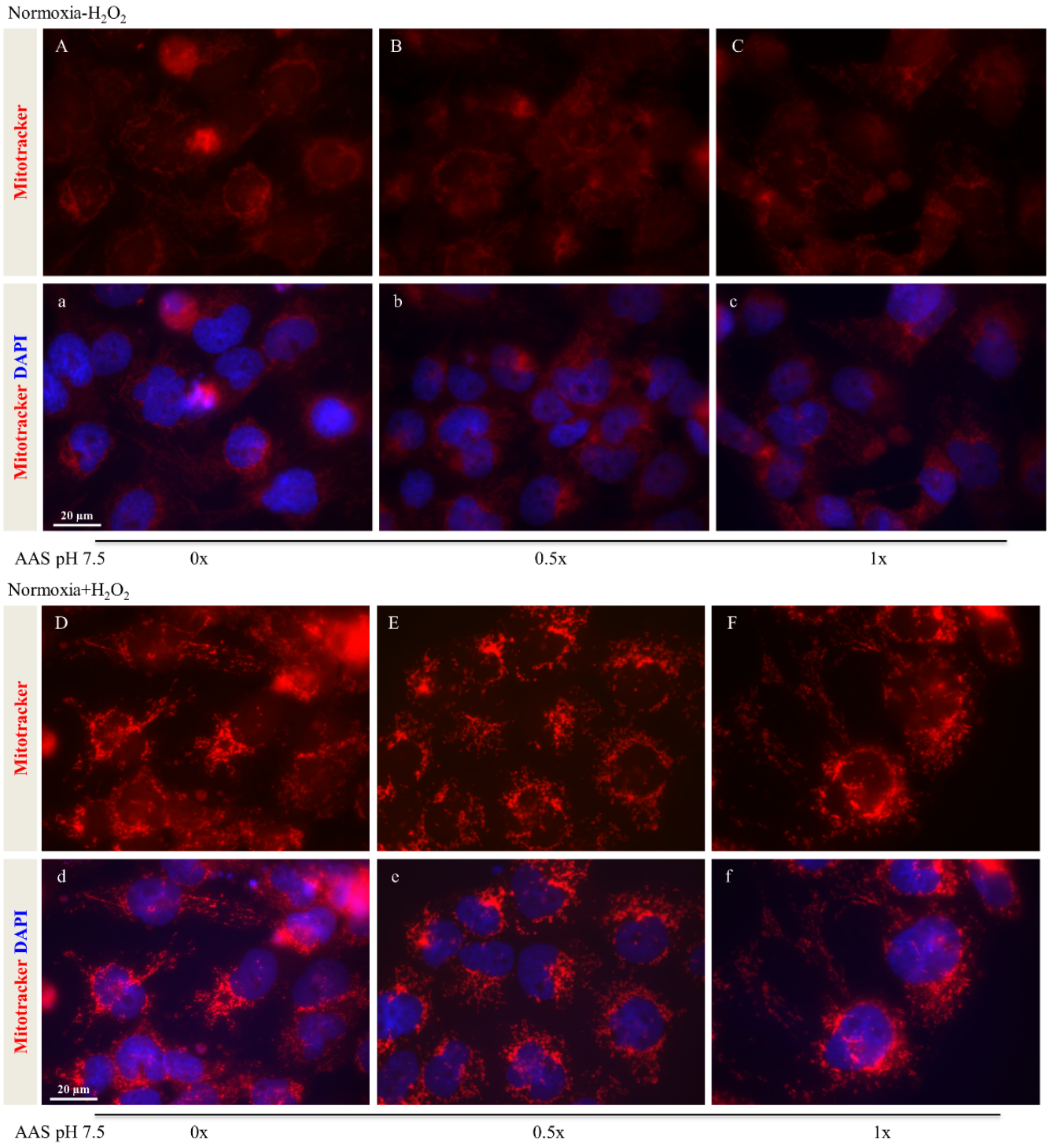


Figure 3. 7 Effects of AAS at pH 7.5 following starvation on mitochondrial morphologies in HK-2 cells.

(A-F) Representative images of Mitotracker-labelled HK-2 cells after treatment with AAS at pH 7.5 in the absence or presence of H_2O_2 following starvation were displayed. (a-f) Overlay images showed that Mitotracker (red) and DAPI (blue) were the same area. Magnification, x100; Scale bars = 20 µm. One field per slide and three slides per treatment group were performed for an n = 3.

3.2.5 Effects of AAS at low pH on HK-2 cells following D/R injury

As the results showed that the oxygen levels during starvation did not have any effects on HK-2 cells, in this section we mainly focused on the cellular responses to AAS in the presence or absence of H_2O_2 after nutrient deprivation in normoxia. As starvation in hypoxic condition was excluded, an appropriate term for this experimental injury would be termed as nutrient deprivation/replenishment (D/R) rather than I/R injury.

Gores et al. (1989) has justified that the cytoprotection by acidic pH infusion was mediated by intracellular pH and that a slight drop in extracellular pH led to a great decline in intracellular pH. It was further observed by Crean et al. (2013) that in HK-2 cells the intracellular pH decreased with the decrease in extracellular pH. In particular, the authors found that media at pH 7.2 caused intracellular pH to decline to pH ~6.9, which may theoretically exert cytoprotection according to the literature. The media at pH 6.4 also caused a decline in intracellular pH to pH ~6.4, and Crean et al. (2013) showed a cytoprotection against cell death caused by glucose and oxygen deprivation. Hence, here we investigated whether low pH could be protective against H_2O_2 mediated damage, and two pH levels including pH 7.2 and 6.4 were chosen to assess the effects of a slight decline in pH (>7.0) and an acidic pH (<7.0) on HK-2 cells following D/R injury.

At pH 7.5 the mitochondrial dysfunction was observed with increasing concentration of AAS, with a strong negative linear relationship between AAS concentration and mitochondrial function ($p < 0.001$, Lin. $p < 0.001$; Figure 3.8 A). The mitochondrial

function was also affected by exogenous H_2O_2; that is, it was lower in the presence of H_2O_2 compared with that in the absence of H_2O_2 ($p = 0.003$; Figure 3.8 A). There was also a strong interaction between AAS and H_2O_2 ($p = 0.019$; Figure 3.8 A). The AAS concentration and mitochondrial function had a strong negative linear relationship, and the presence of H_2O_2 further exacerbated mitochondrial dysfunction ($p = 0.006$; Figure 3.8 A). This again suggested that increasing concentration of AAS in the presence of H_2O_2 exacerbated mitochondrial dysfunction. Compared with the data in 3.2.4 (Figure 3.5 A), the negative linear relationship between AAS concentration and mitochondrial function affected by H_2O_2 was stronger here. This was due to the cell population seeded in the beginning of the experiment, as evidenced by the observation of twice higher MTT absorbance in the control group (0x AAS) here. This experiment was repeated several times (data not shown), and we found that over confluent cell population seeded in the beginning of the experiment led to a greater loss of mitochondrial function driven by amino acids in the presence of H_2O_2. Nevertheless, the negative relationship between AAS concentration and mitochondrial function in all experiments still retained.

At pH 7.2, the results were similar. The mitochondrial dysfunction was observed with increasing concentration of AAS, with a strong negative linear relationship between AAS concentration and mitochondrial function ($p = 0.012$, Lin. $p = 0.005$; Figure 3.8 B). The mitochondrial function was lower in the presence of H_2O_2 compared with that in the absence of H_2O_2 ($p < 0.001$; Figure 3.8 B). At pH 6.4 only H_2O_2 had a strong effect on mitochondrial function ($p < 0.001$; Figure 3.8 C), and a greater loss of mitochondrial function was observed in the presence of H_2O_2 compared with the absence of H_2O_2. These results showed that AAS at low pH did not exert any positive effects on H_2O_2 mediated damage, contrary to the published

literature which showed that pH paradox during reperfusion could be prevented by acidic infusion.

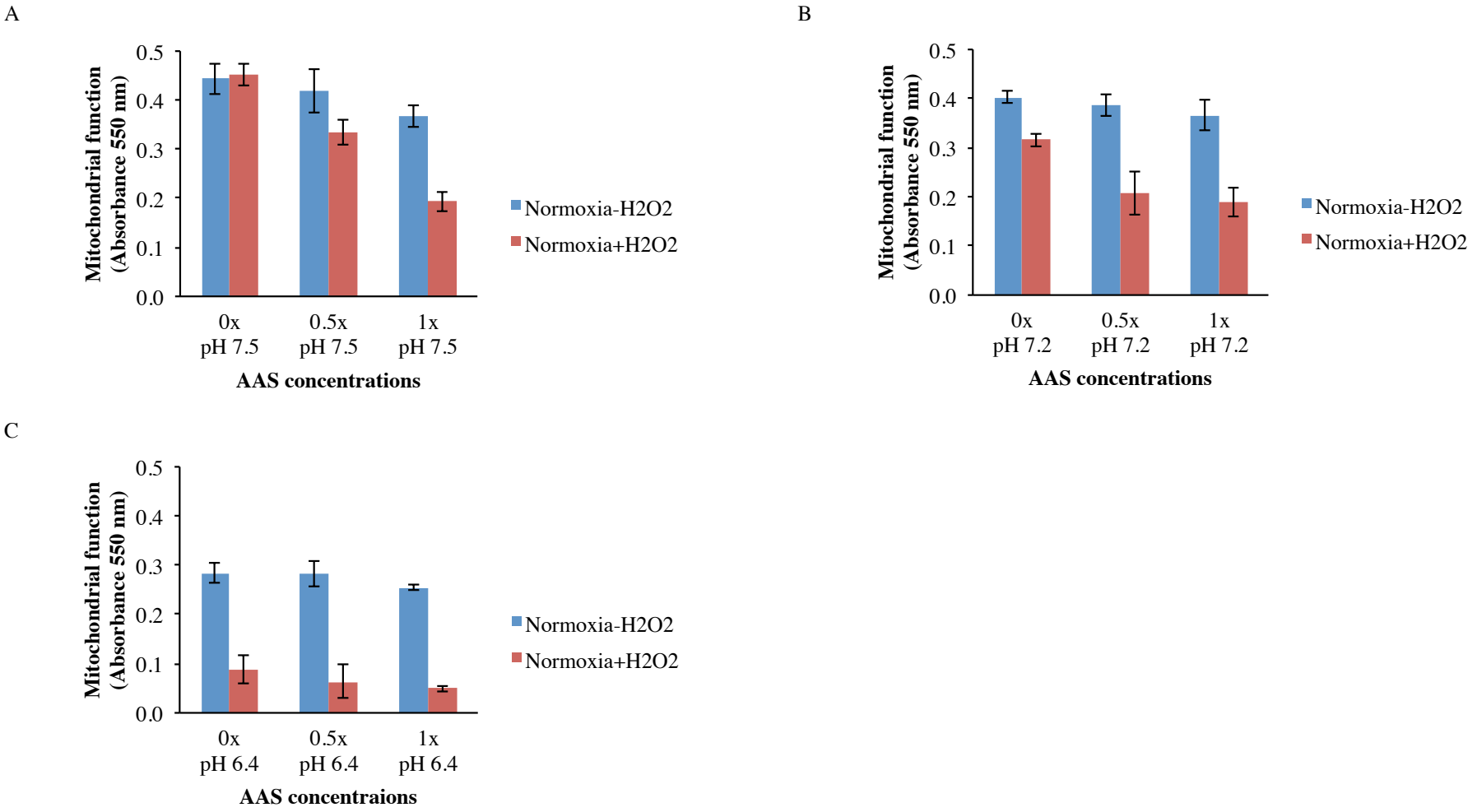


Figure 3. 8 Effects of AAS at physiological and low pH on HK-2 cells following starvation.

Mitochondrial function was measured by MTT assay after treatment with AAS at (A) pH 7.5, (B) pH 7.2 and (C) pH 6.4 with and without H_2O_2 following nutrient deprivation. Each treatment had triplicates per plate and was repeated on three plates for an n = 3. Data were presented as means ± SEM.

3.2.6 Effects of AAS and pH on HK-2 cell viability following D/R injury

As MTT assay measures the mitochondrial function of the viable cell number, it cannot accurately determine cell viability. Hence, in order to further confirm the cell viability after treatment calcein AM was utilised since it can only be taken up and converted to fluorescent dye by live cells and be excluded by dead cells. Ideally, a flow cytometry would be appropriate for the detection of calcein fluorescence, and co-staining with DAPI would allow the quantitative analysis of the viable cell number. However, here the representative images were shown and might be less generalisable as one field per slide and three slides per treatment group were performed.

The cell viability after treatment with AAS was examined. In the absence of H_2O_2 after starvation in normoxia and hypoxia, cytosolic calcein fluorescence could be visualised in HK-2 cells after 24 hours of treatment with 0x (pH 7.5; Figure 3.9 a and d) and 0.5x AAS (pH 6.4; Figure 3.9 b and e). However, there was no fluorescence at all in cells exposed to 1x AAS (pH 3.8; Figure 3.9 c and f), suggesting no viability in all cells remaining attached. In the presence of H_2O_2 after starvation in normoxia and hypoxia, cytosolic calcein fluorescence could be visualised in all cells treated with 0x (pH 7.5; Figure 3.10 a and d) and 0.5x AAS (pH 6.4; Figure 3.10 b and e). However, there was no fluorescence at all in cells treated with 1x AAS (pH 3.8; Figure 3.10 c and f), suggesting no cell viability in all cells remaining attached. We then confirmed the cell viability after treatment with AAS at pH 7.5 adjusted with KOH. In the absence of H_2O_2 after starvation in normoxia and hypoxia, cytosolic calcein fluorescence could be visualised in HK-2 cells treated with 0x, 0.5x and 1x AAS at

pH 7.5 for 24 hours (Figure 3.11). In the presence of H_2O_2 after starvation in normoxia and hypoxia, cytosolic calcein fluorescence decreased with increasing AAS concentration due to the reduction in the cell population (Figure 3.12). However, this required the quantitative analysis to confirm the viable cell number. Additionally, the effect of HBSS at varying pH on HK-2 cell viability was also examined. After starvation in normoxia and hypoxia, the cytosolic calcein fluorescence decreased with the reduction in pH (Figure 3.13-3.16). From pH 7.8 to 6.4, the decreased fluorescence was mainly due to the gradual reduction in the cell number, but this required the quantitative analysis to confirm the viable cell number. However, there was no fluorescence detected in cells treated with HBSS at pH 5.8, 4.8 and 3.8 despite HK-2 cells still remaining attached (Figure 3.13-3.16). This indicated no viability in these attached cells, consistent with the findings from the MTT assay.

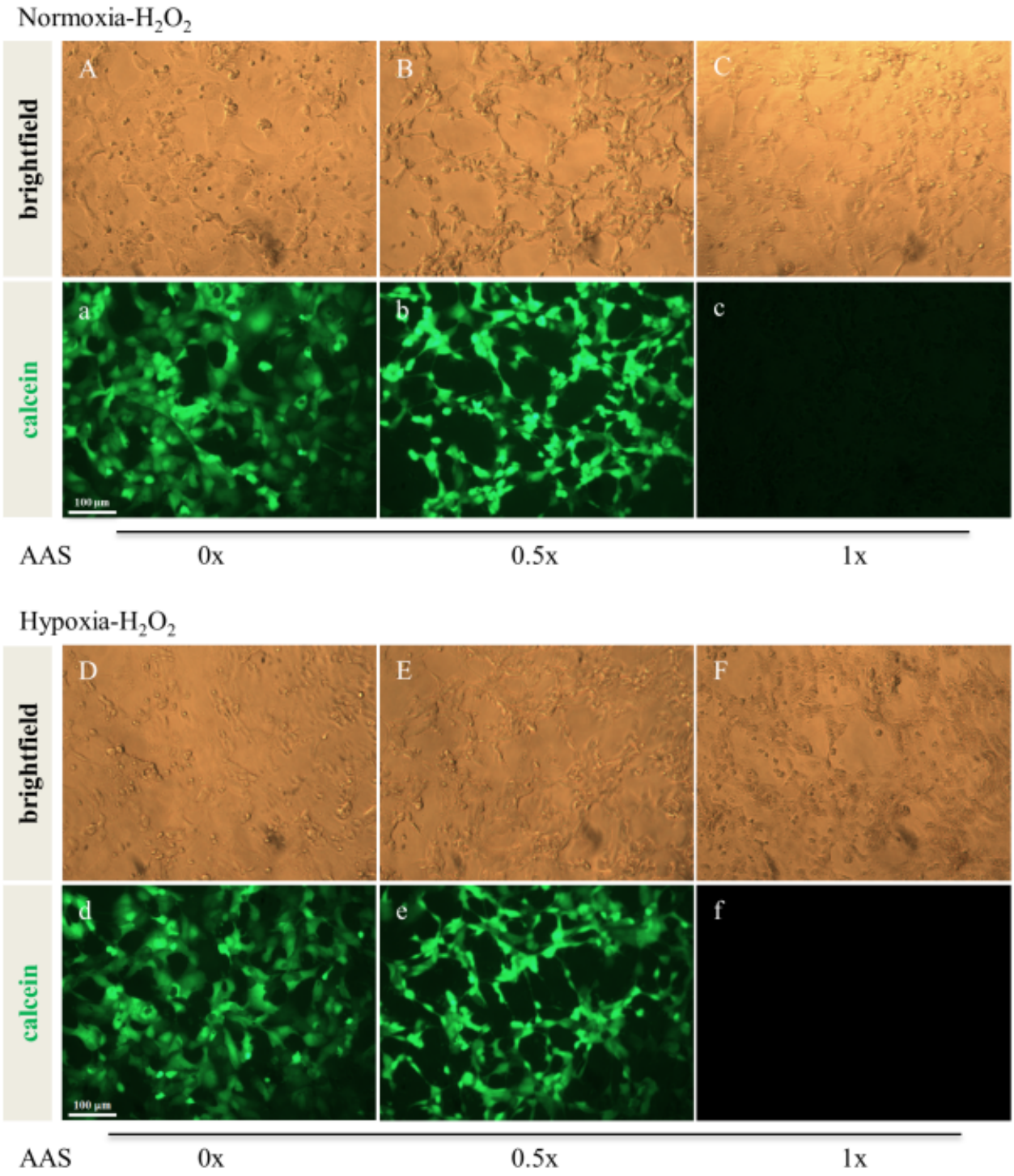


Figure 3. 9 HK-2 cell viability after treatment with AAS following starvation in normoxia or hypoxia.

Representative images of viable cells stained with calcein AM after treatment with 0x (pH 7.5), 0.5x (pH 6.4) and 1x AAS (pH 3.8) following starvation in normoxia or hypoxia were displayed. Magnification, x20; scale bar = 100 μm. One field per slide and three slides per treatment group were performed for an n = 3.

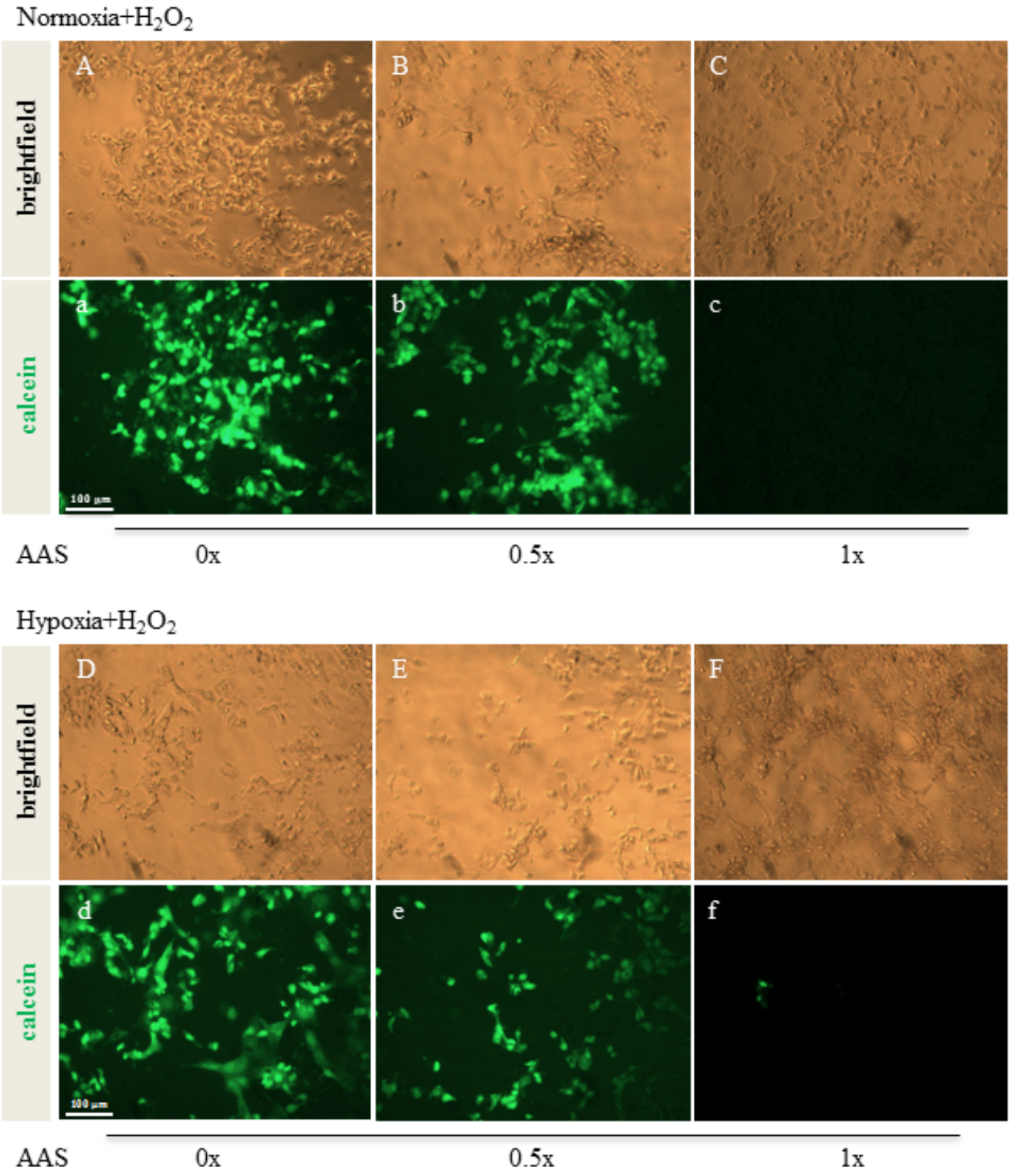


Figure 3. 10 HK-2 cell viability after treatment with AAS in the presence of H_2O_2 following starvation in normoxia or hypoxia.

Representative images of viable cells stained with calcein AM after treatment with 0x (pH 7.5), 0.5x (pH 6.4) and 1x AAS (pH 3.8) in the presence of H_2O_2 following starvation in normoxia or hypoxia were displayed. Magnification, x20; scale bar = 100 μm. One field per slide and three slides per treatment group were performed for an n = 3.

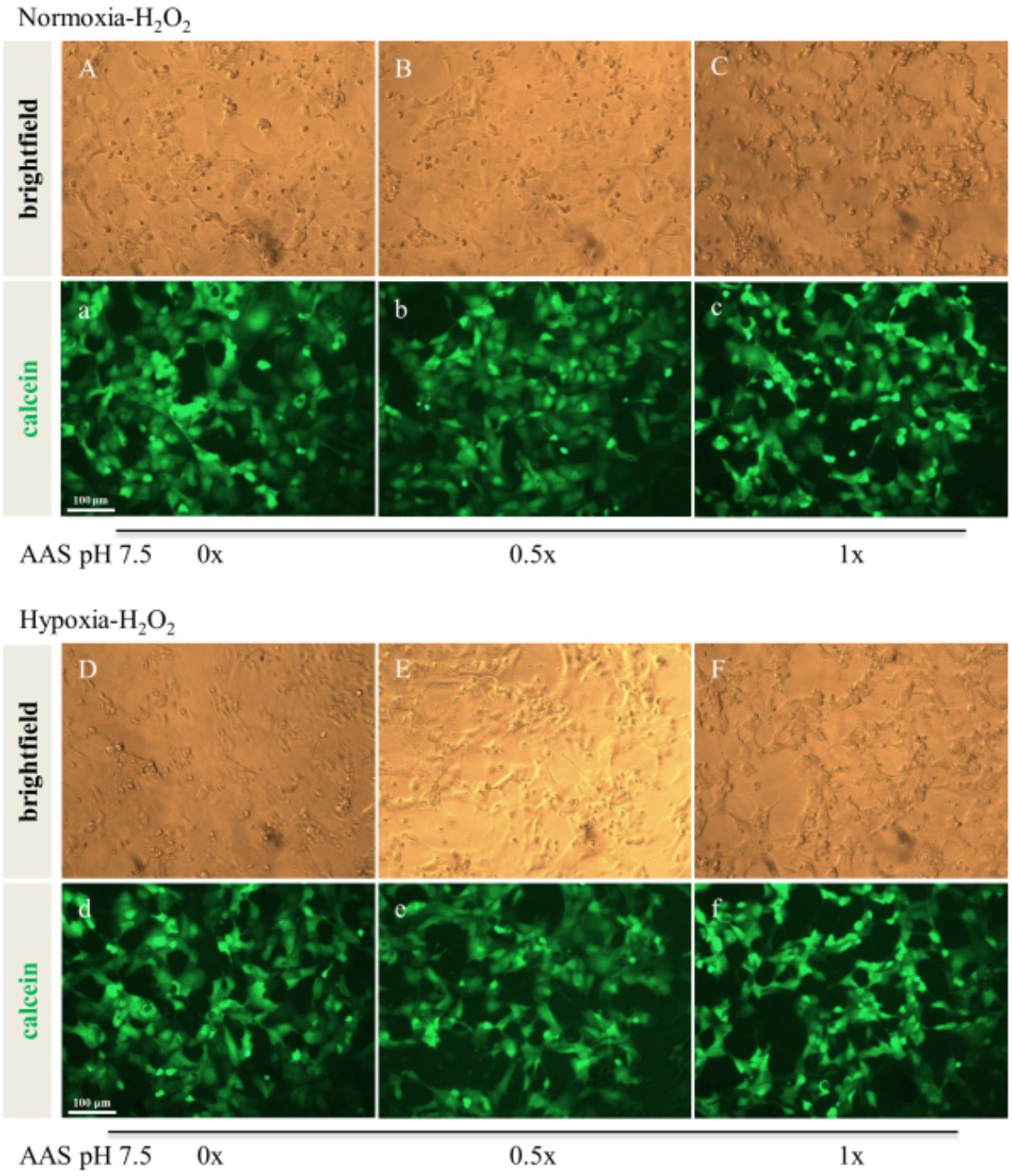


Figure 3. 11 HK-2 cell viability after treatment with AAS at pH 7.5 following starvation in normoxia or hypoxia.

Representative images of viable cells stained with calcein AM after treatment with 0x, 0.5x and 1x AAS at pH 7.5 following starvation in normoxia or hypoxia were displayed. Magnification, x20; scale bar = 100 μm. One field per slide and three slides per treatment group were performed for an n = 3.

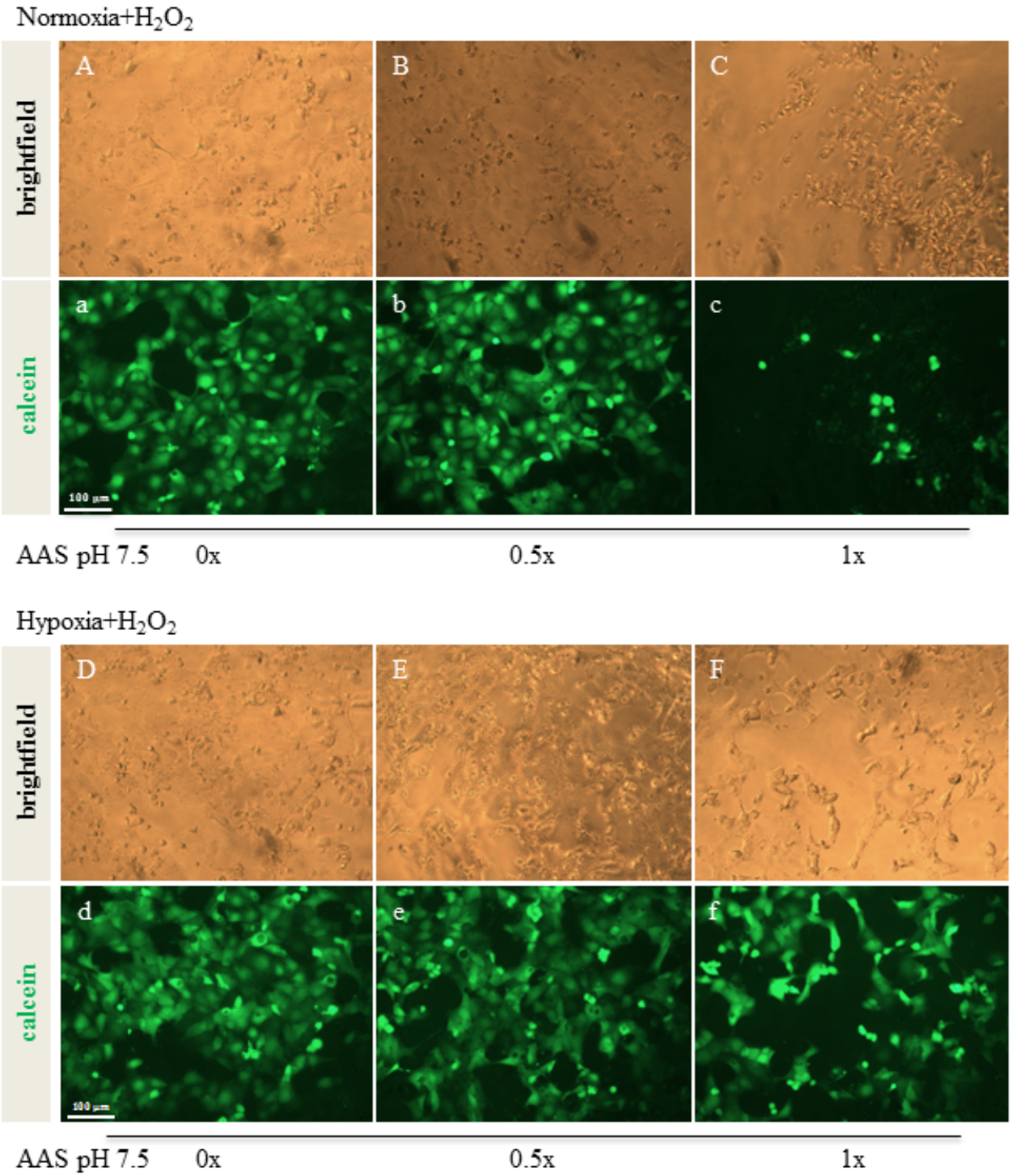


Figure 3. 12 HK-2 cell viability after treatment with AAS at pH 7.5 in the presence of H_2O_2 following starvation in normoxia or hypoxia.

Representative images of viable cells stained with calcein AM after treatment with 0x, 0.5x and 1x AAS at pH 7.5 in the presence of H_2O_2 following starvation in normoxia or hypoxia were displayed. Magnification, x20; scale bar = 100 μm. One field per slide and three slides per treatment group were performed for an n = 3.

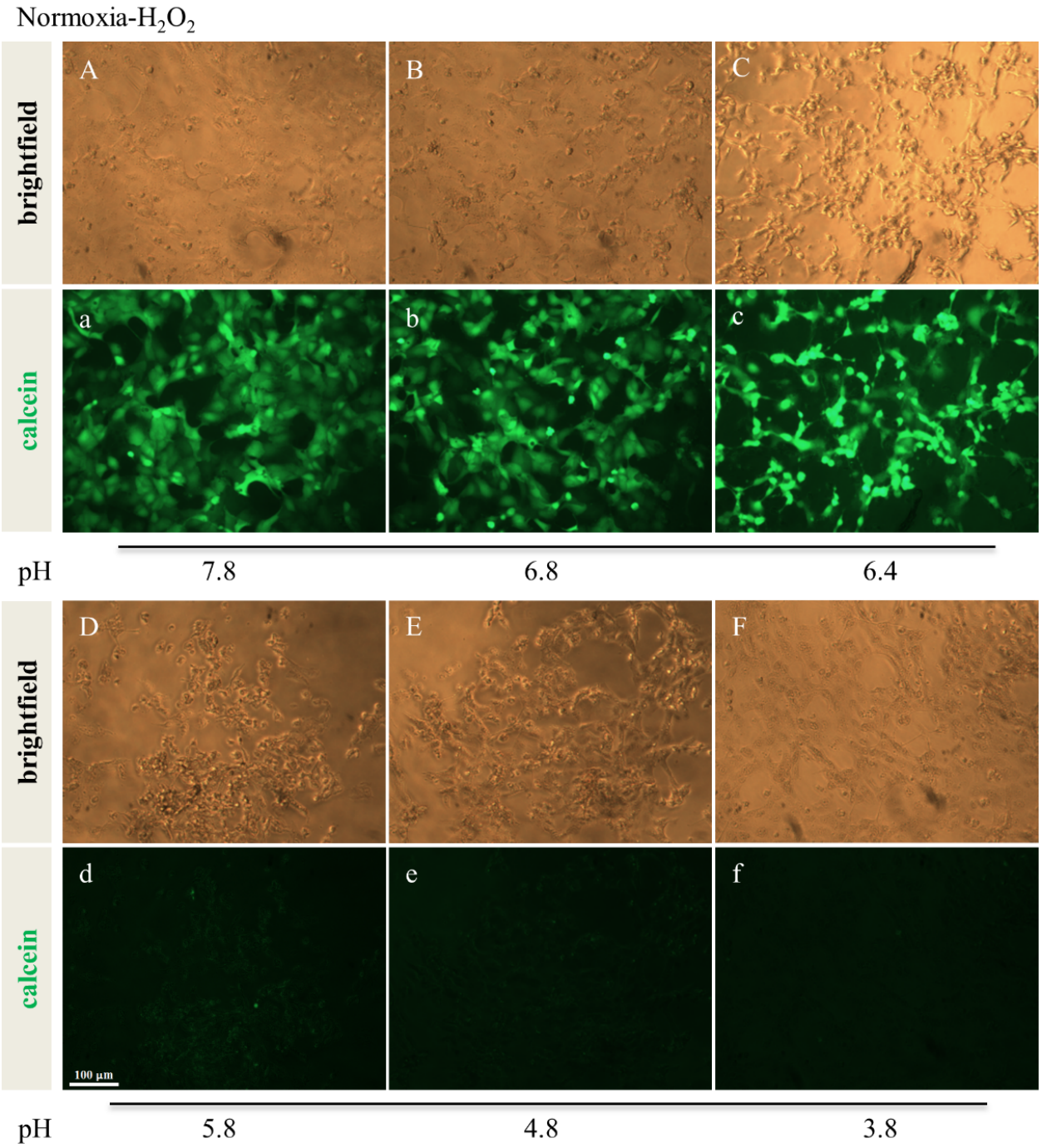


Figure 3. 13 Effects of pH on HK-2 cell viability following starvation in normoxia.

Representative images of viable cells stained with calcein AM after treatment with HBSS at pH 7.8, 6.8, 6.4, 5.8, 4.8 and 3.8 following starvation in normoxia were displayed. Magnification, x20; scale bar = 100 μm. One field per slide and three slides per treatment group were performed for an n = 3.

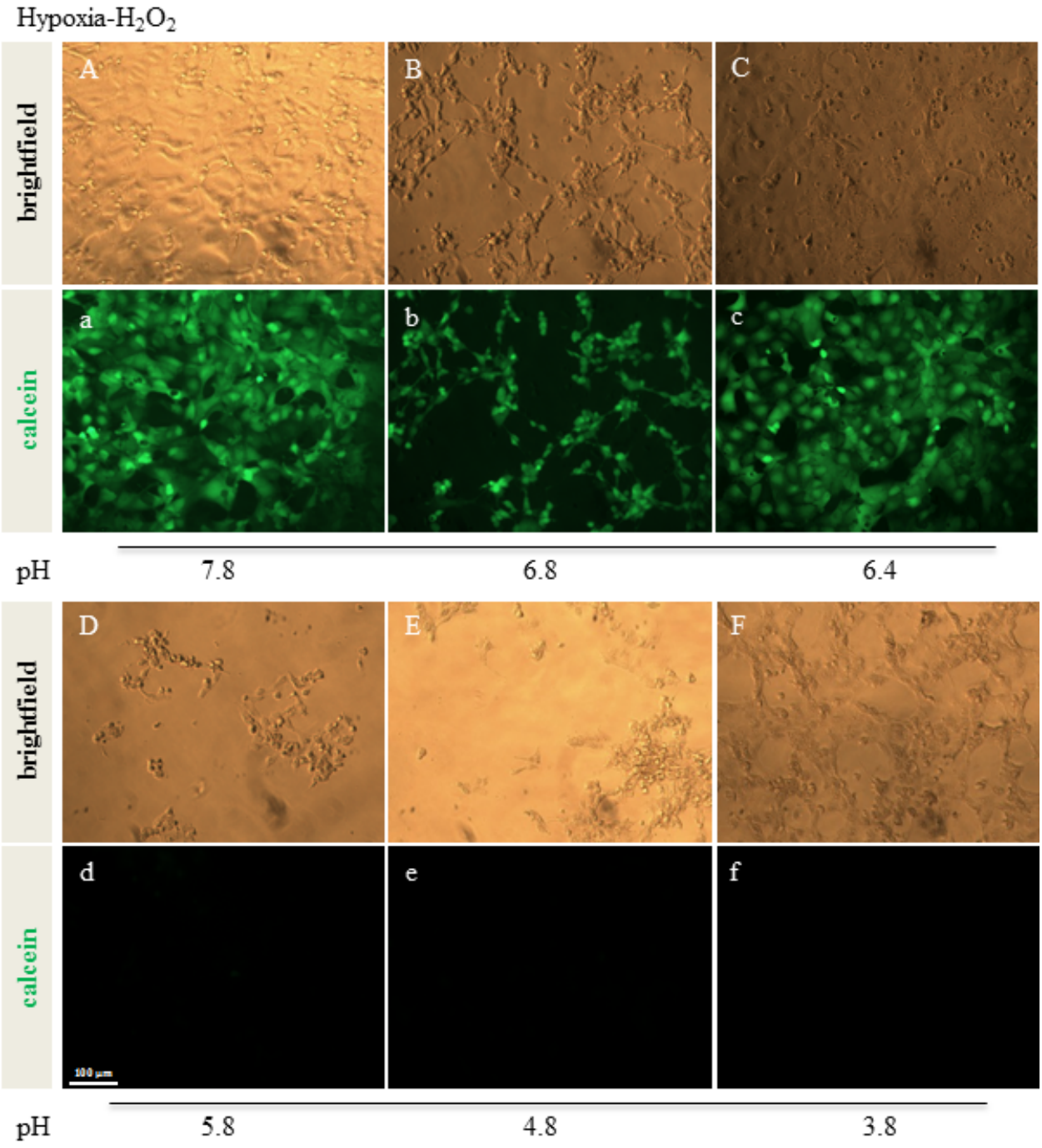


Figure 3. 14 Effects of pH on HK-2 cell viability following starvation in hypoxia.

Representative images of viable cells stained with calcein AM after treatment with HBSS at pH 7.8, 6.8, 6.4, 5.8, 4.8 and 3.8 following starvation in hypoxia were displayed. Magnification, x20; scale bar = 100 μm. One field per slide and three slides per treatment group were performed for an n = 3.

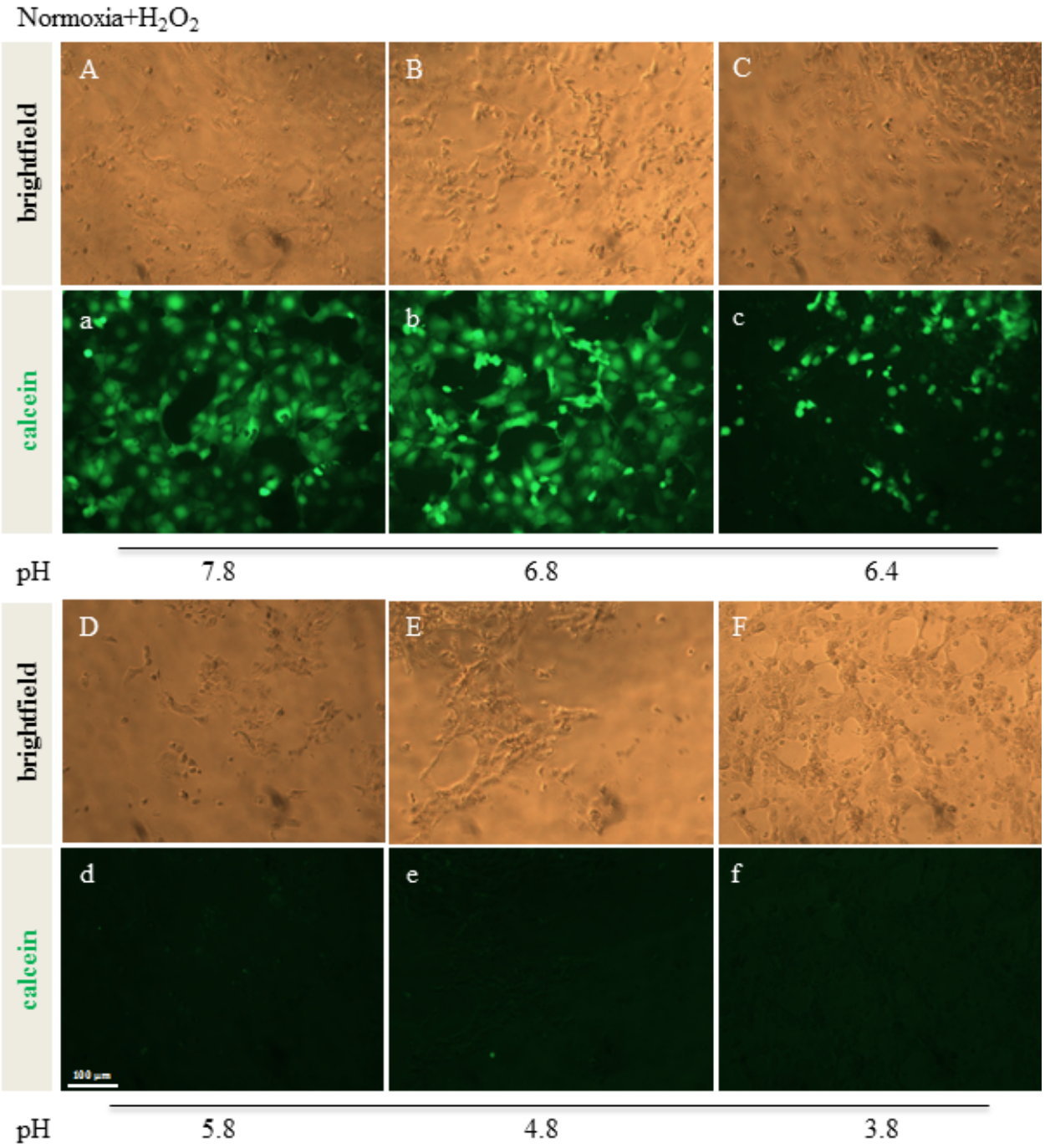


Figure 3. 15 Effects of pH on HK-2 cell viability in the presence of H_2O_2 following starvation in normoxia.

Representative images of viable cells stained with calcein AM after treatment with HBSS at pH 7.8, 6.8, 6.4, 5.8, 4.8 and 3.8 in the presence of H_2O_2 following starvation in normoxia were displayed. Magnification, x20; scale bar = 100 μm. One field per slide and three slides per treatment group were performed for an n = 3.

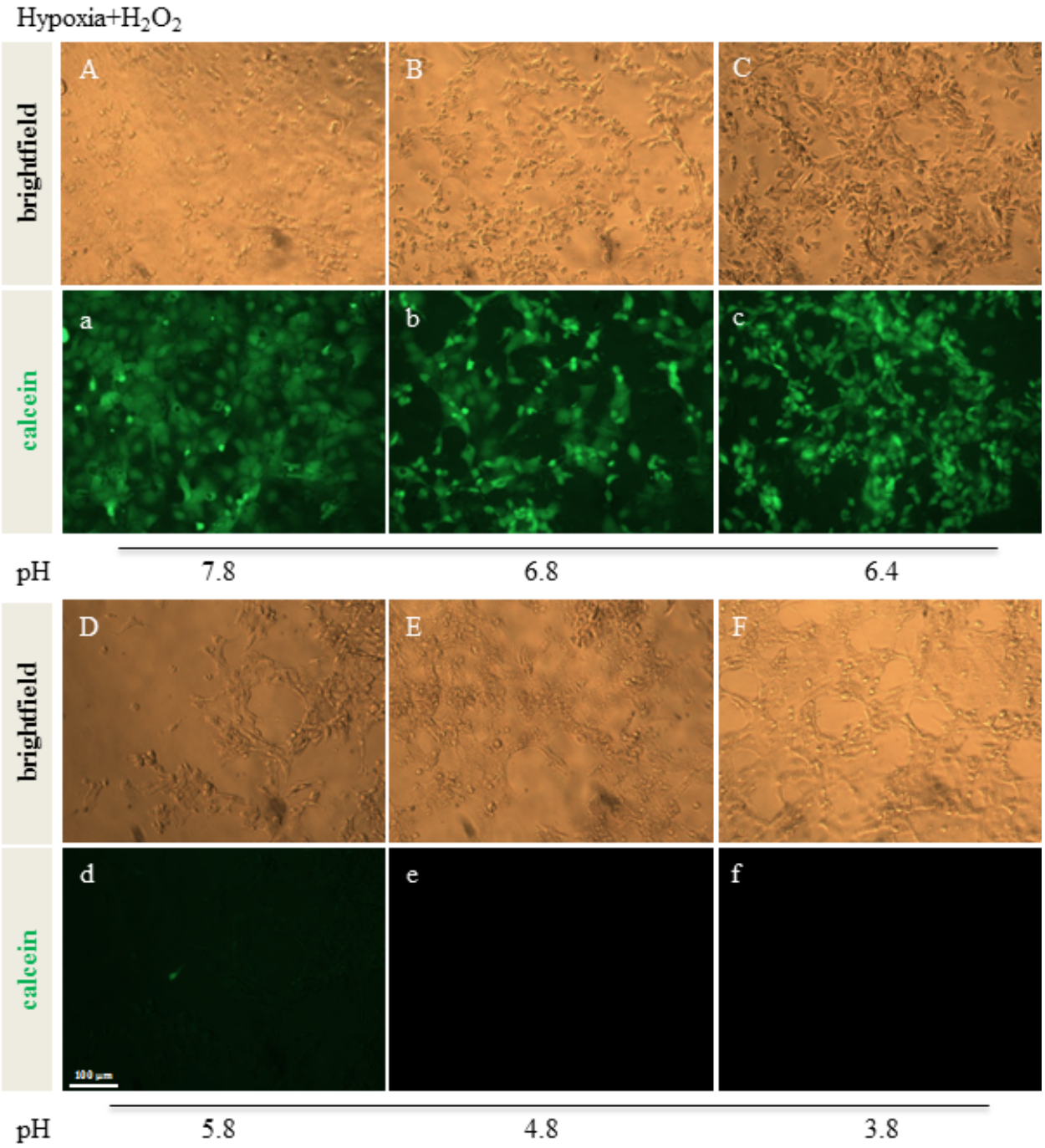


Figure 3. 16 Effects of pH on HK-2 cell viability in the presence of H_2O_2 following starvation in hypoxia.

Representative images of viable cells stained with calcein AM after treatment with HBSS at pH 7.8, 6.8, 6.4, 5.8, 4.8 and 3.8 in the presence of H_2O_2 following starvation in hypoxia were displayed. Magnification, x20; scale bar = 100 μm. One field per slide and three slides per treatment group were performed for an n = 3.

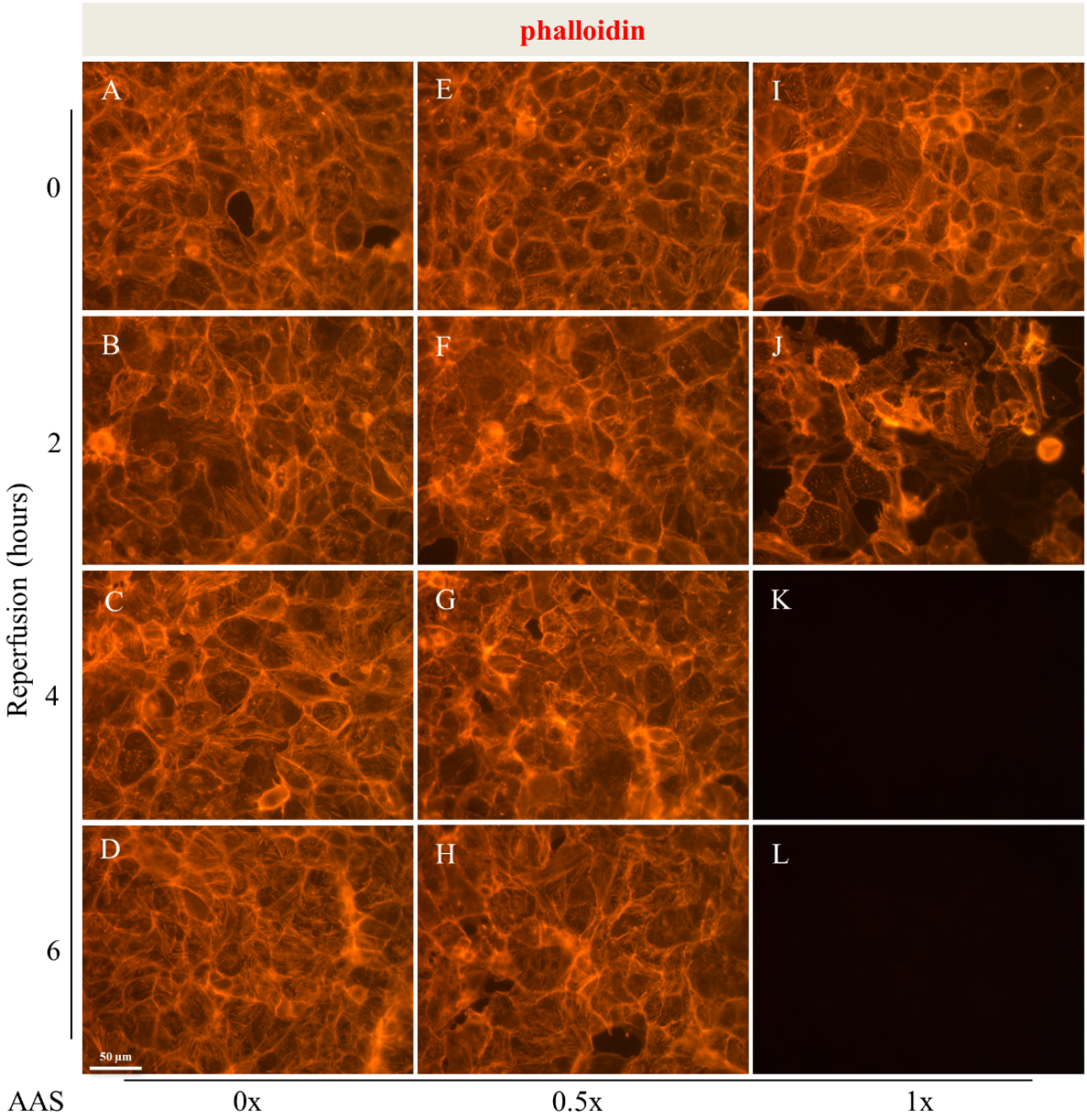
3.2.7 F-actin cytoskeleton alterations in HK-2 cells in response to AAS following simulated I/R injury

As the significant cell detachment occurred after 24 hours of treatment with 0.5x AAS in the presence of H_2O_2 following 24 hours of starvation in normoxia and after 24 hours of treatment with 0x (pH 7.5) or 0.5x (pH 6.4) AAS in the presence of H_2O_2 following 24 hours of starvation in hypoxia, the actin cytoskeleton was assessed with phalloidin labelling. Cell detachment had been previously observed after 24 hours of treatment, and therefore a time course (0-6 hours) of analysis which preceded this event was chosen here. It is important to note that a lower cell density is more appropriate to observe and analyse the changes in filamentous actin. However, here HK-2 cells were still grown into full confluent in order to maintain the consistent experimental protocol throughout the whole study. Additionally, more fields per slide are required for a reproducible observation and quantitative analysis. As one field per slide and three slides per treatment group were obtained without quantitative analysis, the representative images shown here might be less generalisable.

Cells treated with 0x (pH 7.5) and 0.5x (pH 6.4) AAS in the absence of H_2O_2 for 0, 2, 4 and 6 hours following 24 hours of starvation in normoxia (Figure 3.17 A-H and a-h) still maintained an organised F-actin network with long stress fibres. The long cytoplasmic stress fibre F-actin at 2 hours was observed in high power images (Figure 3.19 A and B). By contrast, cells treated with 0x (pH 7.5) and 0.5x (pH 6.4) AAS after starvation in hypoxia showed more cells with cortical stress fibre distribution rather than cytoplasmic stress fibres (Figure 3.18 A-H and a-h; Figure 3.19 D and E). However, to quantify the percentage of the cell number with cortical

or cytoplasmic stress fibres F-actin more fields per slide are required. Furthermore, F-actin was disrupted at 2 hours of treatment with 1x AAS (pH 3.8) in the absence of H_2O_2 (Figure 3.17; Figure 3.18), showing short stress fibres among the cytoplasm and the disappearance of F-actin in some cells. High power images of F-actin at 2 hours of treatment with 1x AAS (pH 3.8) displayed shorter stress fibres and a loss of cytoskeleton (Figure 3.19 C and F) compared with 0x AAS (Figure 3.19 A). After 4 hours, F-actin was completely lost (Figure 3.17; Figure 3.18). Exposure of cells to H_2O_2 showed a large-scale loss of cells in the 0.5x AAS group as seen previously (Figure 3.21), making it difficult to compare with other treatments. Nevertheless, even if there was no loss of cells in the 1x AAS group, it still showed the complete absence of F-actin cytoskeleton (Figure 3.20; Figure 3.21).

Normoxia-H_2O_2



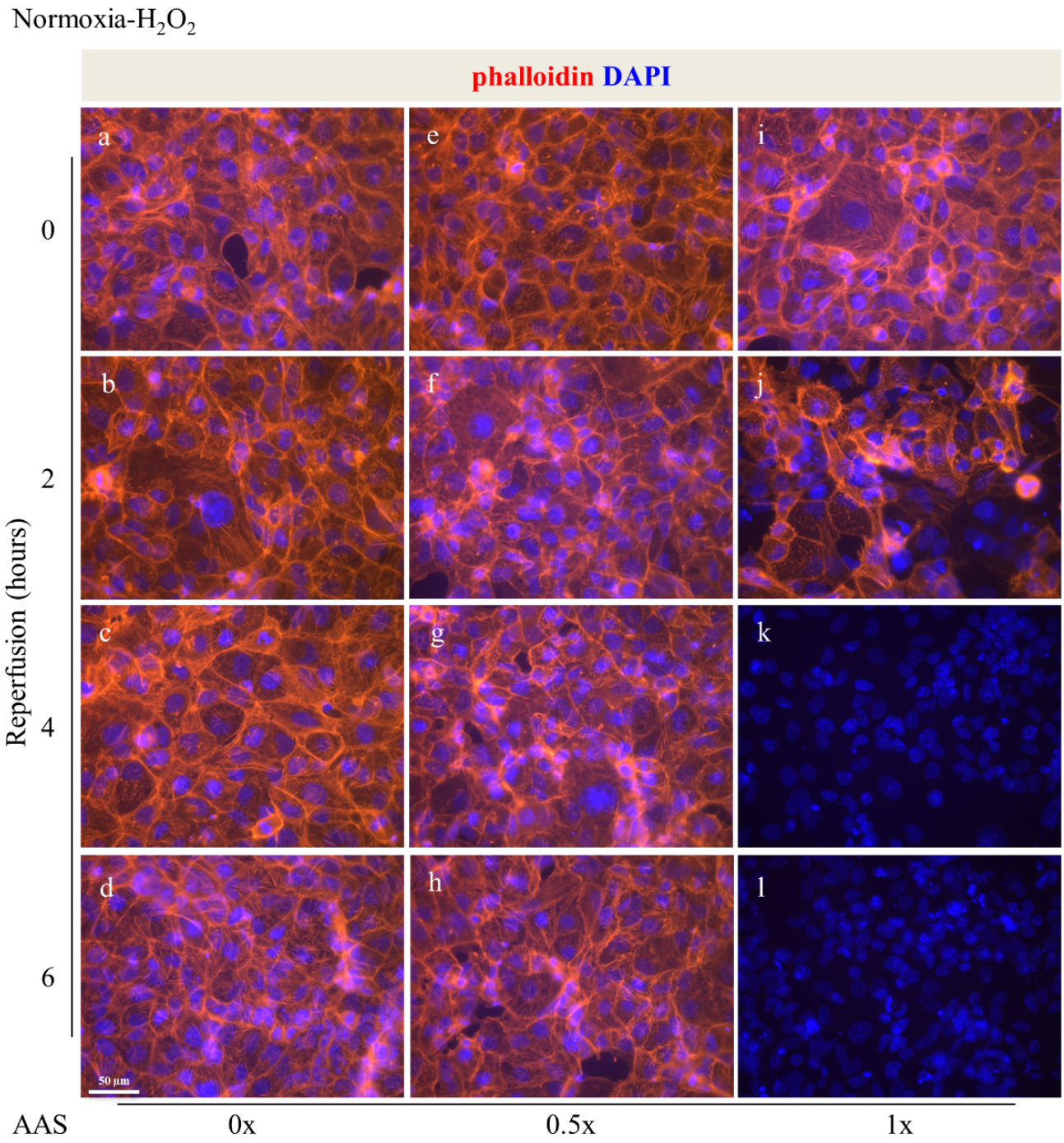
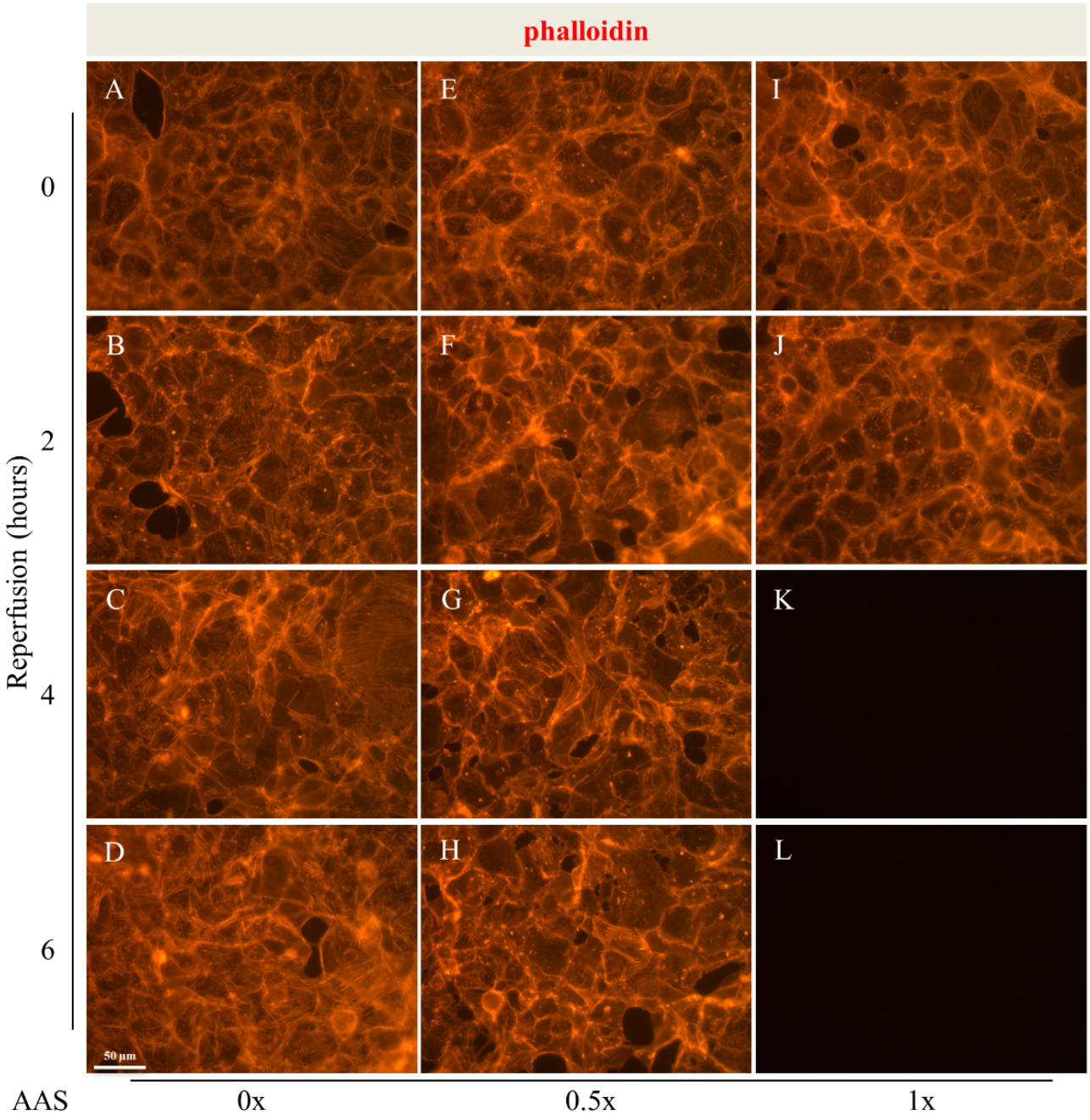


Figure 3. 17 Time course images of phalloidin-labelled HK-2 cells treated with AAS following starvation.

(A-L) Representative images showed phalloidin-labelled HK-2 cells treated with 0x (pH 7.5), 0.5x (pH 6.4) and 1x AAS (pH 3.8) for 6 hours following starvation in normoxia. (a-l) Overlay images showed that phalloidin (red) and DAPI (blue) were the same area. Magnification, x40; Scale bars = 50 µm. One field per slide and three slides per treatment group were performed for an n = 3.


Hypoxia-H_2O_2
phalloidin
A
E
I
B
F
J
C
G
K
D
H
L
0
2
4
6
Reperfusion (hours)
50 μm
AAS
0x
0.5x
1x

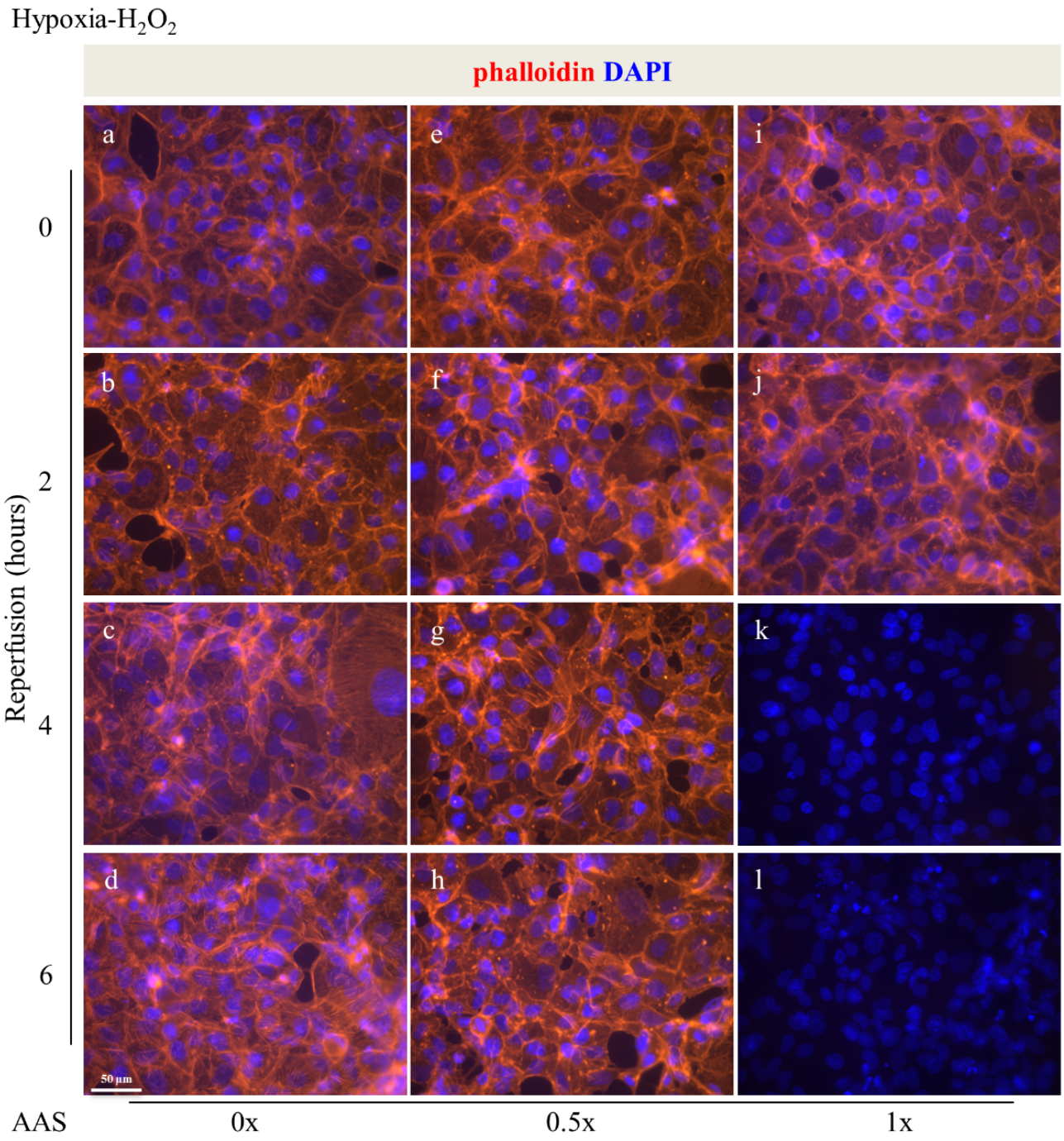


Figure 3. 18 Time course images of phalloidin-labelled HK-2 cells treated with AAS following starvation.

(A-L) Representative images showed phalloidin-labelled HK-2 cells treated with 0x (pH 7.5), 0.5x (pH 6.4) and 1x AAS (pH 3.8) for 6 hours following starvation in hypoxia. (a-l) Overlay images showed that phalloidin (red) and DAPI (blue) were the same area. Magnification, x40; Scale bars = 50 µm. One field per slide and three slides per treatment group were performed for an n = 3.

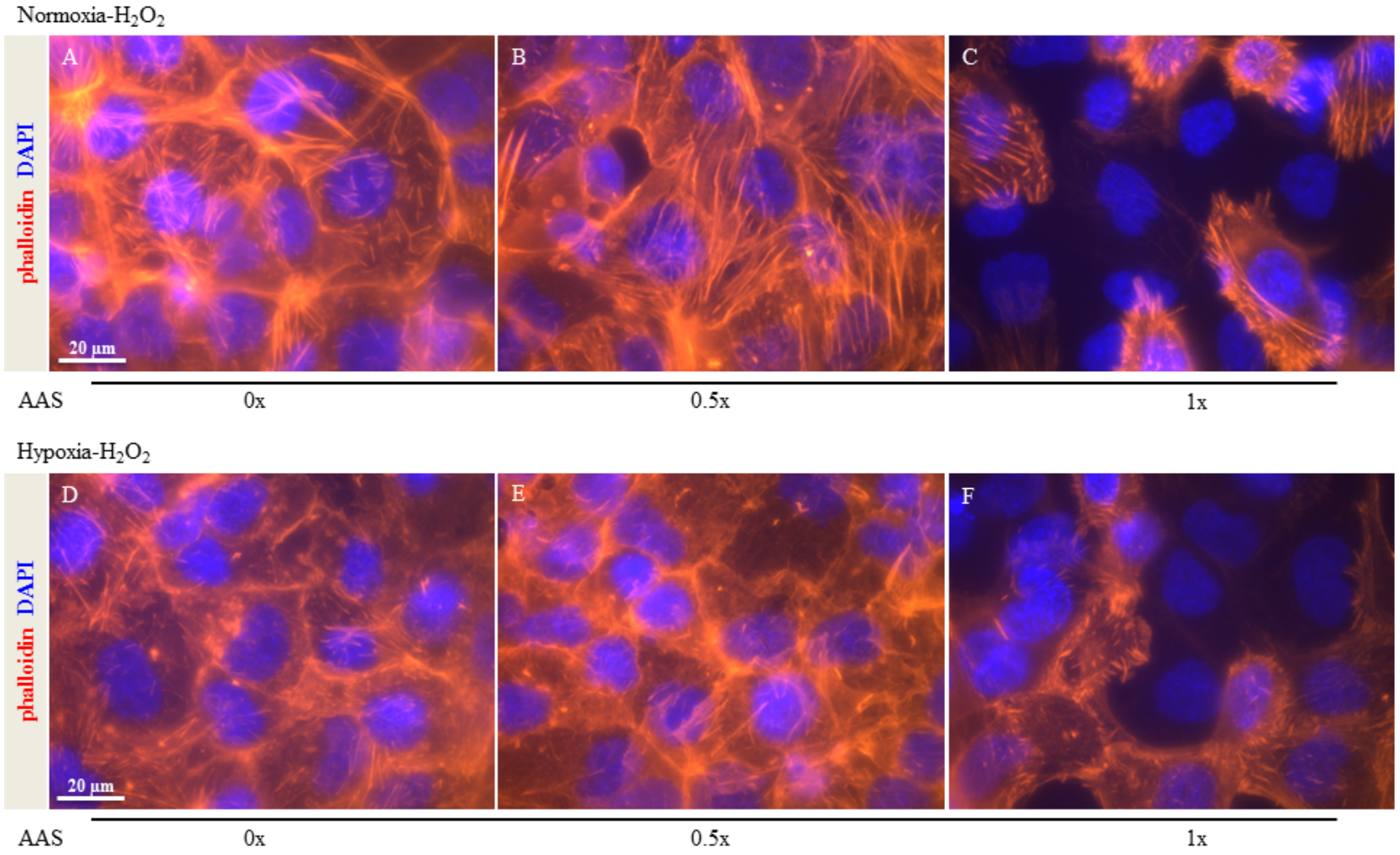
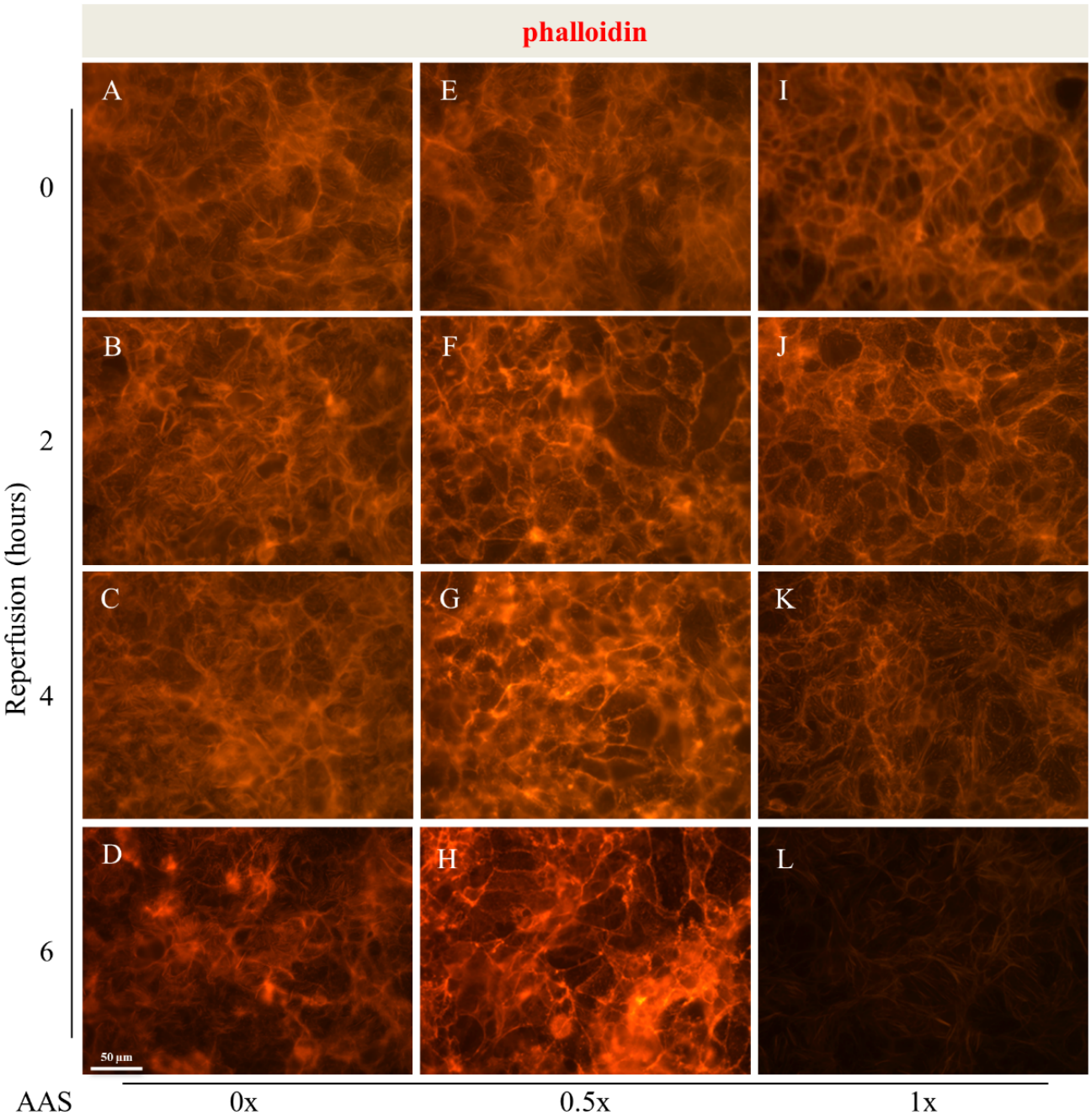


Figure 3. 19 Effects of AAS on F-actin in HK-2 cells at 2 hours following starvation.

Representative high power images of F-actin at 2 hours of treatment with 0x (pH 7.5), 0.5x (pH 6.4) and 1x (pH 3.8) AAS following starvation were acquired. Magnification, x100; scale bar = 20 µm. One field per slide and three slides per treatment group were performed for an n = 3.

Normoxia+H_2O_2



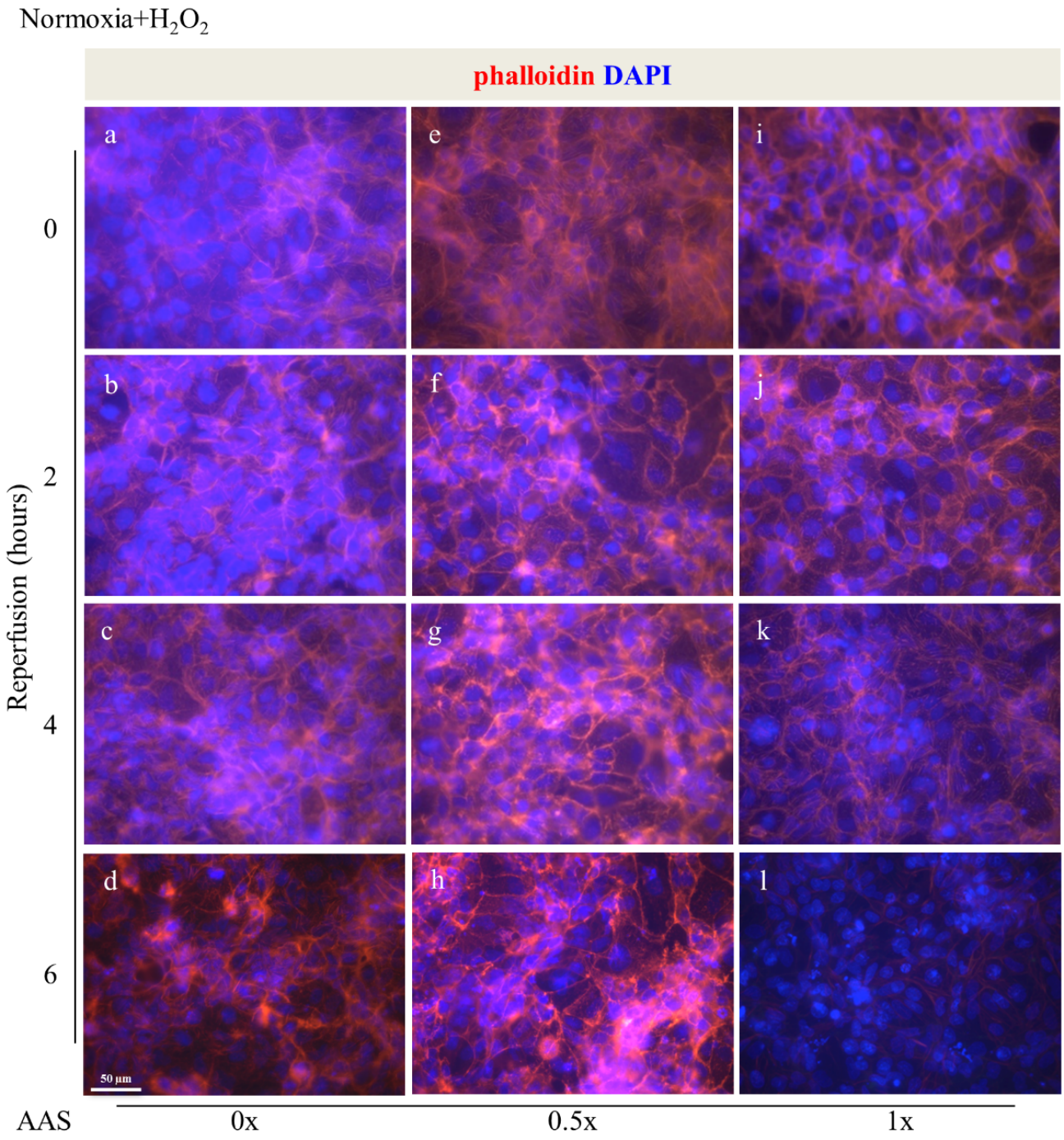
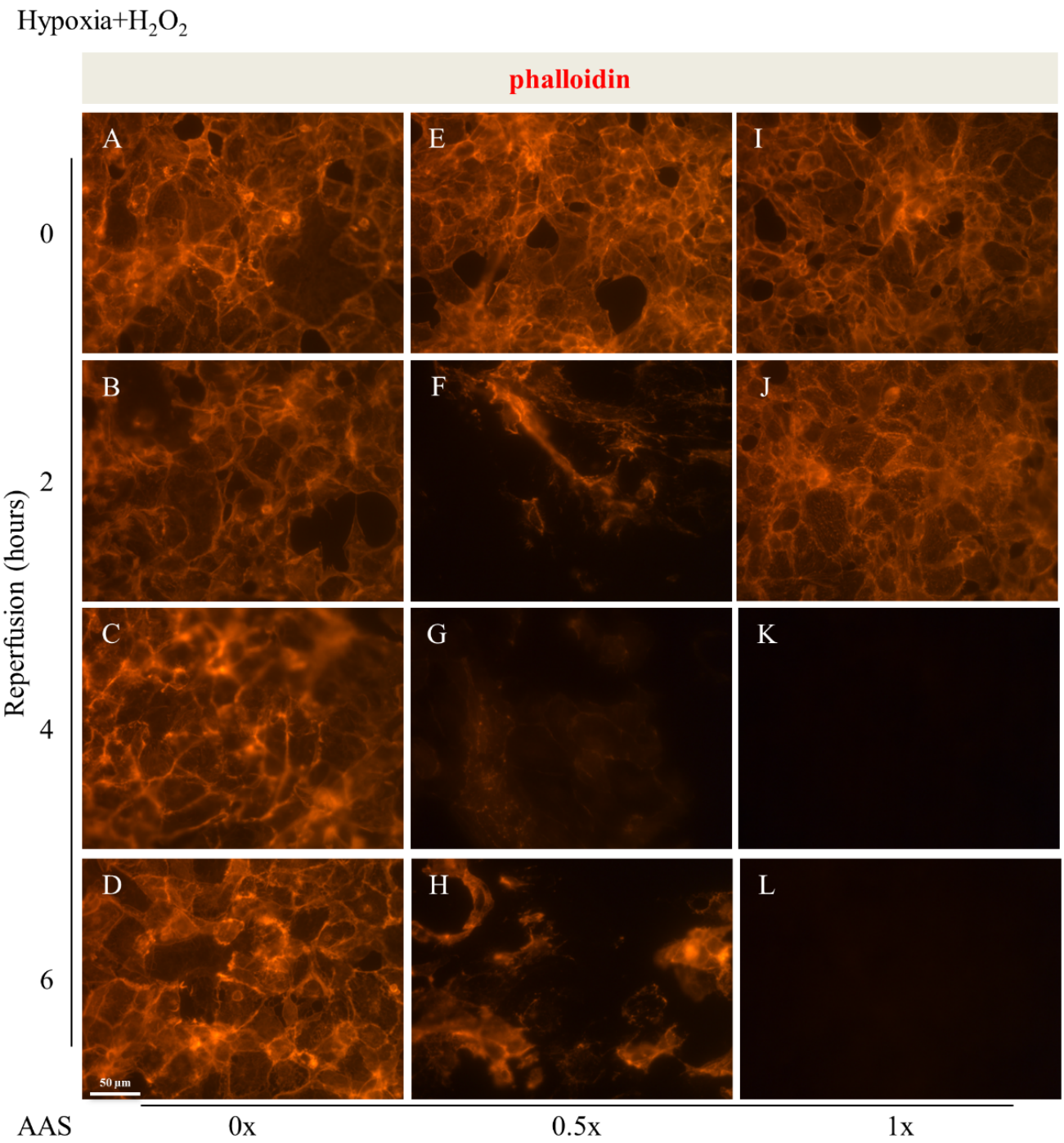


Figure 3. 20 Time course images of phalloidin-labelled HK-2 cells treated with AAS in the presence of H_2O_2 following starvation.

(A-L) Representative images showed phalloidin-labelled HK-2 cells treated with 0x (pH 7.5), 0.5x (pH 6.4) and 1x (pH 3.8) AAS in the presence of H_2O_2 for 6 hours following starvation in normoxia. (a-l) Overlay images showed that phalloidin (red) and DAPI (blue) were the same area. Magnification, x40; Scale bars = 50 µm. One field per slide and three slides per treatment group were performed for an n = 3.


Hypoxia+H_2O_2
phalloidin
A
E
I
B
F
J
C
G
K
D
H
L
0
2
4
6
Reperfusion (hours)
50 µm
AAS
0x
0.5x
1x

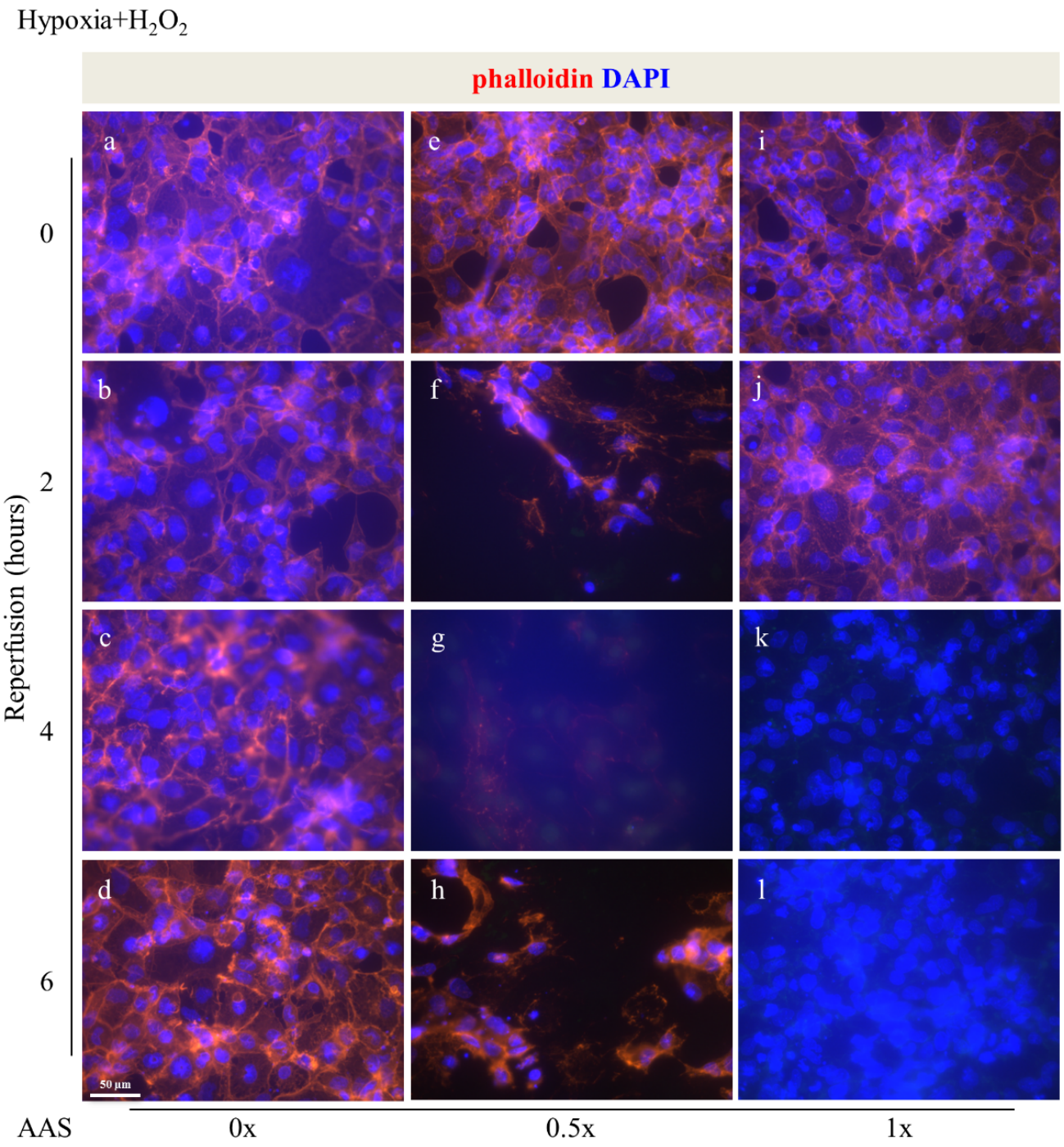
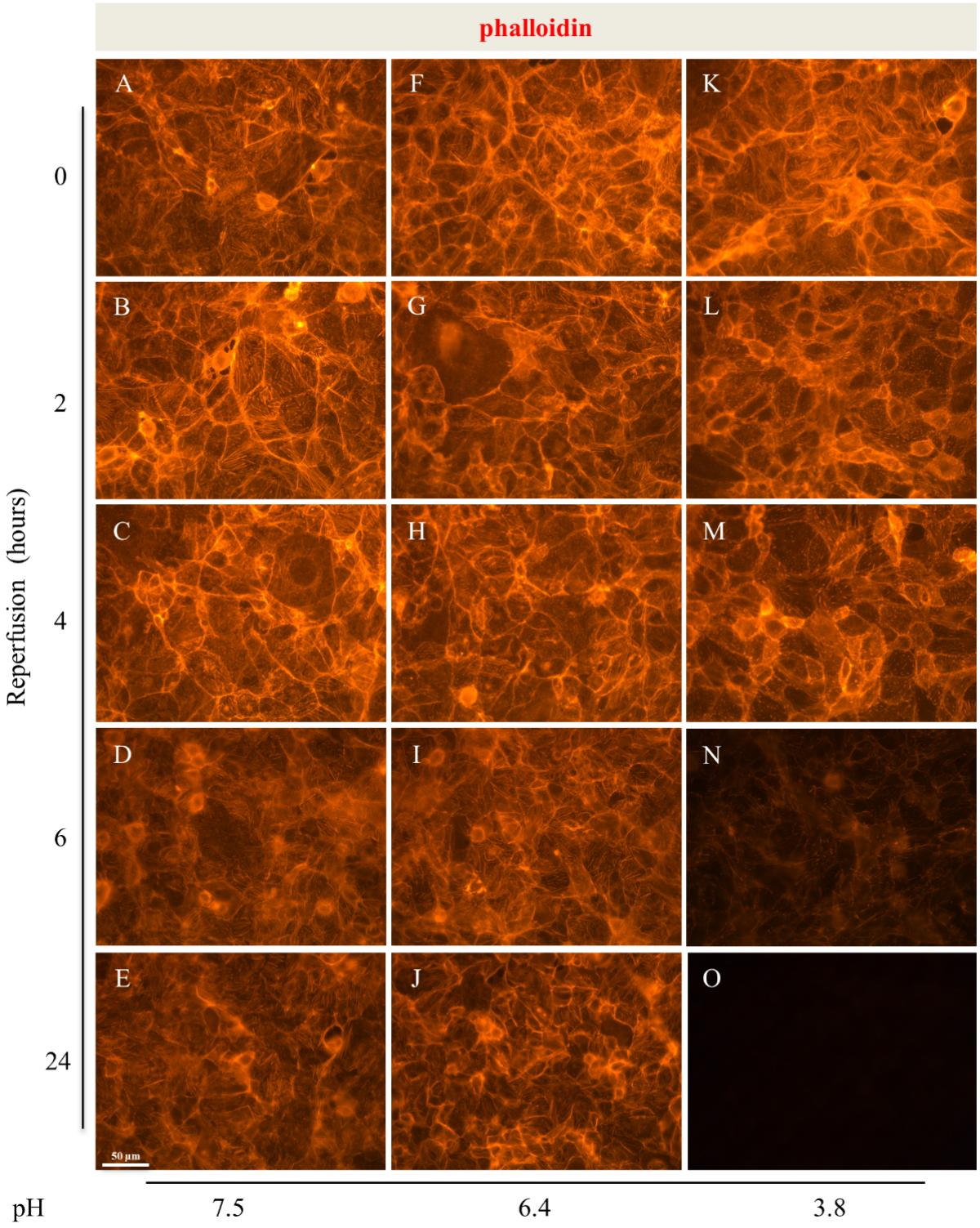


Figure 3. 21 Time course images of phalloidin-labelled HK-2 cells treated with AAS in the presence of H_2O_2 following starvation.

(A-L) Representative images showed phalloidin-labelled HK-2 cells treated with 0x (pH 7.5), 0.5x (pH 6.4) and 1x (pH 3.8) AAS in the presence of H_2O_2 for 6 hours following starvation in hypoxia. (a-l) Overlay images showed that phalloidin (red) and DAPI (blue) were the same area. Magnification, x40; Scale bars = 50 µm. One field per slide and three slides per treatment group were performed for an n = 3.

3.2.8 F-actin cytoskeleton alterations in HK-2 cells in response to pH following D/R injury

To confirm whether F-actin alterations in response to treatment resulted from AAS or pH, F-actin was observed by labelling with phalloidin after treatment with HBSS at pH 7.5, 6.4 and 3.8 for 0, 2, 4, 6 and 24 hours following 24 hours of nutrient deprivation in normoxia. HK-2 cells treated with HBSS at pH 7.5 and 6.4 maintained unaltered F-actin during 24 hours (Figure 3.22 A-J and a-j). The cytoplasmic stress fibres in all cells at 6 hours could be observed in the high power images (Figure 3.23 A and B). However, F-actin staining with phalloidin after treatment with HBSS at pH 3.8 became less bright at 6 hours (Figure 3.22 N and n; Figure 3.23 C) and completely disrupted at 24 hours (Figure 3.22 O and o), suggesting that the F-actin disrupted in a pH dependent manner. As the high cell density and one field per slide obtained did not allow quantitative analysis of the percentage of the cell number with cytoplasmic or cortical stress fibres, these images of the representative areas may be argued to be limited.


Normoxia-H_2O_2
phalloidin
A
F
K
B
G
L
C
H
M
D
I
N
E
J
O
50 μm
0
2
4
6
24
Reperfusion (hours)
pH
7.5
6.4
3.8

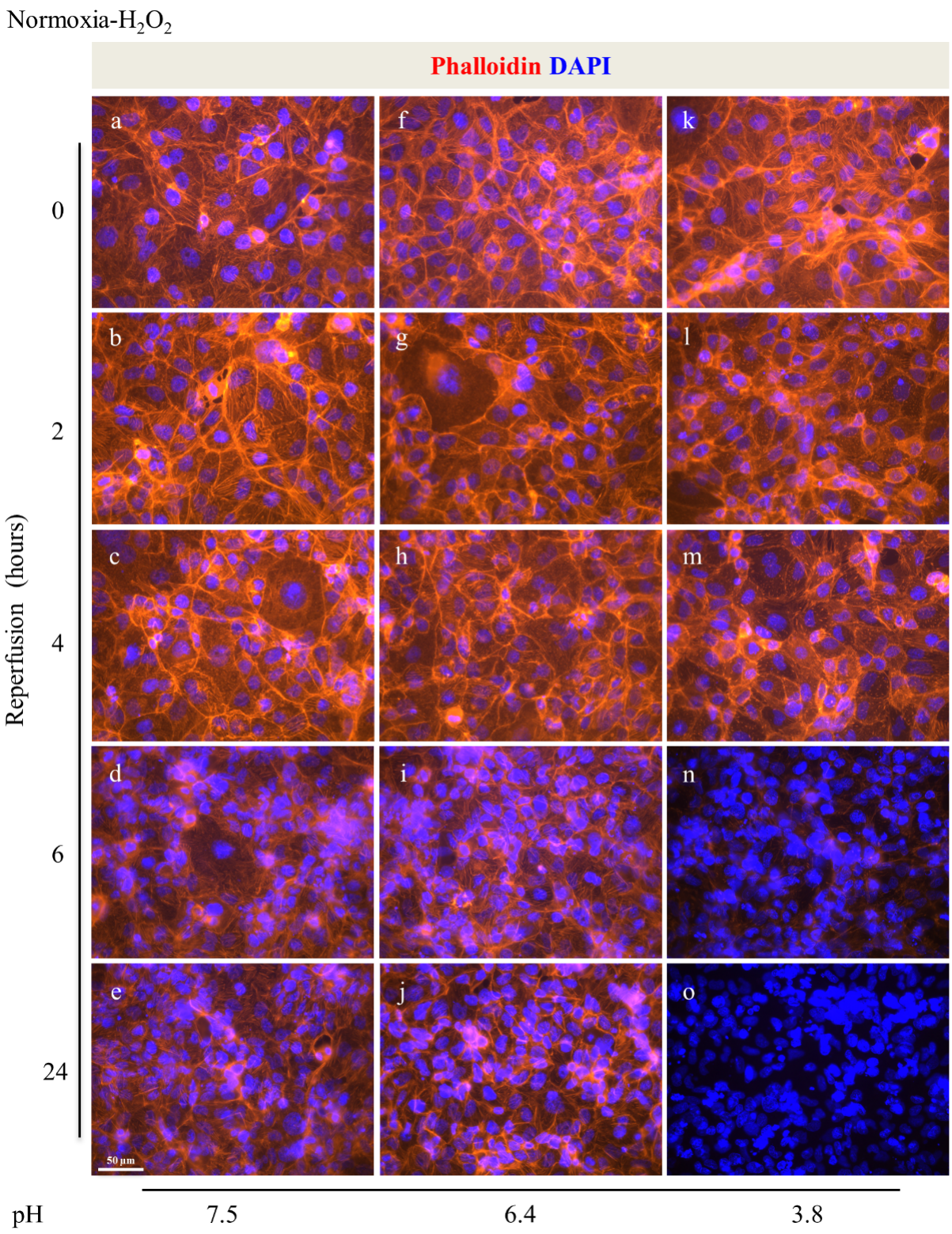


Figure 3. 22 Time course images of phalloidin-labelled HK-2 cells treated with HBSS at varying pH following starvation.

(A-O) Representative images showed phalloidin-labelled HK-2 cells treated with HBSS at pH 7.5, 6.4 and 3.8 for 24 hours following starvation. (a-o) Overlay images showed that phalloidin (red) and DAPI (blue) were the same area. Magnification, x40; Scale bars = 50 µm. One field per slide and three slides per treatment group were performed for an n = 3.

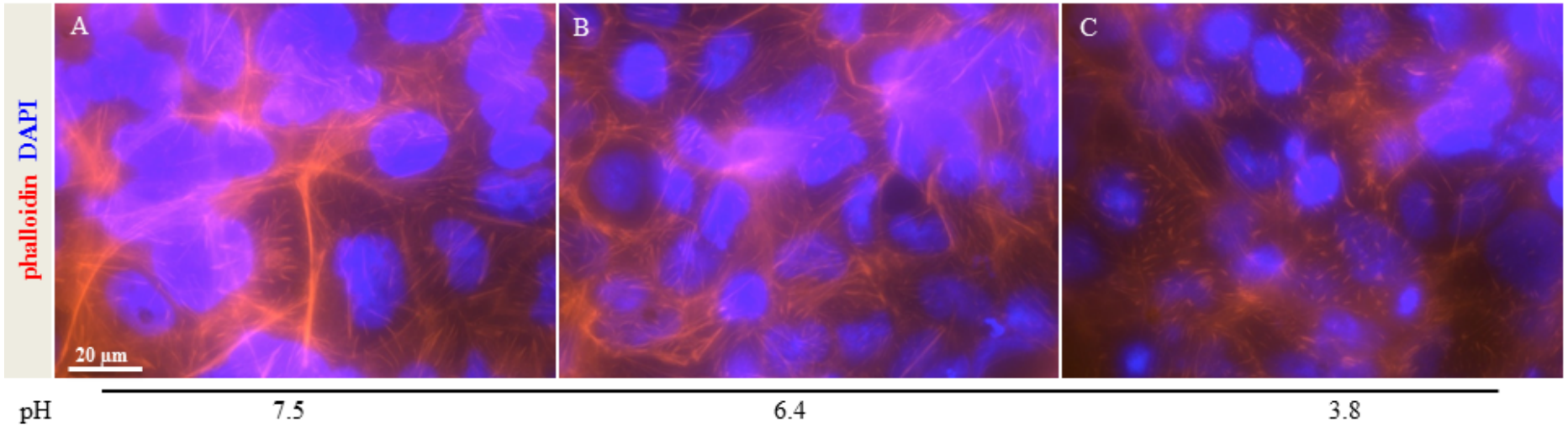


Figure 3. 23 Effects of pH on F-actin in HK-2 cells at 6 hours following starvation.

Representative high power images of F-actin at 6 hours of treatment with HBSS at 7.5, 6.4 and 3.8 following starvation were acquired. Magnification, x100; scale bar = 20 µm. One field per slide and three slides per treatment group were performed for an n = 3.

3.2.9 Intracellular ROS in HK-2 cells treated with AAS after simulated I/R injury

Here we determined i) whether the provision of H_2O_2 as a source of ROS could be a direct extracellular damage or ii) whether the generation of ROS by H_2O_2 may lead to the oxidation of amino acids to form more potent ROS after treatment with AAS following simulated I/R injury. To achieve this, CMH_2DCFDA was incubated with AAS solutions (pH 7.5) and was loaded in HK-2 cells during treatment with AAS (pH 7.5) to detect ROS production.

In the absence of cells, DCF fluorescence in any treatments without H_2O_2 did not show any differences and did not change over time (Figure 3.24). It was found that AAS, H_2O_2, time and all treatment interactions had strong effects on DCF fluorescence (Figure 3.24). There was a strong positive linear and quadratic relationship between AAS concentration and DCF fluorescence ($p < 0.001$; Figure 3.24); that is, DCF fluorescence increased in an AAS concentration dependent manner ($p < 0.001$; Figure 3.24). It was also found that DCF fluorescence was higher in the presence of H_2O_2 compared with that in the absence of H_2O_2 ($p < 0.001$; Figure 3.24) and that it increased in a time dependent manner ($p < 0.001$; Figure 3.24). More importantly, there were strong interactions of i) AAS and H_2O_2, ii) AAS and time, iii) H_2O_2 and time and iv) AAS, H_2O_2 and time (all $p < 0.001$; Figure 3.24), suggesting that ROS levels increased in an AAS concentration dependent manner in the presence of H_2O_2 over time.

In the presence of HK-2 cells, DCF fluorescence was strongly affected by AAS concentration, H_2O_2, oxygen and time (all $p < 0.001$; Figure 3.25). The ROS levels

increased with the increase in concentration of AAS, and the presence of H_2O_2 or starvation in normoxia also enhanced ROS production. These factors also interacted with time, indicating that the increased ROS levels caused by these factors were time dependent (all $p < 0.001$; Figure 3.25). Furthermore, a strong interaction between AAS and H_2O_2 on ROS levels was observed ($p < 0.001$; Figure 3.25). The positive linear relationship between AAS concentration and ROS generation was found to be further enhanced by the presence of H_2O_2 ($p < 0.001$; Figure 3.25). There was also an interaction of AAS, H_2O_2 and oxygen ($p = 0.047$; Figure 3.25), and the quadratic relationship between AAS concentration and ROS levels was positively affected by H_2O_2 and oxygen ($p = 0.040$; Figure 3.25). That is, the increasing AAS concentration in the presence of H_2O_2 following starvation in normoxia enhanced ROS production. The interaction of AAS, H_2O_2 and time again suggested that the positive linear relationship between AAS concentration and ROS levels was further enhanced by the presence of H_2O_2 over time. These results may suggest that amino acids and hydrogen peroxide were likely to form more potent ROS in HK-2 cells and contribute to cellular damage.

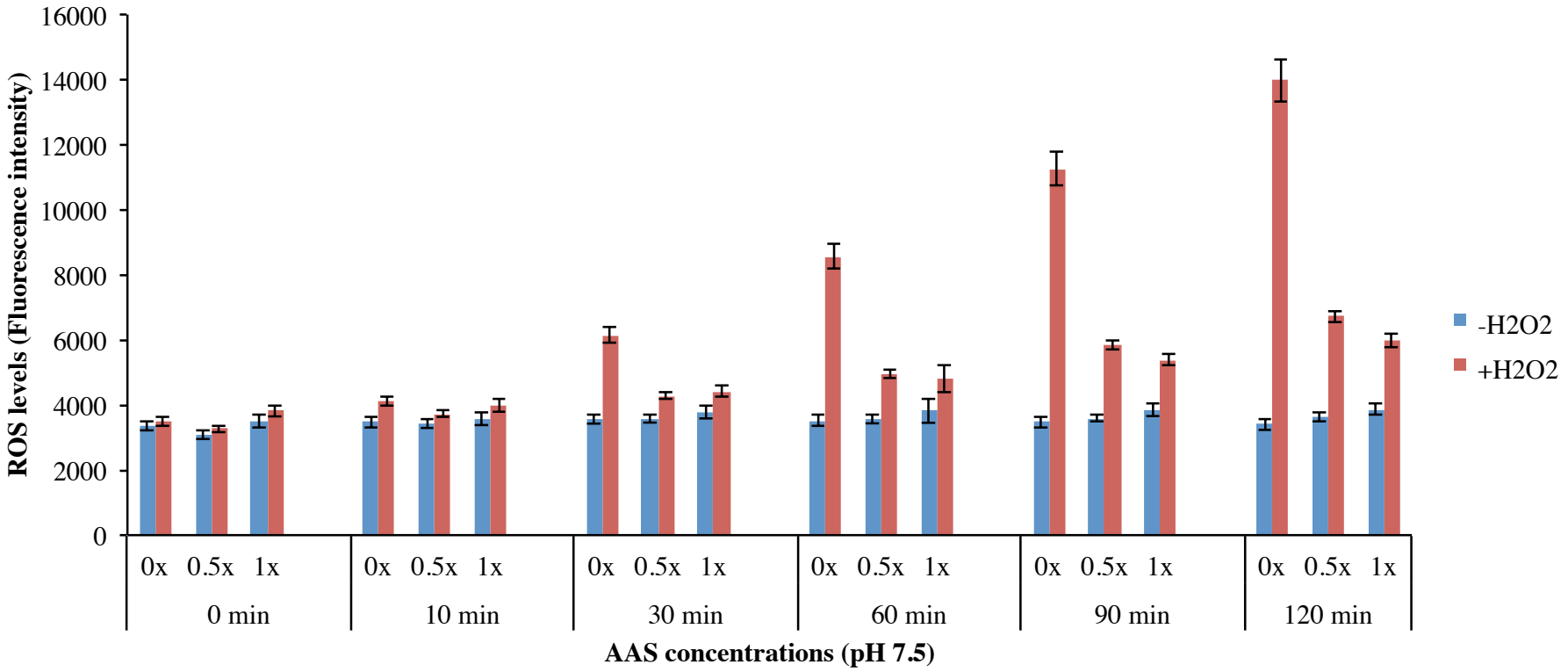


Figure 3. 24 ROS detection in AAS solutions at pH 7.5 with and without H_2O_2.

ROS levels in AAS solutions at pH 7.5 with and without H_2O_2 were determined at 0, 10, 30, 60, 90 and 120 minutes using CM-H_2DCFDA. Data were presented as means ± SEM (n = 3).

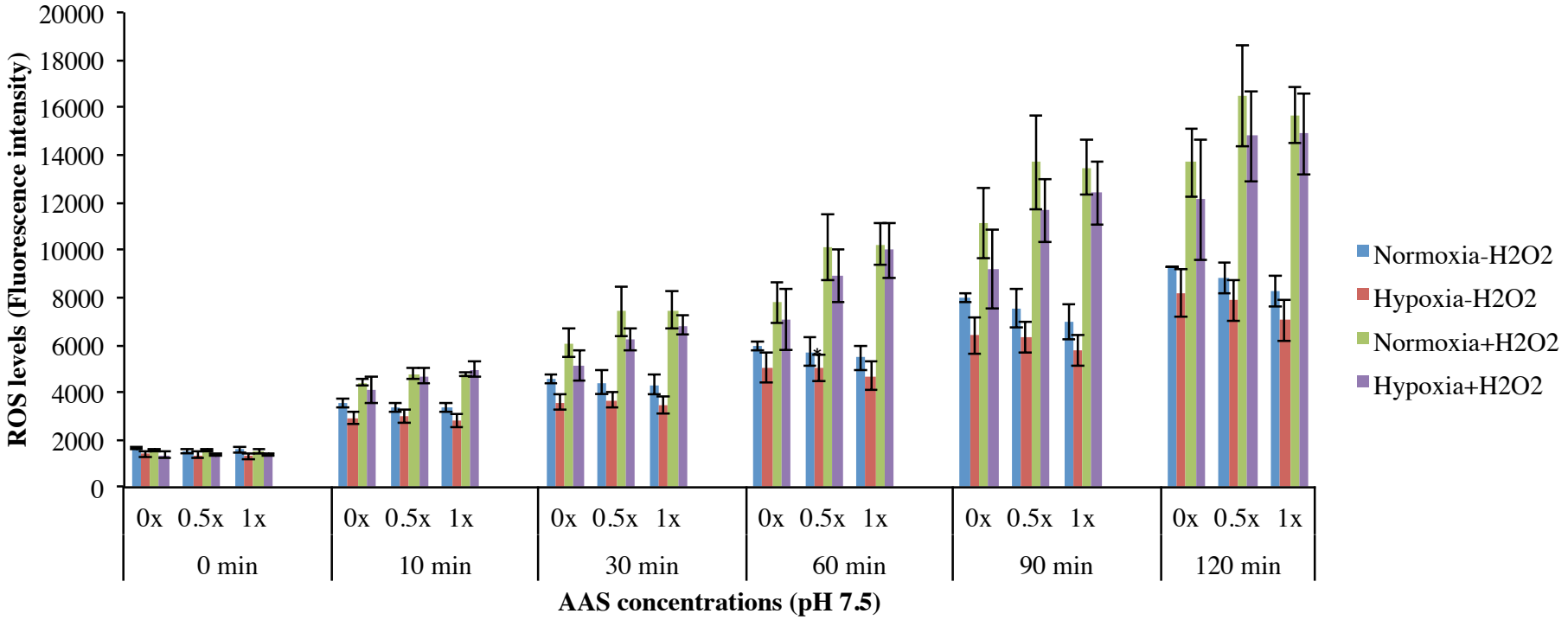


Figure 3. 25 ROS detection in HK-2 cells after treatment with AAS at pH 7.5 with and without H_2O_2 following starvation.

ROS levels in HK-2 cells after treatment with AAS at pH 7.5 with and without H_2O_2 following starvation were determined at 0, 10, 30, 60, 90 and 120 minutes using CM-H_2DCFDA. Data were presented as means ± SEM (n = 3).

3.3 Conclusion

Evidence has shown that not only a burst of ROS generation caused by the return of nutrients and oxygen but also the return of pH to physiological levels are the key to triggering the lethal cell injury during reperfusion (Gores et al., 1988; Shanley et al., 1988; Currin et al., 1991; Zager, Schimpf and Gmur, 1993; Weinberg et al., 1994). Instead of playing a critical role in the kidney recovery from ischaemia, reperfusion causes greater damages than ischaemia. During ischaemia or hypoxia, tissue intracellular pH (pHi) becomes acidotic due to the anaerobic glycolysis and ATP hydrolysis which leads to the accumulation of lactic acid (Hochachka and Mommsen, 1993). The pHi can reduce to pH 6.8-6.3 depending on the tissue types, and many tissues including kidney (Weinberg, 1985; Burnier et al., 1988; Shanley et al., 1988), liver (Gores et al., 1988; Gores et al., 1989; Parivar, Narasimhan and Ross, 1991), heart (Bing, Brooks and Messer, 1973; Pentilla, Glaumann and Trump, 1976) and brain (Jokivarsi et al., 2007; Vaughan-Jones, Spitzer and Swietach, 2009) have been reported to be resistant to oxygen deprivation in such a pH range. Interestingly, tissue necrosis normally occurs during reperfusion rather than ischaemia due to not only ROS generation and inflammation but also the prompt return of extracellular pH to physiological level, exacerbating ischaemic injury and resulting in an abrupt cell death (Zager, Schimpf and Gmur, 1993; Kalogeris et al., 2012). To date, studies have proposed that the 'pH paradox' triggering a rapid cell death involves the MPTP opening upon reperfusion after ischaemic injury.

This chapter established a simulated I/R injury by nutrient deprivation and the replenishment of nutrients in the presence of H_2O_2. The utility of exogenous H_2O_2 was inevitable as hypoxia/reoxygenation did not have any influence on HK-2 cells.

This chapter investigated whether the increase in amino acid supplementation may facilitate HK-2 cell recovery from H_2O_2 damage. Additionally, this chapter assessed whether resupply of amino acids at low pH may exert any protection against H_2O_2 mediated damage. The results presented here showed that after starvation the return of amino acids at the physiological pH (pH 7.5) in the presence of H_2O_2 exacerbated mitochondrial dysfunction in an AAS concentration dependent manner. The data also indicated that AAS per se might be able to scavenge ROS in the absence of cells, whilst AAS with H_2O_2 resulted in an increase in ROS production in the presence of cells. It was proposed that the detrimental effect of AAS may be due to the formation of amino acid peroxides which were likely to become a second toxic messenger to cells or tissues (Gebicki and Gebicki, 1993).

It has been proposed that maintaining acidosis during reperfusion could attenuate cell death. The cytoprotection of acidosis ranging from pH 6.8 to pH 6.0 against I/R injury has been documented in the published literature (Gores et al., 1988; Shanley et al., 1988; Currin et al., 1991; Nishimura, Romer and Lemasters, 1998; Zhang and Lemasters, 2013). This chapter investigated the effects of a range of low pH (pH 6.8-3.8) on HK-2 cells in the presence of H_2O_2 damage following starvation. However, acidic pH appeared to cause a lethal cell injury in the presence of H_2O_2, particularly initiated at pH 6.4. The provision of AAS at pH 6.4 in the presence of H_2O_2 exacerbated a substantial cell death following nutrient deprivation. A further reduction in pH to 3.8 caused a disruption of F-actin, a loss of mitochondrial morphologies and lethal cell death. Although numerous studies showed the cytoprotection of acidic pH at the acute phase of I/R injury (LDH release assay ranging from 10 minutes to 6 hours), several studies have also reported that treatment of acidic pH (pH 6.8-6.2) did not recover cytoskeleton disruption and cell

morphological alterations and eventually led to cell death (Shanley et al., 1988; Gores et al., 1989). Overall, this chapter implicated that the rapid return of circulating nutrients (e.g. free amino acids) in the circulation under oxidative stress was detrimental for the renal proximal tubule cell recovery from I/R injury.

Chapter 4: Cellular responses to amino acids during oxidative stress following nutrient deprivation

Chapter 4: Cellular responses to amino acids during oxidative stress following nutrient deprivation

4.1 Introduction

It is known that the increased oxidative stress induced by a burst generation of ROS is the key to renal I/R injury. Recently other potential mechanisms also began to be uncovered, particularly mTOR signalling pathways and UPR pathways. The rapid activation of mTORC1 upon reperfusion due to the sudden return of nutrients, growth factors and ATP is considered to enhance renal regeneration and functional recovery (Lieberthal et al., 2006). However, emerging evidence showed that mTORC1 activation mediated a variety of renal diseases including I/R injury and directly contributed to ER stress mediated cell apoptosis (Prachasilchai et al., 2008; Kato et al., 2012; Dong et al., 2015). The inhibition of mTORC1 activity by mTOR inhibitors was observed more protective as a result of induction of autophagy, immunosuppression and anti-inflammation (Declèves et al., 2011; Chen et al., 2012; Wang et al., 2013; Zhang et al., 2014). Furthermore, attenuation of mTOR signalling pathways through dietary restriction, particularly amino acid and protein restriction, also demonstrated a certain level of protection against renal I/R injury in animal models (Mitchell et al., 2010; Verweij et al., 2011; Peng et al., 2012; Robertson et al., 2015). A recent study by Robertson et al. (2015) demonstrated that mice fed with protein and calorie restricted diet for a week before I/R injury showed a reduced level of serum urea and lesser tubular destruction and obstruction compared with mice fed with a complete diet. Protein restricted diet exhibited a similar level of protection as non-essential amino acids only diet, but mice fed with essential amino

acid only diet showed a greater increase in serum urea. The authors suggested the compromised protection by essential amino acids was due to the presence of leucine, well known as an mTOR activator. These authors further identified that activation of mTOR by an addition of leptin (an mTOR activator) to protein and calorie restricted diet negated the protection due to the observation of increased serum urea. This indicated that inhibition of mTORC1 signalling pathways displayed a protective role in renal I/R injury. It was proposed that the protection afforded by nutrient restriction was associated with the increased stress resistance by attenuating nutrient or stress sensing pathways (Walter and Ron, 2011; Gallinetti et al., 2013). In the stressed condition such as nutrient deprivation and oxidant injury, cells may adapt to survive by downregulating the important cellular functions including protein synthesis, cell growth and proliferation through the inhibition of mTORC1 (Reiling and Sabatini, 2006). Moreover, in mammalian cells the UPR pathways in the ER may also be activated to participate in the protection from stress. Activation of UPR inhibits protein synthesis through downregulation of gene transcription or translation in order to reduce the misfolded protein overload in the ER (Walter and Ron, 2011). In contrast, activation of mTOR negatively regulates such adaptive stress response.

These studies and current knowledge of the adaptive cellular response to stress may provide an explanation for the results in chapter 3, which showed that the return of amino acids (at pH 7.5) in the presence of H_2O_2 caused a substantial cell death following starvation with increasing AAS concentration. This could be due to the activation of mTOR by essential amino acids which increased protein synthesis and protein load in the ER. Meanwhile, the presence of ROS interfered with protein disulfide bonding through disruption of ER redox homeostasis (Malhotra and Kaufman, 2007). This caused newly synthesised proteins to be inappropriately folded

or unfolded, subsequently leading to ER stress (Chakravarthi and Bulleid, 2004; Molteni et al., 2004) and activating cell apoptosis mediated by UPR downstream JNK signalling pathway (Wouters et al., 2008; Inagi, 2009). In contrast, without resupply of AAS an adaptive response for cell survival could be induced due to the attenuation of protein synthesis and the misfolded protein formation. Hence, UPR could relieve ER stress promptly. This may explain that in chapter 3 the replenishment of 0x AAS at pH 7.5 showed less cell death compared with AAS treated cells in the presence of H_2O_2 following starvation.

Moreover, studies reported that acidic pH also exerted a similar protection afforded by nutrient deprivation/restriction through downregulation of mTOR signalling to attenuate cell growth and protein synthesis. Balgi et al. (2011) showed that reperfusion at acidic pH following starvation interfered with the protein synthesis in MCF-7 human breast cancer cells through the inhibition of growth signalling pathways and Raf/mitogen activated kinases (MEK)/extracellular signal regulated kinases (ERK) of mTOR pathways to negatively affect the energy-consuming anabolic process to respond to metabolic stresses. Marino et al. (2012) suggested that acidic extracellular pH reduced the uptake of amino acids and subsequently inhibited mTOR in melanoma cells. Crean et al. (2013) proposed that acidic pH (pH 6.4) protected against cell death induced by oxygen and glucose deprivation in HK-2 cells through reducing protein synthesis/translation. The authors further observed that acidic pH attenuated UPR activated pro-apoptosis by inhibiting DNA damage inducible transcript 3 (DDIT3) gene mediated by ATF6-CHOP signalling pathway. However, chapter 3 showed that acidic pH did not show any protective effect against H_2O_2 induced oxidative stress following starvation. Nevertheless, it still remains unknown whether acidic pH is protective against oxidative stresses in renal I/R

injury due to the limited literature. The effectiveness was mostly shown in treating heart and liver I/R injury (Kim et al., 2006; Zhang and Lemasters, 2013), and others were mainly associated with cancer research (Balgi et al., 2011; Marino et al., 2012).

Aims and hypothesis

This chapter aimed to investigate i) whether the protective effect of nutrient deprivation against oxidative damage was due to the inhibition of mTOR which potentially decreased protein synthesis and the activation of the UPR, ii) whether the provision of AAS (pH 7.5) in the presence of H_2O_2 following starvation activated mTOR which potentially promoted protein synthesis under oxidative stress, caused accumulation of misfolded proteins in the ER and led to ER stress and iii) whether AAS at acidic pH may inhibit mTOR signalling to reduce global protein synthesis and may potentially inhibit protective chaperone protein expression for cell survival through oxidative stress. To achieve this, HK-2 cells were pre-starved for 24 hours followed by resupply of amino acids at pH 7.5 in HEPES buffering system or at pH 6.4 in bicarbonate buffering system for a short period of time (e.g. 15-60 minutes) in order to assess downstream phosphorylated proteins of mTOR signalling. To assess chaperone protein level over time, HK-2 cells were resupplied with AAS at pH 7.5 and 6.4 for 20 hours following starvation. It was hypothesised that i) nutrient restriction triggered the cellular adaptation by inhibition of mTORC1 and activation of adaptive UPR, whereas resupply of amino acids at pH 7.5 activated mTORC1 and suppressed such a protective cellular response to stresses; and that ii) acidic pH inhibited mTOR signalling and reduced both global proteins for cell growth and protective chaperone proteins for cell survival.

4.2 Results

4.2.1 Effects of AAS at physiological pH following D/R injury on mTOR signalling

Studies uncovered that mTOR activation mediated a variety of renal diseases including I/R injury and directly contributed to ER stress whereas mTOR inhibition through dietary restriction (particularly amino acid or protein restriction) and acidic pH was found to be protective. In chapter 3, the results showed that the return of amino acids at physiological pH in the presence of H_2O_2 caused substantial cell death following starvation in an AAS concentration dependent manner. Hence, we investigated whether this was due to the activation of mTOR by essential amino acids which increased protein synthesis and protein load in the ER. In this chapter, HEPES buffer was included in AAS at pH 7.5 to prevent pH fluctuation after overnight incubation.

To identify the effect of amino acids at pH 7.5 on mTOR signalling pathways following starvation, we focused on the levels of downstream proteins including pS6 and pS6K. The phosphorylation of these two downstream proteins is positively regulated by mTORC1 to promote cell growth (cell mass/size). Active pS6K leading to activation of S6 protein inhibits eukaryotic translation initiation factor 4E (eIF4E)-binding protein 1 (4EBP1), and this releases eIF4E to promote translation for protein synthesis (Reiling and Sabatini, 2006). To perform a positive control, other nutrients including glucose, insulin, leucine and FBS were used. The concentration was chosen according to the published literature and was known to stimulate mTOR signalling after starvation in renal tubular cells such as HK-2 cells and human

embryonic kidney cells (Ramírez-Rangel et al., 2011; Velagapudi et al., 2011). Another positive control was also carried out by treating cells with rapamycin to show an inhibition of mTOR signalling. In addition, the loading control was performed in order to compare within the gel and across three blots. Here the cells treated with 10% FBS after starvation was used as a loading control as this treatment was found to induce a high and constitutive protein expression in previous experiments (data not shown). Hence, within the same gel and across different blots the protein density of cells treated with 10% FBS (Figure 4.1 A, lane 19) and loading control (Figure 4.1 A, lane 25) ideally should be identical. This step was to ensure that i) protein loading was the same across three different gels and that ii) all proteins within the same and across three gels were equally transferred to the membranes.

After starvation, the replenishment of AAS, glucose, insulin, leucine and FBS activated the phosphorylation of p70/85 S6K after 15 minutes (Figure 4.1 A, lane 1-9 and 19). However, the protein levels at 15 minutes were not affected by AAS concentration and H_2O_2 (Figure 4.1 B, left). At 60 minutes, the activated phosphorylation of p70/85 S6K increased in an AAS concentration dependent manner ($p = 0.007$; Figure 4.1 B, right), with a strong positive linear relationship ($p = 0.004$). However, such protein expression was not affected by H_2O_2 and the interaction of AAS and H_2O_2.

The protein level of pS6 was also activated after replenishment of AAS in the presence or absence of H_2O_2 in 15 minutes, and the level was higher in those treated with glucose, insulin and leucine (Figure 4.1 A, lane 7-9). Although AAS did not have effects on the pS6 protein levels at 15 minutes ($p = 0.065$; Figure 4.1 C, left), there was a positive linear trend between AAS concentration and pS6 protein levels

($p = 0.029$; Figure 4.1 C, left). The pS6 protein levels were not affected by H_2O_2 and the interaction of AAS and H_2O_2. At 60 minutes, there were no differences in pS6 levels between 0x, 0.5x and 1x AAS, and pS6 protein levels were not affected by H_2O_2 and the interaction of AAS and H_2O_2 (Figure 4.1 C, right). These suggested that mTOR activation was mainly dependent on AAS concentration and that the presence of H_2O_2 did not influence mTOR activation in response to amino acids.

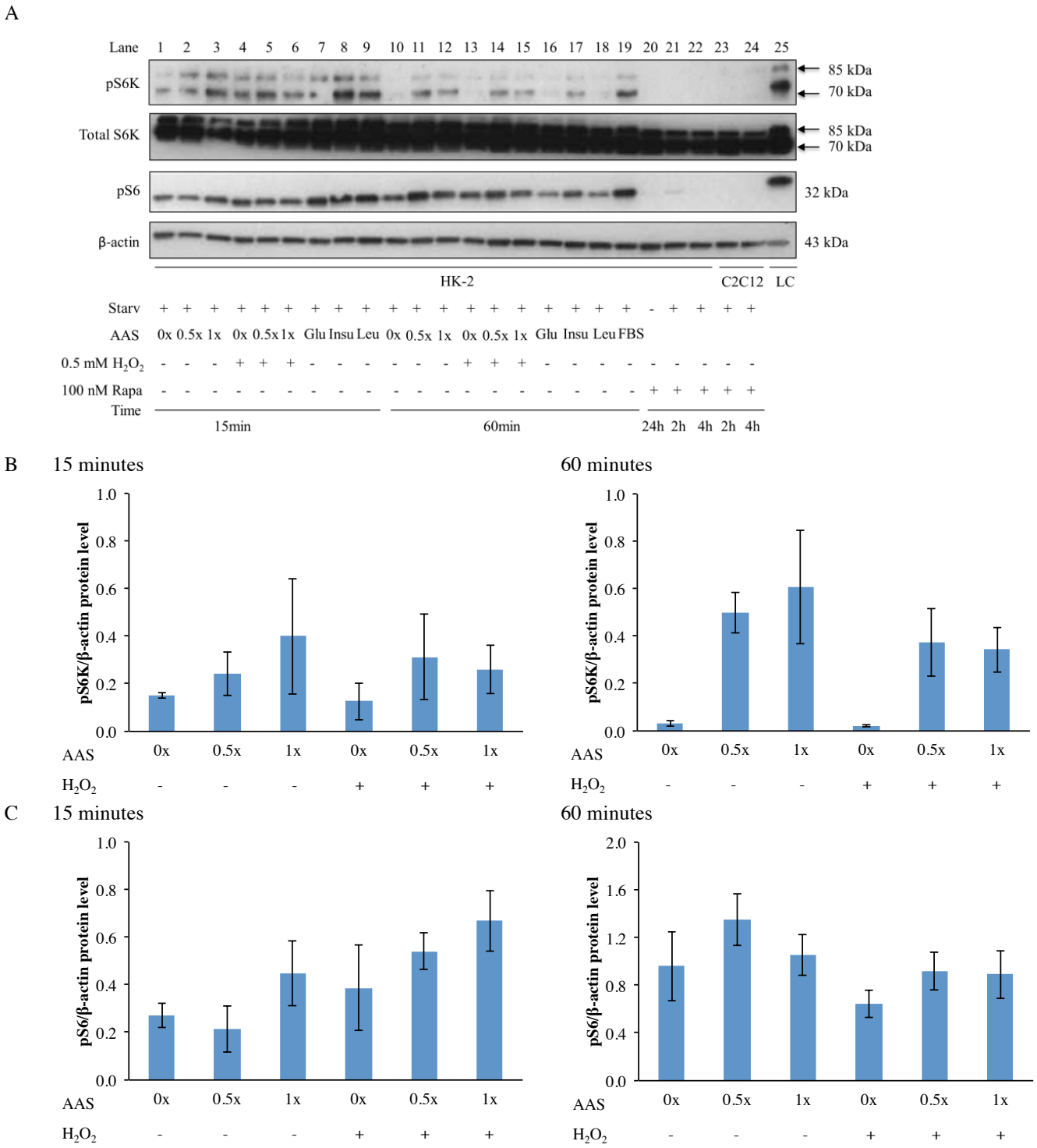


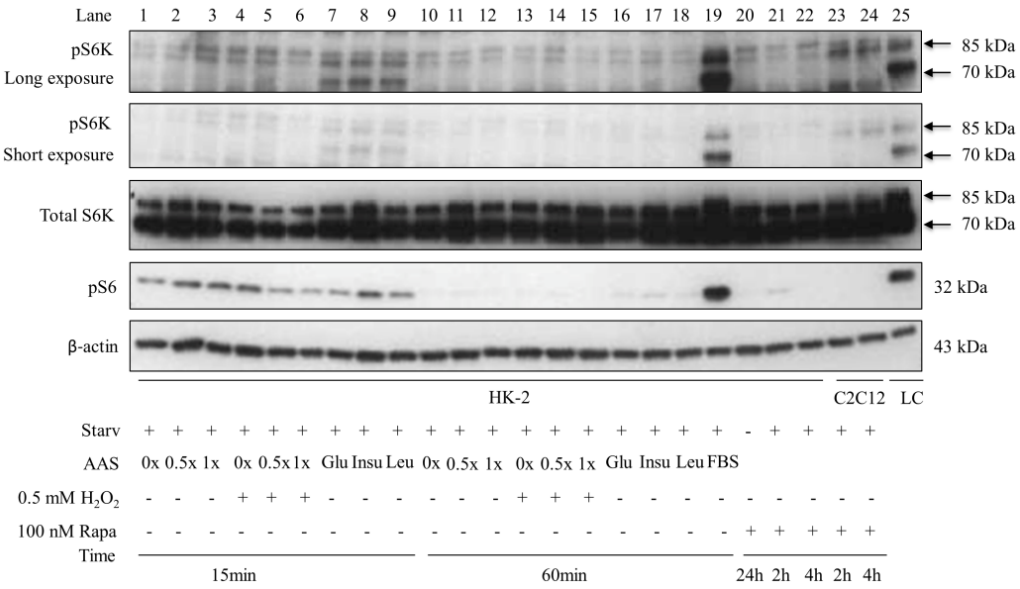
Figure 4. 1 Effects of AAS at pH 7.5 after starvation on mTOR signalling.

(A) Representative immunoblots of pS6K, pS6, total S6K and β-actin protein levels were displayed for pre-starved cells treated with 0x, 0.5x and 1x AAS with and without H_2O_2, glucose, insulin and leucine for 15 and 60 minutes and FBS for 1 hour. HK-2 and C2C12 cells were treated with rapamycin for 2, 4 or 24 hours. LC: loading controls. The bar graphs summarised the relative density of (B) pS6K/β-actin and (C) pS6/β-actin at 15 and 60 minutes in HK-2 cells treated with AAS. Each treatment had triplicates for an n = 3. Data were presented as means ± SEM (n = 3).

4.2.2 Effects of AAS at acidic pH following D/R injury on mTOR signalling

Since studies demonstrated that acidic infusion protected against oxidative and ER stress in I/R injury potentially through inhibition of mTORC1 signalling, we further investigated whether mTOR inhibition by acidic pH also occurred in our model despite no protection observed in chapter 3. After nutrient deprivation, at pH 6.4 the addition of amino acids failed to activate phosphorylation of S6K compared with 10% FBS (pH 7.5) treated cells (Figure 4.2 A). The p70/85 pS6K was slightly activated in cells treated with glucose, insulin and leucine at pH 6.4 at 15 minutes but was completely inhibited at 60 minutes (Figure 4.2 A). Similarly, the pS6 protein was slightly activated in all treatment groups at 15 minutes, but the level was not affected by AAS concentration and H_2O_2 (Figure 4.2 B). At 60 minutes, the phosphorylation of S6 protein was completely inhibited (Figure 4.2 B). These suggested that acidic pH had a strong negative effect on mTOR signalling despite the presence of amino acids.

A



B

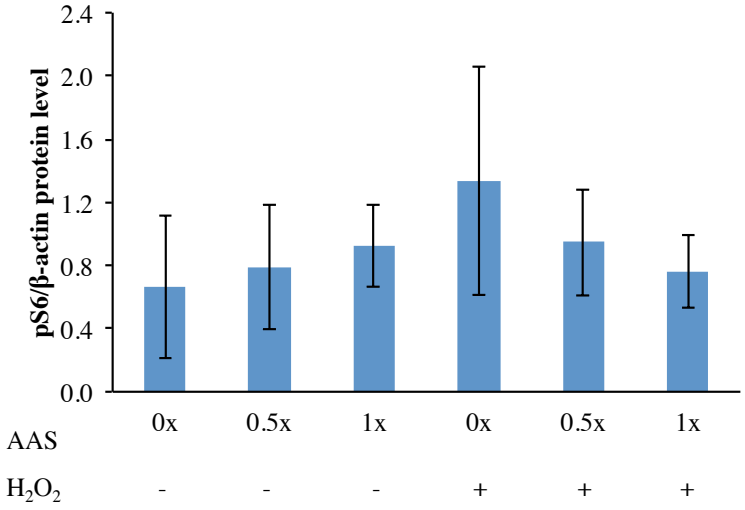


Figure 4. 2 Effects of AAS at pH 6.4 after starvation on mTOR signalling.

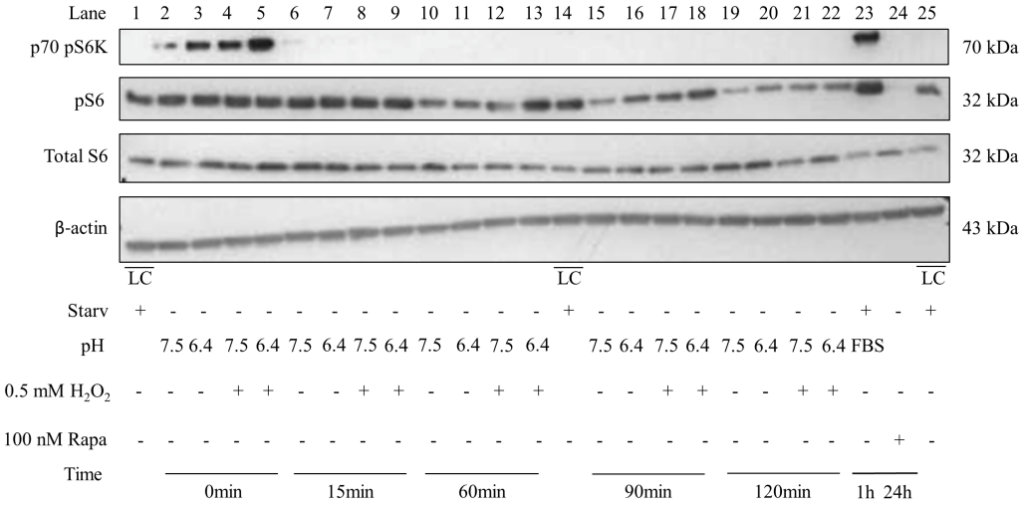
(A) Representative immunoblots of pS6K, pS6, total S6K and β-actin protein levels were displayed for pre-starved cells treated with 0x, 0.5x and 1x AAS with and without H_2O_2, glucose, insulin and leucine for 15 and 60 minutes and FBS for 1 hour. HK-2 and C2C12 cells were treated with rapamycin for 2, 4 or 24 hours. LC: loading controls. (B) The bar graph summarised the relative density of pS6/β-actin at 15 minutes in HK-2 cells treated with AAS. Each treatment had triplicates for an n = 3. Data were presented as means ± SEM (n = 3).

4.2.3 Effects of pH without pre-starvation on mTOR signalling

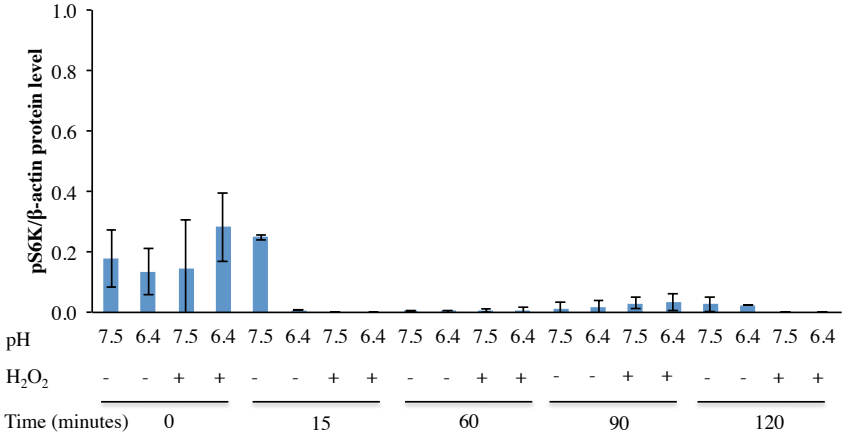
As it was found that AAS at pH 7.5 stimulated mTOR whereas AAS at pH 6.4 failed to activate mTORC1, we further investigated whether there was a direct effect of pH on mTORC1 signalling. To confirm this, the effects of pH 7.5 and 6.4 without pre-starvation on downstream proteins of mTOR were examined. The phosphorylation of S6K was activated at 0 minute and then was completely inhibited after the replacement of media with HBSS at pH 7.5 and 6.4 by 15 minutes (Figure 4.3 A and B). The pS6K was highly activated only in FBS treated cells (Figure 4.3 A and B).

The phosphorylation of S6 protein was constantly activated but gradually reduced after 60 minutes of incubation at both pH 7.5 and 6.4 (Figure 4.3 A and C). The pS6 protein levels were strongly affected by time; that is, it decreased over time ($p < 0.001$; Figure 4.3 A and C). There was also an interaction of H_2O_2 and time ($p = 0.005$), and pS6 protein levels reduced in the presence of H_2O_2 compared with the absence of H_2O_2 over time (Figure 4.3 A and C). However, there were no effects of pH and H_2O_2 and their interaction. As we investigated the effects of these two pH levels in starvation media, this could not confirm whether pH had a direct effect on mTOR. The decline in pS6 protein levels over time could be attributed to the nutrient deficient condition.

A



B



C

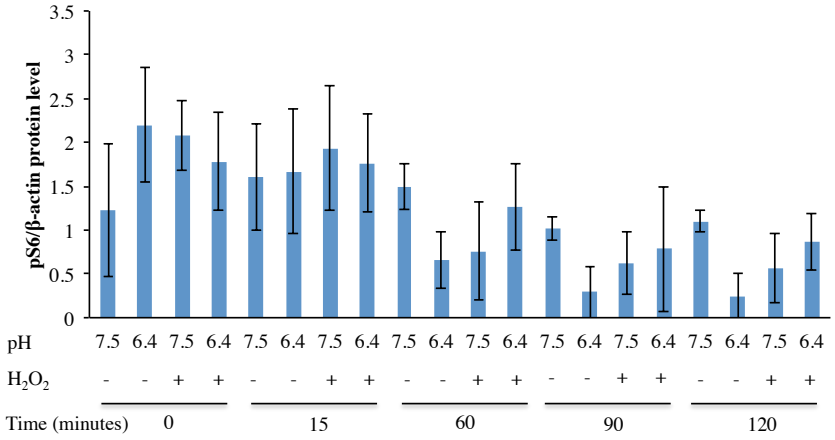


Figure 4. 3 Effects of pH 7.5 and 6.4 in the presence or absence of H_2O_2 without pre-starvation on mTOR signalling.

(A) Representative immunoblots of pS6K, pS6, total S6 and β-actin protein levels were displayed for HK-2 cells treated with HBSS at pH 7.5 and 6.4 with and without H_2O_2 for 0-120 minutes, FBS for 1 hour and rapamycin for 24 hours. LC: loading controls. The bar graphs summarised the relative density of (B) pS6K/β-actin and (C) pS6/β-actin. Each treatment had triplicates for an n = 3. Data were presented as means ± SEM (n = 3).

4.2.4 Intracellular localisation of mTOR to mitochondria in response to AAS following D/R injury

The mTOR has been observed on several locations in cellular systems including mitochondria and lysosomes, and the intracellular localisation of mTOR was detected using immunofluorescence labelling. To validate the antibody, the intracellular location of mTOR was first detected in HK-2 cells growing in the complete DMEM. In such a nutrient sufficient condition, mTOR in a punctate structure aggregated and localised to the perinuclear regions (Figure 4.4 A and B). After treatment with rapamycin, mTOR became small puncta throughout cytoplasm (Figure 4.4 C and D).

In order not to over interpret the results, it is important to acknowledge that only one field per slide and three slides per treatment group were obtained for triplicates. Hence, the quantitative analysis was not carried out. These images for representative areas might be less generalisable. A negative control was not performed for the immunofluorescence labelling, and the efficiency and specificity of the antibody to proteins could be argued. After starvation for 24 hours, mTOR was in a punctate structure in the perinuclear regions after treatment with 0x AAS with and without H_2O_2 (Figure 4.5 A-C; Figure 4.6 A-C), whilst 1 hour of the replenishment with 0.5x and 1x AAS at pH 7.5 with and without H_2O_2 seemed to promote mTOR to aggregate and become a clustered structure in the perinuclear regions (Figure 4.5 D-I; Figure 4.6 D-I). In addition, the provision of FBS, glucose, insulin and leucine at pH 7.5 for 1 hour after starvation also showed the mTOR aggregation in the perinuclear regions (Figure 4.7).

Cells treated with 0x AAS at pH 6.4 with and without H_2O_2 showed a small puncta structure of mTOR among cytoplasm (Figure 4.8 A-C; Figure 4.9 A-C). After treatment with 0.5x and 1x AAS with and without H_2O_2 and other nutrients including glucose, insulin and leucine at pH 6.4 for 1 hour, there were a few small clustered structures of mTOR in the perinuclear regions (Figure 4.8 D-I; Figure 4.9 D-I; Figure 4.10). However, mTOR mostly became more punctate around nuclei and throughout cytoplasm compared with cells treated with nutrients at pH 7.5 (Figure 4.5, 4.6 and 4.7). Furthermore, there was no yellow signal (overlapping of green mTOR and red Mitotracker fluorescence) observed in cells treated with all nutrients at both pH 7.5 and 6.4, indicating no co-localisation of mTOR and mitochondria.

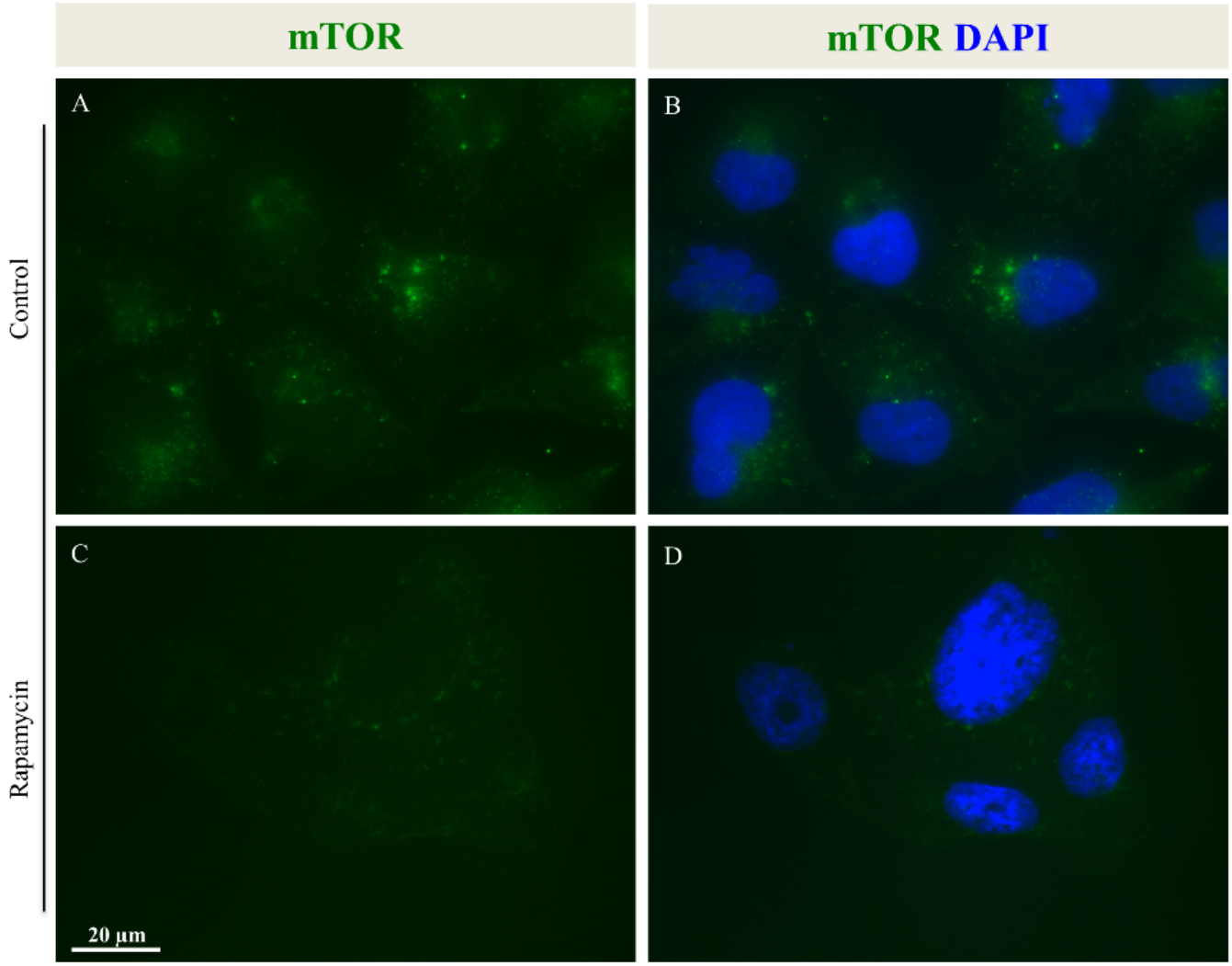


Figure 4. 4 Intracellular localisation of mTOR in HK-2 cells incubated in complete DMEM and rapamycin.

HK-2 cells were (A, B) untreated or (C, D) treated with rapamycin for 24 hours. Overlay images showed that mTOR (green) and DAPI (blue) were the same areas. Magnification, x100; scale bar = 20 µm. One field per slide and three slides per treatment group were performed for an n = 3.

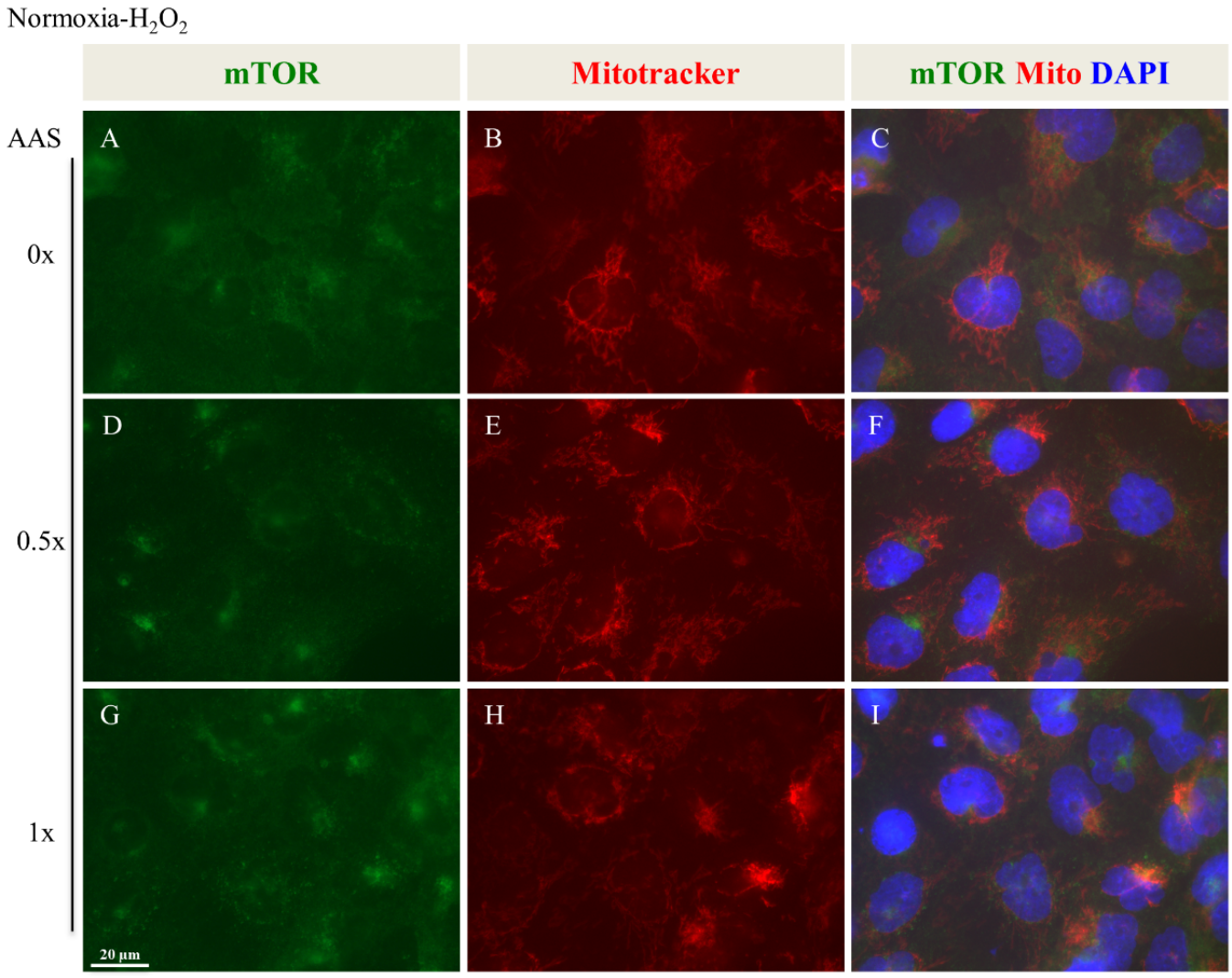


Figure 4. 5 Intracellular localisation of mTOR in response to AAS at pH 7.5 following starvation was independent of mitochondria.

After starvation, HK-2 cells were treated with (A-C) 0x, (D-F) 0.5x and (G-I) 1x AAS at pH 7.5 for 1 hour. Overlay images showed that mTOR (green), Mitotracker (red) and DAPI (blue) were the same areas. Magnification, x100; scale bar = 20 µm. One field per slide and three slides per treatment group were performed for an n = 3.

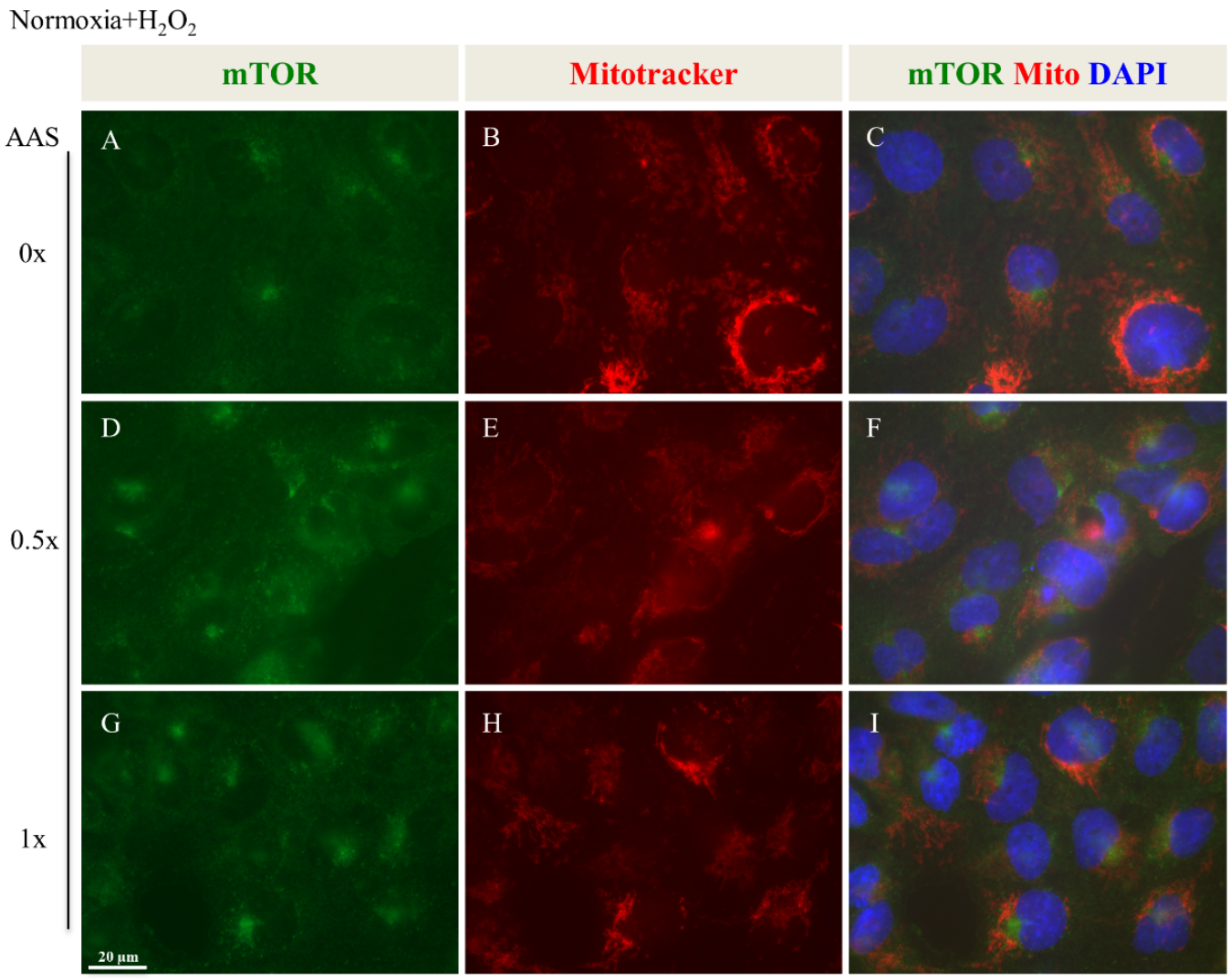


Figure 4. 6 Intracellular localisation of mTOR in response to AAS at pH 7.5 with H_2O_2 following starvation was independent of mitochondria.

After starvation, HK-2 cells were treated with (A-C) 0x, (D-F) 0.5x and (G-I) 1x AAS at pH 7.5 in the presence of H_2O_2 for 1 hour. Overlay images showed that mTOR (green), Mitotracker (red) and DAPI (blue) were the same areas. Magnification, x100; scale bar = 20 µm. One field per slide and three slides per treatment group were performed for an n = 3.

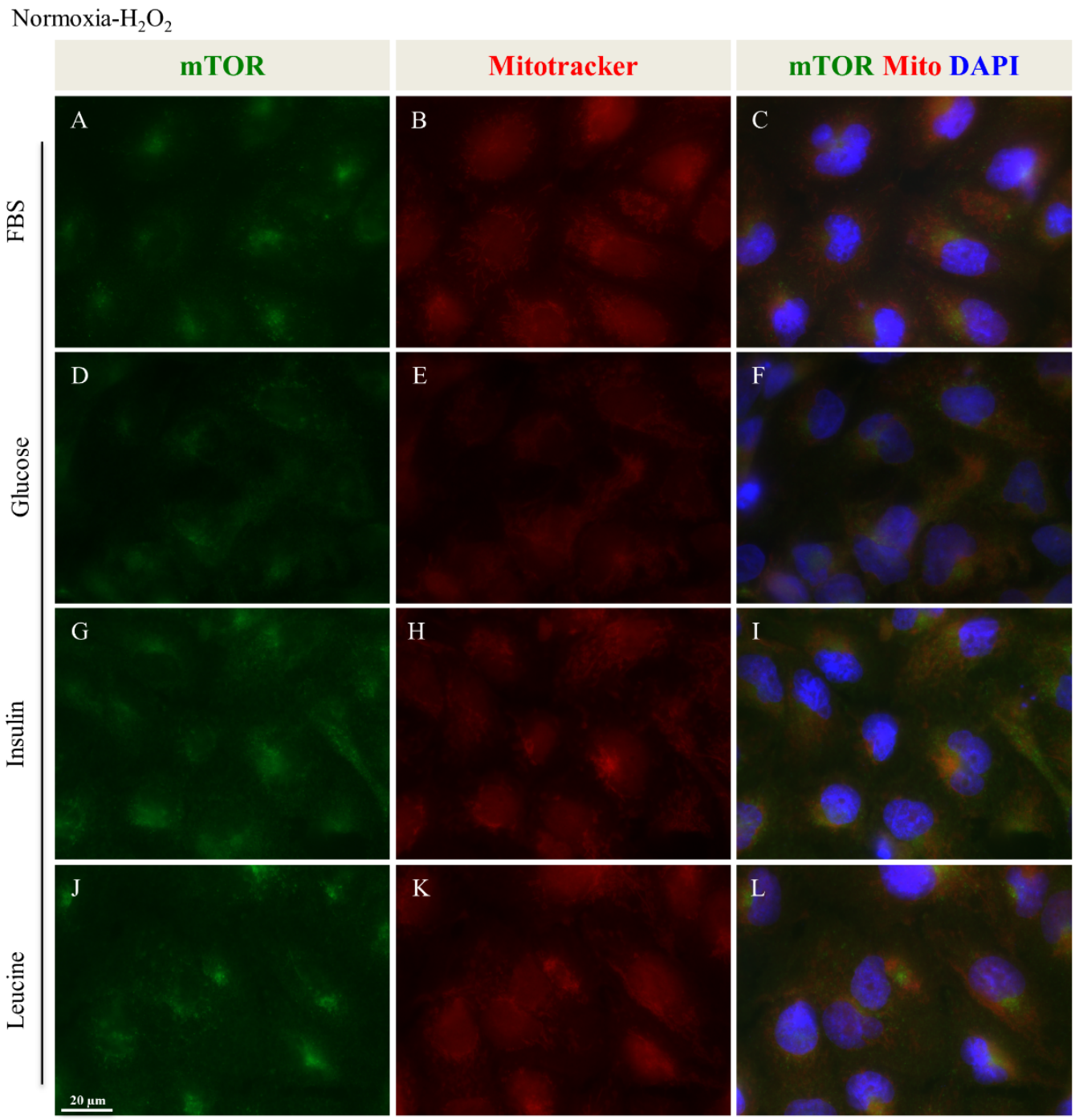


Figure 4. 7 Intracellular localisation of mTOR and mitochondria in response to nutrients at pH 7.5 following starvation was independent of mitochondria.

After starvation, HK-2 cells were treated with (A-C) FBS, (D-F) glucose, (G-I) insulin and (J-L) leucine at pH 7.5 for 1 hour. Overlay images showed that mTOR (green), Mitotracker (red) and DAPI (blue) were the same areas. Magnification, x100; scale bar = 20 µm. One field per slide and three slides per treatment group were performed for an n = 3.

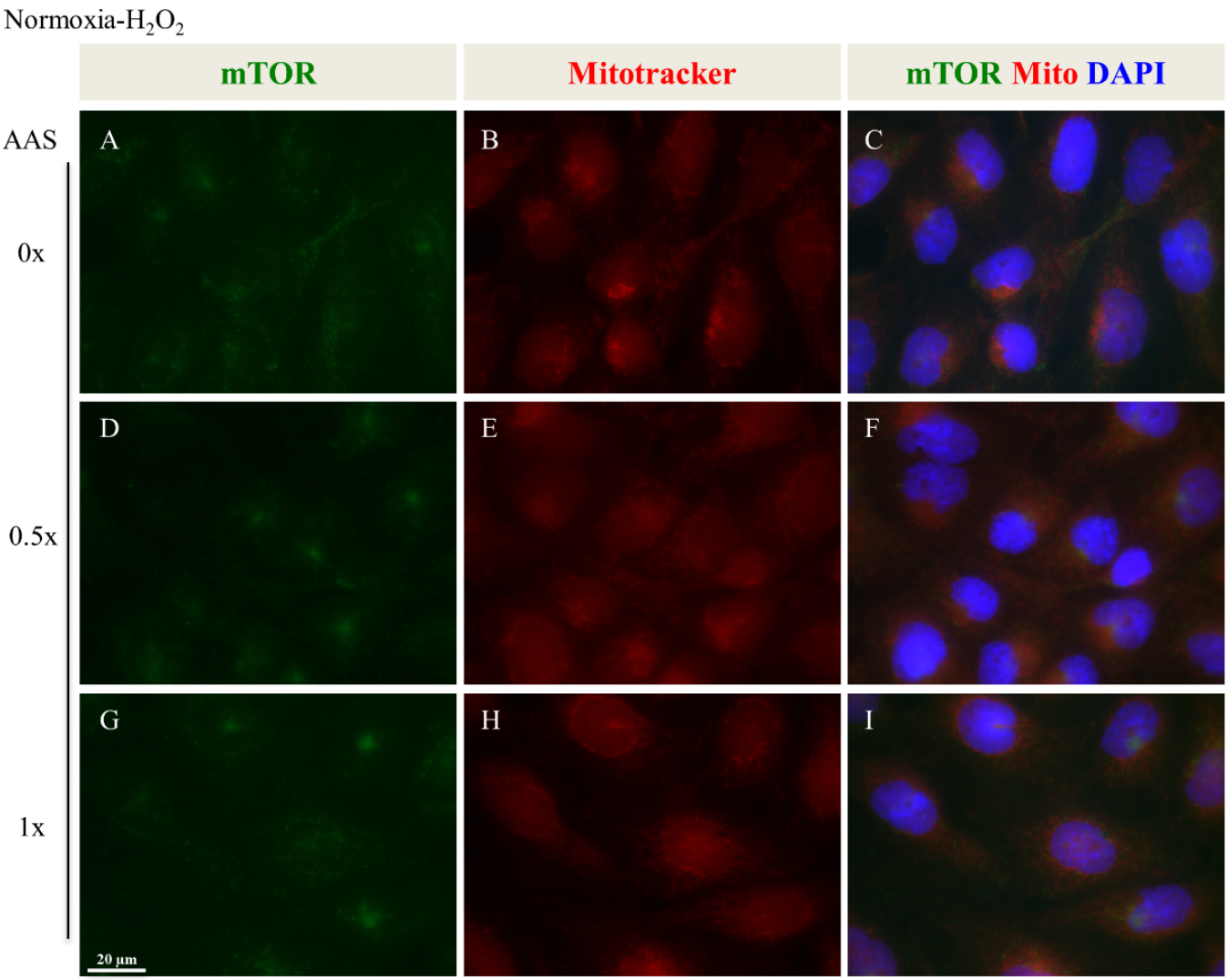


Figure 4. 8 Intracellular localisation of mTOR and mitochondria in response to AAS at pH 6.4 following starvation.

After starvation, HK-2 cells were treated with (A-C) 0x, (D-F) 0.5x and (G-I) 1x AAS at pH 6.4 for 1 hour. Overlay images showed that mTOR (green), Mitotracker (red) and DAPI (blue) were the same areas. Magnification, x100; scale bar = 20 µm. One field per slide and three slides per treatment group were performed for an n = 3.

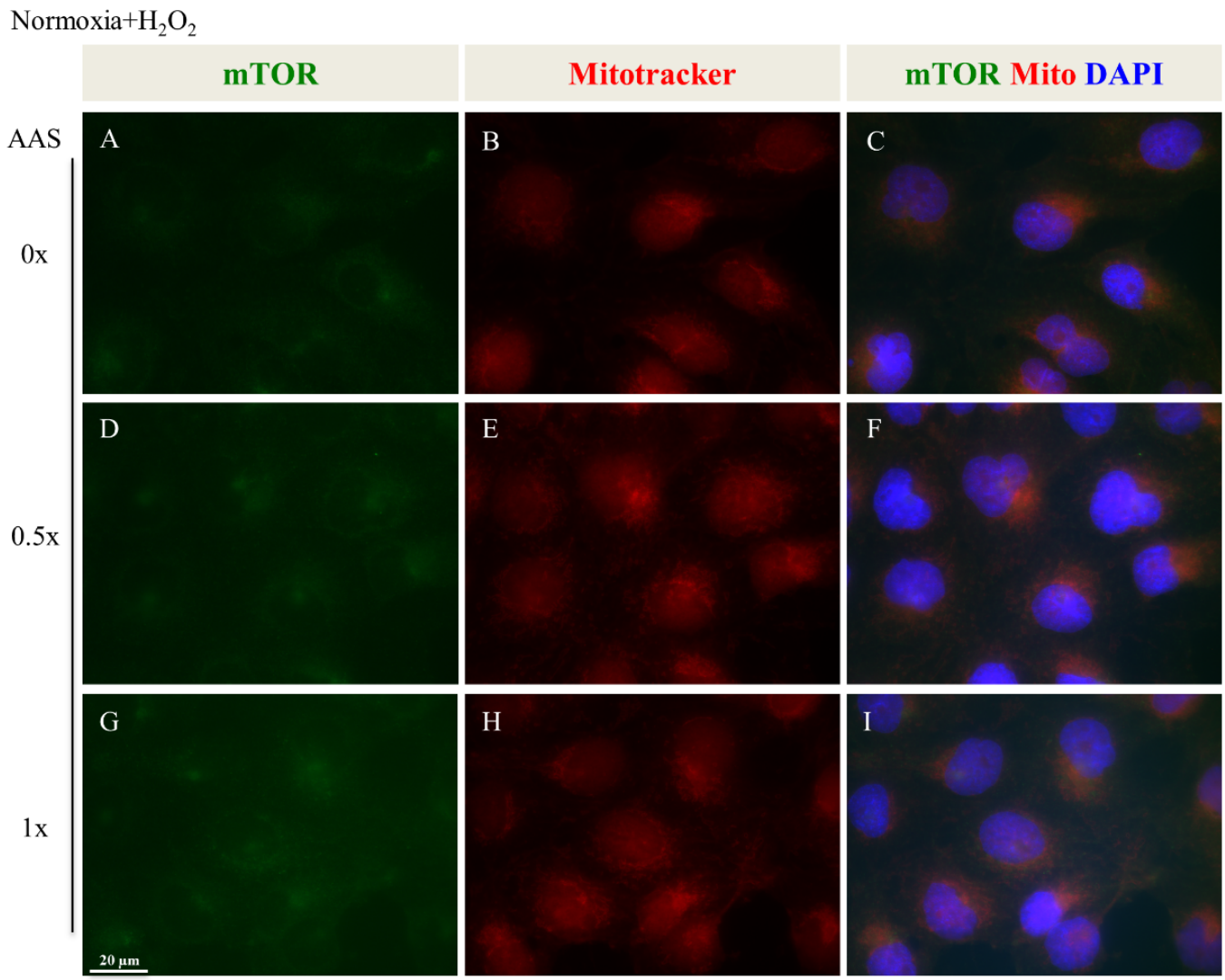


Figure 4. 9 Intracellular localisation of mTOR and mitochondria in response to AAS at pH 6.4 with H_2O_2 following starvation.

After starvation, HK-2 cells were treated with (A-C) 0x, (D-F) 0.5x and (G-I) 1x AAS at pH 6.4 in the presence of H_2O_2 for 1 hour. Overlay images showed that mTOR (green), Mitotracker (red) and DAPI (blue) were the same areas. Magnification, x100; scale bar = 20 µm. One field per slide and three slides per treatment group were performed for an n = 3.

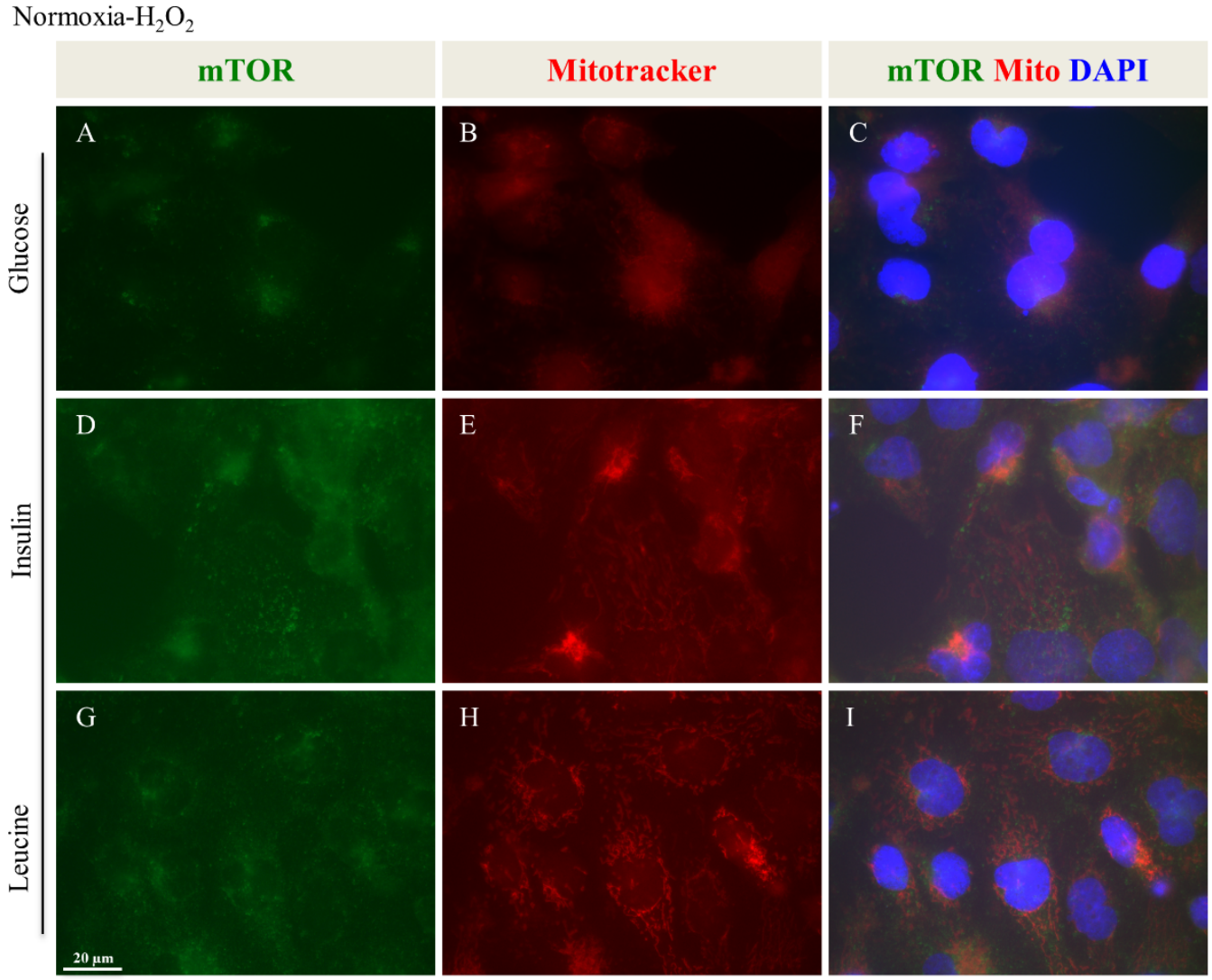


Figure 4. 10 Intracellular localisation of mTOR and mitochondria in response to nutrients at pH 6.4 following starvation.

After starvation, HK-2 cells were treated with (A-C) glucose, (D-F) insulin and (G-I) leucine at pH 6.4 for 1 hour. Overlay images showed that mTOR (green), Mitotracker (red) and DAPI (blue) were the same areas. Magnification, x100; scale bar = 20 µm. One field per slide and three slides per treatment group were performed for an n = 3.

4.2.5 Intracellular localisation of mTOR to lysosomes in response to AAS following D/R injury

This experiment was also performed without a negative control, and only one field per slide and three slides per treatment group were obtained for triplicates. The quantification analysis could not be performed. The images of a representative area per slide might be less generalisable. After starvation for 24 hours, mTOR was in a punctate structure among cytoplasm and nuclei with the lysosomes randomly located on the perinuclear regions after treatment with 0x AAS at pH 7.5 with and without H_2O_2 (Figure 4.11 A-C; Figure 4.12 A-C). However, the replenishment of 0.5x and 1x AAS at pH 7.5 with and without H_2O_2 for 1 hour promoted mTOR to aggregate in the perinuclear regions (Figure 4.11 D-I; Figure 4.12 D-I). The mTOR aggregating in the perinuclear regions occasionally co-localised with lysosomes as the pattern and location of mTOR and lysosomes were almost identical, and some yellow signals were also detected (Figure 4.11 D-I; Figure 4.12 D-I). However, this did not occur for all cells. In addition, the lysosomes were randomly located on the perinuclear regions in the provision of other nutrients including FBS, glucose and insulin (Figure 4.13 A-I). The co-localisation of mTOR and lysosomes was occasionally observed in some cells treated with leucine (Figure 4.13 J-L). Cells treated with AAS and other nutrients at pH 6.4 with and without H_2O_2 for 1 hour showed that mTOR became a small puncta in the perinuclear region and throughout cytoplasm, with no signal of lysosomes (Figure 4.14, 4.15 and 4.16).

The total mTOR protein level was also assessed by immunoblotting to investigate whether it was affected by treatments and pH. This was also to serve as a baseline for the mTOR activation/aggregation structure or inhibition/punctate structure observed

in immunofluorescence labelling. The total mTOR levels were only strongly affected by pH ($p < 0.001$; Figure 4.17), and the level was lower in cells treated with AAS at pH 6.4 compared with pH 7.5. Cells treated with glucose, insulin and leucine at pH 6.4 also showed a lower level of mTOR compared with those treated at pH 7.5 (Figure 4.18). However, the total mTOR levels were not affected by AAS concentration and H_2O_2 (Figure 4.18). There were no changes in protein levels between cells treated with glucose, insulin and leucine (Figure 4.18). These confirmed the observation of mTOR in response to nutrients at pH 7.5 and pH 6.4 respectively in immunofluorescence labelling.

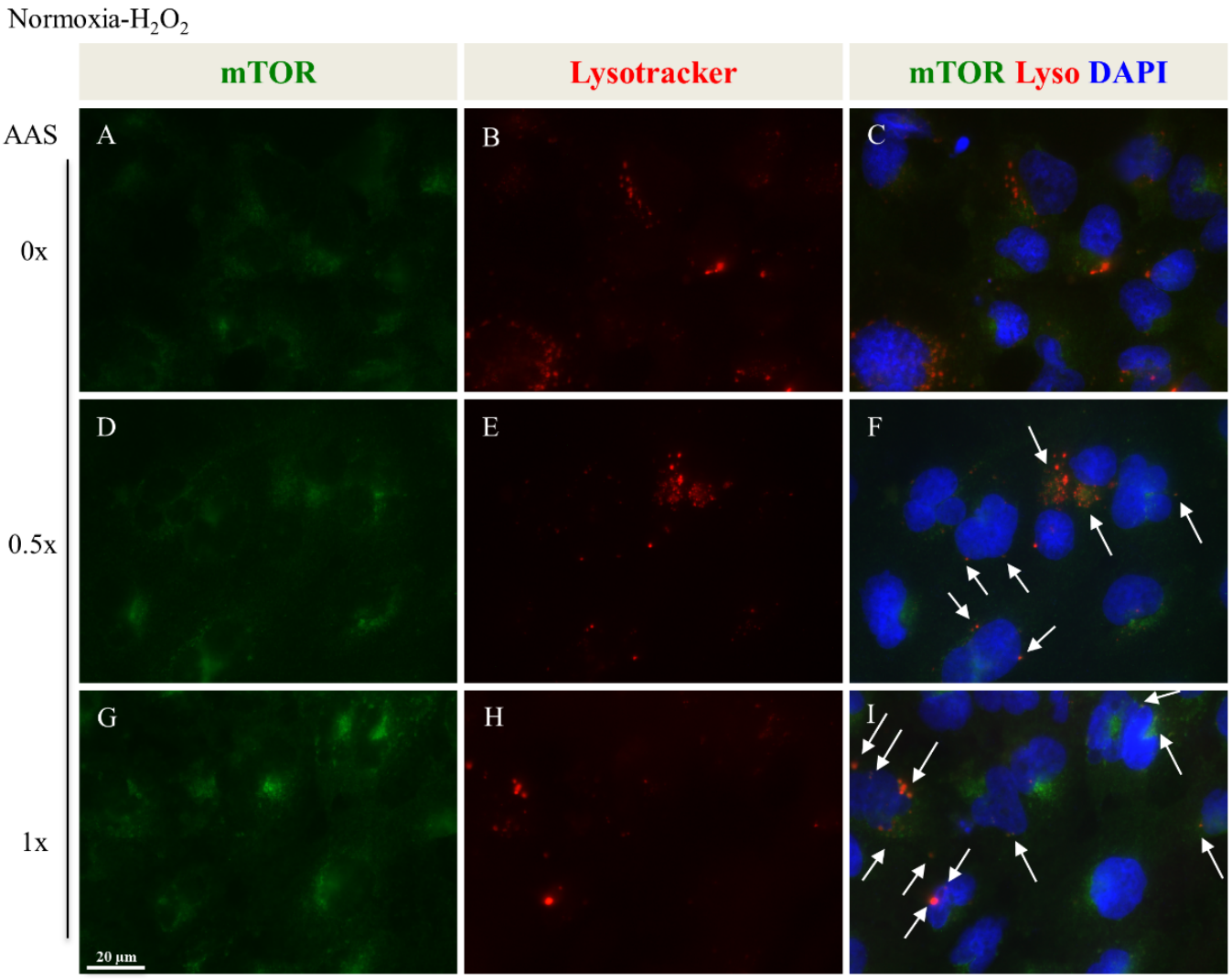


Figure 4. 11 Intracellular localisation of mTOR and lysosomes in response to AAS at pH 7.5 following starvation.

After starvation, HK-2 cells were treated with (A-C) 0x, (D-F) 0.5x and (G-I) 1x AAS at pH 7.5 for 1 hour. Overlay images showed that mTOR (green), Lysotracker (red) and DAPI (blue) were the same areas. Arrows showed the co-localisation of mTOR and Lysotracker. Magnification, x100; scale bar = 20 µm. One field per slide and three slides per treatment group were performed for an n = 3.

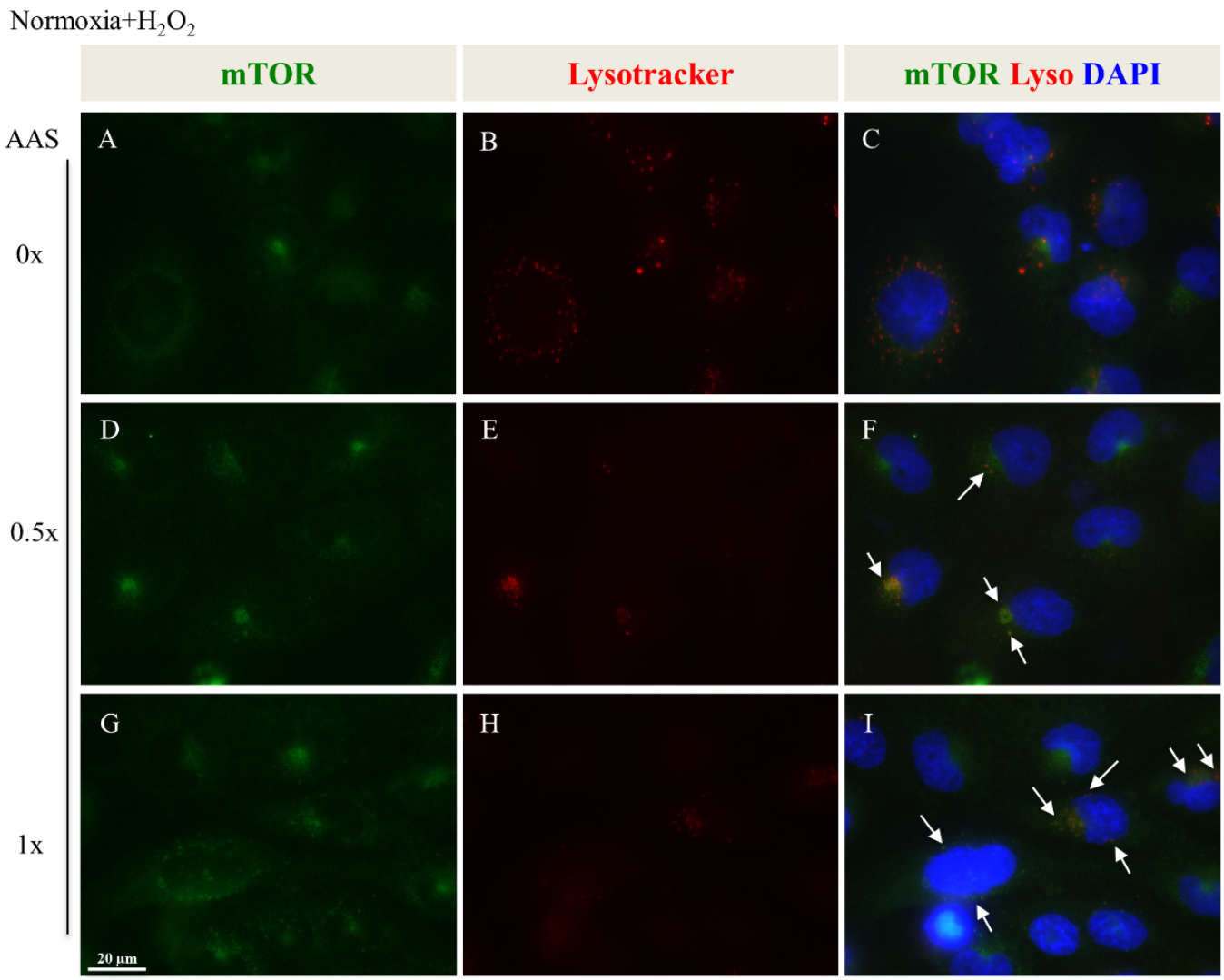


Figure 4. 12 Intracellular localisation of mTOR and lysosomes in response to AAS at pH 7.5 with H_2O_2 following starvation.

After starvation, HK-2 cells were treated with (A-C) 0x, (D-F) 0.5x and (G-I) 1x AAS at pH 7.5 in the presence of H_2O_2 for 1 hour. Overlay images showed that mTOR (green), Lysotracker (red) and DAPI (blue) were the same areas. Arrows showed the co-localisation of mTOR and Lysotracker. Magnification, x100; scale bar = 20 µm. One field per slide and three slides per treatment group were performed for an n = 3.

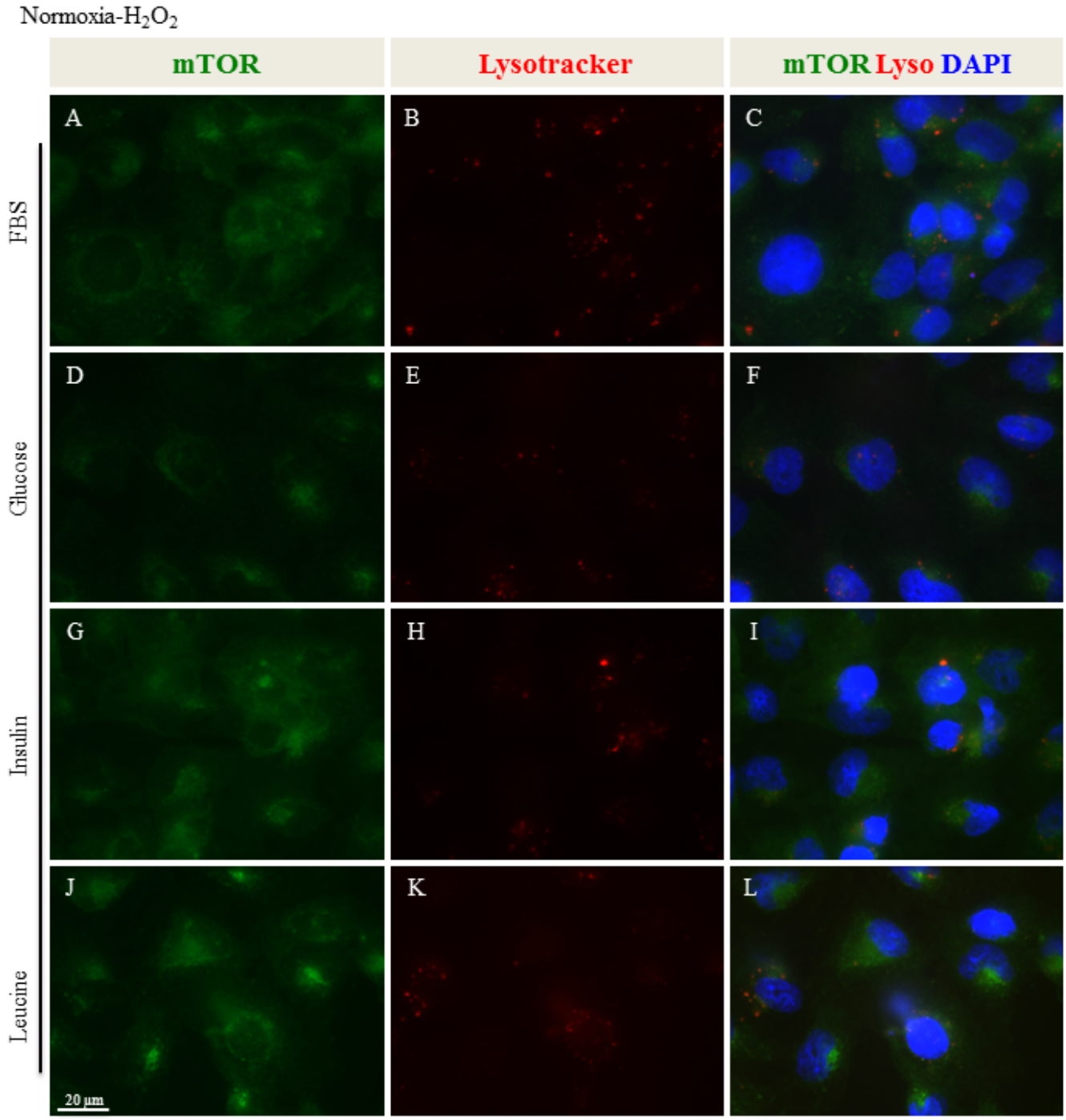


Figure 4. 13 Intracellular localisation of mTOR and lysosomes in response to nutrients at pH 7.5 following starvation.

After starvation, HK-2 cells were treated with (A-C) FBS, (D-F) glucose, (G-I) insulin and (J-L) leucine at pH 7.5 for 1 hour. Overlay images showed that mTOR (green), Lysotracker (red) and DAPI (blue) were the same areas. Magnification, x100; scale bar = 20 µm. One field per slide and three slides per treatment group were performed for an n = 3.

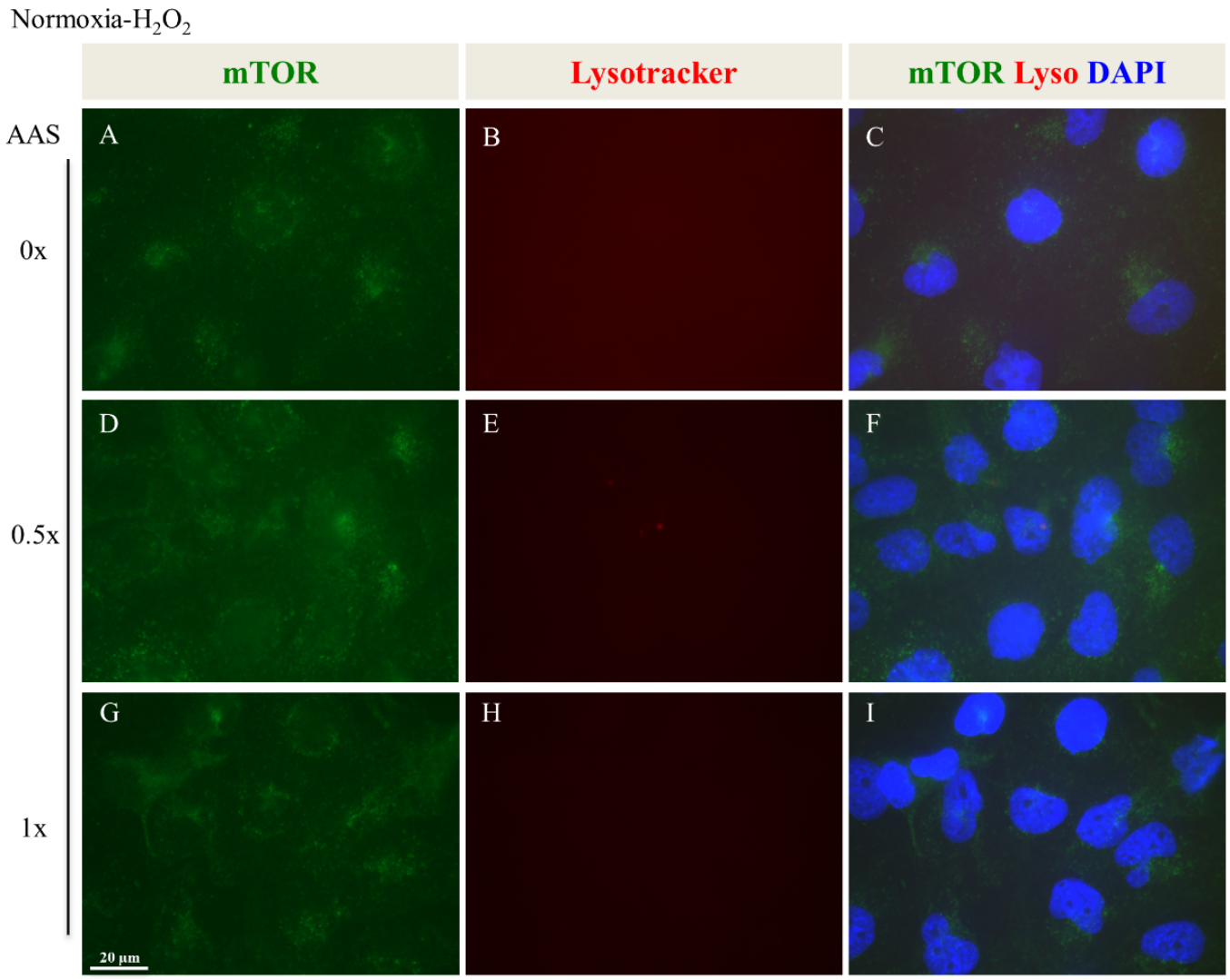


Figure 4. 14 Intracellular localisation of mTOR and lysosomes in response to AAS at pH 6.4 following starvation.

After starvation, HK-2 cells were treated with (A-C) 0x, (D-F) 0.5x and (G-I) 1x AAS at pH 6.4 for 1 hour. Overlay images showed that mTOR (green), Lysotracker (red) and DAPI (blue) were the same areas. Magnification, x100; scale bar = 20 µm. One field per slide and three slides per treatment group were performed for an n = 3.

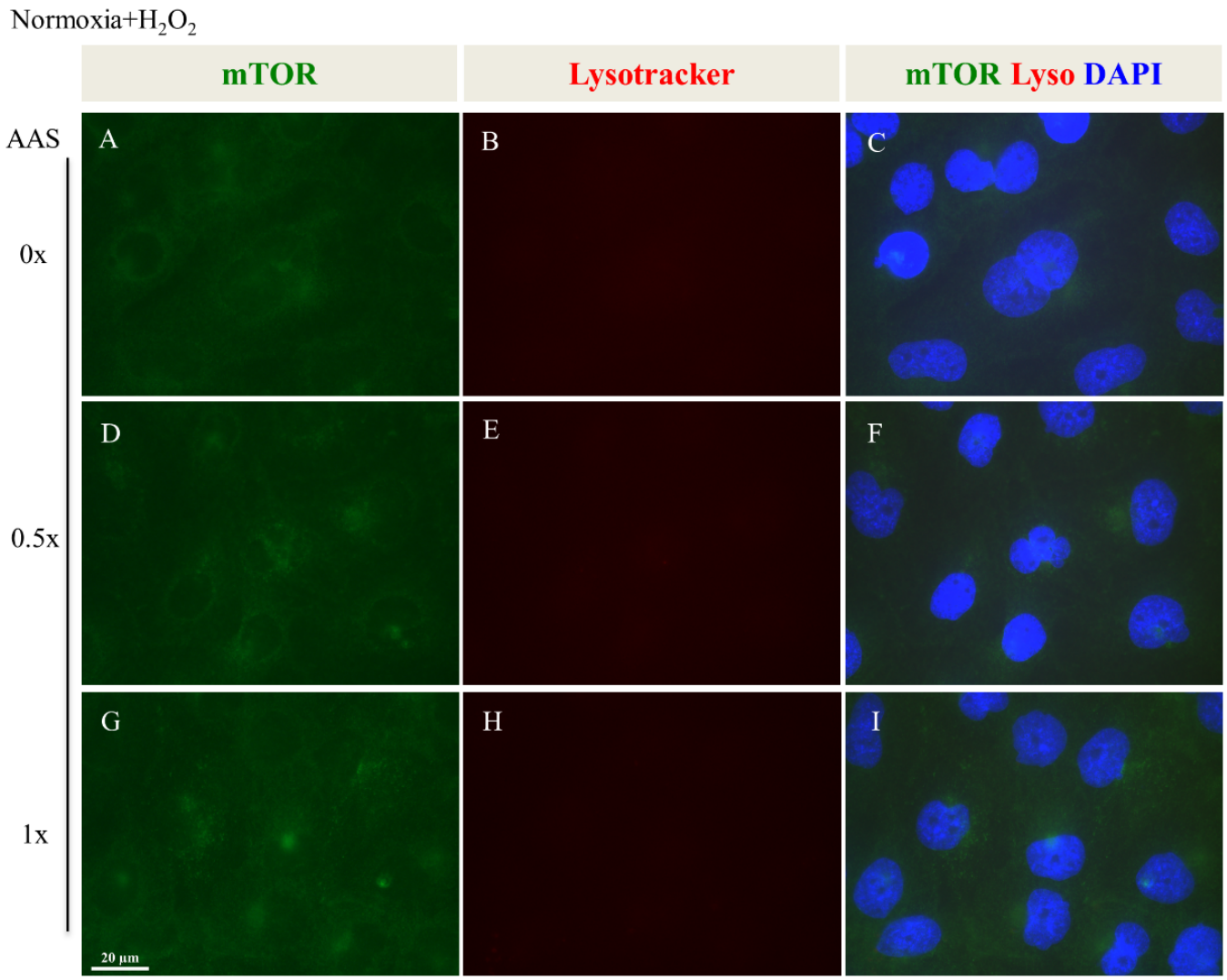


Figure 4. 15 Intracellular localisation of mTOR and lysosomes in response to AAS at pH 6.4 with H_2O_2 following starvation.

After starvation, HK-2 cells were treated with (A-C) 0x, (D-F) 0.5x and (G-I) 1x AAS at pH 6.4 in the presence of H_2O_2 for 1 hour. Overlay images showed that mTOR (green), Lysotracker (red) and DAPI (blue) were the same areas. Magnification, x100; scale bar = 20 µm. One field per slide and three slides per treatment group were performed for an n = 3.

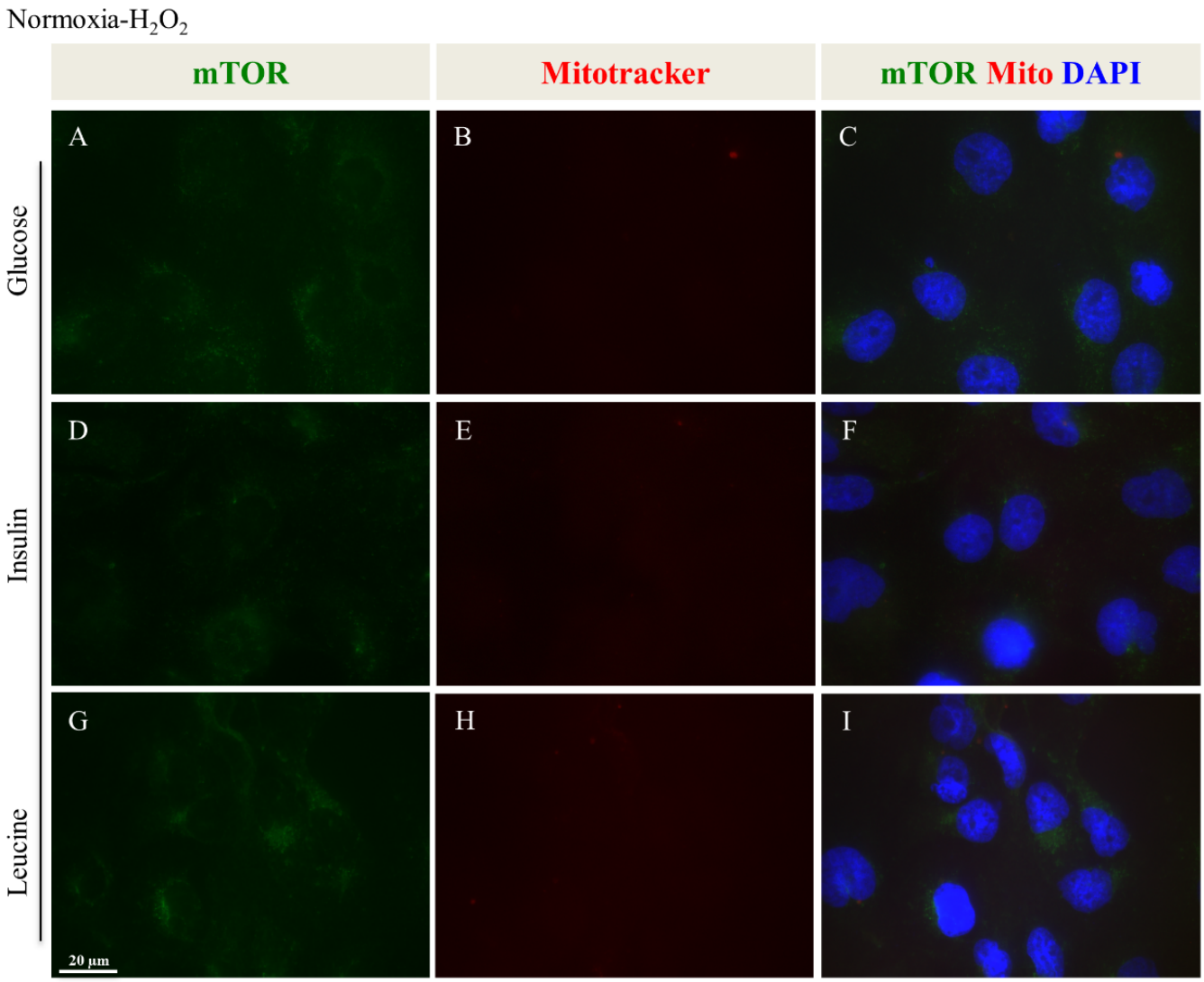


Figure 4. 16 Intracellular localisation of mTOR and lysosomes in response to nutrients at pH 6.4 following starvation.

After starvation, HK-2 cells were treated with (A-C) glucose, (D-F) insulin and (G-I) leucine at pH 6.4 for 1 hour. Overlay images showed that mTOR (green), Mitotracker (red) and DAPI (blue) were the same areas. Magnification, x100; scale bar = 20 µm. One field per slide and three slides per treatment group were performed for an n = 3.

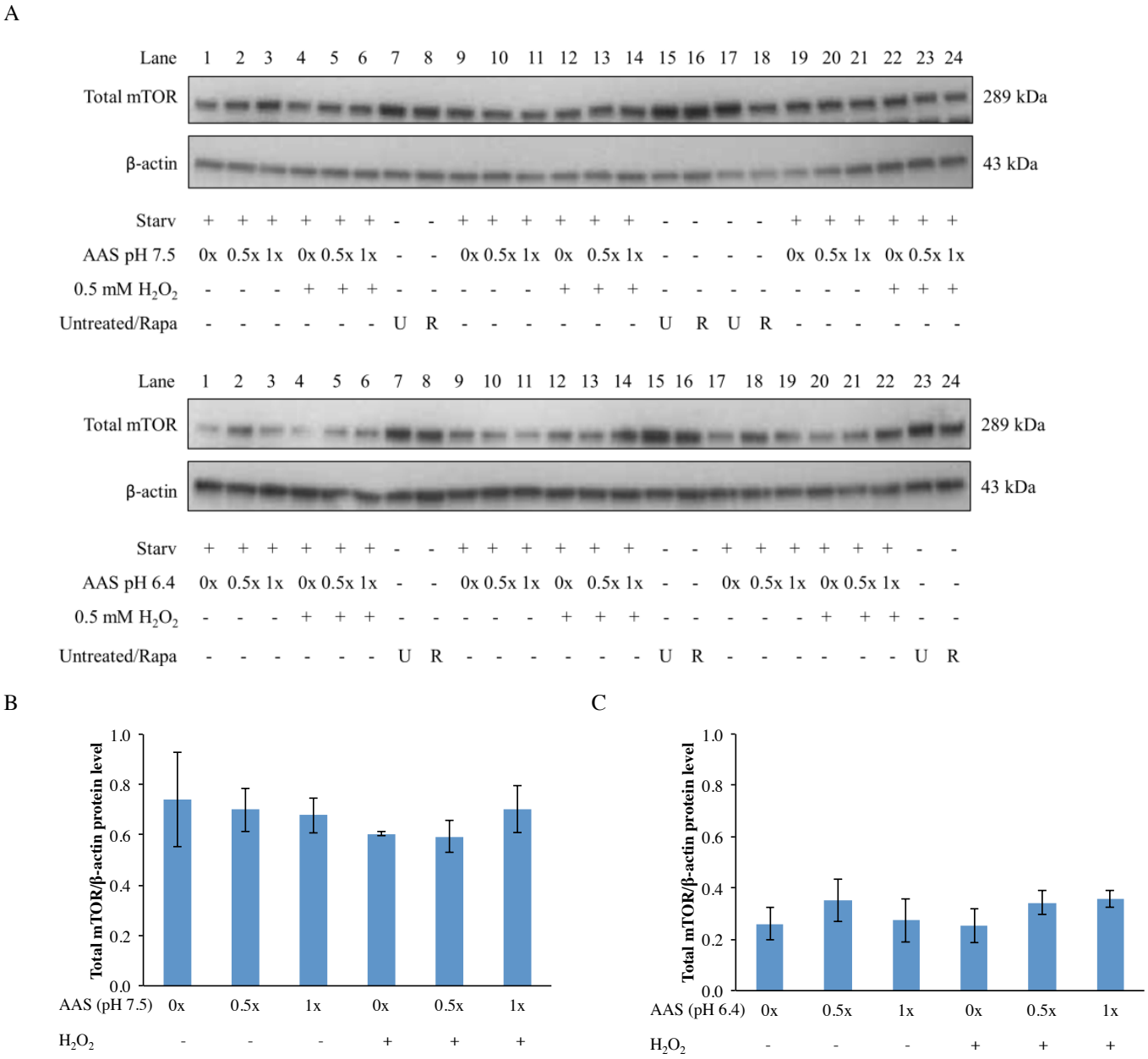


Figure 4. 17 Effects of amino acids at pH 7.5 and 6.4 with and without H_2O_2 following starvation on total mTOR protein levels.

(A) Immunoblots of total mTOR and β-actin protein levels were displayed for cells treated with AAS at pH 7.5 and pH 6.4 with and without H_2O_2 for 1 hour after starvation, untreated and treated with rapamycin for 24 hours. U: untreated; R: rapamycin. The bar graphs summarised the relative density of total mTOR/β-actin in cells treated with AAS at (B) pH 7.5 and (C) pH 6.4. Each treatment had triplicates for an n = 3. Data were presented as means ± SEM (n = 3).

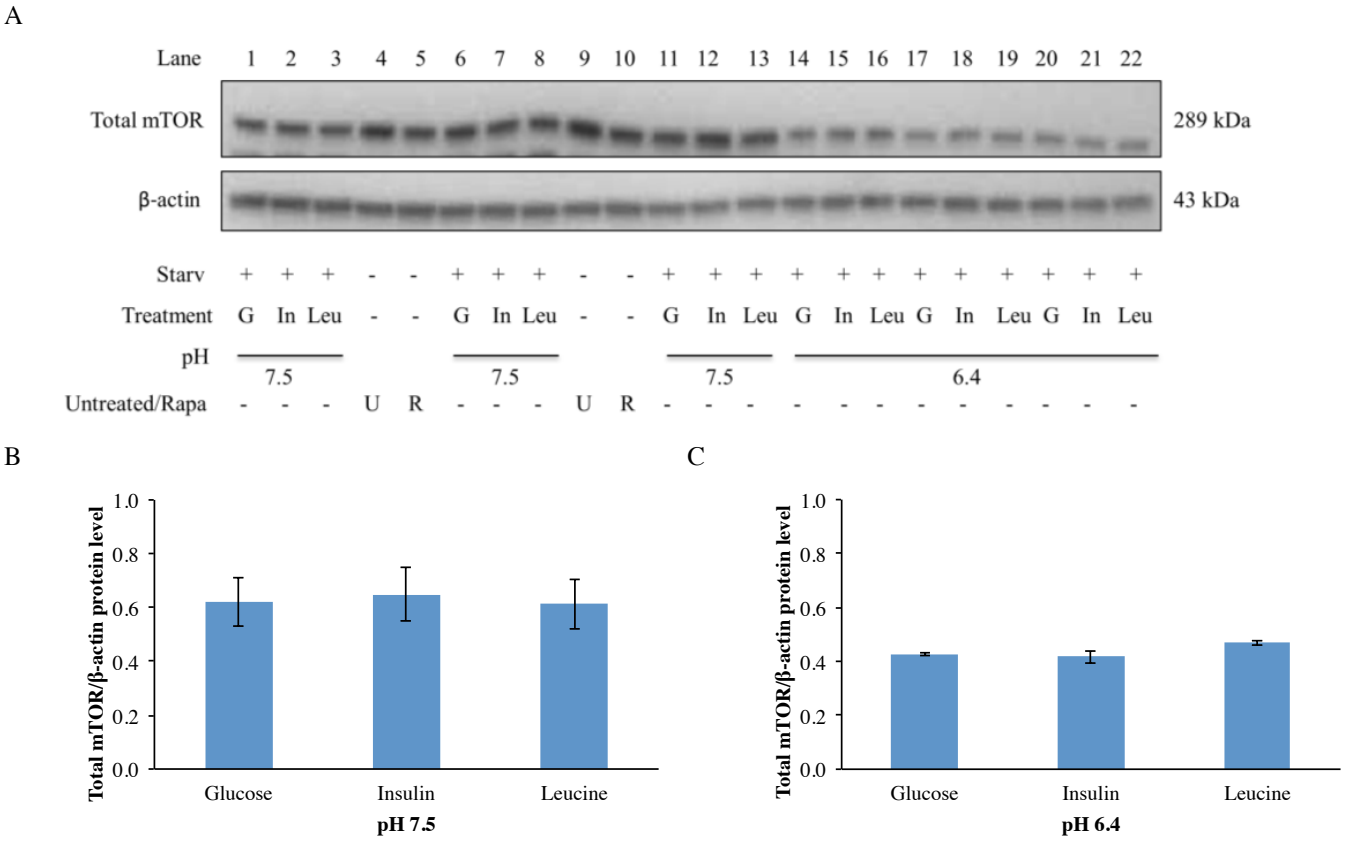


Figure 4. 18 Effects of nutrients at pH 7.5 and 6.4 following starvation on total mTOR.

(A) Immunoblots of total mTOR and β-actin protein levels were displayed for pre-starved HK-2 cells treated with glucose, insulin, leucine for 1 hour, untreated and treated with rapamycin for 24 hours. U: untreated; R: rapamycin. The bar graphs summarised the relative density of total mTOR/β-actin in cells treated with nutrients at (B) pH 7.5 and (C) pH 6.4. Each treatment had triplicates for an n = 3, and U and R group had duplicates. Data were presented as means ± SEM (n = 3).

4.2.6 Effects of AAS at physiological and acidic pH on ER stress sensor protein following D/R injury

To determine whether ER stress was induced and whether UPR was activated following nutrient deprivation and the replenishment of amino acids in the presence of H_2O_2, here the ER stress sensor protein Grp78 was detected using immunoblotting. Although determination of UPR activation requires the detection of its three main transmembrane proteins (e.g. PERK, IRE1 and ATF6) and the downstream proteins, here we examined Grp78 expression since it is known as a key regulator of ER stress transducer. Assessment on this protein only might be limited for testing the hypothesis, but its expression could reveal whether ER stress was induced after resupply of AAS following starvation.

After starvation, Grp78 protein constantly expressed over time after the replenishment of 0x, 0.5x and 1x AAS at pH 7.5 with and without H_2O_2 (Figure 4.19 A, lane 2-19), compared with untreated cells (Figure 4.19 A, lane 20). At 1 hour, there were no differences in Grp78 expression between treatments (Figure 4.19 B). At 4 hours, Grp78 expression decreased with the increase in AAS concentration ($p = 0.043$; Figure 4.19 B), with a negative linear relationship between AAS concentration and Grp78 levels ($p = 0.025$; Figure 4.19 B). The protein level was generally higher in the presence of H_2O_2 compared with the absence of H_2O_2 ($p = 0.002$; Figure 4.19 B). However, there was no interaction between AAS and H_2O_2 on protein expression. At 20 hours, the trend between Grp78 protein levels and AAS concentration ($p = 0.024$; Figure 4.19 B) was positive; that is, increasing AAS concentration enhanced Grp78 expression. However, the protein levels were not

affected by H_2O_2 or the interaction of AAS and H_2O_2. As the Grp78 levels in response to AAS and the concentration-dependent responses changed over time (at 4 and 20 hours), the relationship between AAS and Grp78 expression and the link to ER stress response could not be determined. These results could only suggest that starvation caused ER stress since chaperone proteins were found to express over time in all treatment groups. In contrast, the provision of AAS at pH 6.4 with and without H_2O_2 inhibited Grp78 protein expression within 1 hour (Figure 4.20 A).

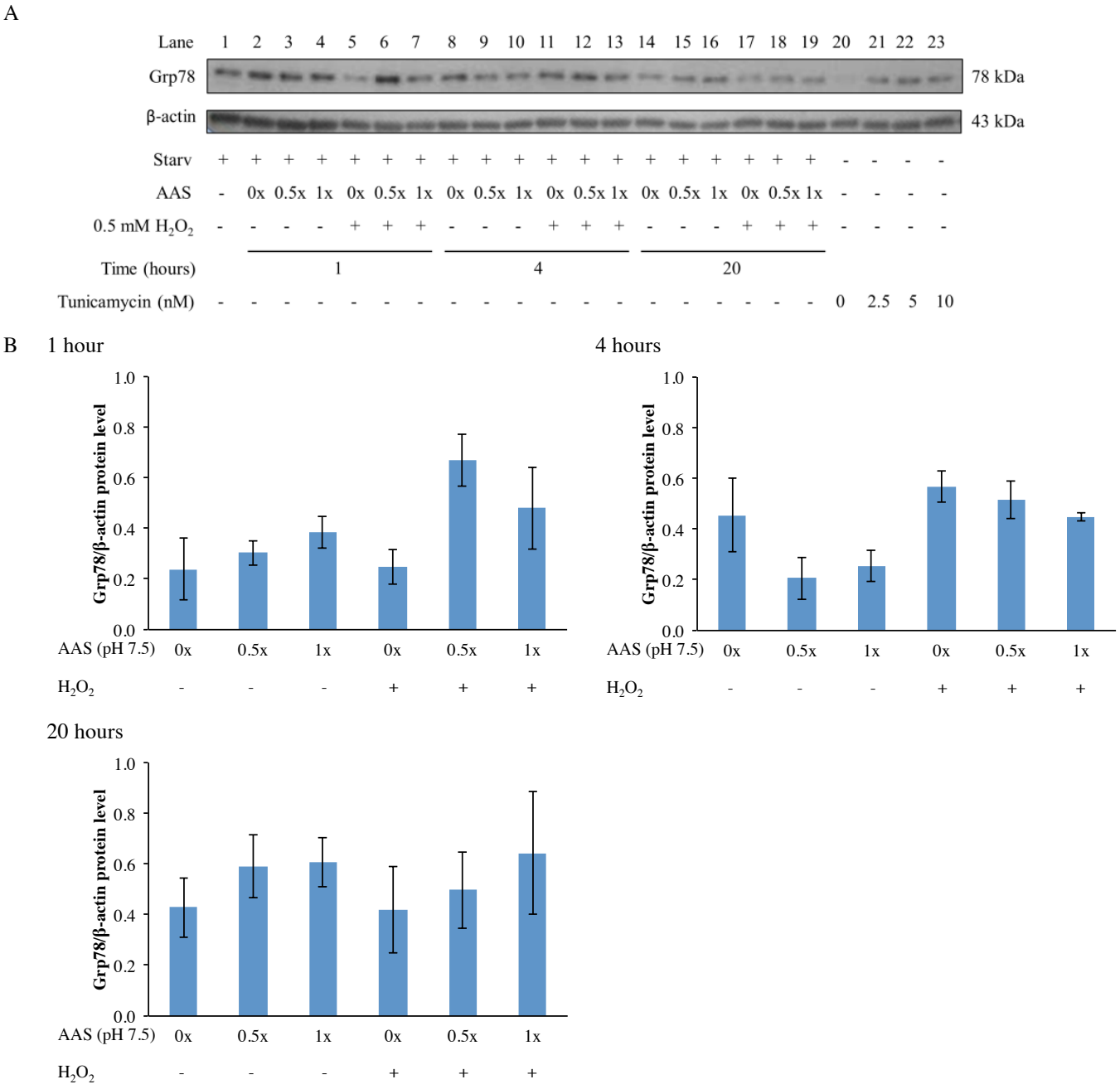
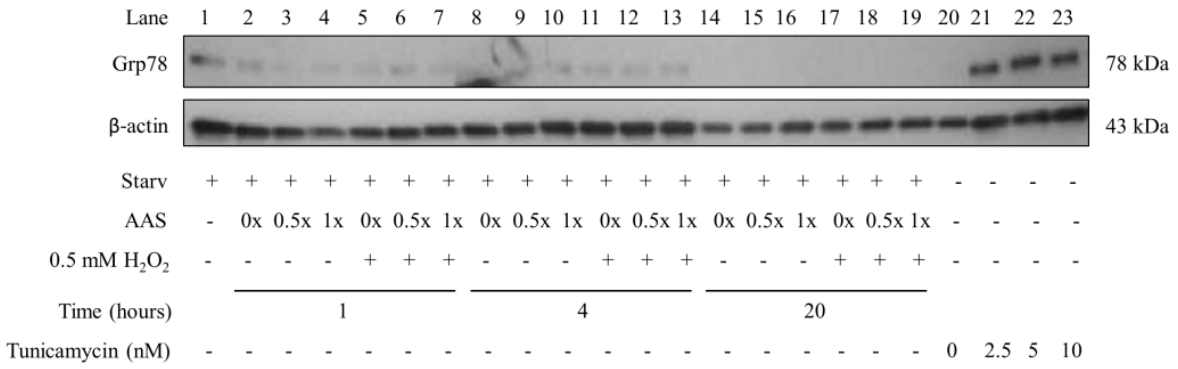


Figure 4. 19 Effects of amino acids at pH 7.5 with and without H_2O_2 following starvation on Grp78.

(A) Representative immunoblots of Grp78 and β-actin protein levels were displayed for pre-starved HK-2 cells treated with 0x, 0.5x and 1x AAS at pH 7.5 with and without H_2O_2 for 0, 1, 4 and 20 hours. Positive control was carried out by incubating cells with 0, 2.5, 5 and 10 μg/ml tunicamycin for 24 hours. (B) The bar graphs summarised the relative density of Grp78/β-actin at each time point. Each treatment had triplicates for an n = 3. Data were presented as means ± SEM (n = 3).

A



B

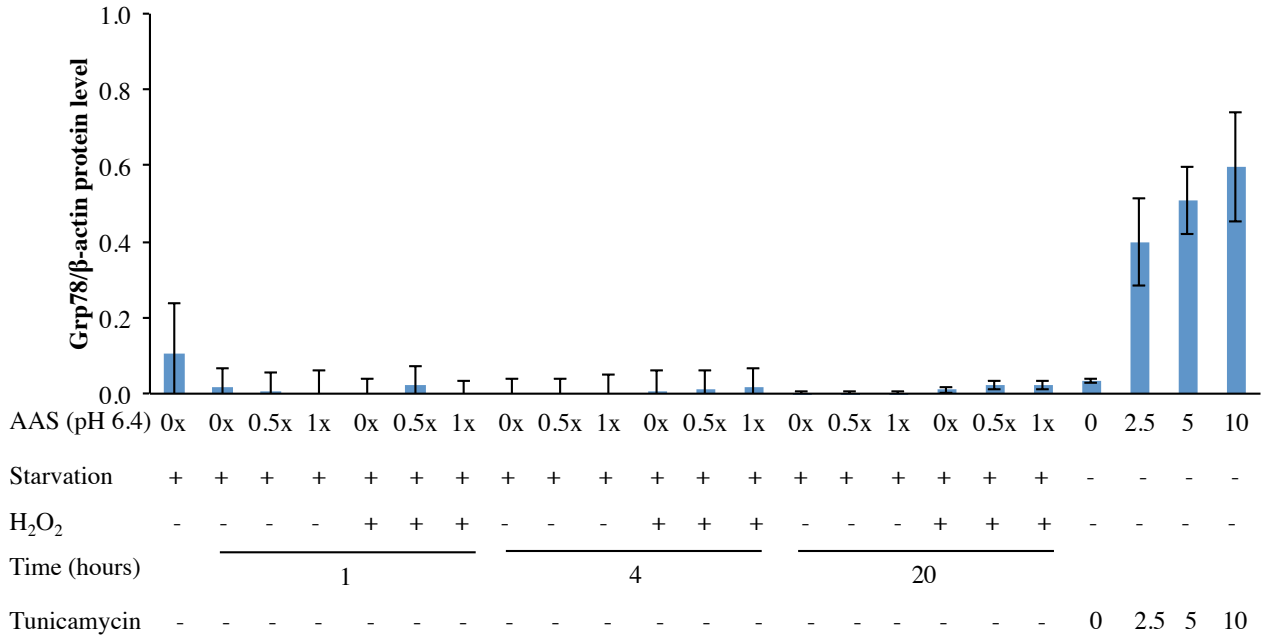


Figure 4. 20 Effects of amino acids at pH 6.4 with and without H_2O_2 following starvation on Grp78.

(A) Representative immunoblots of Grp78 and β-actin protein levels were displayed for pre-starved HK-2 cells treated with 0x, 0.5x and 1x AAS at pH 6.4 with and without H_2O_2 for 0, 1, 4 and 20 hours. Positive control was carried out by incubating cells with 0, 2.5, 5 and 10 μg/ml tunicamycin for 24 hours. (B) The bar graph summarised the relative density of Grp78/β-actin. Each treatment had triplicates for an n = 3. Data were presented as means ± SEM (n = 3).

4.3 Conclusion

After I/R injury, mTOR was found to be markedly activated in order to enhance renal tubular cell proliferation and restore kidney function (Lieberthal et al., 2006). Such an activation of mTOR in response to the rebound of nutrients, growth factors and ATP upon reperfusion after ischaemia can cause ER stress due to the increase in the protein load in the ER (Lieberthal et al., 2006; Inagi, 2009). Additionally, these newly synthesised proteins can be misfolded especially under oxidative stress as ROS can interfere with the protein disulfide bonding (Inagi, 2009). Subsequently, the accumulation of misfolded proteins can overwhelm ER ability in processing these proteins, leading to toxicity (Douglas and Dillin, 2010). Therefore, this chapter investigated whether cell death caused by the provision of amino acids under oxidative damage was due to the activation of mTOR which increased protein synthesis, caused misfolded protein overload in the ER and led to ER stress .

The results showed that the levels of mTOR downstream proteins including pS6K and pS6 were attenuated in cells treated with 0x AAS (pH 7.5) following starvation, and this potentially limited protein synthesis. In contrast, the mTOR signalling was activated in response to the presence of amino acids (pH 7.5) following starvation, evidenced by the observation of upregulated pS6K and pS6 protein expression. The level of activation was found to be positively correlated to AAS concentration. The presence or absence of H_2O_2 did not affect such a relationship, potentially suggesting that the return of amino acids still promoted protein synthesis through mTOR activation even if under oxidant injury.

It was observed that the activation of mTOR was possibly lysosome-dependent but not mitochondria-dependent, but this could not be confirmed as co-localisation only occurred occasionally in some cells. As only one field per slide and three slides per treatment group were obtained, the representative images could be less generalisable. Also, a negative control was not performed, and the efficiency and specificity of the antibody could be argued. These results could not confirm the lysosome-dependent mTOR activation.

We demonstrated that the activation of mTOR signalling by the replenishment of amino acids (pH 7.5) under H_2O_2 mediated damage. The further hypothesis was that this promoted protein synthesis and caused the newly synthesised protein to be oxidatively damaged by ROS and accumulate in the ER and lead to ER stress. To detect whether amino acids imposed a burden on the ER following starvation, this chapter assessed the chaperone protein Grp78, known as a regulator of ER stress transducer. The chaperone protein Grp78 was found to express in all treatment groups over time after starvation, indicating a cellular stress responses following starvation. The expression of Grp78 can result in cell survival or death in different conditions, and its role in diseases remains unknown. For instance, Grp78 has been found to be expressed in tumour cells, and its overexpression protects tumour cells from death and increases the resistence to chemotherapy (Sato et al., 2010). Another study demonstrated that induction of Grp78 expression using ER stress inducer (e.g. tunicamycin) prior to H_2O_2 mediated damage protected from renal tubular cell death (Chandrika et al., 2015). In other cases, overexpression of Grp78 was found to participate in drug-induced nephrotoxicity and cell death (Pallet et al., 2008).

In this chapter, Grp78 protein constantly expressed over time, but its levels did not display a consistent pattern in response to AAS concentration. At 4 hours, Grp78 levels decreased with increasing AAS concentration, and the presence of H_2O_2 enhanced its expression. However, at 20 hours Grp78 levels increased with the increase in AAS concentration. The constant Grp78 expression could only suggest the cellular stress response after starvation. Whether the prolonged Grp78 expression was associated with cell death caused by AAS in the presence of H_2O_2 in chapter 3 was still unclear. To confirm the direct link between AAS at pH 7.5 in the presence of H_2O_2 and Grp78 expression that induced UPR mediated cell death, it still requires the detection of UPR pathways mediated by PERK, IRE1 and ATF6 and apoptotic factors. More importantly, the concentration of H_2O_2 used in this study did not inhibit mTOR signalling. Li et al. (2010) reported that the *in-vivo* injection of ROS-inducing drugs stimulated mTOR activity in all tissues including brain, heart, liver, kidney and muscle. The level of H_2O_2 induced oxidative stress in this thesis could be biologically relevant to the *in-vivo* condition.

Moreover, the provision of AAS and other nutrients including glucose, insulin and leucine at pH 6.4 following starvation was unable to activate mTOR downstream proteins including pS6 and pS6K. Additionally, no lysosomes were detected in such an acidic condition. Although the inactivation of mTOR signalling observed here was consistent with several studies (Balgi et al., 2011; Marino et al., 2012; Crean et al., 2013), acidic pH (pH 6.4) did not show any protection against oxidative damage. Even if inhibition of mTOR by pH 6.4 may potentially reduce global protein synthesis and misfolded protein formation, it still exacerbated cell death upon the replenishment of AAS in the presence of H_2O_2 as shown in MTT assay. As acidic pH

also inhibited chaperone protein expression, this completely blocked the chance for cell survival through oxidative stress.

Chapter 5: The effects of sodium nitrite on ArisA-induced AKI

Chapter 5: The effects of sodium nitrite on ArisA-induced AKI

5.1 Introduction

In Chapter 3 and 4, simulated I/R injury was unable to induce a previously compromised kidney cells using HK-2 cell system. Hence, this chapter established an ArisA-induced AKI model in animals. ArisA-induced AKI has several advantages compared with other commonly used AKI models including bilateral I/R injury and other drug-induced nephrotoxicity. Compared with bilateral I/R, the utility of drugs to induce a successful and consistent AKI is independent of the technical issues such as surgery process and skills (Wei and Dong, 2012). Compared with other commonly used drugs including cyclosporine, gentamycin, cisplatin and folic acid, ArisA-induced nephrotoxicity can be simply achieved by a single low dose of ArisA and can result in a modest AKI at the early stage (within 4-10 days) and lead to interstitial fibrosis after one month (Yang et al., 2010; Novitskaya et al., 2014). A successful AKI induced by drugs is mainly dependent on dose, duration and the selection of experimental models such as species, strains and gender. Inbred male rodents are normally preferred in the AKI research due to the features of high susceptibility and consistency (Park et al., 2004). However, this thesis selected an outbred strain of female mice in order to induce a modest injury (without an overt damage) which allows a full recovery by dietary intervention at the acute phase and to mimic human population which is genetically variable (Festing, 2010).

The nephrotoxicity and genotoxicity of ArisA appear after metabolism by enzymes, CYP reductases, which mainly exist in liver and kidney (Stiborová et al., 2008). In

kidney, ArisA predominately damages the cortical region, with renal proximal tubular epithelial cells being the major target (Chang et al., 2001; Sato et al., 2004; Shibutani et al., 2007). Additionally it was also found to cause endothelial wall thickening in the afferent arterioles, suggesting an ischaemic phenomenon in AAN (De Broe, 1999). Hence, it is an alternative means for inducing renal I/R injury. Evidence has shown that ArisA induced DNA damage triggered G2/M cell cycle arrest in HK-2 cells and porcine proximal tubular epithelial cells (Li, Y. et al., 2006; Yang et al., 2010; Romanov et al., 2015). Recently, this cell cycle arrest was further identified to be associated with the increase in oxidative stress induced by ROS production and lead to apoptosis in a dose-dependent manner in both *in-vitro* and *in-vivo* models (Pozdzik et al., 2008; Zhu et al., 2012; Romanov et al., 2015). Moreover, it was also found that the percentage of cells entering G2/M cell cycle arrest was also positively correlated to the development of fibrosis (Yang et al., 2012; Canaud and Bonventre, 2015). Studies discovered that the tubular epithelial cells arrested in G2/M phase could produce fibrotic factors (e.g. CTGF) and cytokines (e.g. TGF-b1), and therefore it was suggested that G2/M cell cycle arrest could also serve as a novel biomarker for fibrosis and CKD progression (Yang et al., 2012; Canaud and Bonventre, 2015). As G2/M arrest caused by ArisA was shown to lead to interstitial fibrosis (Yang et al., 2012), this chapter additionally intended to determine whether this was shown in the animals.

In addition to examining the consequence of AKI on compromised renal tubular cells, this chapter also intended to establish whether any renoprotective agents might influence kidney response to the damage. Here sodium nitrite supplemented in drinking water was used as a nutritional intervention prior to exposure to ArisA. The purpose of dietary nitrite is to mimic a RIPC programme. It has been evidenced that

administration of exogenous nitrate/nitrite could generate a RIPC-like effect and that its protection was as potent as RIPC (Shiva et al., 2007b). The main principle is to increase circulating and tissue nitrate/nitrite levels, and hence NO is ready to release in the target organ to ameliorate ROS damage during I/R injury (Rassaf et al., 2014). The protection of exogenous nitrate/nitrite against I/R injury has also been demonstrated in many organs including heart (Zhan et al., 2009), liver (Patel et al., 2005), brain (Jung et al., 2006) and kidney (Tripatara et al., 2007; Kanematsu et al., 2008; Declèves et al., 2016). In particular, Declèves et al. (2016) recently showed that L-arginine (a source of NO) supplemented in drinking water protected against ArisA-induced AKI in mice. The authors observed that the increase in NO bioavailability by L-arginine protected from kidney structural and functional damages, ROS damage, inflammation and apoptosis caused by ArisA. This indicated therapeutic effects of dietary nitrite on renal I/R injury, potentially supporting the hypothesis in this chapter.

To date, most studies investigated the therapeutic effects of chronic administration (over 3 days to weeks) of dietary nitrite/nitrate at a low dose on various diseases (0.1 to 1.0 mmol/kg/d) (Lundberg et al., 2011). However, it is important to note that dietary nitrite is readily absorbed and distributed in most tissues and that nitrite bioavailability reaches 95-98% within 1 hour after ingestion (Bryan et al., 2005; Hunault et al., 2009). Therefore, the dose and duration of sodium nitrite (1 mM in drinking water for 24 hours) used in this thesis may theoretically achieve sufficient nitrite bioavailability prior to subsequent injury.

Aims and hypothesis

The aims of this chapter were to determine whether sodium nitrite could protect tubular cells from ArisA induced damage. To achieve this, the protocol was as follows. Mice at 6-8 weeks of age were administered with either drinking water or sodium nitrite supplemented in drinking water for 24 hours followed by intraperitoneal injection of saline or ArisA. Some mice were then sacrificed 24 hours after treatments, with some mice injected with BrdU 24 hours prior to sacrifice. The rest were sacrificed at 35 days thereafter. Considering the relationship between nitrite/nitrate and the current understanding of cytoprotection of nitrite in response to I/R injury in many organs, it was hypothesised that oral administration of sodium nitrite may increase nitrite levels in the circulation and kidney tissue to enhance kidney resistance to ArisA-induced AKI.

5.2 Results

5.2.1 Histopathology of the kidneys

Kidneys were stained with H&E to observe the changes in kidney structures. All groups maintained normal kidney architecture (Figure 5.1 and 5.2). There were no obvious morphological and structural abnormalities in 48-hour (Figure 5.1) and 35-day kidneys (Figure 5.2). The glomeruli, tubules and the basement membranes were intact, and there were no patchy zones and any signs of acute damage such as dilation, epithelial flattening, apoptotic or necrotic cells and casts. The kidneys all showed small regions of interstitial areas among tubules and glomeruli, indicating no effects of ArisA.

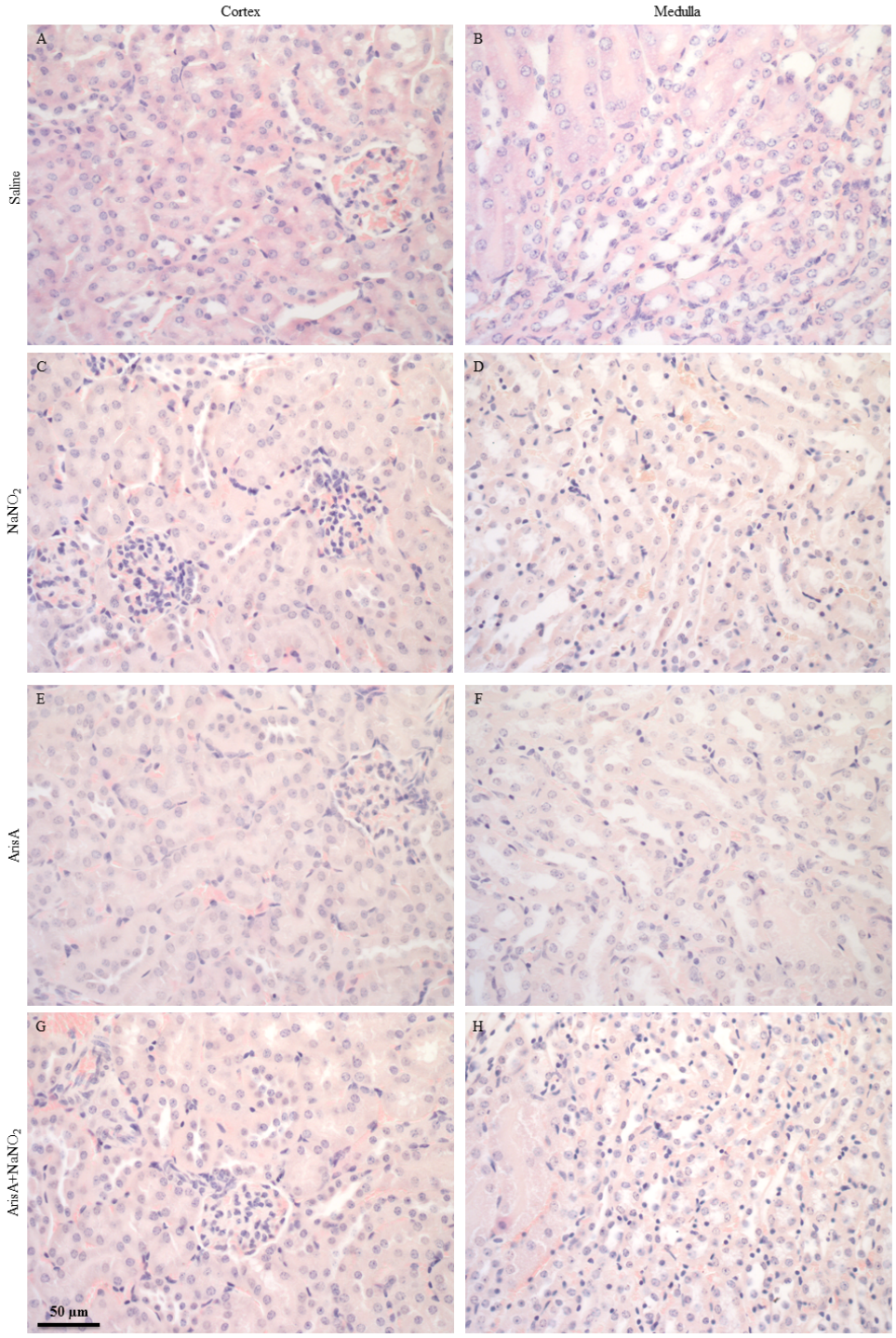


Figure 5. 1 Representative images of H&E stain in 48-hour kidneys.

Representative areas of cortex and medulla in H&E stained kidneys were displayed for (A-B) saline (n = 14), (C-D) $NaNO_2$ (n = 16), (E-F) ArisA (n = 17) and (G-H) ArisA+$NaNO_2$ (n = 16) treated mice. Magnification, x40; scale bar = 50 μm. Ten randomly chosen fields per slide and ten animals per treatment group were obtained.

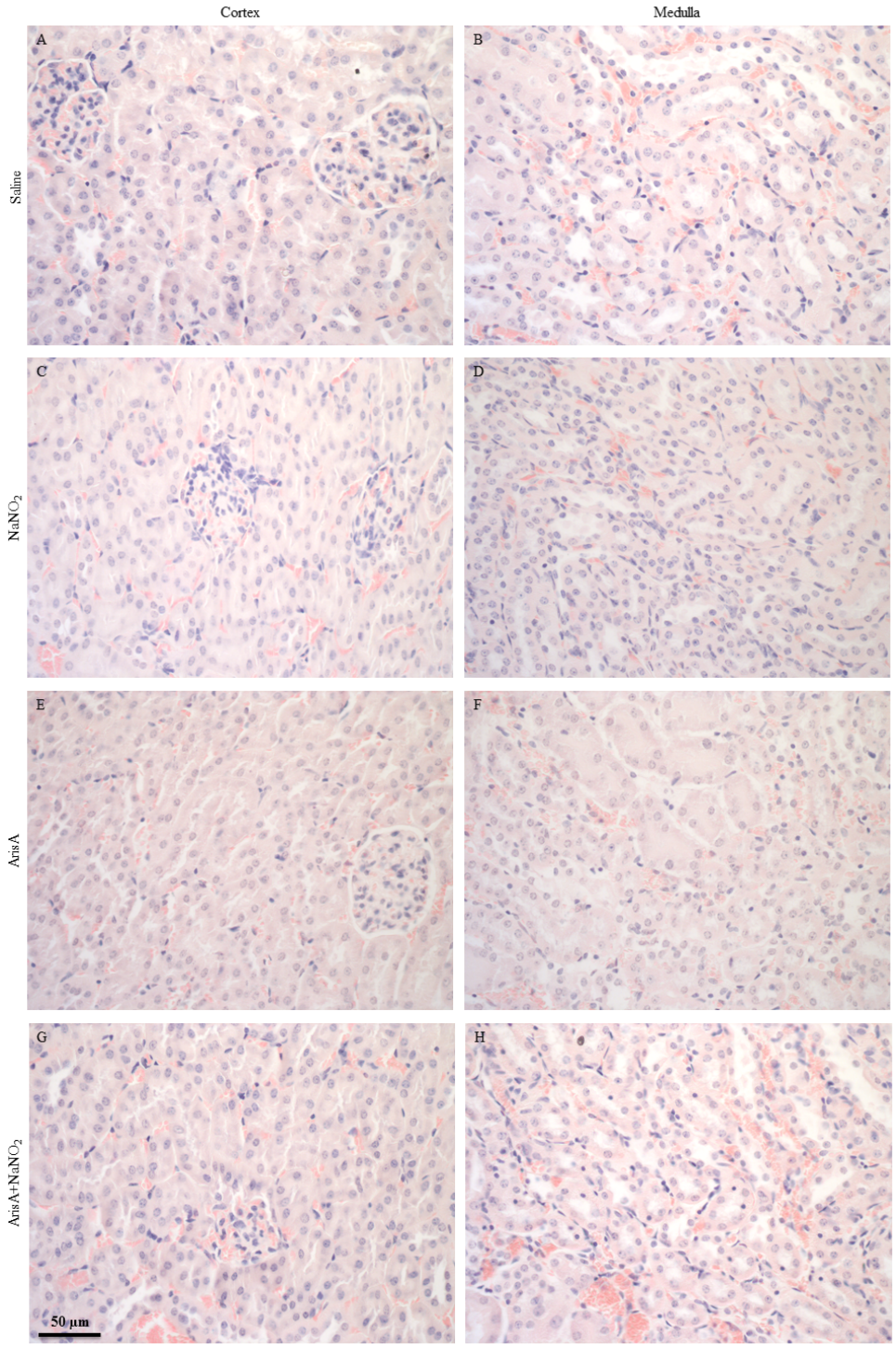


Figure 5. 2 Representative images of H&E stain in 35-day kidneys.

Representative areas of cortex and medulla in H&E stained kidneys were displayed for (A-B) saline (n = 11), (C-D) $NaNO_2$ (n = 17), (E-F) ArisA (n = 15) and (G-H) ArisA+$NaNO_2$ (n = 16) treated mice. Magnification, x40; scale bar = 50 μm. Ten randomly chosen fields per slide and ten animals per treatment group were obtained.

5.2.2 Tubulointerstitial fibrosis assessment by Masson's trichrome stain

Before carrying out Masson's trichrome staining on the experimental sections, the positive controls for the staining protocol were performed in the sections from injured mouse and pig kidneys (Figure 5.3). Only the connective tissues or collagen can be stained by fast green dye; therefore, the green colour will appear in the basement membrane of blood vessels and the fibrotic (collagen covered) areas in the glomeruli, tubules or interstitium (the space between tubules, glomeruli and capillaries). The kidney section from cyclooxygenase-2 knockout mice displayed a positive stain in the glomeruli and interstitium (Figure 5.3 A), and the kidney section from pigs subjected to I/R injury (by renal artery clamping for 40 minutes) also showed a positive stain in the interstitial areas (Figure 5.3 B). Hence, the same protocol was performed on the experimental kidneys at 35 days after treatments to observe whether fibrosis occurred at the chronic phase. Generally, the kidneys after all treatments still maintained normal structures as observed in the H&E staining (Figure 5.4). There were no signs of fibrosis in interstitial areas. Some sections showed glomeruli stained green which may be indicative of fibrosis. However, it could not be clearly identified due to the intact structures, and this also occurred in the control group (Figure 5.4 A). In a few sections, the positive stain was found to appear inside of tubular lumen, and this was not a correct location for fibrosis. Nevertheless, the relative blue/green stained areas in the cortical and medullary region were still quantified using ImageJ software. As there was no obvious fibrosis in the interstitial areas, the colour threshold for quantification of positive stained areas was setup based on the colour (blue/green/grey) of basement membrane of

blood vessels. Overall, there were no significant differences between treatments, suggesting that ArisA did not have any significant impact on this animal model (Figure 5.5).

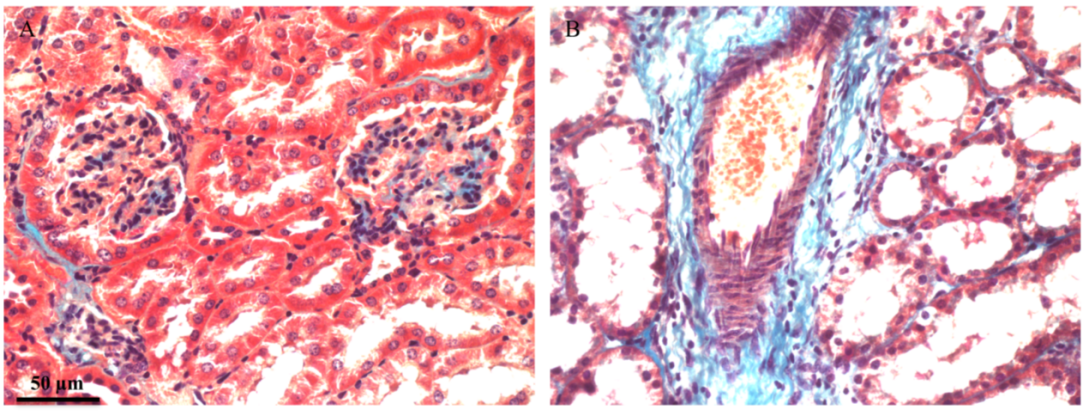


Figure 5. 3 Representative images of Masson's trichrome stained kidneys.

Positive controls were displayed for Masson's trichrome staining in paraffin-embedded kidney sections from (A) cyclooxygenase-2 knockout mice and (B) pigs subjected to I/R injury showed purple nuclei, red cytoplasm and red blood cells and green collagen/connective tissues. Magnification, x40; scale bar = 50 μm.

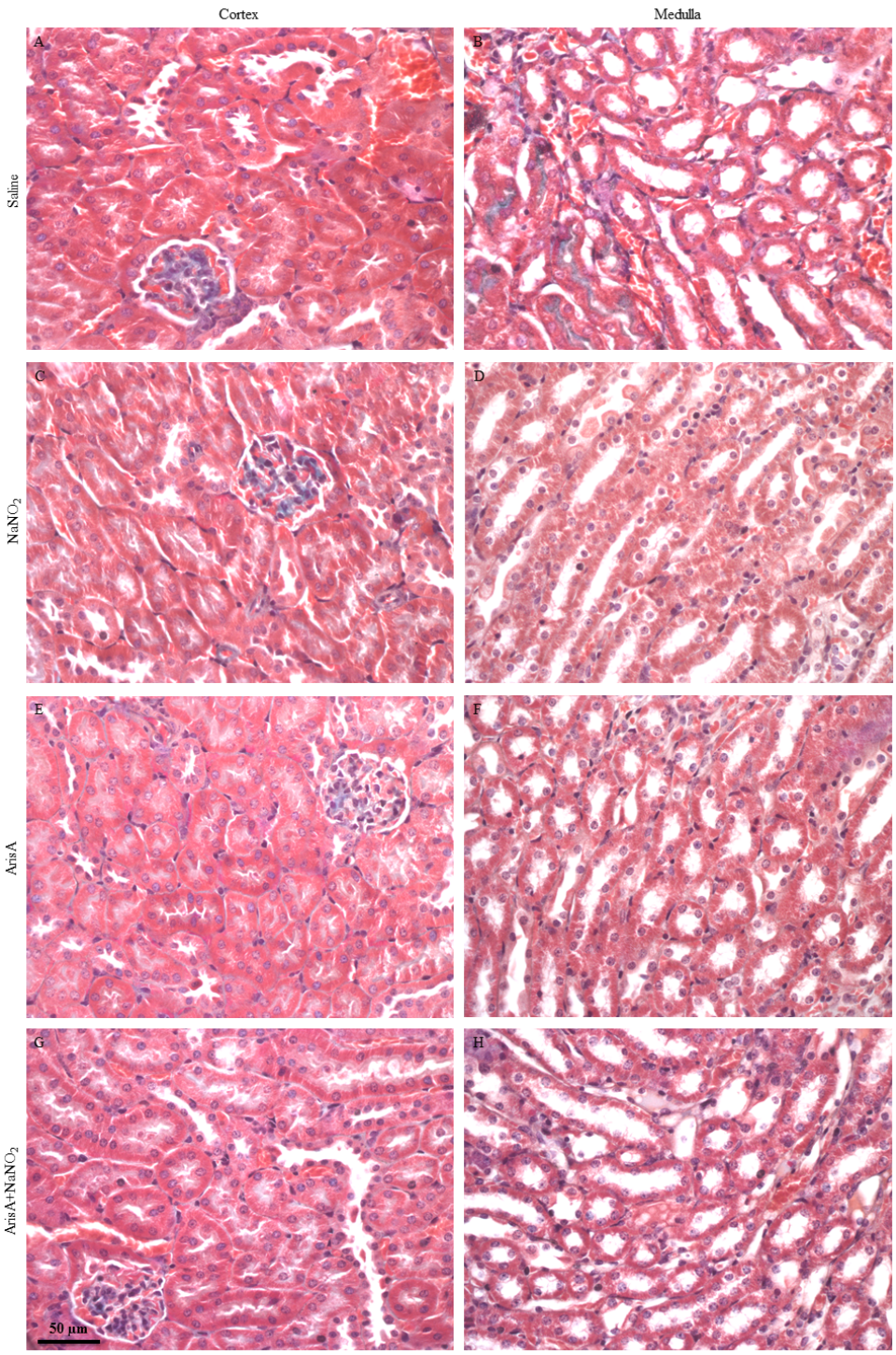
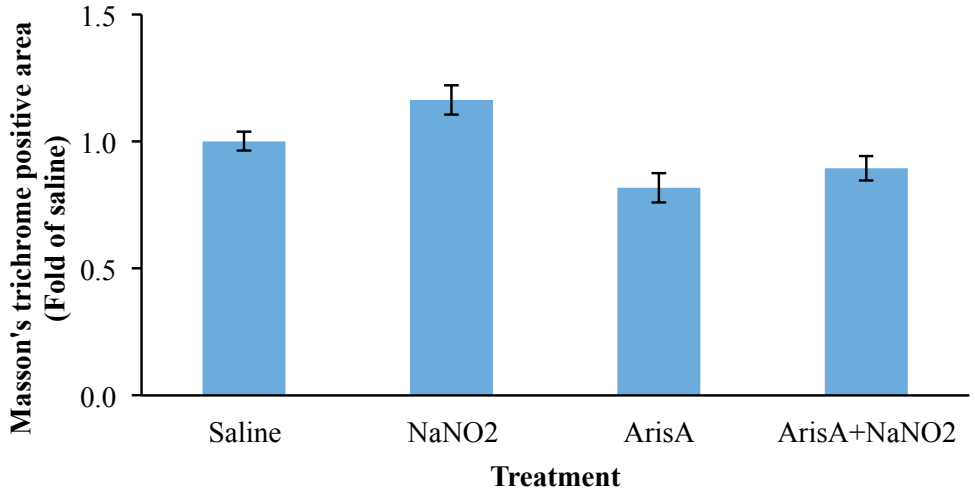


Figure 5. 4 Representative images of Masson's trichrome stain in 35-day kidneys.

Representative areas of cortex and medulla in Masson's trichrome stained kidneys were displayed for (A-B) saline (n = 11), (C-D) $NaNO_2$ (n = 17), (E-F) ArisA (n = 15) and (G-H) ArisA+$NaNO_2$ (n = 16) treated mice. Nuclei, purple; cytoplasm and red blood cells, red; collagen, green. Magnification, x40; scale bar = 50 μm. Ten fields per slide and ten animals per treatment group were obtained.

A



B

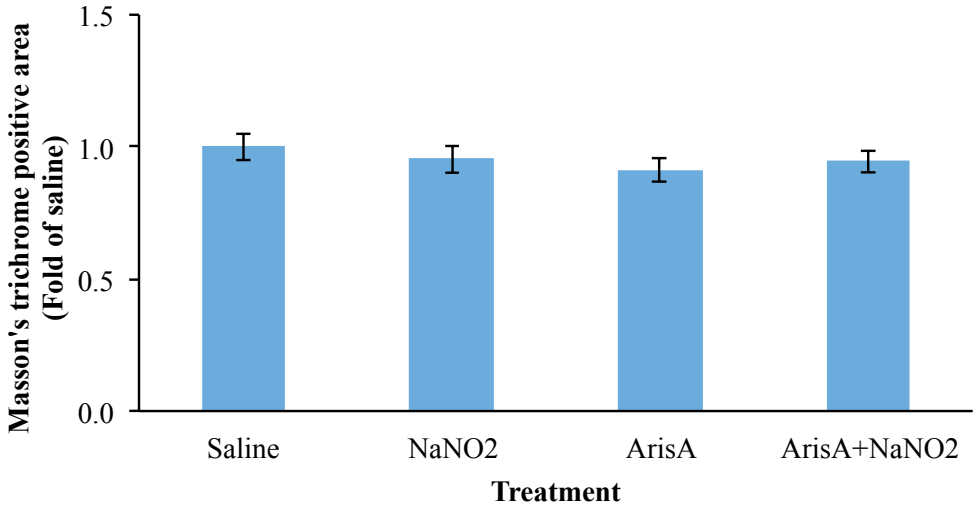


Figure 5. 5 Analyses of Masson's trichrome positive stain in 35-day kidneys.

Relative blue/green stained areas were quantified using ImageJ software. Ten fields each for (A) cortex and (B) medulla in each slide and ten animals for each treatment group were analysed. Data were presented as means ± SEM (n = 10) and fold change compared with saline.

5.2.3 Cell proliferation, survival and recovery

Although there was no structural damage observed in the histological analysis, this still could not conclude that there was no injury caused by ArisA. Since it has been known that within 48 hours after injury there were normally numerous proliferative cells in the cortical areas, we examined those animals injected with BrdU at 48 hours. To identify the proliferative cells, the immunofluorescence labelling and quantification of BrdU+ (incorporated into DNA in S phase) and pH3+ (labeled cells in G2/M phase) cells were performed. Before carrying it out on the experimental sections, the positive control for pH3 immunofluorescence labelling were first performed in the sections of whole mouse embryos (Figure 5.6).

Overall, there were only a few proliferative cells detected in all treatment groups, suggesting that ArisA did not induce any damage. Some BrdU and pH3 positive cells were detected, but the co-localised BrdU and pH3 cells were rarely detected (Figure 5.7). Three fields per section were obtained at a magnification of x20. While more fields are required for the quantitative analysis, three fields were sufficient here due to a low positive cell number. The BrdU and pH3 positively stained cells in both cortical and medullary region were counted and analysed. As the medullary region did not have any proliferative cells, data were not reported here. The positive BrdU+, pH3+ and BrdU+pH3+ cell number was quantified and presented as positive cell number per mm^2 kidney area rather than positive cell number per total cell number, as the DAPI staining disappeared in some sections. After conversion of the $pixels^2$ into mm^2, the cell number reached up to 497 ± 371 positive cells/mm^2 observed in the $NaNO_2$ group (Figure 5.8 D). However, in each section from all treatment groups the positive cell number observed only ranged from 0 to 20 cells. Overall, the

analyses using an Unbalanced ANOVA showed that there were no significant differences in all cases.

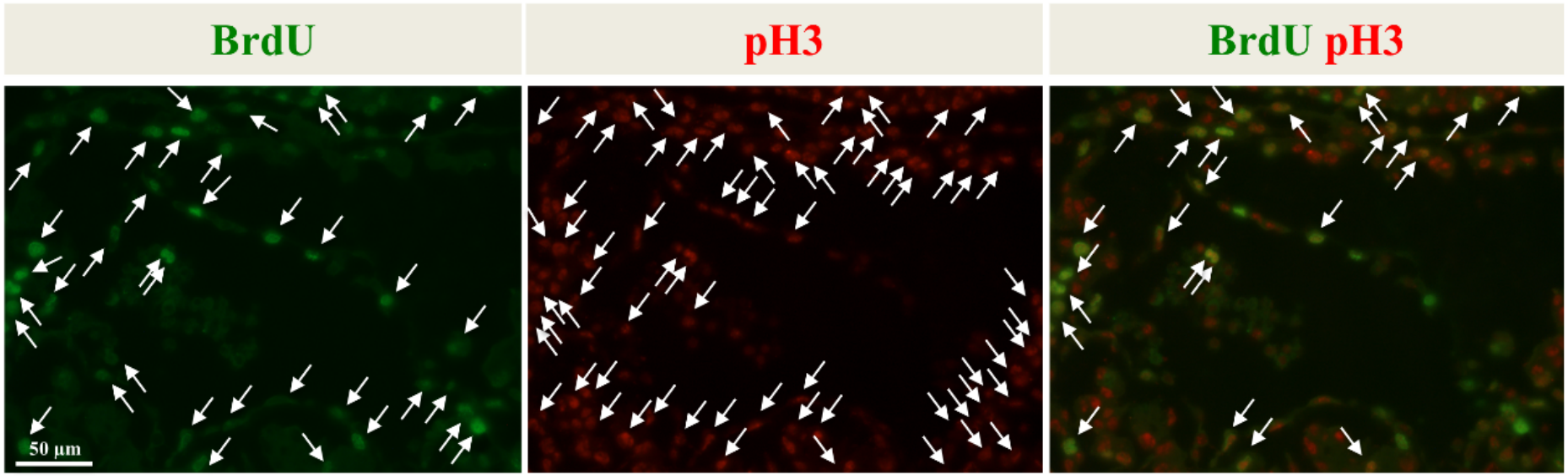


Figure 5. 6 Representative images of positive control for pH3 labelling in sections from mouse embryos.

Mouse embryos were probed with anti-BrdU (green) and anti-pH3 (red). Arrows showed BrdU or pH3 positive cells and BrdU and pH3 co-positive cells from the left to the right panels. Magnification, x40; scale bar = 50 μm.

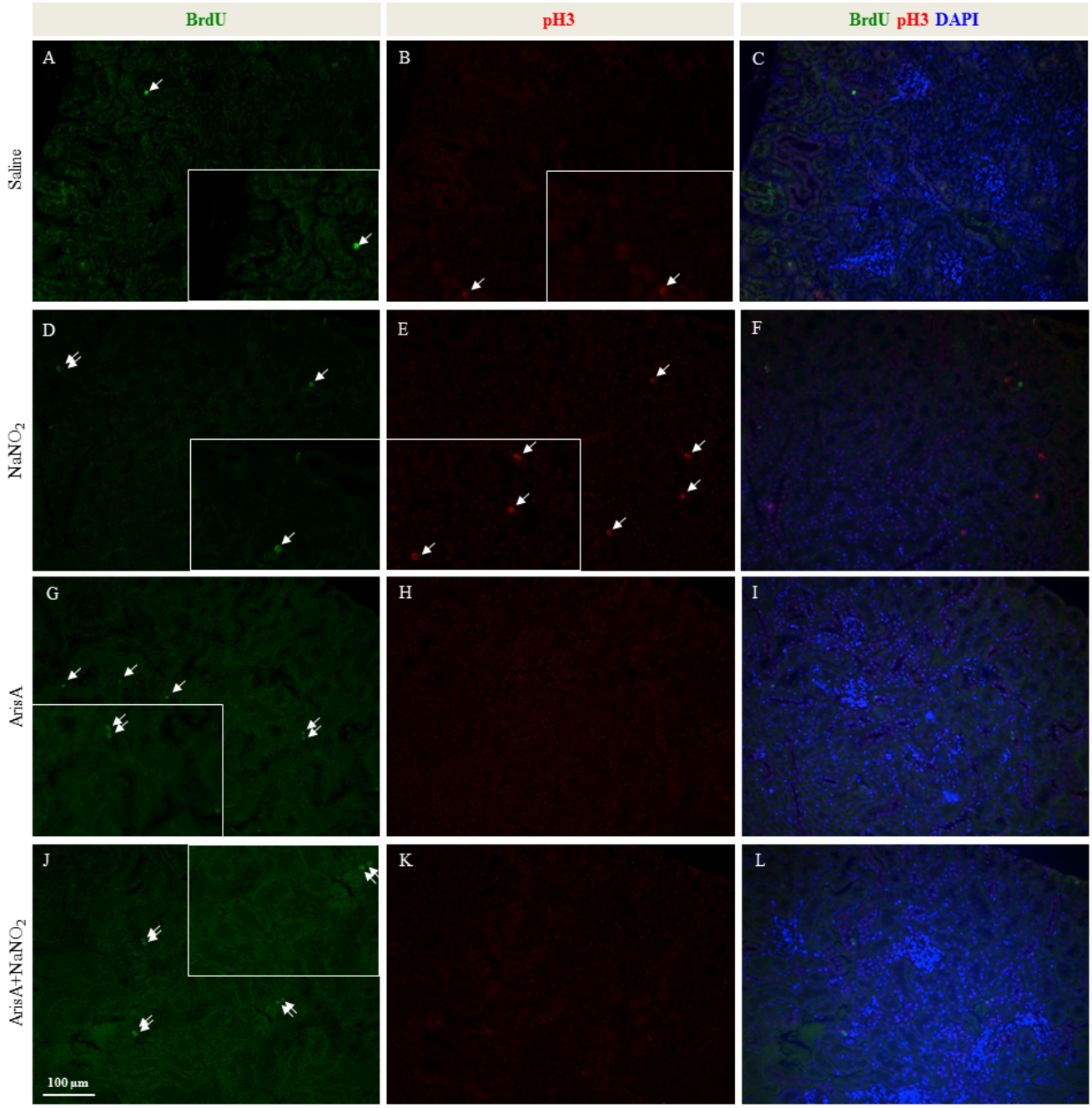
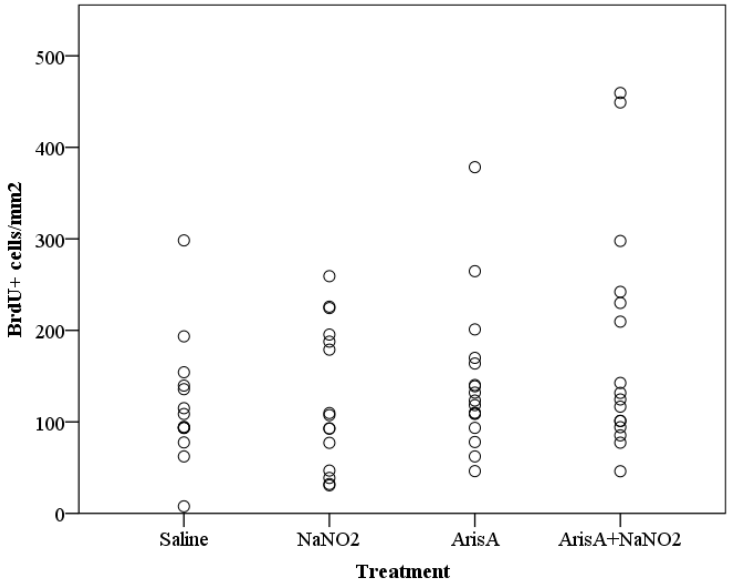


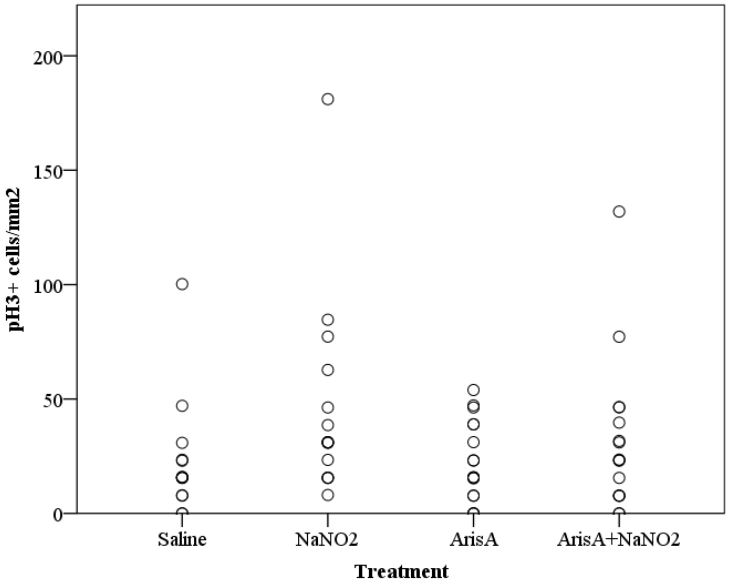
Figure 5. 7 Representative images of BrdU and pH3 labelling in 48-hour kidneys.

Representative areas of renal cortex labelled with BrdU and pH3 were displayed for (A-C) saline (n = 14), (D-F) $NaNO_2$ (n = 16), (G-I) ArisA (n = 17) and (J-L) ArisA+$NaNO_2$ (n = 16) treated mice. Magnification, x20; scale bar = 100 μm. Three randomly chosen fields per slide for all animals were obtained.

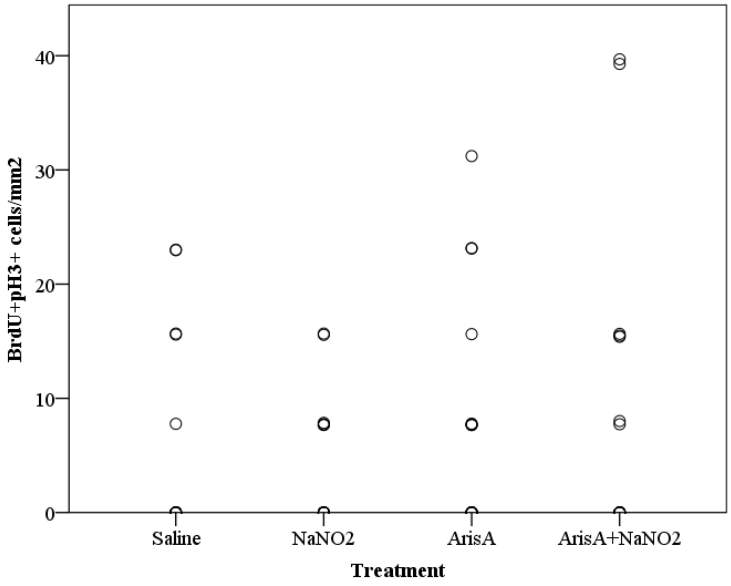
A



B



C



D

Cortex	Saline (n = 14)	Saline+$NaNO_2$ (n = 16)	ArisA (n = 17)	ArisA+$NaNO_2$ (n = 16)
BrdU+cells/mm^2	119 ± 18	497 ± 371	143 ± 19	181 ± 31
pH3+cells/mm^2	22 ± 6	98 ± 53	22 ± 4	32 ± 8
BrdU+pH3+cells/mm^2	6 ± 2	58 ± 54	7 ± 2	8 ± 3

Figure 5. 8 Quantification of BrdU and pH3 positive cell number in cortex.

Dot-plots represented the (A) BrdU+ cell number, (B) pH3+ cell number and (C) BrdU+ and pH3+ cell number per mm^2 kidney area in saline (n = 14), $NaNO_2$ (n = 16), ArisA (n = 17) and ArisA+$NaNO_2$ (n = 16) treated mice. Each dot (an average of three areas per slide) represented the positive cell number per mm^2 of each animal. (D) The table displayed mean values for the positive cell number/mm^2 of each treatment group.

5.2.4 Effects of sodium nitrite on renal gene expression in ArisA-induced AKI

While there were only a few proliferative cells observed, we still intended to examine whether gene expression may be affected by treatments. Here we assessed the renal gene expression in 48-hour kidneys, as 35-day kidneys were unavailable. To examine whether ingestion of nitrite could increase tissue nitrite levels and subsequently become a ready source for NO production, the expression of iNOS and eNOS was assessed. However, there were no differences between treatments (Figure 5.9 A and B; Table 5.1). Since ArisA-induced nephrotoxicity has been found to be associated with the increase in oxidative stress, we examined the expression of NADPH oxidases, particularly NOX-2 and NOX-4, known as the major source of ROS production in kidneys. However, there were no significant differences in *Cyba* and *Cybb* (alpha and bata chain of NOX-2) and *Nox4* expression between treatments (Figure 5.9 C-E; Table 5.1). KIM-1 has been characterised as an ideal biomarker for diagnosis of AKI and CKD. Its upregulation has been observed, particularly in the proximal tubules, after injury compared with normal kidney. However, there were no significant differences between treatments in our model (Figure 5.9 F). Although the expression appeared to be slightly higher in ArisA treated mice compared with that in saline group (Table 5.1), this was mainly due to the outliers which could not represent the responses of the whole population to ArisA.

Moreover, we assessed several fibrosis markers including *Tgfb1*, *Ctgf*, *Col1A1*, *Col4A1* and *Vim* expression to investigate whether these might be upregulated in response to injury, since Yang et al. (2010) showed that these fibrotic molecules were largely secreted by HK-2 cells in response to ArisA-induced nephrotoxicity.

However, such observations might not be shown in *in-vivo* in which fibrosis normally occurs at the chronic phase. Additionally, if there was no acute injury induced in our model fibrosis would not occur, as fibrosis is known as an uncontrolled inflammation and maladaptive repairing process. Overall, the results showed that there were no significant differences between treatments (Figure 5.10; Table 5.1).

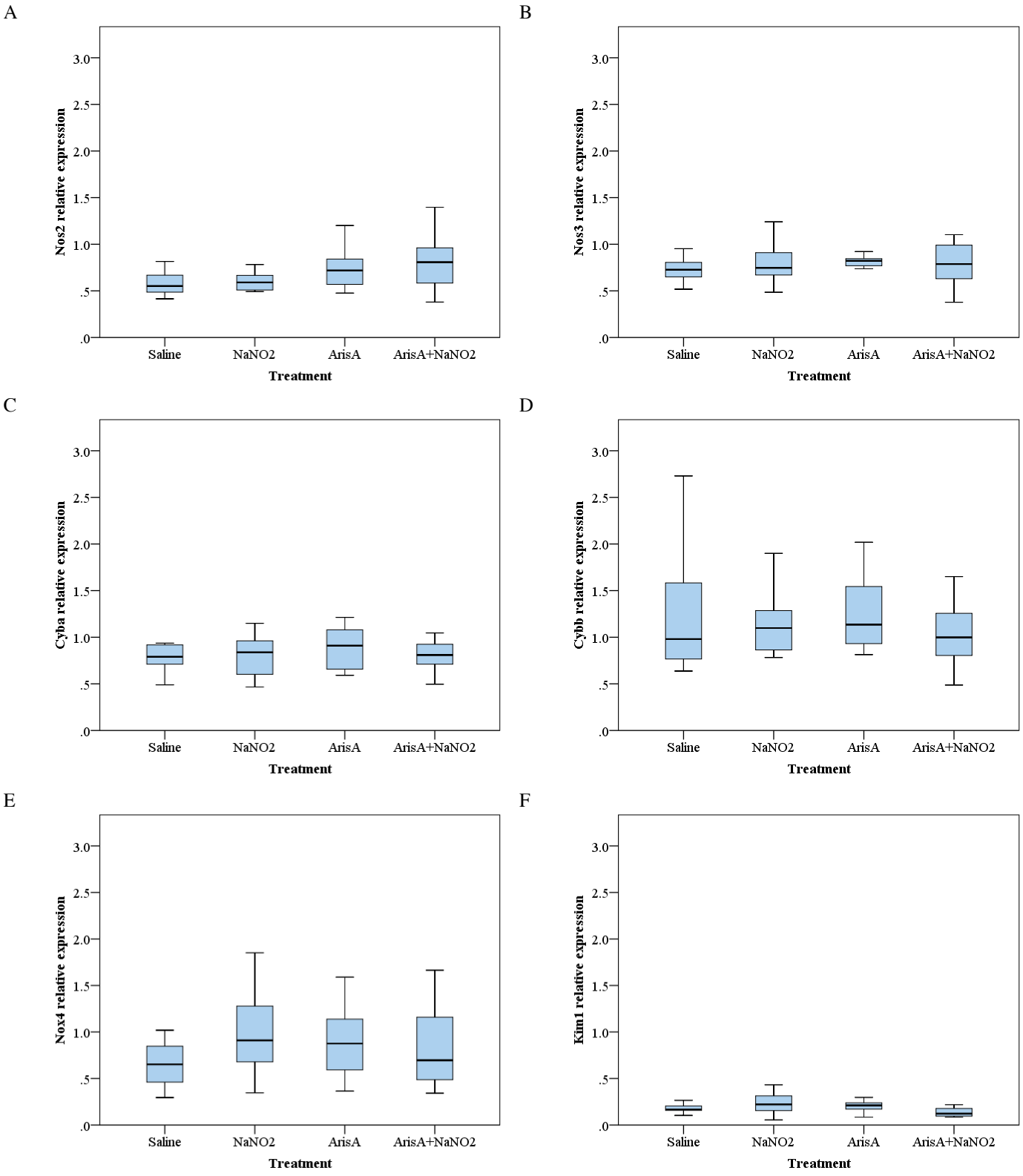


Figure 5. 9 Effects of treatments on renal gene expression in 48-hour kidneys.

Gene expression was examined using qRT-PCR. Quantification of (A) *Nos2*, (B) *Nos3*, (C) *Cyba*, (D) *Cybb*, (E) *Nox4* and (F) *Kim1* expression was normalised against *Tbp*. The box-plots displayed means ± SEM for gene expression in saline (n = 14), $NaNO_2$ (n = 16), ArisA (n = 17) and ArisA+$NaNO_2$ (n = 16) treated mice.

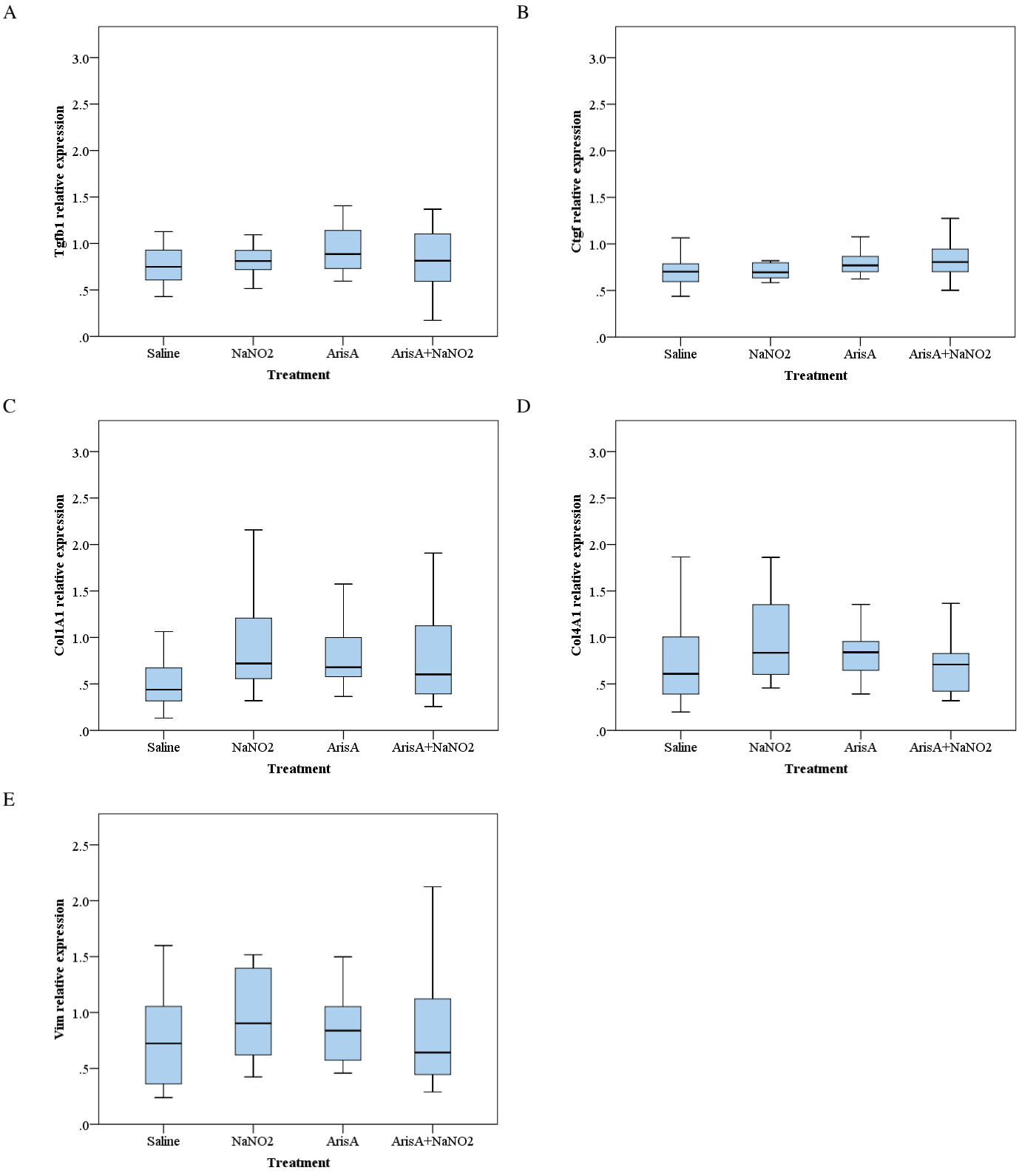


Figure 5. 10 Effects of treatments on renal gene expression in 48-hour kidneys.

Gene expression was examined using qRT-PCR. Quantification of (A) *Tgfb1* (B) *Ctgf*, (C) *Col1A1*, (D) *Col4A1* and (E) *Vim* expression was normalised against *Tbp*. The box-plots displayed means ± SEM for gene expression in saline (n = 14), $NaNO_2$ (n = 16), ArisA (n = 17) and ArisA+$NaNO_2$ (n = 16) treated mice.

Table 5. 1 Effects of sodium nitrite on gene expression in 48-hour kidneys.

	Saline (n = 14)	$NaNO_2$ (n = 16)	ArisA (n = 17)	ArisA+$NaNO_2$ (n = 16)
Nos2	1.00 ± 0.07	0.99 ± 0.09	1.11 ± 0.09	1.16 ± 0.10
Nos3	1.00 ± 0.06	1.05 ± 0.07	1.08 ± 0.06	1.06 ± 0.08
Cyba	1.00 ± 0.07	0.98 ± 0.07	1.07 ± 0.07	0.96 ± 0.05
Cybb	1.00 ± 0.17	0.94 ± 0.07	1.13 ± 0.09	0.92 ± 0.09
Nox4	1.00 ± 0.14	1.15 ± 0.13	1.17 ± 0.15	0.96 ± 0.12
Kim1	1.00 ± 0.65	0.61 ± 0.32	1.53 ± 0.98	0.60 ± 0.27
Tgfb1	1.00 ± 0.09	1.01 ± 0.08	1.20 ± 0.01	1.03 ± 0.05
Ctgf	1.00 ± 0.06	1.09 ± 0.13	0.98 ± 0.06	1.00 ± 0.07
Col1A1	1.00 ± 0.16	1.25 ± 0.20	1.22 ± 0.17	1.30 ± 0.25
Col4A1	1.00 ± 0.14	1.20 ± 0.16	1.26 ± 0.21	1.01 ± 0.15
Vim	1.00 ± 0.12	1.22 ± 0.14	1.30 ± 0.22	1.07 ± 0.16

Gene expression in saline, $NaNO_2$, ArisA and ArisA+$NaNO_2$ treated mice were quantified. Data were presented as means ± SEM and fold change compared with saline. Statistical analyses were performed using an Unbalanced ANOVA.

5.3 Conclusion

It has been shown that ArisA-induced nephrotoxicity is characterised by the early phase of acute injury (within 1-5 days) and the progressive interstitial fibrosis at the chronic phase (after 2-5 weeks) in experimental models (Pozdzik et al., 2008; Yang et al., 2010; Declèves et al., 2016). This thesis intended to develop AKI and interstitial fibrosis in mice by administration of ArisA and to investigate whether dietary sodium nitrite supplemented in drinking water could prevent from the development of AKI and chronic interstitial fibrosis.

It has been demonstrated that renal cell apoptosis and cell cycle arrest induced by a daily injection of 2.5 mg/kg ArisA for 4 days (Declèves et al., 2016) or one-time injection of 5 or 10 mg/kg ArisA could be observed within 1-5 days (Pozdzik et al., 2008; Yang et al., 2010). This chapter also induced AKI by one-time injection of

ArisA at a dose of 5 mg/kg. This was adopted from the study by Yang et al. (2010) as the authors showed that one-time intraperitoneal injection of ArisA resulted in the G2/M cell cycle arrest, evidenced by the observation of BrdU and pH3 co-localisation within 12 hours. The authors also observed an obvious interstitial fibrosis in Masson's trichrome stain, with an upregulation of numerous fibrosis markers including *Tgfb1*, *Ctgf*, *Col1A1* and *Col4A1* on day 42. However, our data did not show any obvious abnormalities in kidney structure and any signs of damage or cell death induced by ArisA in H&E stain in both 48-hour and 35-day kidneys. There were also no abnormalities in interstitial areas and no positive staining of Masson's trichrome in 35-day kidneys, and the quantitative analysis of the positive blue/green stained areas showed no differences between treatment groups. Furthermore, only a few proliferative cells in the cortex in all treatment groups were observed in 48-kidneys labelled with BrdU and pH3, and there were no differences in the BrdU+ and pH3+ cell number in all cases and no co-localisation of BrdU and pH3. This suggested that ArisA did not successfully induce injury in this model.

Although there were no structural damage and proliferative cells observed, this chapter still examined whether gene expression in 48-hour kidneys might be affected by treatments. The expressions of NOS genes including *Nos2* (iNOS) and *Nos3* (eNOS) were first assessed to investigate whether the ingestion of sodium nitrite may increase NOS gene expression which is correlated to the increased NO production. However, there were no significant differences in all cases. The measurement of plasma and kidney nitrite levels would be necessary to confirm such results since it is known that dietary nitrite is readily absorbed and distributed in most tissues and reaches up to 98% nitrite bioavailability within 1 hour after ingestion (Bryan et al., 2005; Hunault et al., 2009).

Furthermore, ArisA-induced AKI has been found to be associated with an increase in ROS production in both *in-vitro* and *in-vivo* models (Pozdzik et al., 2008; Yu et al., 2011; Zhu et al., 2012; Romanov et al., 2015; Declèves et al., 2016), with NOX-2 and NOX-4 being the major source of ROS in renal tubular cells in the cortex (Geiszt et al., 2000; Shiose et al., 2001; Vaziri et al., 2003; Adler and Huang, 2004). However, the data here showed no significant differences in *Nox2* and *Nox4* in all cases. Nevertheless, nephrotoxic drugs could still contribute to a certain level of ROS production which was not measured here, since Declèves et al. (2016) observed high levels of H_2O_2 in the urine and plasma in ArisA treated mice. The expression of the tubular injury marker *Kim1* was assessed, but no differences were found between treatment groups.

The study by Yang et al. (2010) showed that HK-2 cells largely secreted fibrotic factors such as TGFB-1 and collagen into media following treatment with ArisA for 48 hours. Hence, this chapter intended to investigate whether fibrosis markers including *Tgfb1* and *Ctgf* (profibrotic factors), *Col1A1* and *Col4A1* (markers of excessive ECM production) and *Vim* (an indicator of transition of epithelial cells to mesenchymal cells) might have a subtle change in response to treatments. It may be inappropriate to assess fibrosis at such an early phase of injury, as fibrosis normally occurs at the chronic phase. Overall, there were no differences in these genes between treatments. Since fibrosis is characterised by a persistent inflammation and an uncontrolled repairing process, it was not surprising that there were no changes in these genes as ArisA did not successfully induce injury.

The findings here were unable to determine the efficacy of sodium nitrite for the treatment of AKI, since ArisA did not induce any damage in this mouse model. The

model lack of apparent damage in response to ArisA in this chapter could be due to the ICR outbred female mice, which differed from the published studies mostly using inbred male mice (Pozdzik et al., 2008; Yang et al., 2010; Declèves et al., 2016). The purpose of selecting female animals as experimental models was to avoid any overt renal damage shown in male animals, since female animals have been known to be more resistant to AKI compared with males (Park et al., 2004). The use of outbred strain was due to its genetic heterogeneity which is closely relevant to human (Festing, 2010). However, such a model resulted in a lack of sensitivity to injury. The high resistance to AKI and toxicity and false negative and unstable results seemed to be the common issues when using female and outbred animals (Park et al., 2004; Festing, 2010), which was the reason that inbred male animals were mostly preferred as an experimental model in renal research. Nevertheless, it remains unknown whether these treatments contribute to a long-term damage (e.g. mice left for one year after treatments), as mice were only left for 35 days maximum.

Chapter 6: Discussion

Chapter 6: Discussion

6.1 The detrimental effects of amino acids on HK-2 cells following simulated I/R injury

After ischaemia, the return of nutrient supply and oxygen are thought to be crucial for renal recovery. However, it is has been known that the prompt restoration of these components normally leads to a further damage. The presence of nutrients and oxygen drives mitochondrial respiratory reaction to synthesise ATP, and meanwhile this causes a rapid ROS and reactive nitrogen species generation that overwhelms cellular recovery process (Chamoun et al., 2000; Yazihan and Kavas, 2010). Likewise, this thesis showed a substantial cell death with increasing concentration of amino acids in the presence of H_2O_2 after nutrient deprivation. In addition to the return of nutrients and oxygen, other factors including the prompt return of pH to physiological levels and calcium overload in mitochondria have also been proposed to mediate the lethal cell injury after I/R injury (Halestrap, Clarke and Javadov, 2004).

Since 1988 accumulated studies have observed that maintaining acidosis during reperfusion after ischaemic insults could attenuate cell death in various cell types including liver, heart and kidney cells. A previous study by Gores et al. (1988) found that prompt recovery of pH during reperfusion led to an abrupt increase in cell death whereas performing hypoxia at pH 6.0 or reperfusion at pH 6.8 reversed the outcomes in the primary culture of rat hepatocytes. Currin and colleagues (1991) also showed that a rapid return to physiological pH (from pH 6.1 to 7.3) during reoxygenation rapidly increased LDH release. The authors observed that reperfusion

at acidic pH after ischaemia and slow pH return (by slow pH adjustment over 15 minutes during reperfusion) showed no release and reduced LDH release by over 5 fold, respectively. Weinberg and colleagues (1994) indicated that renal I/R injury was ameliorated by the extracellular acidosis (pH 6.9) in the primary culture of rabbit proximal tubule cells. Furthermore, Zhang and Lemasters (2013) investigated the mechanism in the primary culture of the rat hepatocytes. The authors proposed that during ischemia ATP depletion inhibited V-ATPase and subsequently caused lysosomal alkalisation, which releases Fe^{2+} from lysosome to cytoplasm. The translocation of Fe^{2+} into mitochondria through mitochondrial calcium uniporters and participated in the hydroxyl free radical generation through the Fenton reaction upon reperfusion. This resulted in MPTP opening and cell death. The authors also clarify that MPTP-dependent cell death does not occur during ischaemia as it requires the return of oxygen and normal intracellular pH for restoring mitochondrial respiration where ROS is generated. Collectively, these studies indicate that the deleterious effect of reperfusion requires Ca^{2+} and Fe^{2+} overload in mitochondria (via disturbed ionic homeostasis), the prompt return of intracellular pH to physiological levels and subsequent ROS production. Yet, maintaining acidosis (pH < 7.0) during reperfusion may attenuate such phenomena.

Our results showed that the replenishment of amino acids at both physiological pH and low pH exacerbated H_2O_2 damage following nutrient deprivation. These findings did not display a 'pH shock' phenomenon proposed by previous studies. Rather, this may indicate that the return of amino acids in the presence of H_2O_2 was the key to such damage. Moreover, the data showed that amino acids per se might be able to scavenge ROS in the absence of cells, whilst AAS with H_2O_2 resulted in a tremendous ROS production in the presence of cells. It was proposed that the

detrimental effect of AAS may be due to the formation of amino acid peroxides which were likely to become a second toxic messenger to cells or tissues (Gebicki and Gebicki, 1993), although the mechanism was not yet elucidated.

Additionally, this thesis showed that treatment with AAS in the presence of H_2O_2 following starvation resulted in mitochondrial fragmentation. Frank et al. (2012) indicated that even mild oxidative stress induced by H_2O_2 or rotenone (blocks complex I) can trigger mitochondrial fragmentation in mammalian cells. Furthermore, Jheng et al. (2012) demonstrated that the elevated ROS production observed in C2C12 cells in high glucose and fatty acid medium also led to mitochondrial fragmentation. The authors also observed such a phenomenon in the skeletal muscle tissues from obese mice fed with a high-fat diet. The disruption of mitochondrial dynamics is commonly observed in acute tissue injuries since mitochondria mediate apoptosis and necrosis. Studies have reported that mitochondrial fragmentation is a common event in ischaemic models of heart (Ong et al., 2010), brain (Zhao et al., 2014) and kidney (Gall et al., 2012). Brooks et al. (2009) showed that mitochondrial fission occurred in mice subjected to 30 minutes of bilateral renal ischemia followed by 15 minutes of reperfusion and in renal proximal tubular cells after azide-induced ATP depletion or cisplatin-induced nephrotoxicity. This thesis could not confirm whether there were any differences in mitochondrial morphology between 0x, 0.5x and 1x AAS in the presence of H_2O_2 as all appeared to be fragmented, as the analysis of mitochondrial length requires higher power images from confocal microscope. Nevertheless, our results may suggest that H_2O_2 induced a certain level of oxidative stress in mitochondria. The Mitotracker Red was used to observe the mitochondrial morphology, with the initial intention of measuring the mitochondrial membrane potential. Other mitochondrial membrane

potential assay reagents such as TMRE could be an alternative option, but the detection requires the flow cytometry or the live cell imaging. By contrast, live cells labelled with Mitotracker Red could be detected with a plate reader or could be imaged after fixation. This thesis previously used a plate reader to detect the fluorescence to measure the mitochondrial membrane potential, but no signal was detected (data not shown). Therefore, we only presented some representative images of mitochondrial morphologies here. One field per slide and three slides per treatment group were obtained, but it could be argued to be less generalisable. More fields are required for quantifying the changes in mitochondrial morphology. For example, quantifying the length of mitochondria for structural changes (such as tubulation and fragmentation) or the number of cells with tubular and fragmented mitochondria. Also, the microscope setting occasionally altered for exposure time in some samples was not ideal for analysis.

Moreover, unlike other studies the data in this thesis did not show any protective effects of acidic pH (pH 6.4 and 3.8) against H_2O_2 after starvation. Instead, AAS at pH 6.4 exacerbated H_2O_2 damage, and there was no cell viability and cytoskeleton observed in cells treated with AAS at pH 3.8 although cells remained attached. Such different results could be due to the use of immortalised HK-2 cell line and induction of oxidative stress using exogenous H_2O_2 in this thesis. The published literature showing the protection of acidic pH mostly used primary cells isolated from animal tissues, *ex-vivo* or animal models. These models were more biologically relevant and relatively susceptible to experimental I/R injury, for instance, an ATP depletion and cell death could be readily achieved by hypoxia (1% O_2)/reoxygenation (21% O_2) without exogenous H_2O_2. In this thesis, the simulated I/R injury in HK-2 cells was carried out by starvation in normoxia (21% O_2) followed by resupply of AAS in the

presence of H_2O_2 in normoxia, as starvation in hypoxia did not influence the mitochondrial function in HK-2 cells. However, nutrient deprivation in normoxia and the exogenous H_2O_2 could not entirely mimic I/R injury in the *in-vivo* condition. Our model only allowed the investigation of the cellular responses to amino acids under oxidant injury following nutrient deprivation. The induction of I/R protocol which differed from the literature was potentially the reason that acidic pH did not exert any protection, since the cytoprotection afforded by acidic pH was mainly shown in hypoxia/reoxygenation models. Additionally, it has been reported that the immortalised HK-2 cells to serve as an *in-vitro* system was not suitable as they did not express some common *in-vivo* biomarkers such as kidney injury molecule-1 (Huang et al., 2015). Therefore, the current commercially available primary cell line, human renal proximal tubular epithelial cells (hRPTECs), would be an alternative option for future study.

While acidic pH (<7.0) may attenuate the lethal cell injury after I/R injury as indicated in numerous studies (Gores et al., 1988; Shanley et al., 1988; Gores et al., 1989; Currin et al., 1991; Nishimura, Romer and Lemasters, 1998), the recovery of cell morphology and long-term consequences may be overlooked as these studies demonstrated the protection based on short term LDH release assay (ranging from 10 minutes to 6 hours). The irreversible cell morphological alterations, cytoskeletal disruption and ATP depletion were only reported by Shanley et al. (1988), Nishimura and colleagues (1998) and Gores et al. (1989). Shanley et al. (1988) and Nishimura and colleagues (1998) reported that the cytoskeletal disruption and ATP depletion caused by hypoxic injury in the isolated rat kidneys and rat sinusoidal endothelial cells did not recover by acidic pH (pH 6.8 and pH 6.2, respectively) during reperfusion and eventually led to sublethal injury. Moreover, Gores et al. (1989)

continued their previous study in 1988 and found that acidic pHi was unable to inhibit the formation of cell blebs which are common morphological changes occurring in early liver injury. Likewise, our data showed that F-actin was disrupted at pH 6.4 and completely diminished at pH 3.8. Furthermore, the increase in AAS in the presence of H_2O_2 at all pH (from physiological pH to pH 3.8) resulted in a substantial death after starvation, suggesting that the provision of AAS exacerbated H_2O_2 damage after starvation. In addition, this thesis confirmed that such deleterious effects of AAS at physiological and low pH on HK-2 cells following simulated I/R and nutrient depletion/replenishment injury were independent of several factors including osmolality, vitamins and buffering systems (data not shown). The osmolality for all treatments ranged between 260-330 mOsm/kg which cells can endure in the culture system since the osmolality was higher in normal growth media (331 mOsm/kg). We examined whether restoration of vitamin supply as a source of antioxidants in AAS might protect from H_2O_2 mediated damage, but it did not influence the mitochondrial functional responses to AAS (data not shown). Further, we investigated whether buffering systems in reperfusion media might lead to different results in this thesis compared with the published literature which showed that pH paradox during reperfusion was detrimental and could be prevented by acidic infusion. The differences in experimental procedures between this thesis and the published work were the induction of I/R injury protocol and the buffering systems in the reperfusion media. Given that the use of exogenous H_2O_2 to induce oxidant injury was inevitable as hypoxia/reoxygenation did not exhibit any effects on HK-2 cells here, the buffering systems in the reperfusion media could be manipulated to be identical to the literature. Most studies prepared the media in bicarbonate HEPES solution, whereas HBSS used in our system did not contain any Good's buffers

which prevent media pH fluctuation during incubation. In fact, we measured the media pH after overnight incubation using a pH meter and found that AAS at pH 7.5 and pH 6.4 prepared in HBSS declined a little down to pH ~6.6 and ~6.3 respectively. In order to maintain pH constant during the overnight incubation, the Good's buffers including HEPES and MES were included and tested to ensure that these results were not influenced by the drifting pH. We found that MES buffer at pH 6.4 was detrimental to cells (data not shown). This may be the reason that the published studies still used HEPES for buffering pH < 6.8, even if HEPES buffering range is between pH 6.8-8.2. We further found that the buffering system might influence the results as the negative linear trend between AAS (pH 7.5) and mitochondrial function was slightly attenuated in the HEPES buffering system. However, the trend still strongly remained negative. Nevertheless, it might be necessary to include HEPES in the media to prevent from pH fluctuation.

While MTT assay was used throughout chapter 3, it is important to note that MTT assay indirectly measures the viable cell number by detecting the mitochondrial function. Several limitations of MTT assay for measuring cell viability have been reported. For instance, the amount of signal detected depends on the cell metabolic activity as MTT measures the activity of mitochondria enzyme, NADPH dependent cellular oxidoreductase (Riss et al., 2013). The culture condition such as nutrient deprivation, the use of phytochemicals and the utility of cell line with lower metabolic activity can reduce MTT signals (Riss et al., 2013), but such results may not correlate to the cell viability. Another disadvantage of MTT assay is that it is an end point measurement and cannot be used for the time-course study. The signals are dependent on the MTT concentration and incubation time, and the results may vary in each experiment.

The disadvantages of MTT assay can be resolved by other commonly used cell viability assays including trypan blue, propidium iodine, LDH release assay and calcein AM. While these methods have the advantage of excluding viable cells from dead cells, some are costly and require cell counting which is time-consuming and often generates large variations in the results, high content imaging or flow cytometry for an accurate quantitative analysis. Another method using seahorse XF assay may be advantageous as it allows a series of real-time metabolic analysis on mitochondrial function in response to oxidative stress by measuring oxygen consumption rate, glycolysis and oxidative phosphorylation, proton leak (extracellular acidification) and ROS production. Also, after metabolic measurement the cell lysates can be used for western blotting. The most important of all, the results from seahorse assay have a high reproducibility within and across experiments (Dranka et al., 2011). The most disadvantage of this assay is that it requires a series of validation such as testing of cell lines and media and reagent concentration for the experimental protocol, as these factors can lead to under or overestimated metabolic profiles (Dranka et al., 2011). Nevertheless, it is a suitable alternative for our study. Compared with these methods, MTT assay is simpler, inexpensive and efficient for investigating single cell line, HK-2 cells which are highly metabolically active, in our study. This thesis also included the calcein assay with an intention to confirm the MTT results. A flow cytometry to detect the fluorescence signal in viable cells would be ideal, but it was not performed here due to the restricted access to the facility. Alternatively a plate reader was used, and the results were similar to MTT assay. However, there were large variations in the data (data not shown). Hence, this thesis only showed the representative images for each treatment group. One field per slide and three slides per treatment group were performed for triplicates, but this may be

argued to be biased and less generalisable. More fields per slide are required for quantitative analysis, and staining with DAPI may be required for quantifying viable cell number per total cell number. These issues may limit the interpretation of the results. Moreover, there was an issue of the assessment on filamentous actin cytoskeleton. The over confluent cell population in the experiments and a cell loss in some treatment groups made it difficult to make a comparison between treatments. Additionally, this thesis could not quantify the number of cells with cytoplasmic or cortical stress fibres, as the representative images of filamentous actin cytoskeleton were obtained from one field per slide and three slides per treatment group. More fields (10-30 fields) are required from each sample for analysis.

Taken together, this chapter showed that the prompt provision of AAS at a physiological or acidic pH was detrimental to HK-2 cell recovery from simulated I/R and D/R injury. However, there were other factors that may lead to these results. It might be the case that the immortalised HK-2 cell line was unsuitable, although it has been suggested as an appropriate and relevant *in-vitro* model for examining human renal disease (Ryan et al., 1994). A large-scale activation of ROS from the provision of H_2O_2 perhaps leads to the oxidation of amino acids to form more potent ROS. These findings may imply that not only the restoration of pHi but also the prompt return of circulating nutrients (particularly free amino acids) under oxidative stress was deleterious to kidney recovery from I/R injury.

6.2 Cellular responses to amino acids during oxidative stress following nutrient deprivation

Ischaemia/nutrient deprivation may result in oxidative stress accumulation in the metabolic organelles such as mitochondria and the ER, but cells may adapt and survive through the stress by attenuating protein synthesis and cell growth through the inhibition of mTOR (Reiling and Sabatini, 2006) or by activation of adaptive UPR pathways. The principle of these pathways is to limit the protein synthesis, subsequently reducing the oxidatively damaged protein load in the ER. Upon reperfusion, the return of nutrients activates mTOR signalling pathways for renal regeneration; however, the presence of ROS interferes with protein disulfide bonding (Inagi, 2009). When under an oxidising condition, the ER becomes more prone to oxidation (Van der Vlies et al., 2003; Chakravarthi, Jessop and Bulleid, 2006; Malhotra and Kaufman, 2007). Although this oxidising environment promotes protein disulfide bond formation, it also increases disulfide bond mispairing and unfolded protein accumulation due to the ER disulfide isomerase hyperoxidation/inactivation that decreases protein folding capacity (Van der Vlies et al., 2003; Chakravarthi and Bulleid, 2004; Molteni et al., 2004). The accumulation of these damaged proteins subsequently leads to ER stress (Inagi, 2009). In response to ER stress, UPR is activated in order to enhance the protein refolding capacity by upregulating chaperone proteins, to reduce the protein synthesis transnationally and transcriptionally and to increase misfolded protein degradation (Reiling and Sabatini, 2006).

In chapter 3, the data showed the detrimental effect of amino acid supplementation at both pH 7.5 and 6.4 in H_2O_2 induced oxidative damage following starvation. In

chapter 4, it was further investigated whether the provision of amino acids under oxidative damage exacerbating cell death was due to the activation of mTOR increasing protein synthesis and causing misfolded protein overload in the ER. The results showed that 0x AAS in the presence or absence of H_2O_2 attenuated activity of mTOR downstream proteins including pS6K and pS6. In contrast, the replenishment of amino acids at pH 7.5 in the presence of H_2O_2 after starvation activated mTOR signalling pathways as evidenced by the increase in pS6K and pS6 expression. The level of activation was found to solely respond to AAS concentration, independent of H_2O_2. It was surprising that the concentration of H_2O_2 used in this study did not inhibit the mTOR signalling pathways. In fact, ROS was found to stimulate or inactivate mTOR signalling pathways, depending on the cell types, H_2O_2 concentration and the exposure time (Li et al., 2010). For instance, a study by Zhang et al. (2009) showed that in adenocarcinomic human alveolar basal epithelial cells and bovine aortic smooth muscle cells, pre-exposure to 0.25 mM H_2O_2 for 15 minutes significantly decreased the mTOR activation induced by insulin and leucine within 30 minutes. Another study also demonstrated that two hours of exposure to 0.5 mM and 0.7 mM H_2O_2 inhibited mTOR activity through the activation of AMPK pathways in both PC12 neuron cells and primary murine neurons (Chen et al., 2010). In addition, Li et al. (2010) investigated mTOR activity in a variety of cell lines exposed to H_2O_2 and showed that the increase in H_2O_2 concentration or the exposure time stimulated mTOR whilst low dose of H_2O_2 (e.g. <0.5mM in HEK 293 cells; <0.05 mM in MC-3T3-E1 cells for 30 minutes) activated mTOR activity. However, the authors found that *in-vivo* injection of ROS-inducing drugs in fact stimulated mTOR activity in all tissues including brain, heart, liver, kidney and muscle. Hence, the level of H_2O_2-induced oxidative stress in this study could be biologically relevant

to the *in-vivo* condition, and it would be necessary to assess whether mTOR was still active after a longer exposure to AAS in the presence of H_2O_2.

Furthermore, the mTORC1 activation by amino acids was proposed to be associated with their translocation to lysosomes (Sancak et al., 2010; Zoncu et al., 2011). Other proposals suggested that mTOR activation could also be involved in other organelles including mitochondria and the ER (Betz and Hall, 2013). The mechanism is not yet fully understood. It was observed that the active mTOR occasionally co-localised with lysosomes in some cells. However, this thesis could not confirm the lysosome-dependent mTOR activation by amino acids due to no negative control performed and only single field per slide and three slides for each treatment obtained. To confirm this, it would be necessary to test whether mTOR activation by amino acids requires TSC1/TSC2 by genetic deletion as shown in the literature (Sancak et al., 2010). Nevertheless, the findings suggested that resupply amino acids following starvation promoted protein synthesis through activation of mTOR signalling.

Since mTOR was activated in an AAS concentration dependent manner following starvation, this thesis further examined whether increasing protein synthesis by AAS under oxidant injury resulted in misfolded protein formation which induced ER stress. This thesis examined chaperone protein Grp78 expression, as it is known as a key regulator of ER stress transducers and is commonly assessed together with three ER transmembrane proteins (e.g. PERK, IRE1 and ATF6) for detecting UPR pathways in the literature. However, due to the cost of assessing all target proteins this thesis first investigated whether ER stress was induced by resupply of amino acids in the presence of H_2O_2 injury after starvation. Assessing this protein only may seem to be limited as expression of Grp78 could be associated with cell survival or

death. For instance, Grp78 has been found to be expressed by tumor cells, and high expression protected tumor cells from death and increased the resistance to chemotherapy (Sato et al., 2010). Also, another study demonstrated that induction of Grp78 expression using ER stress inducer prior to oxidant injury protected from tubular cell death (Chandrika et al., 2015). In other cases, overexpression of Grp78 contributed to drug-induced nephrotoxicity and cell death (Pallet et al., 2008). In our model, Grp78 protein constantly expressed over time, but the pattern of protein expression was inconsistent. That is, it decreased with increasing AAS concentration at 4 hours, but the levels increased with increasing AAS concentration at 24 hours. The constant Grp78 expression could only suggest the cellular stress responses after starvation. Whether such prolonged Grp78 expression was associated with cell death caused by AAS in the presence of H_2O_2 in chapter 3 was still unclear. To confirm the direct link between AAS at pH 7.5 in the presence of H_2O_2 and Grp78 expression that induced UPR mediated cell death, it still requires the detection of UPR-associated apoptosis (e.g. IRE1-ASK1-JNK or PERK-CHOP pathway) and apoptotic factors. Additionally, the link between mTOR activation by AAS in the presence of H_2O_2 and ER stress was not yet identified here. The current methods to confirm such a relationship in the literature were to investigate whether the change in expression of proteins related to mTOR and UPR pathways synchronised at each time point.

The provision of AAS and other nutrients including glucose, insulin and leucine at pH 6.4 following starvation was unable to activate mTOR downstream proteins including pS6 and pS6K within 60 minutes. These findings were consistent with studies by Balgi et al. (2011) and Marino et al. (2012). Marino et al. (2012) suggested that acidic extracellular pH reduced the uptake of amino acids and subsequently activated phosphorylation of AMPK which positively regulated

autophagy and inhibited mTOR in melanoma cells as a mechanism for cancer cell survival in an acidic stress. However, it was unknown whether the incubation in acidic condition reduced amino acid or other nutrient uptake by HK-2 cells. Moreover, in the detection of co-localised mTOR and Lysotracker there was no sign of Lysotracker in this acidic condition. According to anufacturer's manual, Lysotracker is a weak base reagent that probes acidic compartments of a cell. It passively permeates into cells in dependent of pH gradient between extralysosomal and intralysosomal compartments, is attracted to acidic organelles including lysosomes (~pH 5.0) and slightly protonated to retain on the membranes. Hence, no detection of lysosomes at pH 6.4 could indicate i) that extracellular low pH acidified the entire cellular compartments so that lysosomes could not be specifically detected or ii) that low pH caused extracellular and intracellular pH gradient disruption which prevented from Lysotracker's permeability or iii) acidic pH disrupted lysosomal membranes and caused the proteases leakage to cytoplasm and triggered cell death. If mTOR activation in response to amino acids in HK-2 cells required lysosomes and V-ATPase, the decreased intracellular pH due to the incubation in an acidic condition might enhance V-ATPase to pump protons into lysosomes in order to maintain cytosolic pH. This could shift the function of V-ATPase more prone to act as a proton pump rather than to interact with Ragulator to activate mTOR translocation. Also, if cells were unable to take up amino acids in the acidic condition, low or no amino acids transported into lysosomes could cause inactivation of V-ATPase and hence lead to mTOR inactivation. To improve the detection in this acidic system, the antibody probe of lysosomal associated membrane proteins would be an alternative means for further confirmation.

Recently, Crean and colleagues (2013) proposed that acidic pH (pH 6.4) protected against the oxygen and glucose deprivation induced cell death in HK-2 cells by reducing protein synthesis/translation and attenuated UPR-activated pro-apoptosis mediated by ATF6-CHOP signalling pathway. The model used in this thesis showed that acidic pH (pH 6.4) inhibited mTOR activity but still exacerbated cell death upon the replenishment of AAS in the presence of H_2O_2. It was also observed that such an acidic pH inhibited chaperone protein expression responsible for assisting refolding and clearance of damaged proteins in the ER, completely blocking the chance for cell survival under oxidative damage. However, it remains unknown whether inhibition of Grp78 expression linked to cell death caused by acidic pH, as other protein expression such as pS6 and total mTOR was lower or absent at acidic pH. If mTOR inhibition was the key to the cytoprotection against I/R injury, a dietary restriction such as protein and amino acid restriction would provide a safer and simpler strategy rather than acidic infusion. This thesis also observed that mTOR signalling was inactivated in the absence of amino acids after starvation and that treatment with 0x AAS in the presence of H_2O_2 was less detrimental to mitochondrial function compared with the presence of amino acids. However, such link between mTOR inactivation and cytoprotection still remains to be proved, and this could be due to the use of transformed cell line that is more susceptible to injury. Nevertheless, the dietary restriction has been recently demonstrated to protect from I/R injury induced by surgery in the *in-vivo* models (Mitchell et al., 2010; Verweij et al., 2011; Peng et al., 2012; Robertson et al., 2015).

6.3 The effects of sodium nitrite on ArisA-induced AKI

As this thesis could not mimic I/R injury in the HK-2 cell system, an animal model of AKI was adopted here. The widely used method for induction of AKI is the bilateral I/R, which would be more consistent with chapter 3 and 4. However, to achieve the consistent results of AKI using bilateral I/R, it depends on several factors such as selection of animal models and surgery procedures. Although the animal models with high susceptibility to injury could be used to generate a consistent injury, a successful induction of I/R injury still relies on a good surgery protocol and a well-trained skilful surgeon to perform the operation, minimise surgical trauma and postsurgery care (Wei and Dong, 2012). Alternative method to induce AKI is the drug induced nephrotoxicity by clinically used drugs and nephrotoxic compounds, such as cyclosporine, gentamycin, cisplatin, folic acid and ArisA. These drugs can also generate ischaemic insults by interfering renal haemodynamics and cause tubular injury through ATP depletion, ROS generation and mitochondrial damage, similar to I/R injury (Singh et al., 2012). The severity of drug induced AKI is highly dose and time dependent, and it only requires injection with less technical issues compared with bilateral clamping. Among all these commonly used drugs (Table 1.2), ArisA induced AKI has the most advantage, as it has been demonstrated by many studies that one-time injection at a low dose (5-10 mg/kg) could induce an acute injury that could be observed within 1-5 days and interstitial fibrosis at the chronic phase after 2-5 weeks (Pozdzik et al., 2008; Yang et al., 2010; Declèves et al., 2016). Hence, ArisA induced AKI was adopted in this thesis.

ArisA has been shown to mediate renal damage including tubular injury and acute interstitial fibrosis in part through generation of ROS in both *in-vitro* and *in-vivo*

models (Pozdzik et al., 2008; Yu et al., 2011; Zhu et al., 2012; Romanov et al., 2015; Declèves et al., 2016). It has been identified that NADPH oxidases play a crucial role in ROS production in ArisA-induced AKI models (Pleskova et al., 2006; Declèves et al., 2016). We therefore intended to examine whether this could be observed in animals. As accumulated studies showed that ROS generation could be attenuated by NO through downregulation or suppression of NADPH oxidases in heart and kidney (Pleskova et al., 2006; Selemidis et al., 2007; Declèves et al., 2016), we intended to examine whether dietary inorganic sodium nitrite could prevent from renal damage induced by ArisA.

It has been demonstrated that renal cell apoptosis and cell cycle arrest induced by a daily injection of 2.5 mg/kg ArisA for 4 days (Declèves et al., 2016) or one-time injection of 5 or 10 mg/kg ArisA could be observed within 1-5 days (Pozdzik et al., 2008; Yang et al., 2010). This chapter also intended to induce AKI by one-time injection of ArisA at a dose of 5 mg/kg. The dose was adopted from the study by Yang et al. (2010), as the authors showed that it resulted in the G2/M cell cycle arrest evidenced by the observation of BrdU and pH3 co-localisation within 12 hours and an obvious interstitial fibrosis on day 42.

However, in our study there was an absence of overt cell death at any time point after ArisA injection, contrary to the findings of Yang et al. (2010). Similarly there were no differences in the abundance of proliferative cells after ArisA injection. While Yang et al. (2010) observed the correlation between cell cycle arrest in G2/M and fibrosis, ArisA utilised in this thesis did not induce any acute damage or fibrosis. Even if there was a mild fibrosis, Masson's trichrome stain utilised here was unable to specifically identify the positive stain of fibrotic lesions. Since the fast green dye

stains all connective tissues including basement membrane of vessels and glomerular mesangial matrix and basement membrane, these positive stained areas are also included in the quantification analysis. Another issue of Masson's trichrome stain in this thesis was that fast green dye did not display the colour expected in the images; for example, the basement membrane of blood vessels appeared to be blue and grey. Hence, in the quantification of positive stained areas for fibrosis the colour threshold in the ImageJ software was set up based on blood vessels for all images to determine positive stain of all connective tissues. Also, in a few sections the fast green stain was found to appear inside of tubular lumens, and this was perhaps due to the technical issues. Therefore, even if there was a subtle fibrosis in the kidneys, the assessment of fibrosis using Masson's trichrome stain was not specific to identify such changes. Other stain for fibrosis such as PAS and Sirius red may be recommended.

Although there were no structural damage and proliferative cells observed, this thesis still examined whether there might be a subtle change in gene expression in 48-hour kidneys in response to treatments. It is known that NO is the key mediator to the vascular and renal blood pressure regulation (Majid et al., 2001), and low NO bioavailability was found to be related to the increase in oxidative stress (Araujo et al., 2006). The expressions of NOS genes including *Nos2* and *Nos3* were first assessed to investigate whether the ingestion of sodium nitrite may increase NOS gene expressions which correlate to the increased NO production. Theoretically, the increase in NO production is related to the increased NOS gene or total protein expression (Mount and Power, 2006). However, there were no significant differences in all cases. In fact, it has been pointed out by several studies that the correlation between NO synthesis and NOS gene expression was poor in rat, mouse and human

models (Ortiz et al., 2003; Herrera, Silva and Garvin, 2006). This was because NO synthesis is also mediated by post-translational regulation including protein-protein interaction and multi-site phosphorylation (Shaul et al., 2002; Boo and Jo, 2003; Kone et al., 2003; Ortiz et al., 2003). Hence, assessing the metabolic by-products such as the levels of cGMP and nitrate/nitrite in the urine, plasma or kidneys may provide more reliable results.

ArisA-induced AKI was found associated with the increase in ROS production in numerous *in-vitro* and *in-vivo* models (Pozdzik et al., 2008; Yu et al., 2011; Zhu et al., 2012; Romanov et al., 2015; Declèves et al., 2016). The major source of ROS in kidneys are NADPH oxidases, particularly NOX-2 (Vaziri et al., 2003; Adler and Huang, 2004) and NOX-4 (Geiszt et al., 2000; Shiose et al., 2001) were found abundant in renal tubular cells in the cortex. Emerging data has identified the antioxidant property of NO in heart and kidney through downregulation of NADPH oxidases. Selemidis et al. (2007) discovered that NO donor drugs, having been used as the treatment of hypertension and heart diseases, could also suppress NOX-2 and NOX-4 through S-nitrosylation to reduce ROS generation in the human vascular endothelial cells. Pleskova et al. (2006) also demonstrated that NO donor compounds markedly inhibited ROS production through the suppression of NOX-1 mRNA and protein expressions in rat renal mesangial cells. Recently, Declèves et al. (2016) showed that the administration of NO precursor, L-arginine, in drinking water reduced oxidative stress induced by ArisA through downregulation of *Nox2* expression. However, the data here did not show any statistical differences in *Nox2* and *Nox4* expressions in all cases. Nonetheless, ArisA could still contribute to a certain level of ROS production which was not measured here, since Declèves et al. (2016) observed high H_2O_2 levels in the urine and plasma in ArisA treated mice.

Hence, assessing biomarkers in these metabolic waste products would provide more robust data for further confirmation. In addition, the expression of the tubular injury marker *Kim1* was assessed, but no differences were found between treatment groups. This may further confirm that no injury was induced in this animal model, as it has been known that kidney injury molecule-1 was highly upregulated after injury compared with normal kidneys.

As the source of 35-day kidneys was unavailable here, this thesis assessed some fibrosis markers in 48-hour kidneys. It may be inappropriate to assess fibrosis at such an early phase of injury, as fibrosis normally occurs at the chronic phase. The study by Yang et al. (2010) showed that HK-2 cells largely secreted fibrotic factors such as TGFB-1 and collagen into media following treatment with ArisA for 48 hours. Hence, this thesis intended to investigate whether fibrosis markers including *Tgfb1*, *Ctgf*, *Col1A1* and *Col4A1* and *Vim* might be affected by treatments. Overall, there were no differences in these genes between treatments. Since fibrosis is characterised by a persistent inflammation and an uncontrolled repairing process, it was not surprising that there were no changes in these genes as ArisA did not successfully induce injury. While these drugs did not induce apparent structural abnormalities in kidney, it was still unknown whether there were long-term damage consequences of these treatments as mice were only left for 35 days maximum.

Overall, this study was unable to determine the efficacy of sodium nitrite for the treatment of AKI, since ArisA did not induce any damage in this mouse model. The model lack of sensitivity to ArisA-induced nephrotoxicity could be due to the utility of ICR outbred female mice, compared with the published studies using inbred male mice (Pozdzik et al., 2008; Yang et al., 2010; Declèves et al., 2016). The male

animals have been known to be more susceptible to AKI due to the sex hormones, and hence males are preferred in the renal research as their response to injury is consistent. Inbred strains are preferably and widely used because they are more homogenous, reproducible and genetically stable for producing robust dose-response relationships in toxicological research than outbred stocks, although they are more susceptible to toxicity and often have various spontaneous diseases (Festing, 2010). The initial intention of selecting female animals as an experimental model was to avoid any overt renal damage shown in the literature and allow recovery by dietary intervention, since female animals have been known to be more resistant to AKI compared with males (Park et al., 2004). The use of outbred strain was due to its diverse genetic backgrounds, which is closely relevant to human (Festing, 2010). However, this experimental model resulted in a lack of sensitivity to toxicity. The selection of such experimental model might not be an overall issue of the study, and this could be resolved if a pilot study was performed before the experimental trial.

Chapter 7: Conclusion

Chapter 7: Conclusion

Renal tubular cell attachment/detachment is a common consequence in the cellular pathophysiology of AKI. Ischaemia normally causes the actin cytoskeletal alterations including the rapid loss of cyoskeletal integrity and cell polarity and the disruption of cell-matrix adhesions, subsequently leading to cell death via apoptosis or necrosis if the injury is prolonged (Bacallao et al., 1994; Molitoris, 2004; Bonventre and Yang, 2011). However, the most catastrophic damage normally occurs during reperfusion rather than ischaemia due to the restoration of oxygen leading to a burst of free radical production and the prompt elevated pH that induces MPTP opening, which triggers mitochondrial mediated cell death (Sharfuddin and Molitoris, 2008). Many studies have suggested that maintaining acidosis during reperfusion may inhibit MPTP opening and attenuate cell death. In addition to this, the relationship between renal I/R injury and mTOR signalling pathways and ER stress has been recognised in recent years. The marked activation of mTOR plays a critical role in kidney regeneration and functional recovery after I/R injury. However, the activation of mTOR in response to a sudden return of nutrients and growth factors has also been found to induce ER stress (Inagi, 2009). Under oxidative stress, the newly synthesised proteins can be misfolded due to the interference with disulfide bonding by ROS, leading to ER stress. Under such a circumstance, enhancing protein synthesis could possibly impair the ER functions in terms of processing and clearance of damaged proteins.

The findings in this thesis showed that after starvation the return of amino acids at pH 7.5 in the presence of H_2O_2 induced a substantial cell death with an increase in AAS concentration. Resupply of amino acids in the presence of H_2O_2 also increased

ROS production in the presence of cells, whilst amino acids could possibly possess antioxidant properties in the absence of cells. The mitochondrial fragmentation may also indicate oxidative stress induced by H_2O_2. After starvation, the replenishment of amino acids at pH 7.5 in the presence of H_2O_2 exacerbated mitochondrial dysfunction in an AAS concentration dependent manner. The mTOR signalling was found to be activated in response to amino acids, and the activation level positively correlated to AAS concentration. Its activation was not influenced by the presence of H_2O_2. This suggested that the return of amino acids promoted protein synthesis through mTOR signalling following starvation even if under oxidant injury. The further hypothesis following this finding was that the newly synthesised proteins may be oxidatively damaged and accumulate in the ER and induce ER stress and cell death. To test this, this thesis detected the chaperone protein Grp78 expression, since Grp78 is known as a key regulator of the three transmembrane proteins including PERK, IRE1 and ATF6 for activation of UPR pathways. The Grp78 was found to express over time after all treatments following starvation, and hence its expression could only suggest the constant cellular stress following starvation. These findings were unable to identify the link between the activation of mTOR by amino acids (pH 7.5) under H_2O_2 damage following starvation and ER stress leading to cell death. This still requires the detection of three transmembrane proteins for activation of UPR pathways.

Additionally, a range of low pH (pH 6.8-3.8) was examined, but this thesis did not show any cytoprotection against H_2O_2 damage following starvation. In fact, the replenishment of AAS at acidic pH exacerbated the F-actin disruption and lethal cell injury in the presence of H_2O_2 following starvation. Although resupply of amino acids at acidic pH (pH 6.4) was unable to activate mTOR signalling and could

attenuate global protein synthesis, it also inhibited protective chaperone protein expression and potentially blocked the chance for cell survival through oxidative stress. However, again the link between inhibition of Grp78 and cell death caused by acidic pH was unanswered. In general, it seems that acidic pH negatively affect protein synthesis; for example, we also observed a lower total mTOR level at acidic pH (pH 6.4) compared with that at pH 7.5.

Taken together, these findings may suggest that the rapid return of circulating nutrients (e.g. free amino acids) is detrimental for the renal proximal tubular cell recovery from I/R injury. The activation of mTOR signalling by amino acids promoted protein synthesis even if under oxidative damage, but the link between mTOR activation by amino acids under oxidant injury and ER stress was not yet determined in this thesis. Furthermore, acidic pH to serve as a renoprotective strategy still faces challenges. Although its effectiveness has been shown mostly in *in-vitro* or *ex-vivo* studies, the direct acidic infusion has not yet been applied in any *in-vivo* models. Such strategy still requires the identification of controlling the optimal pH, time-window and long-term health risk.

As this thesis was unable to induce a previously compromised system using HK-2 cell system, an AKI model in mice was established. This thesis investigated the therapeutic properties of another nutrient, sodium nitrite, on the ArisA-induced AKI and fibrosis. The sufficient NO bioavailability is known as a key to protection against oxidative injury induced by I/R injury, drug induced nephrotoxicity and interstitial fibrosis. However, the efficacy of sodium nitrite on AKI could not be determined here, since ArisA did not successfully induce AKI and fibrosis.

While the published literature showed that these nephrotoxic drugs induced kidney structural damage, cell death and interstitial fibrosis, this thesis did not show any abnormalities in kidneys or any signs of cell death. The observation of only a few proliferative cells in BrdU and pH3 labelled 48-hour kidneys again suggested that ArisA did not induce any acute injury. There were no changes in renal gene expression including *Nos2*, *Nos3*, *Nox2*, *Nox4* and *Kim1* for assessment of the correlation of dietary nitrite, NO bioavailability and early signs of acute injury, indicating that ArisA did not have any effects on this animal model. The assessment of fibrosis markers in 48-hour kidneys also did not show any changes. This was not surprising since fibrosis normally occurs at the chronic phase, and we have found that there was no positive stain of Masson's trichrome in 35-day kidneys. While the dose of ArisA was adopted from the published study, it did not successfully induce AKI in this thesis due to the use of the animal model with high susceptibility without a pilot study. While this thesis could not confirm the therapeutic effects of nitrite on renal I/R injury, the improvement of body nitrite pool or NO bioavailability from diet may still possess a certain level of benefit as NO plays a critical role in many physiological processes.

Overall, this thesis implicated that the prompt nutritional supports for AKI may have to be revised, particularly in patients under oxidative stress (e.g. surgical stress). In this case, the delayed nutrient supply or dietary restriction may provide a better strategy. Meanwhile, antioxidant therapy or an increase in NO bioavailability may be considered a priority prior to nutritional support for the treatment of AKI.

Future work

Future work

This thesis was unable to induce an appropriate I/R injury using HK-2 cell system. To induce a simulated I/R injury in this cell line requires exogenous H_2O_2, but the biological relevance can be challenged. Hence, a primary cell line (i.e. commercially available hRPTECs) will be an alternative option for future study. To induce an experimental I/R injury, it will be necessary to perform starvation in hypoxia (5% O_2) followed by the return of nutrients in normoxia (21% O_2) without exogenous H_2O_2. This can also be achieved by drug induced ATP depletion (e.g. KCN) or mitochondrial respiratory chain inhibitor (e.g. antimycin A, an inhibitor of complex III of mitochondrial electron transport) followed by replacement with fresh media/nutrients. For evaluating the effects of pH on this model, it is important to ensure pH to be maintained constant during the incubation. The buffering system should be carefully selected, since this thesis found that MES buffer appeared to have a detrimental effect on cells. Although the buffering range of HEPES is pH 6.8-8.2, it appeared that HEPES was still used for buffering pH 6.4 in some studies.

As it was found that the replenishment of AAS at both pH 7.5 and 6.4 led to cell death, assessing cell death pathways will be essential to understand the mechanisms of how AAS exacerbated oxidative injury. In the mitochondrial morphology assessment, it will be necessary to show co-localisation of Mitotracker with other apoptotic factors such as caspase-3 or cytochrome c to confirm the mitochondria mediated cell death in response to the provision of AAS at pH 7.5 in the presence of H_2O_2 following starvation. Although the cell line and the incubation media might be the limitations in the study, the concentration of H_2O_2 did not inhibit mTOR signalling pathways, which could be biologically relevant. Nevertheless, it is

necessary to examine whether mTOR was still activated after longer exposure to AAS in the presence of H_2O_2 (e.g. 24 hours incubation) as this thesis only examined mTOR signalling in response to 1 hour of resupply of AAS.

If mTOR activation is the key to the ER stress and cell death after D/R injury model, it will be necessary to assess i) protein synthesis, ii) downstream apoptotic pathways, iii) and the activation of UPR pathways (e.g. PERK, IRE1 and ATF6) alongside with MAPK pathways. It is necessary to show whether mTOR activation corresponds to the level of chaperone proteins and UPR proteins at each time point, and hence this may evidence the correlation between mTOR and UPR. Additionally it is necessary to assess whether inhibition of mTOR using rapamycin or induction of autophagy could reverse the outcomes of resupplying AAS under oxidative stress following starvation.

For chapter 5, a pilot study should be included before experimental trial, especially when a different animal model was used. The assessment of plasma creatinine, blood urea nitrogen level and urine production is necessary to see whether kidney function is altered by treatments. Assessment of metabolic waste products or by-products (e.g. nitrite/nitrate, cAMP, H_2O_2 and antioxidant enzymes) from plasma and urine may provide more information for identifying the effectiveness of treatments. PAS staining will be a more specific staining for identifying fibrosis rather than Masson's trichrome.

Chapter 8: References

Chapter 8: References

Abel, R. M., Beck, C. H. Jr., Abbott, W. M., Ryan, J. A. Jr., Barnett, G. O. and Fischer, J. E. (1973) Improved survival from acute renal failure after treatment with intravenous essential L-amino acids and glucose. Results of a prospective, double-blind study. The New England Journal of Medicine, 288, 695-699.

Abu-Amara, M., Yang, S. Y., Quaglia, A., Rowley, P., De Mel, A., Tapuria, N., Seifalian, A., Davidson, B. and Fuller, B. (2011) Nitric oxide is an essential mediator of the protective effects of remote ischaemic preconditioning in a mouse model of liver ischaemia/reperfusion injury. Clinical Science, 121, 257-266.

Adler, S. and Huang, H. (2004) Oxidant stress in kidneys of spontaneously hypertensive rats involves both oxidase overexpression and loss of extracellular superoxide dismutase. American Journal of Physiology-Renal Physiology, 287, 907-913.

Alejandro, V., Nelson, W. J., Huie, P., Sibley, R. K., Dafoe, D., Kuo, P., Scandling, J. D. and Myers, B. D. (1995) Postischemic injury, delayed function and Na+-K+-ATPase distribution in the transplanted kidney. Kidney International, 48, 1308-1315.

Amann, K., Koch, A., Hofstetter, J., Gross, M. L., Haas, C., Orth, S. R., Ehmke, H., Rump, L. C. and Ritz, E. (2001) Glomerulosclerosis and progression: Effect of subantihypertensive doses of alpha and beta blockers. Kidney International, 60(4), 1309-1323.

Amann, K., Rump, L. C., Simonaviciene, A., Oberhauser, V., Wessels, S., Orth, S. R., Gross, M. L., Koch, A., Bielenberg, G. W., Van Kats, J. P., Ehmke, H., Mall, G.

and Ritz, E. (2000) Effects of low dose sympathetic inhibition on glomerulosclerosis and albuminuria in subtotally nephrectomized rats. Journal of the American Society of Nephrology, 11, 1469-1478.

Amores-Sánchez, M. I. and Medina, M. A. (1999) Glutamine, as a precursor of glutathione, and oxidative stress. Molecular Genetics and Metabolism, 67, 100-105.

Appenzeller-Herzog, C. and Hall, M. N. (2012) Bidirectional crosstalk between endoplasmic reticulum stress and mTOR signaling. Trends in Cell Biology, 22(5), 274-282.

Arabi, Y. M., Tamim, H. M., Dhar, G. S., Al-Dawood, A., Al-Sultan, M., Sakkijha, M. H., Kahoul, S. H. and Brits, R. (2011) Permissive underfeeding and intensive insulin therapy in critically ill patients: A randomized controlled trial. American Journal of Clinical Nutrition, 93, 569-577.

Araujo, M. and Welch, W. J. (2006) Oxidative stress and nitric oxide in kidney function. Current Opinion in Nephrology and Hypertension, 15, 72-77.

Baba, M., Furihata, M., Hong, S. B., Tessarollo, L., Haines, D. C., Southon, E., Patel, V., Igarashi, P., Alvord, W. G., Leighty, R., Yao, M., Bernardo, M., Ileva, L., Choyke, P., Warren, M. B., Zbar, B., Linehan, W. M. and Schmidt, L. S. (2008) Kidney-targeted Birt-Hogg-Dube gene inactivation in a mouse model: Erk1/2 and Akt-mTOR activation, cell hyperproliferation, and polycystic kidneys. Journal of the National Cancer Institute, 100(2), 140-154.

Bagetti-Filho, H. J., Sampaio, F. J., Marques, R. G. and Pereira-Sampaio, M. A. (2012) Different from renal artery only clamping, artery and vein clamping causes a

significant reduction in number of rat glomeruli during warm ischemia. Journal of Endourology, 26(10), 1335-1339.

Bakker, R. C., Van Kooten, C., Van de Lagemaat-Paape, M. E., Daha, M. R. and Paul, L. C. (2002) Renal tubular epithelial cell death and cyclosporin A. Nephrology Dialysis Transplantation, 17 (7), 1181-1188.

Balgi, A. D., Diering, G. H., Donohue, E., Lam, K. K. Y., Fonseca, B. D., Zimmerman, C., Numata, M. and Roberge, M. (2011) Regulation of mTORC1 Signaling by pH. PLoS ONE, 6(6), e21549.

Bard, J. B. (2002) Growth and death in the developing mammalian kidney: Signals, receptors and conversations. BioEssays, 24, 72-82.

Basile, D. P., Anderson, M. D. and Sutton, T. A. (2012) Pathophysiology of acute kidney injury. Comprehensive Physiology, 2(2), 1303-1353.

Basile, D. P., Donohoe, D. L., Roethe, K. and Mattson, D. L. (2003) Chronic renal hypoxia after acute ischemic injury: Effects of l-arginine on hypoxia and secondary damage. American Journal of Physiology-Renal Physiology, 284(2), 338-348.

Basile, D. P., Martin, D. R. and Hammerman, M. R. (1998) Extracellular matrix-related genes in kidney after ischemic injury: Potential role for TGF-beta in repair. Journal of the American Society of Nephrology, 275(6), 894-903.

Basireddy, M., Isbell, T. S., Teng, X. Patel, R. P. and Agarwal, A. (2006) Effects of sodium nitrite on ischemia-reperfusion injury in the rat kidney. American Journal of Physioloy-Renal Physiology, 290, 779-786.

Bellomo, R., Cass, A., Cole, L., Finfer, S., Gallagher, M., Lee, J., Lo, S., McArthur, C., McGuinness, S., Norton, R., Myburgh, J., Sheinkestel, C. and The RENAL Study Investigators (2014) Daily protein intake and patient outcomes in severe acute kidney injury: Findings of the Randomized Evaluation of Normal versus Augmented Level of Replacement Therapy (RENAL) trial. Blood Purification, 37, 325-334.

Bellomo, R., Kellum, J. A. and Ronco, C. (2012) Acute kidney injury. Lancet, 380, 756-766.

Bellomo, R., Martin, H., Parkin, G., Love, J., Kearley, Y. and Boyce, N. (1991) Continuous arteriovenous haemodiafiltration in the critically ill: Influence on major nutrient balances. Intensive Care Medicine, 17, 399-402.

Bellomo, R., Seacombe, J., Daskalakis, M., Farmer, M., Wright, C., Parkin, G. and Boyce, N. (1997) A prospective comparative study of moderate versus high protein intake for critically ill patients with acute renal failure. Renal Failure, 19, 111-120.

Bellomo, R., Tan, H. K., Bhonagiri, S., Gopal, I., Seacombe, J., Daskalakis, M. and Boyce, N. (2002) High protein intake during continuous hemodiafiltration: Impact on amino acids and nitrogen balance. International Journal of Artificial Organs, 25, 261-268.

Bendall, J. K., Douglas, G., McNeill, E., Channon, K. M. and Crabtree, M. J. (2014) Tetrahydrobiopterin in cardiovascular health and disease. Antioxidants and Redox Signaling, 20(18), 3040-3077.

Benjamin, D., Colombi, M., Moroni, C. and Hall, M. N. (2011) Rapamycin passes the torch: A new generation of mTOR inhibitors. Drug Discovery, 11, 868-880.

Bernardi, P., Vassanelli, S., Veronese, P., Colonna, R., Szabó, I. and Zoratti, M. (1992) Modulation of the mitochondrial permeability transition pore. Effect of protons and divalent cations. The Journal of Biological Chemistry, 267(5), 2934-2939.

Bertolotti, A., Zhang, Y., Hendershot, L. M., Harding, H. P. and Ron, D. (2000) Dynamic interaction of BiP and ER stress transducers in the unfolded-protein response. Nature Cell Biology, 2, 326-332.

Betz, C. and Hall, M. N. (2013) Where is mTOR and what is it doing there? Journal of Cell Biology, 203, 4, 563-574.

Bielesz, B., Sirin, Y., Si, H., Niranjan, T., Gruenwald, A., Ahn, S., Kato, H., Pullman, J., Gessler, M., Haase, V. H. and Susztak, K. (2010) Epithelial Notch signaling regulates interstitial fibrosis development in the kidneys of mice and humans. Journal of Clinical Investigation, 120(11), 4040-4054.

Bing, O. H. L., Brooks, W. W. and Messer, J. V. (1973) Heart muscle viability following hypoxia: Protective effect of acidosis. Science, 180, 1297-1298.

Bing, P., Maode, L., Li, F. and Sheng, H. (2006) Expression of renal transforming growth factor-beta and its receptors in a rat model of chronic cyclosporine-induced nephropathy. Transplantation Proceedings, 38(7), 2176-2179.

Blaine, J., Chonchol, M. and Levi, M. (2015) Renal control of calcium, phosphate, and magnesium homeostasis. Clinical Journal of the American Society of Nephrology, 10(7), 1257-1272.

Bohle, A., Christensen, J., Kokot, F., Osswald, H., Schubert, B., Kendziorra, H., Pressler, H. and Marcovic-Lipkovski, J. (1990) Acute renal failure in man: New aspects concerning pathogenesis. A morphometric study. American Journal of Nephrology, 10(5), 374-388.

Bolisetty, S., Traylor, A. M., Kim, J., Joseph, R., Ricart, K., Landar, A. and Agarwal, A. (2010) Heme oxygenase-1 inhibits renal tubular macroautophagy in acute kidney injury. Journal of the American Society of Nephrology, 21, 1702-1712.

Bonventre, J. V. (2003) Dedifferentiation and proliferation of surviving epithelial cells in acute renal failure. Journal of the American Society of Nephrology, 14(1), 55-61.

Bonventre, J. V. and Weinberg, J. M. (2003) Recent advances in the pathophysiology of ischemic acute renal failure. Journal of the American Society of Nephrology, 14, 2199-2210.

Bonventre, J. V. and Yang, L. (2011) Cellular pathophysiology of ischemic acute kidney injury. The Journal of Clinical Investigation, 121, 4210-4221.

Bonventre, J. V. and Zuk, A. (2004) Ischemic acute renal failure: An inflammatory disease? Kidney International, 66, 480-485.

Boo, Y. C. and Jo, H. (2003) Flow-dependent regulation of endothelial nitric oxide synthase: Role of protein kinases. American Journal of Physiology-Cell Physiology, 285, 499-508.

Boonla, C., Krieglstein, K., Bovornpadungkitti, S., Strutz, F., Spittau, B., Predanon, C. and Tosukhowong, P. (2011) Fibrosis and evidence for epithelial-mesenchymal

transition in the kidneys of patients with staghorn calculi. BJU International, 108(8), 1336-1345.

Boor, P. and Floege, J. (2011) Chronic kidney disease growth factors in renal fibrosis. Clinical and Experimental Pharmacology and Physiology, 38, 441-450.

Boor, P., Šebeková, K., Ostendorf, T. and Floege, J. (2007) Treatment targets in renal fibrosis. Nephrology Dialysis Transplantation, 22(12), 3391-3407.

Borthwick, L. A., Wynn, T. A. and Fisher, A. J. (2013) Cytokine mediated tissue fibrosis. Biochimica et Biophysica Acta, 1832(7), 1049-1060.

Braga, T. T., Agudelo, J. S. H. and Camara, N. O. S. (2015) Macrophages during the fibrotic process: M2 as friend and foe. Frontiers in Immunology, 6, 602.

Brezis, M. and Rosen, S. (1995) Hypoxia of the renal medulla - Its implications for disease. The New England Journal of Medicine, 332(10), 647-655.

Briggs, J. P., Kriz, W. and Schnermann, J. B. (2014) Overview of kidney function and structure. In: Gilbert, S. and Weiner, D. E. (Eds.) National kidney foundation primer on kidney diseases, 6th edition, 1-18. Philadelphia: Saunders Elsevier.

Brooks, C., Wei, Q., Cho, S. G. and Dong, Z. (2009) Regulation of mitochondrial dynamics in acute kidney injury in cell culture and rodent models. Journal of Clinical Investigation, 119, 1275-1285.

Brown, D. and Wagner, C. A. (2012) Molecular mechanisms of acid-base sensing by the kidney. Journal of the American Society of Nephrology, 23(5), 774-780.

Brown, G. C. (1999) Nitric oxide and mitochondrial respiration. Biochimica et Biophysica Acta, 1411(2-3), 351-369.

Brown, J. R., Kramer, R. S., Coca, S. G., and Parikh, C. R. (2010) Duration of acute kidney injury impacts long-term survival after cardiac surgery. The Annals of Thoracic Surgery, 90, 1142-1149.

Bryan, N. S., Calvert, J. W., Elrod, J. W., Gundewar, S., Ji, S. Y. and Lefer, D. J. (2007) Dietary nitrite supplementation protects against myocardial ischemia-reperfusion injury. Proceedings of the National Academy of Sciences, 104, 19144-19149.

Bryan, N. S., Calvert, J. W., Gundewar, S. and Lefer, D. J. (2008) Dietary nitrite restores NO homeostasis and is cardioprotective in endothelial nitric oxide synthase-deficient mice. Free Radical Biology and Medicine, 45, 468-474.

Bryan, N. S., Fernandez, B. O., Bauer, S. M., Garcia-Saura, M. F., Milsom, A. B., Rassaf, T., Maloney, R. E., Bharti, A., Rodriguez, J. and Feelisch, M. (2005) Nitrite is a signaling molecule and regulator of gene expression in mammalian tissues. Nature Chemical Biology, 1, 290-297.

Btaiche, I. F., Mohammad, R. A., Alaniz, C. and Mueller, B. A. (2008) Amino acid requirements in critically ill patients with acute kidney injury treated with continuous renal replacement therapy. Pharmacotherapy, 28(5), 600-613.

Buchberger, A., Bukau, B. and Sommer, T. (2010) Protein quality control in the cytosol and the endoplasmic reticulum: Brothers in arms. Molecular Cell, 40(2), 238-252.

Bukau, B., Weissman, J. and Horwich, A. (2006) Molecular chaperones and protein quality control. Cell, 125(3), 443-451.

Burnier, M., Van Putten, V. J., Schieppati, A. and Schrier, R. W. (1988) Effect of extracellular acidosis on 45Ca uptake in isolated hypoxic proximal tubules. American Journal of Physiology-Renal Physiology, 254, 839-846.

Burwell, L. S., Nadtochiy, S. M. and Brookes, P. S. (2009) Cardioprotection by metabolic shut-down and gradual wake-up. Journal of Molecular and Cellular Cardiology, 46(6), 804-810.

Bush, K. T., Keller, S. H. and Nigam, S. K. (2000) Genesis and reversal of the ischemic phenotype in epithelial cells. Journal of Clinical Investigation, 106(5), 621-626.

Canaud, G. and Bonventre, J. V. (2015) Cell cycle arrest and the evolution of chronic kidney disease from acute kidney injury. Nephrology Dialysis Transplantation, 30(4), 575-583.

Cano, N. J. M., Aparicio, M., Brunori, G., Carrero, J. J., Cianciaruso, B., Fiaccadori, E., Lindholm, B., Teplan, V., Fouque, D. and Guarnieri, G. (2009) ESPEN guidelines on parenteral nutrition: Adult renal failure. Clinical Nutrition, 28, 401-414.

Cao, S. S. and Kaufman, R. J. (2014) Endoplasmic reticulum stress and oxidative stress in cell fate decision and human disease. Antioxidants and Redox Signaling, 21(3), 396-413.

Carlisle, R. E., Brimble, E., Werner, K. E., Cruz, G. L., Ask, K., Ingram, A. J. and Dickhout, J. G. (2014) 4-Phenylbutyrate inhibits tunicamycin-induced acute kidney injury via CHOP/GADD153 repression. PLoS ONE, 9(1), e84663.

Carlson, E. A., Rao, E. K. and Yan, S. S. (2013) From a cell's viewpoint: Targeting mitochondria in Alzheimer's disease. Drug Discovery Today: Therapeutic Strategies, 10(2), 91-98.

Casaer, M. P., Mesotten, D., Hermans, G., Wouters, P. J., Schetz, M., Meyfroidt, G., Van Cromphaut, S., Ingels, C., Meersseman, P., Muller, J., Vlasselaers, D., Debaveye, Y., Desmet, L., Dubois, J., Van Assche, A., Vanderheyden, S., Wilmer, A. and Van den Berghe, G. (2011) Early versus late parenteral nutrition in critically ill adults. The New England Journal of Medicine, 365, 506-517.

Casaer, M. P., Wilmer, A., Hermans, G., Wouters, P. J., Mesotten, D. and Van den Berghe, G. (2013) Role of disease and macronutrient dose in the randomized controlled EPaNIC trial: A post hoc analysis. American Journal of Respiratory and Critical Care Medicine, 187, 247-255.

Case, J., Khan, S., Khalid, R. and Khan, A. (2013) Epidemiology of acute kidney injury in the intensive care unit. Critical Care Research and Practice, e479730.

Cerdá, J., Liu, K. D., Cruz, D. N., Jaber, B. L., Koyner, J. L., Heung, M., Okusa, M. D. and Faubel, S. (2015) Promoting kidney function recovery in patients with AKI requiring RRT. Clinical Journal of the American Society of Nephrology, 10(10), 1859-1867.

Chakravarthi, S. and Bulleid, N. J. (2004) Glutathione is required to regulate the formation of native disulphide bonds within proteins entering the secretory pathway. Journal of Biological Chemistry, 279, 39872-39879.

Chakravarthi, S., Jessop, C. E. and Bulleid, N. J. (2006) The role of glutathione in disulphide bond formation and endoplasmic-reticulum-generated oxidative stress. EMBO reports, 7, 271-275.

Chamoun, F., Burne, M., O'Donnell, M. and Rabb, H. (2000) Pathophysiological role of selectins and their ligands in ischaemia reperfusion injury. Frontiers in Bioscience, 5, 103-109.

Chandrika, B. B., Yang, C., Ou, Y., Feng, X., Muhoza, D., Holmes, A. F., Theus, S., Deshmukh, S., Haun, R. S. and Kaushal, G. P. (2015) Endoplasmic reticulum stress-induced autophagy provides cytoprotection from chemical hypoxia and oxidant injury and ameliorates renal ischemia-reperfusion injury. PLoS ONE, 10(10), e0140025.

Chang, C. H., Wang, Y. M., Yang, A. H. and Chiang, S. S. (2001) Rapidly progressive interstitial renal fibrosis associated with Chinese herbal medications. American Journal of Nephrology, 21, 441-448.

Chatterjee, P. K. (2007) Novel pharmacological approaches to the treatment of renal ischemia-reperfusion injury: A comprehensive review. Naunyn-Schmiedeberg's Archives of Pharmacology, 376(1-2), 1-43.

Chawla, L. S., Amdur, R. L., Amodeo, S., Kimmel, P. L. and Palant, C. E. (2011) The severity of acute kidney injury predicts progression to chronic kidney disease. Kidney International, 79(12), 1361-1369.

Chawla, L. S. and Kimmel, P. L. (2012) Acute kidney injury and chronic kidney disease: An integrated clinical syndrome. Kidney International, 82, 516-524.

Chen, B. L., Wang, L. T., Huang, K. H., Wang, C. C., Chiang, C. K. and Liu, S. H. (2014) Quercetin attenuates renal ischemia/reperfusion injury via an activation of AMP-activated protein kinase-regulated autophagy pathway. The Journal of Nutritional Biochemistry, 25(11), 1226-1234.

Chen, G., Chen, H., Wang, C., Peng, Y., Sun, L, Liu, H. and Liu, F. (2012) Rapamycin ameliorates kidney fibrosis by inhibiting the activation of mTOR signaling in interstitial macrophages and myofibroblasts. PLoS ONE, 7(3), e33626.

Chen, L., Xu, B., Liu, L., Luo, Y., Yin, J., Zhou, H., Chen, W., Shen, T., Han, X. and Huang, S. (2010) Hydrogen peroxide inhibits mTOR signaling by activation of AMPKalpha leading to apoptosis of neuronal cells. Laboratory Investigation, 90(5), 762-773.

Chertow, G. M., Burdick, E., Honour, M., Bonventre, J. V. and Bates, D. W. (2005) Acute kidney injury, mortality, length of stay, and costs in hospitalized patients. Journal of the American Society of Nephrology, 16(11), 3365-3370.

Chirino, Y. I. and Pedraza-Chaverri, J. (2009) Role of oxidative and nitrosative stress in cisplatin-induced nephrotoxicity. Elsevier, 61(3), 223-242.

Choi, K. H., Kim, T. II, Chong, D. L., Lee, H. Y. and Han, D. S. (2000) Gentamicin induced apoptosis of renal tubular epithelial (LLC-PK1) cells. The Korean Journal of Internal Medicine, 15(3), 218-223.

Chouchani, E. T., Pell, V. R., Gaude, E., Aksentijević, D., Sundier, S. Y., Robb, E. L., Logan, A., Nadtochiy, S. M., Ord, E. N. J., Smith, A. C., Eyassu, F., Shirley, R., Hu, C. H., Dare, A. J., James, A. M., Rogatti, S., Hartley, R. C., Eaton, S., Costa, A. S. H., Brookes, P. S., Davidson, S. M., Duchen, M. R., Saeb-Parsy, K., Shattock, M. J., Robinson, A. J., Work, L. M., Frezza, C., Krieg, T. and Murphy, M. P. (2014) Ischaemic accumulation of succinate controls reperfusion injury through mitochondrial ROS. Nature, 515(7527), 431-435.

Chwieralski, C. E., Welte, T. and Bühling, F. (2006) Cathepsin-regulated apoptosis. Apoptosis, 11, 143-149.

Coca, S. G., Singanamala, S. and Parikh, C. R. (2012) Chronic kidney disease after acute kidney injury: A systematic review and meta-analysis. Kidney international, 81(5), 442-448.

Coffman, T. M. (2005) Clinical approach to the diagnosis acute renal failure. In: Greenberg, A. (Ed.) Primer on kidney diseases. Pennsylvania: Saunders Elsevier.

Cohen, M. V., Yang, X. M. and Downey, J. M. (2007) The pH hypothesis of postconditioning: Staccato reperfusion reintroduces oxygen and perpetuates myocardial acidosis. Circulation, 115(14), 1895-1903.

Contestabile, A. and Ciani, E. (2004) Role of nitric oxide in the regulation of neuronal proliferation, survival and differentiation. Neurochemistry International, 45(6), 903-914.

Cosyns, J. P., Dehoux, J. P., Guiot, Y., Goebbels, R. M., Robert, A., Bernard, A. M. and Van Ypersele de Strihou, C. (2001) Chronic aristolochic acid toxicity in rabbits: A model of Chinese herbs nephropathy? Kidney International, 59, 2164-2173.

Crean, D., Felicea, L., Pierreb, P., Jenningse, P. and Leonard, M. O. (2013) Inhibition of protein translation as a mechanism of acidotic pH protection against ischaemic injury through inhibition of CREB mediated tRNA synthetase expression. Experimental Cell Research, 319, 3116-3127.

Crean, D., Felicea, L., Taylor, C. T., Rabb, H., Jenningse, P. and Leonard, M. O. (2012) Glucose reintroduction triggers the activation of Nrf2 during experimental ischemia reperfusion. Molecular Cell Biochemistry, 366, 231-238.

Crompton, M. (1999) The mitochondrial permeability transition pore and its role in cell death. Biochemical Journal, 341, 233-249.

Cruthirds, D. L., Novak, L., Akhi, K. M., Sanders, P. W., Thompson, J. A. and MacMillan-Crow, L. A. (2003) Mitochondrial targets of oxidative stress during renal ischemia/reperfusion. Archives of Biochemistry and Biophysics, 412(1), 27-33.

Cummings, B. S. and Schnellmann, R. G. (2002) Cisplatin-induced renal cell apoptosis: Caspase 3-dependent and -independent pathways. Journal of Pharmacology and Experimental Therapeutics, 302(1), 8-17.

Cunard, R. and Sharma, K. (2011) The endoplasmic reticulum stress response and diabetic kidney disease. American Journal of Physiology-Renal Physiology, 300, 1054-1061.

Cunnington, C., Assche, T. V., Shirodaria, C., Kylintireas, I., Lindsay, A. C., Lee, J. M., Antoniades, C., Margaritis, M., Lee, R., Cerrato, R., Crabtree, M. J., Francis, J. M., Sayeed, R., Ratnatunga, C., Pillai, R., Choudhury, R. P., Neubauer, S. and Channon, K. M. (2012) Systemic and vascular oxidation limits the efficacy of oral

tetrahydrobiopterin treatment in patients with coronary artery disease. Circulation, 125, 1356-1366.

Currin, R. T., Gores, G. J., Thurman, R. G. and Lemasters, J. J. (1991) Protection by acidotic pH against anoxic cell killing in perfused rat liver: Evidence for a pH paradox. The FASEB Journal, 5(2), 207-210.

Cybulsky, A. V. (2013) The intersecting roles of endoplasmic reticulum stress, ubiquitin-proteasome system, and autophagy in the pathogenesis of proteinuric kidney disease. Kidney International, 84, 25-33.

Daghar, P. C. (2004) Apoptosis in ischemic renal injury: Roles of GTP depletion and p53. Kidney International, 66, 506-508.

Dahm, C. C., Moore, K. and Murphy, M. P. (2006) Persistent S-nitrosation of complex I and other mitochondrial membrane proteins by S-nitrosothiols but not nitric oxide or peroxynitrite. Implications for the interaction of nitric oxide with mitochondria. The Journal of Biological Chemistry, 281, 10056-10065.

D'Amico, G. and Bazzi, C. (2003) Pathophysiology of proteinuria. Kidney International, 63(3), 809-825.

Danilczyk, U. and Penninger, J. M. (2006) Angiotensin-converting enzyme II in the heart and the kidney. Circulation Research, 98, 463-471.

Darling, N. J. and Cook, S. J. (2014) The role of MAPK signalling pathways in the response to endoplasmic reticulum stress. Biochimica et Biophysica Acta, 1843, 2150-2163.

Debelle, F. D., Vanherweghem, J. L. and Nortier, J. L. (2008) Aristolochic acid nephropathy: A worldwide problem. Kidney International, 74, 158-169.

De Broe, M. E. (1999) On a nephrotoxic and carcinogenic slimming regimen. American Journal of Kidney Disease, 33, 1171-1173.

Declèves, A. E., Jadot, I., Colombaro, V., Martin, B., Voisin, V., Habsch, I., De Prez, E., Nortier, J. and Caron, N. (2016) Protective effect of nitric oxide in aristolochic acid-induced toxic acute kidney injury: An old friend with new assets. Experimental Physiology, 101(1), 193-206.

Declèves, A. E., Mathew, A. V., Cunard, R. and Sharma, K. (2011) AMPK mediates the initiation of kidney disease induced by a high-fat diet. Journal of the American Society of Nephrology, 22(10), 1846-1855.

Dejam, A., Hunter, C. J., Tremonti, C., Pluta, R. M., Hon, Y. Y., Grimes, G., Partovi, K., Pelletier, M. M., Oldfield, E. H., Cannon 3rd, R. O., Schechter, A. N. and Gladwin, M. T. (2007) Nitrite infusion in humans and nonhuman primates: Endocrine effects, pharmacokinetics, and tolerance formation. Circulation, 116(16), 1821-1831.

Devarajan, P. (2005) Cellular and molecular derangements in acute tubular necrosis. Current Opinion in Pediatrics, 17(2), 193-199.

Devarajan, P. (2006) Update on mechanisms of ischemic acute kidney injury. Journal of the American Society of Nephrology, 17, 1503-1520.

Dezfulian, C., Shiva, S., Alekseyenko, A., Pendyal, A., Beiser, D. G., Munasinghe, J. P., Anderson, S. A., Chesley, C. F., Vanden Hoek, T. L. and Gladwin, M. T. (2009)

Nitrite therapy after cardiac arrest reduces reactive oxygen species generation, improves cardiac and neurological function, and enhances survival via reversible inhibition of mitochondrial complex I. Circulation, 120(10), 897-905.

Dickhout, J. G., Carlisle, R. E. and Austin, R. C. (2014) Interrelationship between cardiac hypertrophy, heart failure, and chronic kidney disease: Endoplasmic reticulum stress as a mediator of pathogenesis. Circulation Research, 108(5), 629-642.

Dobashi, K., Ghosh, B., Orak, J. K., Singh, I. and Singh, A. K. (2000) Kidney ischemia-reperfusion: Modulation of antioxidant defenses. Molecular and Cellular Biochemistry, 205(1), 1-11.

Doctor, R. B. and Mandel, L. J. (1991) Minimal role of xanthine oxidase and oxygen free radicals in rat renal tubular reoxygenation injury. Journal of the American Society of Nephrology, 1(7), 959-969.

Doig, G. S., Simpson, F., Bellomo, R., Heighes, P. T., Sweetman, E. A., Chesher, D., Pollock, C., Davies, A., Botha, J., Harrigan, P. and Reade, M. C. (2015) Intravenous amino acid therapy for kidney function in critically ill patients: A randomized controlled trial. Intensive Care Medicine, 41, 7, 1197-1208.

Dong, G., Liu, Y., Zhang, L., Huang, S., Ding, H. F. and Dong, Z. (2015) mTOR contributes to ER stress and associated apoptosis in renal tubular cells. American Journal of Physiology-Renal Physiology, 308, 267-274.

Douglas, P. M. and Dillin, A. (2010) Protein homeostasis and aging in neurodegeneration. Journal of Cell Biology, 190, 719-729.

Dranka, B. P., Benavides, G. A., Diers, A. R., Giordano, S., Zelickson, B. R., Reily, C., Zou, L., Chatham, J. C., Hill, B. G., Zhang, J., Landar, A. and Darley-Usmar, V. M. (2011) Assessing bioenergetic function in response to oxidative stress by metabolic profiling. Free Radical Biology and Medicine, 51(9), 1621-1635.

Druml, W. (2001) Nutritional management of acute renal failure. American Journal of Kidney Disease, 37, 89-94.

Druml, W., Fischer, M., Liebisch, B., Lenz, K. and Roth, E. (1994) Elimination of amino acids in renal failure. American Journal of Clinical Nutrition, 60, 418-423.

Duranski, M. R., Greer, J. J. M., Dejam, A., Jaganmohan, S., Hogg, N., Langston, W., Patel, R. P., Yet, S. F., Wang, X., Kevil, C. G., Gladwin, M. T. and Lefer, D. J. (2005) Cytoprotective effects of nitrite during in vivo ischemia-reperfusion of the heart and liver. Journal of Clinical Investigation, 115(5), 1232-1240.

Eaton, D. C. and Pooler, J. P. (2013) Structure and function of the kidneys. In: Vander's Renal Physiology, 5th edition, 15-26. Philadelphia: Saunders Elsevier.

Efeyan, A., Zoncu, R. and Sabatini, D. M. (2012) Amino acids and mTORC1: From lysosomes to disease. Trends in Molecular Medicine, 18(9), 524-533.

El Mohammed, M., Mouedden, G., Mingeot-Leclercq, M. P. and Tulkens, P. M. (2000) Gentamicin-induced apoptosis in renal cell lines and embryonic rat fibroblasts. Toxicological Sciences, 56(1), 229-239.

Erdogan, H., Fadillioglu, E., Yagmurca, M., Uçar, M. and Irmak, M. K. (2006) Protein oxidation and lipid peroxidation after renal ischemia-reperfusion injury:

Protective effects of erdosteine and N-acetylcysteine. Journal of Urology and Research, 34, 41-46.

Esposito, E., Mondello, S., Di Paola, R., Mazzon, E., Italiano, D., Paterniti, I., Mondello, P., Aloisi, C. and Cuzzocrea, S. (2011) Glutamine contributes to ameliorate inflammation after renal ischemia/reperfusion injury in rats. Naunyn-Schmiedeberg's Archives of Pharmacology, 383(5), 493-508.

Esson, M. L. and Schrier, R. W. (2002) Diagnosis and treatment of acute tubular necrosis. Annals of Internal Medicine, 137, 744-752.

Farooqi, S. and Dickhout, J. G. (2016) Major comorbid disease processes associated with increased incidence of acute kidney injury. World Journal of Nephrology, 5(2), 139-146.

Farris, A. B. and Colvin, R. B. (2012) Renal interstitial fibrosis: Mechanisms and evaluation in: Current opinion in nephrology and hypertension. Current Opinion in Nephrology and Hypertension, 21(3), 289-300.

Ferris, S. P., Kodali, V. K. and Kaufman, R. J. (2014) Glycoprotein folding and quality-control mechanisms in protein-folding diseases. Disease Models and Mechanisms, *7*(3), 331-341.

Festing, M. F. W. (2010) Inbred strains should replace outbred stocks in toxicology, safety testing, and drug development. Toxicologic Pathology, 38, 681-690.

Fiaccadori, E., Parenti, E. and Maggiore, U. (2008) Nutritional support in acute kidney injury. Journal of Nephrology, 21(5), 645-656.

Fiaccadori, E., Regolisti, G. and Cabassi, A. (2010) Specific nutritional problems in acute kidney injury, treated with non-dialysis and dialytic modalities. Nephrology Dialysis Transplantation Plus, 3, 1-7.

Filardy, A. A., Pires, D. R., Nunes, M. P., Takiya, C. M., Freire-de-Lima, C. G., Ribeiro-Gomes, F. L. and DosReis, G. A. (2010) Proinflammatory clearance of apoptotic neutrophils induces an IL-12(low)IL-10(high) regulatory phenotype in macrophages. Journal of Immunology, 185, 2044-2050.

Fingar, D. C., Richardson, C. J., Tee, A. R., Cheatham, L., Tsou, C. and Blenis, J. (2004) mTOR controls cell cycle progression through its cell growth effectors S6K1 and 4E-BP1/eukaryotic translation initiation factor 4E. Molecular and Cellular Biology, 24, 200-216.

Fingar, D. C., Salama, S., Tsou, C., Harlow, E. and Blenis, J. (2002) Mammalian cell size is controlled by mTOR and its downstream targets S6K1 and 4EBP1/eIF4E. Genes and Development, 16, 1472-1487.

Forbes, M. S., Thornhill, B. A., Park, M. H. and Chevalier, R. L. (2007) Lack of endothelial nitric-oxide synthase leads to progressive focal renal injury. American Journal of Pathology, 170(1), 87-99.

Frank, S., Gaume, B., Bergmann-Leitner, E. S., Leitner, W. W., Robert, E. G., Catez, F., Smith, C. L. and Youle, R. J. (2001) The role of dynamin-related protein 1, a mediator of mitochondrial fission, in apoptosis. Developmental Cell, 1, 515-525.

Fujita, M., Asanuma, H., Hirata, A., Wakeno, M., Takahama, H., Sasaki, H., Kim, J., Takashima, S., Tsukamoto, O., Minamino, T., Shinozaki, Y., Tomoike, H., Hori, M. and Kitakaze, M. (2007) Prolonged transient acidosis during early reperfusion

contributes to the cardioprotective effects of postconditioning. American Journal of Physiology-Heart and Circulatory Physiology, 292(4), 2004-2008.

Funk, J. A. and Schnellmann, R. G. (2012) Persistent disruption of mitochondrial homeostasis after acute kidney injury. American Journal of Physiology-Renal Physiology, 302, 853-864.

Gall, J. M., Wang, Z., Liesa, M., Molina, A., Havasi, A., Schwartz, J. H., Shirihai, O., Borkan, S. C. and Bonegio, R. G. (2012) Role of mitofusin 2 in the renal stress response. PLoS ONE, 7(1), e31074.

Gallinetti, J., Harputlugil, E. and Mitchell, J. R. (2013) Amino acid sensing in dietary-restriction-mediated longevity: Roles of signal-transducing kinases GCN2 and TOR. Biochemical Journal, 449(1), 1-10.

Gandolfo, M. T., Jang, H. R., Bagnasco, S. M., Ko, G. J., Agreda, P., Satpute, S. R., Crow, M. T., King, L. S. and Rabb, H. (2009) Foxp3+ regulatory T cells participate in repair of ischemic acute kidney injury. Kidney International, 76(7), 717-729.

Garg, H. K. and Bryan, N. S. (2009) Dietary sources of nitrite as a modulator of ischemia/reperfusion injury. Kidney International, 75, 1140-1144.

Garza-Quintero, R., Ortehga-Lopez, J., Stein, J. H. and Venkatachalam, M. A. (1990) Alanine protects rabbit proximal tubules against anoxic injury in vitro. American Journal of Physiology-Renal Physiology, 258, 1075-1083.

Gebicki, S. and Gebicki, J. M. (1993) Formation of peroxides in amino acids and proteins exposed to oxygen free radicals. Biochemical Journal, 289, 743-749.

Geiszt, M., Kopp, J. B., Varnai, P. and Leto, T. L. (2000) Identification of renox, an NAD(P)H oxidase in kidney. Proceedings of the National Academy of Sciences, 97, 8010-8014.

Genovese, F., Manresa, A. A., Leeming, D. J., Karsdal, M. A. and Boor, P. (2014) The extracellular matrix in the kidney: A source of novel non-invasive biomarkers of kidney fibrosis? Fibrogenesis and Tissue Repair, 7, 4.

Gores, G. J., Nieminen, A. L., Fleishman, K. E., Dawson, T. L., Herman, B. and Lemasters, J. (1988) Extracellular acidosis delays onset of cell death in ATP-depleted hepatocytes. American Journal of Physiology, 255, 315-322.

Gores, G. J., Nieminen, A. L., Wray, B. E., Herman, B. and Lemasters, J. (1989) Intracellular pH during "chemical hypoxia" in cultured rat hepatocytes: Protection by intracellular acidosis against the onset of cell death. Journal of Clinical Investigation, 83, 386-396.

Grahammer, F., Haenisch, N., Steinhardt, F., Sandner, L., Roerden, M., Arnold, F., Cordts, T., Wanner, N., Reichardt, W., Kerjaschki, D., Ruegg, M. A., Hall, M. N., Moulin, P., Busch, H., Boerries, M., Walz, G., Artunc, F. and Huber, T. B. (2014) mTORC1 maintains renal tubular homeostasis and is essential in response to ischemic stress. Proceedings of the National Academy of Sciences, 111(27), 2817-2826.

Greene, E. L. and Paller, M. S. (1994) Calcium and free radicals in hypoxia/reoxygenation injury of renal epithelial cells. American Journal of Physiology-Renal Physiology, 266(1), 13-20.

Greka, A. and Mundel, P. (2012) Cell biology and pathology of podocytes. Annual Review of Physiology, 74, 299-323.

Grollman, A. P., Shibutani, S., Moriya, M., Miller, F., Wu, L., Moll, U., Suzuki, N., Fernandes, A., Rosenquist, T., Medverec, Z., Jakovina, K., Brdar, B., Slade, N., Turesky, R. J., Goodenough, A. K., Rieger, R., Vukelić, M. and Jelaković, B. (2007) Aristolochic acid and the etiology of endemic (Balkan) nephropathy. Proceedings of the National Academy of Sciences, 104, 12129-12134.

Gryglewski, R. J., Palmer, R. M. J. and Moncada, S. (1986) Superoxide anion is involved in the breakdown of endothelium-derived vascular relaxing factor. Nature, 320, 454-456.

Guarnieri, G., Situlin, R. and Toigo, G. (2005) Chapter 13. The kidney. In: Gibney, M. J., Elia, M., Ljungqvist, O. and Dowsett, J. (Eds.) Clinical nutrition. Oxford: Blackwell Science.

Gunst, J., Vanhorebeek, I., Casaer, M. P., Hermans, G., Wouters, P. J., Dubois, J., Claes, K., Schetz, M. and Van den Berghe, G. (2013) Impact of early parenteral nutrition on metabolism and kidney injury. Journal of the American Society Nephrology, 24, 995-1005.

Gupta, A., Puri, V., Sharma, R. and Puri, S. (2012) Folic acid induces acute renal failure (ARF) by enhancing renal prooxidant state. Experimental and Toxicologic Pathology, 64, 3, 225-232.

Haigis, M. C. and Yankner, B. A. (2010) The aging stress response. Molecular Cell, 40, 333-344.

Hakroush, S., Moeller, M. J., Theilig, F., Kaissling, B., Sijmonsma, T. P., Jugold, M., Akeson, A. K., Traykova-Brauch, M., Hosser, H., Hähnel, B., Gröne, H. J., Koesters, R. and Kriz, W. (2009) Effects of increased renal tubular vascular endothelial growth factor (VEGF) on fibrosis, cyst formation, and glomerular disease. American Journal of Pathology, 175(5), 1883-1895.

Halestrap, A. P., Clarke, S. J. and Javadov, S. A. (2004) Mitochondrial permeability transition pore opening during myocardial reperfusion - A target for cardioprotection. Cardiovascular Research, 61, 372-385.

Hall, N. A. and Fox, A. J. (2006) Renal replacement therapies in critical care. Continuing Education in Anaesthesia Critical Care and Pain, 6(5), 197-202.

Hallman, M. A., Zhuang, S. and Schnellmann, R. G. (2008) Regulation of dedifferentiation and redifferentiation in renal proximal tubular cells by the epidermal growth factor receptor. The Journal of Pharmacology and Experimental Therapeutics, 325, 520-528.

Hara, K., Yonezawa, K., Weng, Q. P., Kozlowski, M. T., Belham, C. and Avruch, J. (1998) Amino acid sufficiency and mTOR regulate p70 S6 kinase and eIF-4E BP1 through a common effector mechanism. Journal of Biological Chemistry, 273(23), 14484-14494.

Haraldsson, B. and Sorensson, J. (2004) Why do we not all have proteinuria? An update of our current understanding of the glomerular barrier. News Physiological Sciences, 19, 7-10.

Hardie, D. G., Hawley, S. A. and Scott, J. W. (2006) AMP-activated protein kinase-development of the energy sensor concept. Journal of Physiology, 574, 7-15.

Harding, H. P., Zhang, Y., Bertolotti, A., Zeng, H. and Ron, D. (2000) Perk is essential for translational regulation and cell survival during the unfolded protein response. Molecular Cell, 5, 897-904.

Harrison, R. (2002) Structure and function of xanthine oxidoreductase: Where are we now? Free Radical Biology and Medicine, 33(6), 774-797.

Hausenloy, D. J., Mwamure, P. K., Venugopal, V., Harris, J., Barnard, M., Grundy, E., Ashley, E., Vichare, S., Di Salvo, C., Kolvekar, S., Hayward, M., Keogh, B., MacAllister, R. J. and Yellon, D. M. (2007) Effect of remote ischaemic preconditioning on myocardial injury in patients undergoing coronary artery bypass graft surgery: A randomised controlled trial. Lancet, 370, 575-579.

Havasi, A. and Borkan, S. C. (2011) Apoptosis and acute kidney injury. Kidney International, 80, 29-40.

Haworth, R. A. and Hunter, D. R. (1979) The Ca2+-induced membrane transition in mitochondria: II. Nature of the Ca2+ trigger site. Archives of Biochemistry and Biophysics, 195 (2), 460-467.

Hendgen-Cotta, U. B., Merx, M. W., Shiva, S., Schmitz, J., Becher, S., Klare, J. P., Steinhoff, H. J., Goedecke, A., Schrader, J., Gladwin, M. T., Kelm, M. and Rassaf, T. (2008) Nitrite reductase activity of myoglobin regulates respiration and cellular viability in myocardial ischemia-reperfusion injury. Proceedings of the National Academy of Sciences of the United States of America, 105(29), 10256-10261.

Herlitz, L. C., Mohan, S., Stokes, M. B., Radhakrishnan, J., D'Agati, V. D. and Markowitz, G. S. (2010) Tenofovir nephrotoxicity: Acute tubular necrosis with

distinctive clinical, pathological, and mitochondrial abnormalities. Kidney International, 78(11), 1171-1177.

Herrera, M., Silva, G. and Garvin, J. L. (2006) A high-salt diet dissociates NO synthase-3 expression and NO production by the thick ascending limb. Hypertension, 47, 95-101.

Heusch, G. (2013) Cardioprotection: Chances and challenges of its translation to the clinic. Lancet, 381, 166-175.

Hickey, E. J., Raje, R. R., Reid, V. E., Gross, S. M. and Ray, S. D. (2001) Diclofenac induced in vivo nephrotoxicity may involve oxidative stress-mediated massive genomic DNA fragmentation and apoptotic cell death. Free Radical Biology and Medicine, 31(2), 139-152.

Higashi, Y., Sasaki, S., Nakagawa, K., Fukuda, Y., Matsuura, H., Oshima, T. and Chayama, K. (2002) Tetrahydrobiopterin enhances forearm vascular response to acetylcholine in both normotensive and hypertensive individuals. American Journal of Hypertension, 15(4), 326-332.

Hochachka, P. W. and Mommsen, T. P. (1993) Protons and anaerobiosis. Science, 219, 1391-1397.

Holley, J. L. (2005) Clinical approach to the diagnosis acute renal failure. In: Greenberg, A. (Ed.) Primer on kidney diseases. Pennsylvania: Saunders Elsevier.

Hollien, J., Lin, J. H., Li, H., Stevens, N., Walter, P. and Weissman, J. S. (2009) Regulated Ire1-dependent decay of messenger RNAs in mammalian cells. Journal of Cell Biology, 186, 323-331.

Huang, J. X., Kaeslin, G., Ranall, M. V., Blaskovich, M. A., Becker, B., Butler, M. S., Little, M. H., Lash, L. H. and Cooper, M. A. (2015) Evaluation of biomarkers for in vitro prediction of drug-induced nephrotoxicity: Comparison of HK-2, immortalized human proximal tubule epithelial, and primary cultures of human proximal tubular cells. Pharmaceutical Research, 3(3), e00148.

Huang, P. L. (2009) eNOS, metabolic syndrome and cardiovascular disease. Trends in Endocrinology and Metabolism, 20, 295-302.

Huang, P. L., Huang, Z., Mashimo, H., Bloch, K. D., Moskowitz, M. A., Bevan, J. A. and Fishman, M. C. (1995) Hypertension in mice lacking the gene for endothelial nitric oxide synthase. Nature, 377(6546), 239-2342.

Humes, H. D. (1995) Chapter 7. Acute renal failure. In: Shayman, J. A. (Ed.) Renal pathophysiology. Philadelphia: J. B. Lippincott.

Humes, H. D., Nakamura, T., Cieslinski, D. A., Miller, D., Emmons, R. V. and Border, W. A. (1993) Role of proteoglycans and cytoskeleton in the effects of TGF-beta 1 on renal proximal tubule cells. Kidney International, 43, 575-584.

Humphreys, B. D., Valerius, M. T., Kobayashi, A., Mugford, J. W., Soeung, S., Duffield, J. S., McMahon, A. P. and Bonventre, J. V. (2008) Intrinsic epithelial cells repair the kidney after injury. Cell Stem Cell, 2(3), 284-291.

Hunault, C. C., Van Velzen, A. G., Sips, A. J., Schothorst, R. C. and Meulenbelt, J. (2009) Bioavailability of sodium nitrite from an aqueous solution in healthy adults. Toxicology Letters, 190, 48-53.

Hung, C. C., Ichimura, T., Stevens, J. L. and Bonventre, J. V. (2003) Protection of renal epithelial cells against oxidative injury by endoplasmic reticulum stress preconditioning is mediated by ERK1/2 activation. The Journal of Biological Chemistry, 278, 31, 29317-29326.

Hwang, C., Sinskey, A. J. and Lodish, H. F. (1992) Oxidized redox state of glutathione in the endoplasmic reticulum. Science, 257, 1496-1502.

Hwang, J. K., Kim, J. M., Kim, Y. K., Kim, S. D., Park, S. C., Kim, J. I., Nam, H. W., Kim, J. and Moon, I. S. (2013) The early protective effect of glutamine pretreatment and ischemia preconditioning in renal ischemia-reperfusion injury of rat. Transplantation Proceeding, 45(9), 3203-3208.

IARC (2002) Some traditional herbal medicines, some mycotoxins, naphthalene and styrene. IARC Monographs on Evaluation of Carcinogenic Risks to Humans, 82, 1-556.

Ichimura, T., Finch, P. W., Zhang, G., Kan, M. and Stevens, J. L. (1996) Induction of FGF-7 after kidney damage: A possible paracrine mechanism for tubule repair. American Journal of Physiology-Renal Physiology, 271, 967-976.

Igawa, T., Matsumoto, K., Kanda, S., Saito, Y. and Nakamura, T. (1993) Hepatocyte growth factor may function as a renotropic factor for regeneration in rats with acute renal injury. American Journal of Physiology-Renal Physiology, 265(1), 61-69.

Imai, M. and Kokko, J. P. (1974) Sodium chloride, urea, and water transport in the thin ascending limb of Henle. Generation of osmotic gradients by passive diffusion of solutes. Journal of Clinical Investigation, 53(2), 393-402.

Imgrund, M., Gröne, E., Gröne, H. J., Kretzler, M., Holzman, L., Schlöndorff, D. and Rothenpieler, U. W. (1999) Re-expression of the developmental gene Pax-2 during experimental acute tubular necrosis in mice 1. Kidney International, 56(4), 1423-1431.

Inagi, R. (2009) Endoplasmic reticulum stress in the kidney as a novel mediator of kidney injury. Nephron Experimental Nephrology, 112, 1-9.

Inagi, R., Ishimoto, Y. and Nangaku, M. (2014) Proteostasis in endoplasmic reticulum - New mechanisms in kidney disease. Nature Reviews Nephrology, 10, 369-378.

Inoki, K., Zhu, T. and Guan, K. L. (2003) TSC2 mediates cellular energy response to control cell growth and survival. Cell, 115(5), 577-590.

Ishani, A., Xue, J. L., Himmelfarb, J., Eggers, P. W., Kimmel, P. L., Molitoris, B. A. and Collins, A. J. (2009) Acute kidney injury increases risk of ESRD among elderly. Journal of the American Society of Nephrology, 20, 223-228.

Jain, M., Nilsson, R., Sharma, S., Madhusudhan, N., Kitami, T., Souza, A. L., Kafri, R., Kirschner, M. W., Clish, C. B. and Mootha, V. K. (2012) Metabolite profiling identifies a key role for glycine in rapid cancer cell proliferation. Science, 336(6084), 1040-1044.

Janssen, W. M., Beekhuis, H., De Bruin, R., De Jong, P. E. and De Zeeuw, D. (1995) Noninvasive measurement of intrarenal blood flow distribution: Kinetic model of renal 123I-hippuran handling. American Journal of Physiology-Renal Physiology, 269(4), 571-580.

Jennings, P., Koppelstaetter, C., Aydin, S., Abberger, T., Wolf, A. M., Mayer, G. and Pfaller, W. (2007) Cyclosporine A induces senescence in renal tubular epithelial cells. American Journal of Physiology-Renal Physiology, 293(3), 831-838.

Jerkic, M., Varagic, J., Jovovic, D., Radujković-Kuburović, G., Nastić-Mirić, D., Adanja-Grujić, G., Marković-Lipkovski, J., Dimitrijević, J., Miloradović, Z. and Vojvodić, S. B. (1999) L-arginine reduces tubular cell injury in acute post-ischaemic renal failure. Nephrology Dialysis Transplantation, 14, 1398-1407.

Jesinkey, S. R., Funk, J. A., Stallons, L. J., Wills, L. P., Megyesi, J. K., Beeson, C. C. and Schnellmann, R. G. (2014) Formoterol restores mitochondrial and renal function after ischemia-reperfusion injury. Journal of the American Society of Nephrology, 25(6), 1157-1162.

Jheng, H. F., Tsai, P. J., Guo, S. M., Kuo, L. H., Chang, C. S., Su, I. J., Chang, C. R. and Tsaia, Y. S. (2012) Mitochondrial fission contributes to mitochondrial dysfunction and insulin resistance in skeletal muscle. Molecular and Cellular Biology, 32(2), 309-319.

Jiang, M., Liu, K., Luo, J. and Dong, Z. (2010) Autophagy is a renoprotective mechanism during in vitro hypoxia and in vivo ischemia-reperfusion injury. American Journal of Pathology, 176(3), 1181-1192.

Jiang, W. G., Martin, T. A., Parr, C., Davies, G., Matsumoto, K. and Nakamura, T. (2005) Hepatocyte growth factor, its receptor, and their potential value in cancer therapies. Critical Reviews in Oncology/Hematology, 53(1), 35-69.

Jokivarsi, K. T., Grohn, H. I., Grohn, O. H. and Kauppinen, R. A. (2007) Proton transfer ratio, lactate, and intracellular pH in acute cerebral ischemia. Magnetic Resonance in Medicine, 57, 647-653.

Jung, C. H., Ro, S. H., Cao, J., Otto, N. M. and Kim, D. H. (2010) mTOR regulation of autophagy. FEBS Letters, 584, 1287-1295.

Jung, K. H., Chu, K., Ko, S. Y., Lee, S. T., Sinn, D. I., Park, D. K., Kim, J. M., Song, E. C., Kim, M. and Roh, J. K. (2006) Early intravenous infusion of sodium nitrite protects brain against in vivo ischemia-reperfusion injury. Stroke, 37, 2744-2750.

Kadkhodaee, M., Gobe, G. C., Willgoss, D. A. and Endre, Z. H. (1998) DNA fragmentation reduced by antioxidants following ischaemia-reperfusion in the isolated perfused rat kidney. Nephrology, 4(3), 163-175.

Kakoki, M., Hirata, Y., Hayakawa, H., Suzuki, E., Nagata, D., Tojo, A., Nishimatsu, H., Nakanishi, N., Hattori, Y., Kikuchi, K., Nagano, T. and Omata, M. (2000) Effects of tetrahydrobiopterin on endothelial dysfunction in rats with ischemic acute renal failure. Journal of the American Socirty of Nephrology, 11(2), 301-309.

Kalogeris, T., Baines, C. P., Krenz, M. and Korthuis, R. J. (2012) Cell biology of ischemia/reperfusion injury. International Review of Cell and Molecular Biology, 298, 229-317.

Kanematsu, Y., Yamaguchi, K., Ohnishi, H., Motobayashi, Y., Ishizawa, K., Izawa, Y., Kawazoe, K., Kondo, S., Kagami, S., Tomita, S., Tsuchiya, K. and Tamaki, T. (2008) Dietary doses of nitrite restore circulating nitric oxide level and improve renal injury in L-NAME-induced hypertensive rats. American Journal of Physiology-Renal Physiology, 295(5), 1457-1462.

Kang, D. H., Hughes, J., Mazzali, M., Schreiner, G. F. and Johnson, R. J. (2001) Impaired angiogenesis in the remnant kidney model: II. Vascular endothelial growth factor administration reduces renal fibrosis and stabilizes renal function. Journal of the American Society of Nephrology, 12(7), 1448-1457.

Kapuya, O., Vinodb, P. K. and Bánhegyia, G. (2014) mTOR inhibition increases cell viability via autophagy induction during endoplasmic reticulum stress - An experimental and modeling study. FEBS Letters, 4, 704-713.

Karlberg, L., Norlen, B. J., Ojteg, G. and Wolgast, M. (1983) Impaired medullary circulation in postischemic acute renal failure. Acta Physiologica, 118, 11-17.

Karmazyn, M., Sostaric, J. V. and Gan, X. T. (2001) The myocardial Na+/H+ exchanger: A potential therapeutic target for the prevention of myocardial ischaemic and reperfusion injury and attenuation of postinfarction heart failure. Drugs, 61, 375-389.

Kase, H., Hashikabe, Y., Uchida, K., Nakanishi, N. and Hattori, Y. (2005) Supplementation with tetrahydrobiopterin prevents the cardiovascular effects of angiotensin II-induced oxidative and nitrosative stress. Journal of Hypertension, 23(7), 1375-1382.

Kato, H., Nakajima, S., Saito, Y., Takahashi, S., Katoh, R. and Kitamura, M. (2012) mTORC1 serves ER stress-triggered apoptosis via selective activation of the IRE1-JNK pathway. Cell Death and Differentiation, 19, 310-320.

Kaushal, G. P., Basnakian, A. P. and Shah, S. V. (2004) Apoptotic pathways in ischemic renal failure. Kidney International, 66, 500-505.

Kawai, Y. and Gemba, M. (2007) Cisplatin-induced renal injury in LLC-PK1 cells. Japanese Society for Alternatives to Animal Experiments, 14, 453-456.

Kellerman, P. S., Clark, R. A., Hoilien, C. A., Linas, S. L. and Molitoris, B. A. (1990) Role of microfilaments in maintenance of proximal tubule structural and functional integrity. American Journal of Physiology-Renal Physiology, 259, 279-285.

Kelly, K. J., Baird, N. R. and Greene, A. L. (2001) Induction of stress response proteins and experimental renal ischemia/reperfusion. Kidney International, 59(5), 1798-1802.

Kerr, M., Bedford, M., Matthews, B. and O'Donoghue, D. (2014) The economic impact of acute kidney injury in England. Nephrology Dialysis Transplantation, 29, 1362-1368.

Kidney Disease Improving Global Outcomes (2012) KDIGO Clinical practice guideline for acute kidney injury. Official Journal of the International Society of Nephrology, 2(1), 1-138.

Kim, D. H., Sarbassov, D. D., Ali, S. M., King, J. E., Latek, R. R., Erdjument-Bromage, H., Tempst, P. and Sabatini, D. M. (2002) mTOR interacts with raptor to form a nutrient-sensitive complex that signals to the cell growth machinery. Cell, 110, 163-175.

Kim, H. Y. (2009) Renal handling of ammonium and acid base regulation. Electrolytes and Blood Pressure, 7(1), 9-13.

Kim, J. S., Jin, Y. and Lemasters, J. J. (2006) Reactive oxygen species, but not Ca2+ overloading, trigger pH- and mitochondrial permeability transition-dependent death of adult rat myocytes after ischemia-reperfusion. American Journal of Physiology-Heart and Circulatory Physiology, 290, 2024-2034.

Kim, M. G., Kim, S. C., Ko, Y. S., Lee, H. Y., Jo, S. K. and Cho, W. (2015) The role of M2 macrophages in the progression of chronic kidney disease following acute kidney injury. PLoS ONE, 10(12), e0143961.

Kim, M. G., Koo, T. Y., Yan, J. J., Lee, E., Han, K. H., Jeong, J. C., Ro, H., Kim, B. S., Jo, S. K., Oh, K. H., Surh, C. D., Ahn, C. and Yang, J. (2013) IL-2/anti-IL-2 complex attenuates renal ischemia-reperfusion injury through expansion of regulatory T cells. Journal of the American Society of Nephrology, 24(10), 1529-1536.

Klatt, P., Schmidt, K., Lehner, D., Glatter, O., Bachinger, H. P. and Mayer, B. (1995) Structural analysis of porcine brain nitric oxide synthase reveals a role for tetrahydrobiopterin and L-arginine in the formation of an SDS-resistant dimer. EMBO Journal, 14(15), 3687-3695.

Koeppen, B. M. and Stanton, B. A. (2013) Structure and functions of the kidneys. In: Renal physiology, 5th edition, 15-26. Philadelphia: Saunders Elsevier.

Kone, B. C. (2004) Nitric oxide synthesis in the kidney: Iso-forms, biosynthesis, and functions in health. Seminar in Nephrology, 24, 299-315.

Kramann, R., Kobayashi, A. and Humphreys, B. D. (2013) Differentiated kidney epithelial cells repair injured proximal tubule. Proceedings of the National Academy of Sciences, 111, 1527-1532.

Kroshian, V. M., Sheridan, A. and Lieberthal, W. (1994) Functional and cytoskeletal changes induced by sublethal injury in proximal tubular epithelial cells. American Journal of Physiology-Renal Physiology, 266, 21-30.

Kruidering, M., Van De Water, B., De Heer, E., Mulder, G. J. and Nagelkerke, J. F. (1997) Cisplatin-induced nephrotoxicity in porcine proximal tubular cells: Mitochondrial dysfunction by inhibition of complexes I to IV of the respiratory chain. Journal of Pharmacology and Experimental Therapeutics, 280(2), 638-649.

Kubes, P., Suzuki, M. and Granger, D. N. (1991) Nitric oxide: An endogenous modulator of leukocyte adhesion. Proceedings of the National Academy of Sciences, 88(11), 4651-4655.

Kulkarni, O. P., Hartter, I., Mulay, S. R., Hagemann, J., Darisipudi, M. N., Kumar VR, S., Romoli, S., Thomasova, D., Ryu, M., Kobold, S. and Anders, H. J. (2014) Toll-like receptor 4-induced IL-22 accelerates kidney regeneration. Journal of the American Society of Nephrology, 25(5), 978-989.

Kurian, G. A. and Pemaih, B. (2014) Standardization of in vitro cell-based model for renal ischemia and reperfusion injury. Indian Journal of Pharmaceutical Sciences, 76(4), 348-353.

Kurts, C., Panzer, U., Anders, H. J. and Rees, A. J. (2013) The immune system and kidney disease: Basic concepts and clinical implications. Nature Reviews Immunology, 13, 738-753.

Kusaka, J., Koga, H., Hagiwara, S., Hasegawa, A., Kudo, K. and Noguchi, T. (2012) Age-dependent responses to renal ischemia-reperfusion injury. Journal of Surgical Research, 172(1), 153-158.

Lafrance J. P. and Miller, D. R. (2010) Acute kidney injury associates with increased long-term mortality. Journal of the American Society of Nephrology, 21(2), 345-352.

Lameire, N., Van Biesen, W. and Vanholder, R. (2005) Acute renal failure. Seminar, 365, 417-430.

Lameire, N. H. and Vanholder, R. (2004) Pathophysiology of ischaemic acute renal failure. Best Practice and Research Clinical Anaesthesiology, 18, 21-36.

Larsen, F. J., Schiffer, T. A., Borniquel, S., Sahlin, K., Ekblom, B., Lundberg, J. O. and Weitzberg, E. (2011) Dietary inorganic nitrate improves mitochondrial efficiency in humans. Cell Metabolism, 13, 149-159.

Lazzeri, E., Crescioli, C., Ronconi, E., Mazzinghi, B., Sagrinati, C., Netti, G. S., Angelotti, M. L., Parente, E., Ballerini, L., Cosmi, L., Maggi, L., Gesualdo, L., Rotondi, M., Annunziato, F., Maggi, E., Lasagni, L., Serio, M., Romagnani, S., Vannelli, G. B. and Romagnani, P. (2007) Regenerative potential of embryonic renal multipotent progenitors in acute renal failure. Journal of the American Society of Nephrology, 18(12), 3128-3138.

Leblanc, M., Kellum, J. A., Gibney, R. T., Lieberthal, W., Tumlin, J. and Mehta, R. (2005) Risk factors for acute renal failure: Inherent and modifiable risks. Current Opinion in Critical Care, 11(6), 533-536.

Lech, M. and Anders, H. J. (2013) Macrophages and fibrosis: How resident and infiltrating mononuclear phagocytes orchestrate all phases of tissue injury and repair. Biochimica et Biophysica Acta, 1832, 7, 989-997.

Lech, M., Avila-Ferrufino, A., Allam, R., Segerer, S., Khandoga, A., Krombach, F., Garlanda, C., Mantovani, A. and Anders, H. J. (2009) Resident dendritic cells prevent postischemic acute renal failure by help of single Ig IL-1 receptor-related protein. Journal of Immunology, 183, 4109-4118.

Lee, K., Tirasophon, W., Shen, X., Michalak, M., Prywes, R., Okada, T., Yoshida, H., Mori, K. and Kaufman, R. J. (2002) IRE1-mediated unconventional mRNA splicing and S2P-mediated ATF6 cleavage merge to regulate XBP1 in signaling the unfolded protein response. Genes and Development, 16, 452-466.

Lee, S., Huen, S., Nishio, H., Nishio, S., Lee, H. K., Choi, B. S., Ruhrberg, C. and Cantley, L. G. (2011) Distinct macrophage phenotypes contribute to kidney injury and repair. Journal of the American Society of Nephrology, 22 (2), 317-326.

Lewington, A. and Kanagasundaram, S. (2011) Clinical practice guidelines. Acute kidney injury. Hampshire, United Kindon: UK Renal Association.

Li, B., Cohen, A., Hudson, T. E., Motlagh, D., Amrani, D. L. and Duffield, J. S. (2010) Mobilized human hematopoietic stem/progenitor cells promote kidney repair after ischemia/reperfusion injury. Circulation, 121(20), 2211-2220.

Li, H., Samouilov, A., Liu, X. and Zweier, J. L. (2003) Characterization of the magnitude and kinetics of xanthine oxidase-catalyzed nitrate reduction: Evaluation of its role in nitrite and nitric oxide generation in anoxic tissues. Biochemistry, 42(4), 1150-1159.

Li, M., Zhao, L., Liu, J., Liu, A., Jia, C., Ma, D., Jiang, Y. and Bai, X. (2010) Multi-mechanisms are involved in reactive oxygen species regulation of mTORC1 signaling. Cellular Signalling, 22, 1469-1476.

Li, M. O., Wan, Y. Y., Sanjabi, S., Robertson, A. K. and Flavell, R. A. (2006a) Transforming growth factor beta regulation of immune responses. Annual Review of Immunology, 24, 99-146.

Li, S., Wu, P., Yarlagadda, P., Vadjunec, N. M., Proia, A. D., Harris, R. A. and Portilla, D. (2004) PPAR alpha ligand protects during cisplatin-induced acute renal failure by preventing inhibition of renal FAO and PDC activity. American Journal of Physiology-Renal Physiology, 286(3), 572-580.

Li, X., Liu, M., Bedja, D., Thoburn, C., Gabrielson, K., Racusen, L. and Rabb, H. (2012) Acute renal venous obstruction is more detrimental to the kidney than arterial occlusion: Implication for murine models of acute kidney injury. American Journal of Physiology-Renal Physiology, 302(5), 519-525.

Li, Y., Liu, Z., Guo, X., Shu, J., Chen, Z. and Li, L. (2006) Aristolochic acid I-induced DNA damage and cell cycle arrest in renal tubular epithelial cells in vitro. Archives of Toxicology, 80(8), 524-532.

Li, Z. Y., Liu, B., Yu, J., Yang, F. W., Luo, Y. N. and Ge, P. F. (2012) Ischaemic postconditioning rescues brain injury caused by focal ischaemia/reperfusion via attenuation of protein oxidization. Journal of International Medical Research, 40(3), 954-966.

Lidder, S. and Webb, A. J. (2012) Vascular effects of dietary nitrate (as found in green leafy vegetables and beetroot) via the nitrate-nitrite-nitric oxide pathway. British Journal of Clinical Pharmacology, 75(3), 677-696.

Lieberthal, W. (2008) Macroautophagy: A mechanism for mediating cell death or for promoting cell survival? Kidney International, 74, 555-557.

Lieberthal, W., Fuhro, R., Andry, C., Patel, V. and Levine, J. S. (2006) Rapamycin delays but does not prevent recovery from acute renal failure: Role of acquired tubular resistance. Transplantation, 82, 17-22.

Lieberthal, W., Fuhro, R., Andry, C. C., Rennke, H., Abernathy, V. E., Koh, J. S., Valeri, R. and Levine, J. S. (2001) Rapamycin impairs recovery from acute renal failure: Role of cell-cycle arrest and apoptosis of tubular cells. American Journal of Physiology-Renal Physiology, 281, 693-706.

Lieberthal, W. and Levine, J. S. (2009) The role of the mammalian target of rapamycin (mTOR) in renal disease. Journal of the American Society of Nephrology, 20, 2493-2502.

Lieberthal, W. and Levine, J. S. (2012) Mammalian target of rapamycin and the kidney. I. The signaling pathway. American Journal of Physiology-Renal Physiology, 303(1), 1-10.

Lieberthal, W. and Nigam, S. K. (2000) Acute renal failure. II. Experimental models of acute renal failure: Imperfect but indispensable. American Journal of Physiology-Renal Physiology, 278(1), 1-12.

Lim, B. J., Yang, H. C. and Fogo, A. B. (2014) Animal models of regression/progression of kidney disease. Drug Discovery Today, 11, 45-51.

Lin, F., Cordes, K., Li, L., Hood, L., Couser, W. G., Shankland, S. J. and Igarashi, P. (2003) Hematopoietic stem cells contribute to the regeneration of renal tubules after renal ischemia-reperfusion injury in mice. Journal of the American Society of Nephrology, 14(5), 1188-1199.

Lin, S. L., Li, B., Rao, S. Yeo, E. J., Hudsona, T. E., Nowlina, B. T., Peia, H., Chen, L., Zhenge, J. J., Carrollf, T. J., Pollardg, J. W., McMahonh, A. P., Langc, R. A. and Duffielda, J. S. (2010) Macrophage Wnt7b is critical for kidney repair and regeneration. Proceedings of the National Academy of Sciences, 107(9), 4194-4199.

Linz, W. J. and Busch, A. E. (2003) NHE-1 inhibition: From protection during acute ischaemia/reperfusion to prevention/reversal of myocardial remodeling. Naunyn-Schmiedeberg's Archives of Pharmacology, 368, 239-246.

Liu, H. and Baliga, R. (2003) Cytochrome P450 2E1 null mice provide novel protection against cisplatin-induced nephrotoxicity and apoptosis. Kidney International, 63, 1687-1696.

Liu, H. and Baliga, R. (2005) Endoplasmic reticulum stress-associated caspase 12 mediates cisplatin-induced LLC-PK1 cell apoptosis. Journal of the American Society of Nephrology, 16(7), 1985-1992.

Liu, H. H. (2013) Identification of optimal concentration of amino acid supplements for prevention of acute kidney injury. MSc Dissertation. University of Nottingham.

Liu, K. D. and Chertow, G. M. (2008) Chapter 10. Acute renal failure. In: Fauci, A. S., Braunwald, E., Kasper, D. L., Hauser, S. L., Longo, D. L., Jameson, J. L. and Loscalzo, J. (Eds.) Harrison's principles of internal medicine. New York: McGraw-Hill.

Liu, L., Cash, T. P., Jones, R. G., Keith, B., Thompson, C. B. and Simon, M. C. (2006) Hypoxia-induced energy stress regulates mRNA translation and cell growth. Molecular Cell, 21, 521-531.

Liu, Y. (2011) Cellular and molecular mechanisms of renal fibrosis. Nature Reviews Nephrology, 7, 684-696.

Lloberas, N., Cruzado, J. M., Franquesa, M., Herrero-Fresneda, I., Torras, J., Alperovich, G., Rama, I., Vidal, A. and Grinyó, J. M. (2006) Mammalian target of rapamycin pathway blockade slows progression of diabetic kidney disease in rats. Journal of the American Society of Nephrology, 17, 1395-1404.

Lo, L. J., Go, A. S., Chertow, G. M., McCulloch, C. E., Fan, D., Ordonez, J. D. and Hsu, C. Y. (2009) Dialysis-requiring acute renal failure increases the risk of progressive chronic kidney disease. Kidney International, 76, 893-899.

Loewith, R., Jacinto, E., Wullschleger, S., Lorberg, A., Crespo, J. L., Bonenfant, D., Oppliger, W., Jenoe, P. and Hall, M. N. (2002) Two TOR complexes, only one of which is rapamycin sensitive, have distinct roles in cell growth control. Molecular Cell, 10, 457-468.

Loverre, A., Ditonno, P., Crovace, A., Gesualdo, L., Ranieri, E., Pontrelli, P., Stallone, G., Infante, B., Schena, A., Di Paolo, S., Capobianco, C., Ursi, M., Palazzo, S., Battaglia, M., Selvaggi, F. P., Schena, F. P. and Grandaliano, G. (2004) Ischemia reperfusion induces glomerular and tubular activation of proinflammatory and antiapoptotic pathways: Differential modulation by rapamycin. Journal of the American Society of Nephrology, 15, 2675-2686.

Lu, P., Liu, F., Yao, Z., Wang, C. Y., Chen, D. D., Tian, Y., Zhang, J. H. and Wu, Y. H. (2005) Nitrite-derived nitric oxide by xanthine oxidoreductase protects the liver against ischemia-reperfusion injury. Hepatobiliary and Pancreatic Diseases International, 4(3), 350-355.

Lundberg, J. O., Carlstro ¨m, M., Larsen, F. J. and Weitzberg, E. (2011) Roles of dietary inorganic nitrate in cardiovascular health and disease. Cardiovascular Research, 89, 525-532.

Lundberg, J. O. and Govoni, M. (2004) Inorganic nitrate is a possible source for systemic generation of nitric oxide. Free Radical Biology and Medicine, 37, 395-400.

Lundberg, J. O. and Weitzberg, E. (2005) NO generation from nitrite and its role in vascular control. Arteriosclerosis, Thrombosis, and Vascular Biology, 25, 915-922.

Lundberg, J. O. N., Weitzberg, E., Lundberg, J. M. and Alving, K. (1994) Intragastric nitric oxide production in humans: Measurement in expelled air. Gut, 35, 1543-1546.

Macias, W. L., Alaka, K. J., Murphy, M. H., Miller, M. E., Clark, W. R. and Mueller, B. A. (1996) Impact of the nutritional regimen on protein catabolism and nitrogen balance in patients with acute renal failure. Journal of Parenteral and Enteral Nutrition, 20, 56-62.

Maddocks, O. D. K., Berkers, C. R., Mason, S. M., Zheng, L., Blyth, K., Gottlieb, E. and Vousden, K. H. (2012) Serine starvation induces stress and p53-dependent metabolic remodeling in cancer cells. Nature, 493(7433), 542-546.

Maeshima, A., Takahashi, S., Nakasatomi, M. and Nojima, Y. (2015) Diverse cell populations involved in regeneration of renal tubular epithelium following acute kidney injury. Stem Cells International, 2015, 964849.

Maher, A. R., Milsom, A. B., Gunaruwan, P., Abozguia, K., Ahmed, I., Weaver, R. A., Thomas, P., Ashrafian, H., Born, G. V., James, P. E. and Frenneaux, M. P. (2008)

Hypoxic modulation of exogenous nitrite-induced vasodilation in humans. Circulation, 117, 670-677.

Majid, D. S. and Navar, L. G. (2001) Nitric oxide in the control of renal hemodynamics and excretory function. American Journal of Hypertension, 14, 74-82.

Malhotra, J. D. and Kaufman, R. J. (2007) Endoplasmic reticulum stress and oxidative stress: A vicious cycle or a double-edged sword? Antioxidants and Redox Signaling, 9(12), 2277-2293.

Marino, M. L., Pellegrini, P., Lernia, G. D., Djavaheri-Mergny, M., Brnjic, S., Zhang, X., Hägg, M., Linder, S., Fais, S., Codogno, P. and De Milito, A. (2012) Autophagy is a protective mechanism for human melanoma cells under acidic stress. Journal of Biological Chemistry, 287(36), 30664-30676.

Markowitz, G. S. and Perazella, M. A. (2005) Drug-induced renal failure: A focus on tubulointerstitial disease. Clinica Chimica Acta, 351(1-2), 31-47.

Martinou, J. C. and Green, D. R. (2001) Breaking the mitochondrial barrier. Nature Reviews Molecular Cell Biology, 2, 63-67.

Matejka, G. L. and Jennische, E. (1992) IGF-I binding and IGF-I mRNA expression in the post-ischemic regenerating rat kidney. Kidney International, 42(5), 1113-1123.

Mayer, B. and Werner, E. R. (1995) In search of a function for tetrahydrobiopterin in the biosynthesis of nitric oxide. Naunyn-Schmiedeberg's Archives of Pharmacology, 351, 453-463.

McClellan, A. J., Tam, S., Kaganovich, D. and Frydman, J. (2005) Protein quality control: Chaperones culling corrupt conformations. Nature Cell Biology, 7, 736-741.

McKnight, G. M., Smith, L. M., Drummond, R. S., Duncan, C. W., Golden, M. and Benjamin, N. (1997) Chemical synthesis of nitric oxide in the stomach from dietary nitrate in humans. Gut, 40, 211-214.

Megyesi, J., Di Mari, J., Udvarhelyi, N., Price, P. M. and Safirstein, R. (1995) DNA synthesis is dissociated from the immediate-early gene response in the post-ischemic kidney. Kidney International, 48(5), 1451-1458.

Mehta, R. L., Kellum, J. A., Shah, S. V., Molitoris, B. A., Ronco, C., Warnock, D. G., Levin, A. and Acute Kidney Network (2007) Acute kidney injury network: Report of an initiative to improve outcomes in acute kidney injury. Critical Care, 11(2), R31.

Mei, N., Arlt, V. M., Phillips, D. H., Heflich, R. H. and Chen, T. (2006) DNA adduct formation and mutation induction by aristolochic acid in rat kidney and liver. Mutation Research, 602, 83-91.

Metallo, C. M., Gameiro, P. A., Bell, E. L., Mattaini, K. R., Yang, J., Hiller, K., Jewell, C. M., Johnson, Z. R., Irvine, D. J., Guarente, L., Kelleher, J. K., Vander Heiden, M. G., Iliopoulos, O. and Stephanopoulos, G. (2011) Reductive glutamine metabolism by IDH1 mediates lipogenesis under hypoxia. Nature, 481(7381), 380-384.

Metcalfe, W., Simpson, M., Khan, I. H., Prescott, G. J., Simpson, K., Smith, W. C. and MacLeod, A. M. (2002) Acute renal failure requiring renal replacement therapy: Incidence and outcome. An International Journal of Medicine, 95, 579-583.

Miklós, Z., Kürthy, M., Degrell, P., Ranczinger, E., Vida, M., Lantos, J., Arató, E., Sínay, L., Hardi, P., Balatonyi, B., Ferencz, S., Jávor, S., Kovács, V., Borsiczky, B., Wéber, G., Rőth, E. and Jancsó, G. (2012) Ischaemic postconditioning reduces serum and tubular TNF-α expression in ischaemic-reperfused kidney in healthy rats. Clinical Hemorheology and Microcirculation, 50(3), 167-178.

Millar, T. M., Stevens, C. R., Benjamin, N., Eisenthal, R., Harrison, R. and Blake, D. R. (1998) Xanthine oxidoreductase catalyses the reduction of nitrates and nitrite to nitric oxide under hypoxic conditions. FEBS Letters, 427(2), 225-228.

Mingeot-Leclercq, M. P. and Tulkens, P. M. (1999) Aminoglycosides: Nephrotoxicity. Antimicrobial Agents and Chemotherapy, 43(5), 1003-1012.

Mitchell, J. R., Verweij, M., Brand, K., Van de Ven, M., Goemaere, N., Van den Engel, S., Chu, T., Forrer, F., Mu¨ ller, C., De Jong, M., Van IJcken, W., IJzermans, J. N. M., Hoeijmakers, J. H. J. and De Bruin, R. W. F. (2010) Short-term dietary restriction and fasting precondition against ischemia reperfusion injury in mice. Aging Cell, 9, 40-53.

Mocan, M. Z., Mocan, H., Gacar, M. N., Özgür, G. K. and Uluutku, M. H. (1995) Effect of essential amino acid supplementation in acute renal failure. International Urology and Nephrology, 27, 4, 503-510.

Moens, A. L. and Kass, D. A. (2006) Tetrahydrobiopterin and cardiovascular disease. Arteriosclerosis, Thrombosis, and Vascular Biology, 26, 2439-2444.

Molitoris, B. (1993) Na+-K+-ATPase that redistributes to apical membrane during ATP depletion remains functional. American Journal of Physiology-Renal Physiology, 265, 693-697.

Molteni, S. N., Fassio, A., Ciriolo, M. R., Filomeni, G., Pasqualetto, E., Fagioli, C. and Sitia, R. (2004) Glutathione limits Ero1-dependent oxidation in the endoplasmic reticulum. Journal of Biological Chemitry, 279, 32667-32673.

Moradi, H. and Wang, P. H. (2013) Renoprotective mechanisms of ischemic postconditioning in ischemia-reperfusion injury: Improved mitochondrial function and integrity. Nephrology Dialysis Transplantation, 28(11), 2667-2669.

Morales, A. I., Detaille, D., Prieto, M., Puente, A., Briones, E., Arévalo, M., Leverve, X., López-Novoa, J. M. and El-Mir, M. Y. (2010) Metformin prevents experimental gentamicin-induced nephropathy by a mitochondria-dependent pathway. Kidney International, 77, 861-869.

Morigi, M., Rota, C., Montemurro, T., Montelatici, E., Lo Cicero, V., Imberti, B., Abbate, M., Zoja, C., Cassis, P., Longaretti, L., Rebulla, P., Introna, M., Capelli, C., Benigni, A., Remuzzi, G. and Lazzari, L. (2010) Life-sparing effect of human cord blood-mesenchymal stem cells in experimental acute kidney injury. Stem Cells, 28(3), 513-522.

Mount, P. F. and Power, D. A. (2006) Nitric oxide in the kidney: Functions and regulation of synthesis. Acta Physiology, 187, 433-446.

Murakami, M., Ichisaka, T., Maeda, M., Oshiro, N., Hara, K., Edenhofer, F., Kiyama, H., Yonezawa, K. and Yamanaka, S. (2004) mTOR is essential for growth and proliferation in early mouse embryos and embryonic stem cells. Molecular and Cellular Biology, 24(15), 6710-6718.

Nakagawa, T., Sato, W., Glushakova, O., Heinig, M., Clarke, T., Campbell-Thompson, M., Yuzawa, Y., Atkinson, M. A., Johnson, R. J. and Croker, B. (2007)

Diabetic endothelial nitric oxide synthase knockout mice develop advanced diabetic nephropathy. Journal of the American Society of Nephrology, 18(2), 539-550.

Nakayama, T., Sato, W., Kosugi, T., Zhang, L., Campbell-Thompson, M., Yoshimura, A., Croker, B. P., Johnson, R. J. and Nakagawa, T. (2009) Endothelial injury due to eNOS deficiency accelerates the progression of chronic renal disease in the mouse. American Journal of Physiology-Renal Physiology, 296(2), 317-327.

Nakayama, T., Sato, W., Yoshimura, A., Zhang, L., Kosugi, T., Campbell-Thompson, M., Kojima, H., Croker, B. P. and Nakagawa, T. (2010) Endothelial von Willebrand factor release due to eNOS deficiency predisposes to thrombotic microangiopathy in mouse aging kidney. American Journal of Pathology, 176(5), 2198-2208.

Nash, K., Hafeez, A. and Hou, S. (2002) Hospital-acquired renal insufficiency. American Journal of Kidney Disease, 39, 930-936.

National Heart, Lung, and Blood Institute Acute Respiratory Distress Syndrome (ARDS) Clinical Trials Network, Rice, T. W., Wheeler, A. P., Thompson, B. T., Steingrub, J., Hite, R. D., Moss, M., Morris, A., Dong, N. and Rock, P. (2012) Initial trophic vs full enteral feeding in patients with acute lung injury: The EDEN randomized trial. JAMA, 307, 795-803.

National Institute for Health and Care Excellence (2013) Acute kidney injury: Prevention, detection and management of acute kidney injury up to the point of renal replacement therapy. London, United Kingdom: NICE.

Naughton, C. (2008) Drug-induced nephrotoxicity. American Family Physician, 78(6), 743-750.

Nazarewicz, R. R., Bikineyeva, A. and Dikalov, S. I. (2013) Rapid and specific measurements of superoxide using fluorescence spectroscopy. Journal of Biomolecular Screening, 18(4), 498-503.

Nishimura, Y., Romer, L. H. and Lemasters, J. J. (1998) Mitochondrial dysfunction and cytoskeletal disruption during chemical hypoxia to cultured rat hepatic sinusoidal endothelial cells: The pH paradox and cytoprotection by glucose, acidotic pH, and glycine. Hepatology, 27(4), 1039-1049.

Noiri, E., Nakao, A., Uchida, K., Tsukahara, H., Ohno, M., Fujita, T., Brodsky, S. and Goligorsky, M. S. (2001) Oxidative and nitrosative stress in acute renal ischemia. American Journal of Physiology-Renal Physiology, 281(5), 948-957.

Nony, P. A. and Schnellmann, R. G. (2003) Mechanisms of renal cell repair and regeneration after acute renal failure. The Journal of Pharmacology and Experimental Therapeutics, 304, 905-912.

Novitskaya, T., McDermott, L., Zhang, K. X., Chiba, T., Paueksakon, P., Hukriede, N. A. and De Caestecker, M. P. (2014) A PTBA small molecule enhances recovery and reduces postinjury fibrosis after aristolochic acid-induced kidney injury. American Journal of Physiology-Renal Physiology, 306(5), 496-504.

Nurko, S., Sogabe, K., Davis, J., Roeser, N., Defrain, M., Chien, A., Hinshaw, D., Athey, B., Meixner, W., Venkatachalam, M. and Weinberg, J. (1996) Contribution of actin cytoskeletal alterations to ATP depletion and calcium-induced proximal tubule cell injury. American Journal of Physiology-Renal Physiology, 270, 39-52.

Okada, H., Kikuta, T., Kobayashi, T., Inoue, T., Kanno, Y., Takigawa, M., Sugaya, T., Kopp, J. B. and Suzuki, H. (2005) Connective tissue growth factor expressed in

tubular epithelium has a pivotal role in renal fibrogenesis. Journal of the American Society of Nephrology, 16, 133-143.

Olliges, A., Wimmer, S. and Nüsing, R. M. (2011) Defects in mouse nephrogenesis induced by selective and non-selective cyclooxygenase-2 inhibitors. British Journal of Pharmacology, 163, 927-936.

Ong, S. B., Subrayan, S., Lim, S. Y., Yellon, D. M., Davidson, S. M. and Hausenloy, D. J. (2010) Inhibiting mitochondrial fission protects the heart against ischemia/reperfusion injury. Circulation, 121, 2012-2022.

Ortiz, P., Stoos, B. A., Hong, N. J., Boesch, D. M., Plato, C. F. and Garvin, J. L. (2003) High-salt diet increases sensitivity to NO and eNOS expression but not NO production in THALs. Hypertension, 41, 682-687.

Ozcan, U., Ozcan, L., Yilmaz, E., Düvel, K., Sahin, M., Manning, B. D. and Hotamisligil, G. S. (2008) Loss of the tuberous sclerosis complex tumor suppressors triggers the unfolded protein response to regulate insulin signaling and apoptosis. Molecular Cell, 29, 541-551.

Paller, M. S., Neumann, T. V., Knobloch, E. and Patten, M. (1991) Reactive oxygen species and rat renal epithelial cells during hypoxia and reoxygenation. Kidney International, 40, 6, 1041-1049.

Pallet, N., Bouvier, N., Bendjallabah, A., Rabant, M., Flinois, J. P., Hertig, A., Legendre, C., Beaune, P., Thervet, E. and Anglicheau, D. (2008) Cyclosporine-induced endoplasmic reticulum stress triggers tubular phenotypic changes and death. American Journal of Transplantation, 8, 2283-2296.

Pallet, N., Bouvier, N., Legendre, C., Gilleron, J., Codogno, P., Beaune, P., Thervet, E. and Anglicheau, D. (2008) Autophagy protects renal tubular cells against cyclosporine toxicity. Autophagy, 4, 783-791.

Palmer, B. F. (2002) Renal dysfunction complicating the treatment of hypertension. The New England Journal of Medicine, 347(16), 1256-1261.

Parivar, F., Narasimhan, P. T. and Ross, B. (1991) Renal corticomedullary metabolite gradients during graded arterial occlusion: A localized 31P magnetic resonance spectroscopy study. Journal of the American Society of Nephrology, 2, 200-211.

Park, K. M., Kim, J. I., Ahn, Y., Bonventre, A. J. and Bonventre, J. V. (2004) Testosterone is responsible for enhanced susceptibility of males to ischemic renal injury. Journal of Biological Chemistry, 10, 279(50), 52282-52292.

Patel, R. P., Yet, S. F., Wang, X., Kevil, C. G., Gladwin, M. T. and Lefer, D. J. (2005) Cytoprotective effects of nitrite during in vivo ischemia-reperfusion of the heart and liver. Journal of Clinical Investigation, 115, 1232-1240.

Patil, N. K., Parajuli, N., MacMillan-Crow, L. A. and Mayeux, P. R. (2014) Inactivation of renal mitochondrial respiratory complexes and manganese superoxide dismutase during sepsis: Mitochondria-targeted antioxidant mitigates injury. American Journal of Physiology-Renal Physiology, 306(7), 734-743.

Patschan, D., Krupincza, K., Patschan, S., Zhang, Z., Hamby, C. and Goligorsky, M. S. (2006) Dynamics of mobilization and homing of endothelial progenitor cells after acute renal ischemia: Modulation by ischemic preconditioning. American Journal of Physiology-Renal Physiology, 291(1), 176-185.

Patschan, D., Patschan, S. and Müller, G. A. (2011) Endothelial progenitor cells in acute ischemic kidney injury: Strategies for increasing the cells' renoprotective competence. International Journal of Nephrology, 2011, e828369.

Pawluczyk, I. Z. A., Patel, S. R. and Harris, K. P. G. (2006) The role of the α-1 adrenoceptor in modulating human mesangial cell matrix production. Nephrology Dialysis Transplantation, 21(9), 2417-2424.

Peng, W., Robertson, L., Gallinetti, J., Mejia, P., Vose, S., Charlip, A., Chu, T. and Mitchell, J. R. (2012) Surgical stress resistance induced by single amino acid deprivation requires Gcn2 in mice. Science Translational Medicine, 4(118), 118ra11.

Pentilla, A., Glaumann, H. and Trump, B. F. (1976) Studies on the modification of the cellular response to injury: IV. Protective effect of extracellular acidosis against anoxia, thermal, and p-chloromercuribenzene sulfonic acid treatment of isolated rat liver cells. Life Science, 18, 1419-1430.

Perazella, M. A. (2009) Renal vulnerability to drug toxicity. Clinical Journal of the American Society of Nephrology, 4, 1275-1283.

Pereira, M. A., Zanetta, D. M. C. and Abdulkader, R. C. R. M. (2012) The real importance of pre-existing comorbidities on long-term mortality after acute kidney injury. PLoS ONE, 7(10), e47746.

Petrat, F., Boengler, K., Schulz, R. and De Groot, H. (2012) Glycine, a simple physiological compound protecting by yet puzzling mechanism(s) against ischaemia-reperfusion injury: Current knowledge. British Journal of Pharmacology, 165(7), 2059-2072.

Peyrou, M. and Cribb, A. E. (2007) Effect of endoplasmic reticulum stress preconditioning on cytotoxicity of clinically relevant nephrotoxins in renal cell lines. Toxicology in Vitro, 21, 878-886.

Pierce, G. L., Jablonski, K. L., Walker, A. E., Seibert, S. M., DeVan, A. E., Black, S. M., Sharma, S. and Seals, D. R. (2012) Tetrahydrobiopterin supplementation enhances carotid artery compliance in healthy older men: A pilot study. American Journal of Hypertension, 25(10), 1050-1054.

Pleskova, M., Beck, K. F., Behrens, M. H., Huwiler, A., Fichtlscherer, B., Wingerter, O., Brandes, R. P., Mulsch, A. and Pfeilschifter, J. (2006) Nitric oxide down-regulates the expression of the catalytic NADPH oxidase subunit Nox1 in rat renal mesangial cells. The FASEB Journal, 20, 139-141.

Pozdzik, A., Salmon, I. J., Debelle, F. D., Decaestecker, C., Van den Branden, C., Verbeelen, D., Deschodt-Lanckman, M. M., Vanherweghem, J. L. and Nortier, J. L. (2008) Aristolochic acid induces proximal tubule apoptosis and epithelial to mesenchymal transformation. Kidney International, 73, 595-607.

Prachasilchai, W., Sonoda, H., Yokota-Ikeda, N., Oshikawa, S., Aikawa, C., Uchida, K., Ito, K., Kudo, T., Imaizumi, K. and Ikeda, M. (2008) A protective role of unfolded protein response in mouse ischemic acute kidney injury. European Journal of Pharmacology, 592, 138-145.

Price, P. M., Safirstein, R. L. and Megyesi, J. (2004) Protection of renal cells from cisplatin toxicity by cell cycle inhibitors. American Journal of Physiology-Renal Physiology, 286(2), 378-384.

Price, P. M., Yu, F., Kaldis, P., Aleem, E., Nowak, G., Safirstein, R. L. and Megyesi, J. (2006) Dependence of cisplatin-induced cell death in vitro and in vivo on cyclin-dependent kinase 2. Journal of the American Society of Nephrology, 17(9), 2434-2442.

Public Health England (2014) Chronic kidney disease prevalence model. HM Government, United Kingdom.

Puigmulé, M., López-Hellin, J., Suñé, G., Tornavaca, O., Camaño, S., Tejedor, A. and Meseguer, A. (2009) Differential proteomic analysis of cyclosporine A-induced toxicity in renal proximal tubule cells. Nephrology Dialysis Transplantation, 24 (9), 2672-2686.

Qi, W., Twigg, S., Chen, X., Polhill, T. S., Poronnik, P., Gilbert, R. E. and Pollock, C. A. (2005) Integrated actions of transforming growth factor-beta1 and connective tissue growth factor in renal fibrosis. American Journal of Physiology-Renal Physiology, 288, 800-809.

Qiao, X., Xu, J., Yang, Q. J., Du, Y., Lei, S., Liu, Z. H., Liu, X. and Liu, H. (2013) Transient acidosis during early reperfusion attenuates myocardium ischemia reperfusion injury via PI3k-Akt-eNOS signaling pathway. Oxidative Medicine and Cellular Longevity, 2013, 1-6.

Quiros, Y., Vicente-Vicente, L., Morales, A. I., López-Novoa, J. M. and López-Hernández, F. J. (2010) An integrative overview on the mechanisms underlying the renal tubular cytotoxicity of gentamicin. Toxicological Sciences, 119(2), 245-256.

Raat, N. J., Noguchi, A. C., Liu, V. B., Raghavachari, N., Liu, D., Xu, X., Shiva, S., Munson, P. J. and Gladwin, M. T. (2009) Dietary nitrate and nitrite modulate blood

and organ nitrite and the cellular ischemic stress response. Free Radical Biology and Medicine, 47(5), 510-517.

Racusen, L. C., Monteil, C., Sgrignoli, A., Lucskay, M., Marouillat, S., Rhim, J. G. S. and Morin, J. P. (1996) Cell-lines with extended in vitro growth potential from human renal proximal tubule: Characterization, response to inducers, and comparison with established cell lines. Journal of Laboratory and Clinical Medicine, 129(3), 318-329.

Radomski, M. W., Palmer, R. M. and Moncada, S. (1990) An L-arginine/nitric oxide pathway present in human platelets regulates aggregation. Proceedings of the National Academy of Sciences, 87, 5193-5197.

Ramírez-Rangel, I., Bracho-Valdés, I., Vázquez-Macías, A., Carretero-Ortega, J., Reyes-Cruz, G. and Vázquez-Prado, J. (2011) Regulation of mTORC1 complex assembly and signaling by GRp58/ERp57. Molecular and Cellular Biology, 31(8), 1657-1671.

Rao, R. V. and Bredesen, D. E. (2004) Misfolded proteins, endoplasmic reticulum stress and neurodegeneration. Current Opinion in Cell Biology, 16(6), 653-662.

Rassaf, T., Totzeck, M., Hendgen-Cotta, U. B., Shiva, S., Heusch, G. and Kelm, M. (2014) Circulating nitrite contributes to cardioprotection by remote ischemic preconditioning. Circulation Research, 114, 1601-1610.

Razvickas, C. V., Borges, F. T., De Oliveira, A. S., Schor, N. and Boim, M. A. (2013) The effect of hypoxia and reoxygenation in the response of mesangial cells to angiotensin II in vitro. Jornal Brasileiro De Nefrologia, 35(4), 259-264.

Regec, A. L., Trifillis, A. L. and Trump, B. F. (1986) The effect of gentamicin on human renal proximal tubular cells. Toxicologic Pathology, 14(2), 238-241.

Reiling, J. H. and Sabatini, D. M. (2006) Stress and mTORture signaling. Oncogene, 25(48), 6373-6383.

Ren, Y., Garvin, J. L. and Carretero, O. A. (2001) Efferent arteriole tubuloglomerular feedback in the renal nephron. Kidney International, 59(1), 222-229.

Rennke, H. G. and Denker, B. M. (2014) Chapater 11. Acute renal failure. In: Renal pathophysiology: The essentials, 4th edition. Philadelphia: Lippincott Williams and Wilkins.

Rhoden, E., Teloken, C., Lucas, M., Rhoden, C., Mauri, M., Zettler, C., Bello-Klein, A. and Barros, E. (2000) Protective effect of allopurinol in the renal ischemia-reperfusion in uninephrectomized rats. General Pharmacology, 35(4), 189-193.

Ricca, L., Lemoine, A., Cauchy, F., Hamelin, J., Sebagh, M., Esposti, D. D., Salloum, C., Vibert, E., Balducci, G. and Azoulay, D. (2015) Ischemic postconditioning of the liver graft in adult liver transplantation. Transplantation, 99(8), 1633-1643.

Rice, T. W., Mogan, S., Hays, M. A., Bernard, G. R., Jensen, G. L. and Wheeler, A. P. (2011) Randomized trial of initial trophic versus full-energy enteral nutrition in mechanically ventilated patients with acute respiratory failure. Critical Care Medicine, 39, 967-974.

Riss, T. L., Moravec, R. A., Niles, A. L., Duellman, S., Benink, H. A., Worzella, T. J. and Minor, L. (2013) Cell viability assays. In: Sittampalam, G. S., Coussens, N. P.,

Brimacombe, K., Grossman, A., Arkin, M., Auld, D., Austin, C., Bejcek, B., Glicksman, M., Inglese, J., Iversen, P. W., Li, Z., McGee, J., McManus, O., Minor, L., Napper, A., Peltier, J. M., Riss, T., Trask, Jr. O. J. and Weidner, J. (Eds.) Assay guidance manual [Internet]. Bethesda (MD): Eli Lilly and Company and the National Center for Advancing Translational Sciences. Available at: https://www.ncbi.nlm.nih.gov/books/NBK144065/. Accessed 13rd February 2017.

Roberts, P. R., Black, K. W. and Zaloga, G. P. (1997) Enteral feeding improves outcome and protects against glycerol-induced acute renal failure in the rat. American Journal of Respiratory and Critical Care Medicine, 156, 1265-1269.

Rodríguez-Sinovas, A., Cabestrero, A., García del Blanco, B., Inserte, J., García, A. and García-Dorado, D. (2009) Intracoronary acid infusion as an alternative to ischemic postconditioning in pigs. Basic Research in Cardiology, 104(6), 761-771.

Romanov, V., Whyard, T. C., Waltzer, W. C., Grollman, A. P. and Rosenquist, T. (2015) Aristolochic acid-induced apoptosis and G2 cell cycle arrest depends on ROS generation and MAP kinases activation. Archives of Toxicology, 89(1), 47-56.

Rosen, S. and Stillman, I. E. (2008) Acute tubular necrosis is a syndrome of physiologic and pathologic dissociation. Journal of the American Society of Nephrology, 19, 871-887.

Rossiello, M. R., Laconi, E., Rao, P. M., Rajalakshmi, S. and Sarma, D. S. R. (1993) Induction of hepatic nodules in the rat by aristolochic acid. Cancer Letters, 71, 83-87.

Ryan, M. J., Johnson, G., Kirk, J., Fuerstenberg, S. M., Zager, R. A. and Torok-Storb, B. (1994) HK-2: An immortalized proximal tubule epithelial cell line from normal adult human kidney. Kidney International, 45(1), 48-57.

Saat, T. C., Van den Akker, E. K., IJzermans, J. N. M., Dor, F. J. M. F. and De Bruin, R. W. F. (2016) Improving the outcome of kidney transplantation by ameliorating renal ischemia reperfusion injury: Lost in translation? Journal of Translational Medicine, 14, 20, 1-9.

Sabbagh, R., Chawla, A., Tisdale, B., Kwan, K., Chatterjee, S., Kwiecien, J. M. and Kapoor, A. (2011) Renal histopathology features according to various warm ischemia times in porcine laparoscopic and open surgery model. Canadian Urological Association Journal, 5(1), 40-43.

Sabbahy, M. E. and Vaidya, V. S. (2011) Ischemic kidney injury and mechanisms of tissue repair. Wiley Interdiscipinary Reviews Systems Biology and Medicine, 3(5), 606-618.

Sáenz-Morales, D., Conde, E., Escribese, M. M., García-Martos, M., Alegre, L., Blanco-Sánchez, I. and García-Bermejo, M. L. (2009) ERK1/2 mediates cytoskeleton and focal adhesion impairment in proximal epithelial cells after renal ischemia. Cellular Physiology and Biochemistry, 23, 285-294.

Sancak, Y., Bar-Peled, L., Zoncu, R., Markhard, A. L., Nada, S. and Sabatini, D. M. (2010) Ragulator-Rag complex targets mTORC1 to the lysosomal surface and is necessary for its activation by amino acids. Cell, 141, 290-303.

Sancak, Y., Peterson, T. R., Shaul, Y. D., Lindquist, R. A., Thoreen, C. C., Bar-Peled, L. and Sabatini, D. M. (2008) The Rag GTPases bind raptor and mediate amino acid signaling to mTORC1. Science, 320, 1496-1501.

Sanders, M. J., Grondin, P. O., Hegarty, B. D., Snowden, M. A. and Carling, D. (2007) Investigating the mechanism for AMP activation of the AMP-activated protein kinase cascade. Biochemical Journal, 403(1), 139-148.

Sands, J. M. and Layton, H. E. (2009) The physiology of urinary concentration: An update. Seminars in Nephrology, 29(3), 178-195.

Satake, A., Takaoka, M., Nishikawa, M., Yuba, M., Shibata, Y., Okumura, K., Kitano, K., Tsutsui, H., Fujii, K., Kobuchi, S., Ohkita, M. and Matsumura, Y. (2008) Protective effect of 17b-estradiol on ischemic acute renal failure through the PI3K/Akt/eNOS pathway. Kidney International, 73, 308-317.

Sato, M., Yao, V. J., Arap, W. and Pasqualini, R. (2010) GRP78 signaling hub a receptor for targeted tumor therapy. Advances in Genetics, 69, 97-114.

Sato, N., Takahashi, D., Chen, S. M., Tsuchiya, R., Mukoyama, T., Yamagata, S., Ogawa, M., Yoshida, M., Kondo, S., Satoh, N. and Ueda, S. (2004) Acute nephrotoxicity of aristolochic acids in mice. Journal of Pharmacology and Pharmacotherapeutics, 56, 221-229.

Schaudies, R. P. and Johnson, J. P. (1993) Increased soluble EGF after ischemia is accompanied by a decrease in membrane-associated precursors. American Journal of Physiology, 264(3), 523-531.

Scheinkestel, C. D., Kar, L., Marshall, K., Bailey, M., Davies, A., Nyulasi, I. and Tuxen, D. V. (2003) Prospective randomized trial to assess caloric and protein needs of critically ill, anuric, ventilated patients requiring continuous renal replacement therapy. Nutrition, 19 (11-12), 909-916.

Schetz, M., Dasta, J., Goldstein, S. and Golper, T. (2005) Drug-induced acute kidney injury. Current Opinion in Critical Care, 11(6), 555-565.

Schneider, R., Raff, U., Vornberger, N., Schmidt, M., Freund, R., Reber, M., Schramm, L., Gambaryan, S., Wanner, C., Schmidt, H. H. and Galle, J. (2003) L-Arginine counteracts nitric oxide deficiency and improves the recovery phase of ischemic acute renal failure in rats. Kidney International, 64, 216-225.

Schnellmann, R. G. and Williams, S. W. (1998) Proteases in renal cell death: Calpains mediate cell death produced by diverse toxicants. Renal Failure, 20, 679-686.

Schrier, R. W., Wang, W., Poole, B. and Mitra, A. (2004) Acute renal failure: Definition, diagnosis, pathogenesis, and therapy. The Journal of Clinical Investigation, 114, 5-14.

Schröder, E. and Eaton, P. (2008) Hydrogen peroxide as an endogenous mediator and exogenous tool in cardiovascular research: Issues and considerations. Current Opinion in Pharmacology, 8(2), 153-159.

Schwartz, I. F., Schwartz, D., Traskonov, M., Chernichovsky, T., Wollman, Y., Gnessin, E., Topilsky, I., Levo, Y. and Iaina, A. (2002) L-arginine transport is augmented through up-regulation of tubular CAT-2 mRNA in ischemic acute renal failure in rats. Kidney International, 62, 1700-1706.

Selemidis, S., Dusting, G. J., Peshavariya, H., Kemp-Harper, B. K. and Drummond, G. R. (2007) Nitric oxide suppresses NADPH oxidase-dependent superoxide production by S-nitrosylation in human endothelial cells. Cardiovascular Research, 15, 75(2), 349-358.

Sengupta, S., Peterson, T. R. and Sabatini, D. M. (2010) Regulation of the mTOR complex 1 pathway by nutrients, growth factors, and stress. Molecular Cell, 40(2), 310-322.

Setoguchi, S., Mohri, M., Shimokawa, H. and Takeshita, A. (2001) Tetrahydrobiopterin improves endothelial dysfunction in coronary microcirculation in patients without epicardial coronary artery disease. Journal of the American College of Cardiology, 38(2), 493-498.

Shanley, P. F., Shapiro, J. I., Chan, L., Burke, T. J. and Johnson, G. C. (1988) Acidosis and hypoxic medullary injury in the isolated perfused kidney. Kidney International, 34, 791-796.

Sharfuddin, A. A. and Molitoris, B. A. (2008) Chapter 76. Pathophysiology of acute kidney injury. In: Alpern, R. J. and Hebert, S. C. (Eds.) Seldin and Giebisch's The kidney: Physiology and pathophysiology. New York: Lippincott Williams and Wilkins.

Sharfuddin, A. A. and Molitoris, B. A. (2011) Pathophysiology of ischemic acute kidney injury. Nature Reviews Nephrology, 7, 189-200.

Sharma, A., Mucino, M. J. and Ronco, C. (2014) Renal Functional reserve and renal recovery after acute kidney injury. Nephron Clinical Practice, 127, 94-100.

Shaul, P. W. (2002) Regulation of endothelial nitric oxide synthase: Location, location, location. Annual Review of Physiology, 64, 749-774.

Shi, Q., Feng, Y. N., Fang, J. and Xu, K. (2009) Pretreatment with glutamine attenuates anoxia/reoxygenation injury of human proximal renal tubular epithelial cells via induction of heme oxygenase-1. Pharmacology, 84, 1-8.

Shibutani, S., Dong, H., Suzuki, N., Ueda, S., Miller, F. and Grollman, A. P. (2007) Selective toxicity of aristolochic acids I and II. Drug Metabolism and Disposition, 35, 1217-1222.

Shillingford, J. M., Murcia, N. S., Larson, C. H., Low, S. H., Hedgepeth, R., Brown, N., Flask, C. A., Novick, A. C., Goldfarb, D. A., Kramer-Zucker, A., Walz, G., Piontek, K. B., Germino, G. G. and Weimbs, T. (2006) The mTOR pathway is regulated by polycystin-1, and its inhibition reverses renal cystogenesis in polycystic kidney disease. Proceedings of the National Academy of Sciences, 103, 5466-5471.

Shiose, A., Kuroda, J., Tsuruya, K., Hirai, M., Hirakata, H., Naito, S., Hattori, M., Sakaki, Y. and Sumimoto, H. (2001) A novel superoxide-producing NAD(P)H oxidase in kidney. Journal of Biological Chemistry, 276, 1417-1423.

Shiva, S., Huang, Z., Grubina, R., Sun, J., Ringwood, L.A., MacArthur, P. H., Xu, X., Murphy, E., Darley-Usmar, V. M. and Gladwin, M. T. (2007a) Deoxymyoglobin is a nitrite reductase that generates nitric oxide and regulates mitochondrial respiration. Circulation Research, 100(5), 654-661.

Shiva, S., Sack, M. N., Greer, J. J., Duranski, M., Ringwood, L. A., Burwell, L., Wang, X., MacArthur, P. H., Shoja, A., Raghavachari, N., Calvert, J. W., Brookes, P. S., Lefer, D. J. and Gladwin, M. T. (2007b) Nitrite augments tolerance to ischemia/reperfusion injury via the modulation of mitochondrial electron transfer. Journal of Experimental Medicine, 204(9), 2089-2102.

Sigma-Aldrich. Product information. Dulbecco's modified Eagles medium (DME). Available at: http://www.sigmaaldrich.com/content/dam/sigma-aldrich/docs/Sigma/Formulation/d6546for.pdf. Accessed 23rd October 2016.

Sileria, P., Sicaa, G., Gentileschia, P., Venzaa, M., Manzellia, A., Palmierib, G., Spagnolib, L. G., Testac, G., Benedettic, E. and Gasparia, A. L. (2004) Ischemic preconditioning protects intestine from prolonged ischemia. Transplantation Proceedings, 36(2), 283-285.

Silver, S. A., Cardinal, H., Colwell, K., Burger, D. and Dickhout, J. G. (2015) Acute kidney injury: Preclinical innovations, challenges, and opportunities for translation. Canadian Journal of Kidney Health and Disease, 2, 30.

Singbartl, K. and Kellum, J. A. (2012) AKI in the ICU: Definition, epidemiology, risk stratification, and outcomes. Kidney International, 81, 819-825.

Singer, P. (2007) High-dose amino acid infusion preserves diuresis and improves nitrogen balance in non-oliguric acute renal failure. Wien Klin Wochenschr, 119, 218-222.

Singh, A. P., Muthuraman, A., Jaggi, A. S., Singh, N., Grover, K. and Dhawan, R. (2012) Animal models of acute renal failure. Pharmacological Reports, 64, 31-44.

Smith, E. M., Finn, S. G., Tee, A. R., Browne, G. J. and Proud, C. G. (2005) The tuberous sclerosis protein TSC2 is not required for the regulation of the mammalian target of rapamycin by amino acids and certain cellular stresses. Journal of Biological Chemistry, 280, 18717-18727.

Smith, K. D., Wrenshall, L. E., Nicosia, R. F., Pichler, R., Marsh, C. L., Alpers, C. E., Polissar, N. and Davis, C. L. (2003) Delayed graft function and cast nephropathy associated with tacrolimus plus rapamycin use. Journal of the American Society of Nephrology, 14, 1037-1045.

Sola, A., Palacios, L., Lopez-Marti, J., Ivorra, A., Noguera, N., Gomez, R., Villa, R., Aguilo, J. and Hotter, G. (2003) Multiparametric monitoring of ischemia reperfusion in rat kidney: Effect of ischemic preconditioning. Transplantation, 75, 744-749.

Solez, K., Morel-Maroger, L. and Sraer, J. D. (1979) The morphology of "acute tubular necrosis" in man: Analysis of 57 renal biopsies and a comparison with the glycerol model. Medicine (Baltimore), 58, 362-376.

Solez, K., Racusen, L. C., Marcussen, N., Slatnik, I., Keown, P., Burdick, J. F. and Olsen, S. (1993) Morphology of ischemic acute renal failure, normal function, and cyclosporine toxicity in cyclosporine-treated renal allograft recipients. Kidney International, 43(5), 1058-1067.

Spurgeon, K. R., Donohoe, D. L. and Basile, D. P. (2005) Transforming growth factor-beta in acute renal failure: Receptor expression, effects on proliferation, cellularity, and vascularization after recovery from injury. American Journal of Physiology-Renal Physiology, 288(3), 568-577.

Stiborová, M., Frei, E., Arlt, V. M. and Schmeiser, H. H. (2008) Metabolic activation of carcinogenic aristolochic acid, a risk factor for Balkan endemic nephropathy. Mutation Research, 658, 55-67.

Sucher, R., Gehwolf, P., Oberhuber, R., Hermann, M., Margreiter, C., Werner, E. R., Obrist, P., Schneeberger, S., Ollinger, R., Margreiter, R. and Brandacher, G. (2010)

Tetrahydrobiopterin protects the kidney from ischemia-reperfusion injury. Kidney International, 77(8), 681-689.

Surendran, K. and Kopan, R. (2011) Chromatin-based mechanisms of renal epithelial differentiation. Journal of the American Society of Nephrology, 22(7), 1208-1212.

Sureshbabu, A., Ryter, S. W. and Choi, M. E. (2015) Oxidative stress and autophagy: Crucial modulators of kidney injury. Redox Biology, 4, 208-214.

Susantitaphong, P., Cruz, D. N., Cerda, J., Abulfaraj, M., Alqahtani, F., Koulouridis, I. and Jaber, B. L. (2013) World incidence of AKI: A meta-analysis. Clinical Journal of the American Society of Nephrology, 8, 1482-1493.

Suschek, C. V., Schewe, T., Sies, H. and Kroncke, K. D. (2006) Nitrite, a naturally occurring precursor of nitric oxide that acts like a 'prodrug'. Journal of Biological Chemistry, 387(5), 499-506.

Suzuki, C., Isaka, Y., Takabatake, Y., Tanaka, H., Koike, M., Shibata, M., Uchiyama, Y., Takahara, S. and Imai, E. (2008) Participation of autophagy in renal ischemia/reperfusion injury. Biochemical and Biophysical Research Communications, 368, 100-106.

Suzuki, S., Takamura, S., Yoshida, J., Shinzawa, Y., Niwa, O. and Tamatani, R. (1995) Comparison of gentamicin nephrotoxicity between rats and mice. Comparative Biochemistry and Physiology, 112(1), 15-28.

Sykes, E. K., Mactier, S. and Christopherson, R. I. (2016) Melanoma and the unfolded protein response. Cancers, 8, 30, 1-18.

Takimoto, E., Champion, H. C., Li, M., Ren, S., Rodriguez, E. R., Tavazzi, B., Lazzarino, G., Paolocci, N., Gabrielson, K. L., Wang, Y. and Kass, D. A. (2005) Oxidant stress from nitric oxide synthase-3 uncoupling stimulates cardiac pathologic remodeling from chronic pressure load. Journal of Clinical Investigation, 115, 1221-1231.

Tang, R., Yang, C., Tao, J. L., You, Y. K., An, N., Li, S. M., Wu, H. L. and Liu, H. F. (2011) Epithelial-mesenchymal transdifferentiation of renal tubular epithelial cells induced by urinary proteins requires the activation of PKC-alpha and beta I isozymes. Cell Biology International, 35, 953-959.

Taylor, J., Harris, A. and Moss, J. (2011) Prevent this silent killer: Care of the acutely unwell. Health Service Journal supplement, 1-9.

Tejero, J. and Stuehr, D. (2013) Tetrahydrobiopterin in nitric oxide synthase. IUBMB Life, 65(4), 358-365.

Terada, Y., Tanaka, H., Okado, T., Shimamura, H., Inoshita, S., Kuwahara, M. and Sasaki, S. (2003) Expression and function of the developmental gene Wnt-4 during experimental acute renal failure in rats. Journal of the American Society of Nephrology, 14(5), 1223-1233.

The World Bank: GDP per capita (current US$). Available at: http://data.worldbank.org/indicator/NY.GDP.PCAP.CD. Accessed 25th October 2015a.

The World Bank: How we classify countries. Available at: http://data.worldbank.org/indicator/SP.POP.65UP.TO.ZS. Accessed 25th October 2015b.

Thermo Fisher Scientific. Media formulation. 11130 - MEM amino acid solution (50x) liquid. Available at: https://www.thermofisher.com/uk/en/home/technical-resources/media-formulation.164.html. Accessed 23rd October 2016.

Thielmann, M., Kottenberg, E., Kleinbongard, P., Wendt, D., Gedik, N., Pasa, S., Price, V., Tsagakis, K., Neuhauser, M., Peters, J., Jakob, H. and Heusch, G. (2013) Cardioprotection and improved prognosis by remote ischaemic preconditioning in a single-center randomised, double-blind controlled trial of coronary artery bypass surgery. Lancet, 382, 597-604.

Tnava, O. and Gu, W. (2013) The hunger games: p53 regulates metabolism upon serine starvation. Cell Metabolism, 17(2), 1559-1561.

Tögel, F., Isaac, J. and Westenfelder, C. (2004) Hematopoietic stem cell mobilization-associated granulocytosis severely worsens acute renal failure. Journal of the American Society of Nephrology, 15(5), 1261-1267.

Tögel, F. E. and Westenfelder, C. (2012) Kidney protection and regeneration following acute injury: Progress through stem cell therapy. American Journal of Kidney Diseases, 60(6), 1012-1022.

Tolins, J. P. and Raij, L. (1991) Effects of amino acid infusion on renal hemodynamics. Role of endothelium-derived relaxing factor. Hypertension, 17, 1045-1051.

Torras, J., Herrero-Fresned, I., Lloberas, N., Riera, M., Cruzado, J. M. and Grinyo, M. (2002) Promising effects of ischemic preconditioning in renal transplantation. Kidney International, 61, 2218-2227.

Torres, V. E., Boletta, A., Chapman, A., Gattone, V., Pei, Y., Qian, Q., Wallace, D. P., Weimbs, T. and Wüthrich, R. P. (2010) Prospects for mTOR inhibitor use in patients with polycystic kidney disease and hamartomatous diseases. Clinical Journal of the American Society of Nephrology, 5(7), 1312-1329.

Tripatara, P., Patel, N. S., Webb, A., Rathod, K., Lecomte, F. M., Mazzon, E., Cuzzocrea, S., Yaqoob, M. M., Ahluwalia, A. and Thiemermann, C. (2007) Nitrite-derived nitric oxide protects the rat kidney against ischemia/reperfusion injury in vivo: Role for xanthine oxidoreductase. Journal of the American Society of Nephrology, 18, 570-580.

Tsai, Y. C. and Weissman, A. M. (2010) The unfolded protein response, degradation from the endoplasmic reticulum, and cancer. Genes and Cancer, 1(7), 764-778.

Vahed, S. Z., Samadi, N. and Ardalan, M. (2014) Diagnosis of interstitial fibrosis and tubular atrophy in kidney allograft - Implementation of microRNAs. Iranian Journal of Kidney Disease, 8, 4-12.

Van den Akker, E. K., Manintveld, O. C., Hesselink, D. A., De Bruin, R. W., Ijzermans, J. N. and Dor, F. J. (2013) Protection against renal ischemia-reperfusion injury by ischemic postconditioning. Transplantation, 95(11), 1299-1305.

Van der Vlies, D., Makkinje, M., Jansens, A., Braakman, I., Verkleij, A. J., Wirtz, K. W. and Post, J. A. (2003) Oxidation of ER resident proteins upon oxidative stress: Effects of altering cellular redox/antioxidant status and implications for protein maturation. Antioxidants and Redox Signaling, 5, 381-387.

Vanhorebeek, I., Gunst, J., Derde, S., Derese, I., Boussemaere, M., Guiza, F., Martinet, W., Timmermans, J. P., D'Hoore, A., Wouters, P. J. and Van den Berghe,

G. (2011) Insufficient activation of autophagy allows cellular damage to accumulate in critically ill patients. Journal of Clinical Endocrinology and Metabolism, 96, 633-645.

Van Nieuwenhoven, F. A., Jensen, L. J., Flyvbjerg, A. and Goldschmeding, R. (2005) Imbalance of growth factor signalling in diabetic kidney disease: Is connective tissue growth factor (CTGF, CCN2) the perfect intervention point? Nephrology Dialysis Transplantation, 20(1), 6-10.

Vaughan-Jones, R. D., Spitzer, K. W. and Swietach, P. (2009) Intracellular pH regulation in heart. Journal of Molecular and Cellular Cardiology, 46, 318-331.

Vaziri, N. D., Dicus, M., Ho, N. D., Boroujerdi-Rad, L. and Sindhu, R. K. (2003) Oxidative stress and dysregulation of superoxide dismutase and NADPH oxidase in renal insufficiency. Kidney International, 63, 179-185.

Velagapudi, C., Bhandari, B. S., Abboud-Werner, S., Simone, S., Abboud, H. E. and Habib, S. L. (2011) The tuberin/mTOR pathway promotes apoptosis of tubular epithelial cells in diabetes. Journal of the American Society of Nephrology, 22(2), 262-273.

Verweij, M., Van de Ven, M., Mitchell, J. R., Van den Engel, S., Hoeijmakers, J. H., Ijzermans, J. N. and De Bruin, R. W. (2011) Glucose supplementation does not interfere with fasting-induced protection against renal ischemia/reperfusion injury in mice. Transplantation, 92(7), 752-758.

Voisine, C., Pedersen, J. S. and Morimoto, R. I. (2010) Chaperone networks: Tipping the balance in protein folding diseases. Neurobiology of Disease, 40, 12-20.

Wald, R., Quinn, R. R., Luo, J., Li, P., Scales, D. C., Mamdani, M. M. and Ray, J. G. (2009) Chronic dialysis and death among survivors of acute kidney injury requiring dialysis. The Journal of the American Medical Association, 302, 1179-1185.

Walter, P. and Ron, D. (2011) The unfolded protein response: From stress pathway to homeostatic regulation. Science, 334, 1081-1086.

Wang, L. T., Chen, B. L., Wu, C. T., Huang, K. H., Chiang, C. K. and Liu, S. H. (2013) Protective role of AMP-activated protein kinase-evoked autophagy on an in vitro model of ischemia/reperfusion-induced renal tubular cell injury. PLoS ONE, 8(11), e79814.

Wang, M. and Kaufman, R. J. (2014) The impact of the endoplasmic reticulum protein-folding environment on cancer development. Nature Reviews Cancer, 14(9), 581-597.

Wang, S. N., LaPage, J. and Hirschberg, R. (2000) Role of glomerular ultrafiltration of growth factors in progressive interstitial fibrosis in diabetic nephropathy. Kidney International, 57(3), 1002-1014.

Wang, W., Mitra, A., Poole, B., Falk, S., Lucia, M. S., Tayal, S. and Schrier, R. (2004) Endothelial nitric oxide synthase-deficient mice exhibit increased susceptibility to endotoxin-induced acute renal failure. American Journal of Physiology-Renal Physiology, 287(5), 1044-1048.

Wang, Y., He, J., Pei, X. and Zhao, W. (2013) Systematic review and meta-analysis of mesenchymal stem/stromal cells therapy for impaired renal function in small animal models. Nephrology (Carlton), 18(3), 201-208.

Webb, A., Bond, R., McLean, P., Uppal, R., Benjamin, N. and Ahluwalia, A. (2004) Reduction of nitrite to nitric oxide during ischemia protects against myocardial ischemia-reperfusion damage. Proceedings of the National Academy of Sciences, 101, 1368-13688.

Webb, A. J., Patel, N., Loukogeorgakis, S., Okorie, M., Aboud, Z., Misra, S., Rashid, R., Miall, P., Deanfield, J., Benjamin, N., MacAllister, R., Hobbs, A. J. and Ahluwalia, A. (2008) Acute blood pressure lowering, vasoprotective, and antiplatelet properties of dietary nitrate via bioconversion to nitrite. Hypertension, 51, 784-790.

Wei, Q. and Dong, Z. (2012) Mouse model of ischemic acute kidney injury: Technical notes and tricks. American Journal of Physiology-Renal Physiology, 303(11), 1487-1494.

Weight, S. C. and Nicholson, M. L. (1996) Renal ischaemia-reperfusion injury. British Journal of Surgery, 83, 162-170.

Weinberg, J. M. (1985) Oxygen-deprivation-induced injury to isolated rabbit kidney tubules. Journal of Clinical Investigation, 76(3), 1193-1208.

Weinberg, J. M., Davis, J. A., Roeser, N. F. and Venkatachalam, M. A. (1994) Role of intracellular pH during cytoprotection of proximal tubule cells by glycine or acidosis. Journal of the American Society of Nephrology, 5, 1314-1323.

Weinberg, J. M., Roeser, N. F., Davis, J. A. and Venkatachalam, M. A. (1997) Glycine-protected, hypoxic, proximal tubules develop severely compromised energetic function. Kidney International, 52, 140-151.

Weiner, I. D., Mitch, W. E. and Sands, J. M. (2015) Urea and ammonia metabolism and the control of renal nitrogen excretion. Clinical Journal of the American Society of Nephrology, 10(8), 1444-1458.

Weinstein, J. R. and Anderson, S. (2010) The aging kidney: Physiological changes. Advances in Chronic Kidney Disease, 17(4), 302-307.

Wen, X., Peng, Z., Li, Y., Wang, H., Bishop, J. V., Chedwick, L. R., Singbartl, K. and Kellum, J. A. (2012) One dose of cyclosporine A is protective at initiation of folic acid-induced acute kidney injury in mice. Nephrology Dialysis Transplantation, 27(8), 3100-3109.

Wever, K. E., Menting, T. P., Rovers, M., Van der Vliet, J. A., Rongen, G. A., Masereeuw, R., Ritskes-Hoitinga, R., Hooijmans, C. R. and Warlé, M. (2012) Ischemic preconditioning in the animal kidney, a systematic review and meta-analysis. PLoS ONE, 7, e32296.

Wijermars, L. G., Bakker, J. A., De Vries, D. K., Van Noorden, C. J., Bierau, J., Kostidis, S., Mayboroda, O. A., Tsikas, D., Schaapherder, A. F. and Lindeman, J. H. (2017) The hypoxanthine-xanthine oxidase axis is not involved in the initial phase of clinical transplantation-related ischemia/reperfusion injury. American Journal of Physiology-Renal Physiology, 312(3), 457-464.

Wilson, P. D. and Schrier, R. W. (1986) Nephron segment and calcium as determinants of anoxic cell death in renal cultures. Kidney International, 29(6), 1172-1179.

Wischmeyer, P. E. (2007) Glutamine: Mode of action in critical illness. Critical Care Medicine, 35(9), 541-544.

Witzgall, R., Brown, D., Schwarz, C. and Bonventre, J. V. (1994) Localization of proliferating cell nuclear antigen, vimentin, c-fos, and clusterin in the post-ischemic kidney. Evidence for a heterogeneous genetic response among nephron segments, and a large pool of mitotically active and dedifferentiated cells. Journal of Clinical Investigation, 93, 2175-2188.

Wojtala, A., Bonora, M., Malinska, D., Pinton, P., Duszynski, J. and Wieckowski, M. R. (2014) Methods to monitor ROS production by fluorescence microscopy and fluorometry. Methods in Enzymology, 542, 243-262.

Wouters, B. G. and Koritzinsky, M. (2008) Hypoxia signalling through mTOR and the unfolded protein response in cancer. Nature Reviews Cancer, 8, 851-864.

Wu, H., Chen, G., Wyburn, K. R., Yin, J., Bertolino, P., Eris, J. M., Alexander, S. I., Sharland, A. F. and Chadban, S. J. (2007) TLR4 activation mediates kidney ischemia/reperfusion injury. Journal of Clinical Investigation, 117(10), 2847-2859.

Wu, H. H., Hsiao, T. Y., Chien, C. T. and Lai, M. K. (2009) Ischemic conditioning by short periods of reperfusion attenuates renal ischemia/reperfusion induced apoptosis and autophagy in the rat. Journal of Biomedical Science, 16(1), 19.

Wynn, T. A. (2007) Common and unique mechanisms regulate fibrosis in various fibroproliferative diseases. The Journal of Clinical Investigation, 117, 524-529.

Yaffe, D. and Saxel, O. (1977) Serial passaging and differentiation of myogenic cells isolated from dystrophic mouse muscle. Nature, 270(5639), 72-727.

Yamamizu, K., Shinozaki, K., Ayajiki, K., Gemba, M. and Okamura, T. (2007) Oral administration of both tetrahydrobiopterin and L-arginine prevents endothelial

dysfunction in rats with chronic renal failure. Journal of Cardiovascular Pharmacology, 49(3), 131-139.

Yamamoto, K., Sato, T., Matsui, T., Sato, M., Okada, T., Yoshida, H., Harada, A. and Mori, K. (2007) Transcriptional induction of mammalian ER quality control proteins is mediated by single or combined action of ATF6 and XBP1. Developmental Cell, 13, 365-376.

Yang, H. C., Zuo, Y. and Fogo, A. B. (2010) Models of chronic kidney disease. Drug Discovery Today, 7(1), 13-19.

Yang, L., Besschetnova, T. Y., Brooks, C. R., Shah, J. V. and Bonventre, J. V. (2010) Epithelial cell cycle arrest in G2/M mediates kidney fibrosis after injury. Nature Medicine, 16(5), 535-543.

Yazihan, N. and Kavas, G. O. (2010) Protective effect of erythropoietin in renal ischemia-reperfusion injury. The Open Drug Discovery Journal, 2, 3-7.

Yokoi, H., Mukoyama, M., Nagae, T., Mori, K., Suganami, T., Sawai, K., Yoshioka, T., Koshikawa, M., Nishida, T., Takigawa, M., Sugawara, A. and Nakao, K. (2004) Reduction in connective tissue growth factor by antisense treatment ameliorates renal tubulointerstitial fibrosis. Journal of the American Society of Nephrology, 15(6), 1430-1440.

Yonehana, T. and Gemba, M. (1995) Hypoxia and reoxygenation-induced injury of renal epithelial cells: Effect of free radical scavengers. Journal of pharmacology, 68, 231-234.

Yoshida, T., Sugiura, H., Mitobe, M., Tsuchiya, K., Shirota, S., Nishimura, S., Shiohira, S., Ito, H., Nobori, K., Gullans, S. R., Akiba, T. and Nitta, K. (2008) ATF3 protects against renal ischemia-reperfusion injury. Journal of the American Society of Nephrology, 19(2), 217-224.

Yu, F. Y., Wu, T. S., Chen, T. W. and Liu, B. H. (2011) Aristolochic acid I induced oxidative DNA damage associated with glutathione depletion and ERK1/2 activation in human cells. Toxicology in Vitro, 25, 810-816.

Zager, R. A., Fuerstenberg, S. M., Baehr, P. H., Myerson, D. and Torok-Storb, B. (1994) An evaluation of antioxidant effects on recovery from postischemic acute renal failure. Journal of the American Society of Nephrology, 4(8), 1588-1597.

Zager, R. A., Schimpf, B. A. and Gmur, D. J. (1993) Physiological pH. Effects on posthypoxic proximal tubular injury. Circulation Research, 72, 837-846.

Zarbock, A., Schmidt, C., Van Aken, H., Wempe, C., Martens, S., Zahn, P. K., Wolf, B., Goebel, U., Schwer, C. I., Rosenberger, P., Haeberle, H., Görlich, D., Kellum, J. A. and Meersch, M. (2015) Effect of remote ischemic preconditioning on kidney injury among high-risk patients undergoing cardiac surgery: A randomized clinical trial. The Journal of the American Medical Association, 313(21), 2133-2141.

Zella, S., Schmittc, R., Wittinga, S., Kreipea, H. and Becker, J. U. (2013) Hypoxia induces mesenchymal gene expression in renal tubular epithelial cells: An in vitro model of kidney transplant fibrosis. Nephron Extra, 3, 50-58.

Zhan, J., Nakao, A., Sugimoto, R., Dhupar, R., Wang, Y., Wang, Z., Billiar, T. R. and McCurry, K. R. (2009) Orally administered nitrite attenuates cardiac allograft rejection in rats. Surgery, 146(2), 155-165.

Zhang, C., Zheng, L., Li, L., Wang, L., Li, L., Huang, S., Gu, C., Zhang, L., Yang, C., Zhu, T. and Rong, R. (2014) Rapamycin protects kidney against ischemia reperfusion injury through recruitment of NKT cells. Journal of Translational Medicine, 12, 224.

Zhang, D. D. (2006) Mechanistic studies of the Nrf2-Keap1 signaling pathway. Drug Metabolism Reviews, 38, 769-789.

Zhang, L., Kimball, S. R., Jefferson, L. S. and Shenberger, J. S. (2009) Hydrogen peroxide impairs insulin-stimulated assembly of mTORC1. Free Radical Biology and Medicine, 46(11), 1500-1509.

Zhang, M. Z., Yao, B., Yang, S., Jiang, L., Wang, S., Fan, X., Yin, H., Wong, K., Miyazawa, T., Chen, J., Chang, I., Singh, A. and Harris, R. C. (2012) CSF-1 signaling mediates recovery from acute kidney injury. The Journal of Clinical Investigation, 122(12), 4519-4532.

Zhang, X. and Lemasters, J. J. (2013) Translocation of iron from lysosomes to mitochondria during ischaemia predisposes to injury after reperfusion in rat hepatocytes. Free Radical Biology and Medicine, 63, 243-253.

Zhang, Y., Zou, Z., Li, Y. K., Yuan, H. B. and Shi, X. Y. (2009) Glutamine-induced heat shock protein protects against renal ischaemia-reperfusion injury in rats. Nephrology, 14(6), 573-580.

Zhang, Y. L., Zhang, J., Cui, L. Y. and Yang, S. (2015) Autophagy activation attenuates renal ischemia-reperfusion injury in rats. Experimental Biology and Medicine (Maywood), 240(12), 1590-1598.

Zhao, Y. X., Cui, M., Chen, S. F., Dong, Q. and Liu, X. Y. (2014) Amelioration of ischemic mitochondrial injury and Bax-dependent outer membrane permeabilization by Mdivi-1. CNS Neuroscience and Therapeutics, 20, 528-538.

Zhu, S., Wang, Y., Jin, J., Guan, C., Li, M., Xi, C., Ouyang, Z., Chen, M., Qiu, Y., Huang, M. and Huang, Z. (2012) Endoplasmic reticulum stress mediates aristolochic acid I-induced apoptosis in human renal proximal tubular epithelial cells. Toxicology in Vitro, 26, 663-671.

Zimmermann, K. C. and Green, D. R. (2001) How cells die: Apoptosis pathways. Journal of Allergy and Clinical Immunology, 108, 99-103.

Zoncu, R., Bar-Peled, L., Efeyan, A., Wang, S., Sancak, Y. and Sabatini, D. M. (2011) mTORC1 senses lysosomal amino acids through an inside-out mechanism that requires the vacuolar H+-ATPase. Science, 334, 678-683.

Zuk, A., Bonventre, J. V. and Matlin, K. S. (2001) Expression of fibronectin splice variants in the postischemic rat kidney. American Journal of Physiology-Renal Physiology, 280(6), 1037-1053.

Zweier, J. L., Wang, P., Samouilov, A. and Kuppusamy, P. (1995) Enzyme-independent formation of nitric oxide in biological tissues. Nature Medicine, 1, 804-809.